

**Synthesis, characterization, and application of polyethylene glycol modified insulin
for oral delivery using complexation hydrogels**

A Thesis

Submitted to the Faculty

of

Drexel University

by

Anthony D. Tuesca

in partial fulfillment of the
requirements for the degree

of

Doctor of Philosophy

February 2008

© Copyright 2008

Anthony D. Tiesca. All Rights Reserved.

Dedications

I would like to dedicate this dissertation to my loving wife Molly. You first drew me to Philadelphia and Drexel University, but more importantly, your support and love are what carried me through my work there.

Acknowledgements

It is difficult to acknowledge everyone who has helped me over the last 4 ½ years in my graduate work in earning my Ph.D. The work was difficult and I could not have done it without support and help. First and foremost, I wish to thank my wife Molly who has supported me throughout my graduate work. She has been steadfast and loving, made my difficulties less difficult, and always been there when I needed her.

I also need to thank my advisor Anthony Lowman. He is the reason that I decided to pursue a doctorate degree in the first place and without his influence I would not be where I am now. When I first came to Drexel University, I was set on a path to pursue my master's degree and I was resolute. Tony made me realize the value of continuing my education and in the process I have learned much more than just my subject; I have learned the value of continued excellence, education, and personal development throughout one's career.

I wish to thank my parents who instilled in me perseverance and faith in my abilities. I did not heed their advice until later in my life, but not too late to make a difference.

I would like to thank my committee members: Guiseppe Palmese, Yossef Elabd, Jeffrey Joseph, and Aleister Saunders. They have been invaluable mentors in my doctorate progress. They have also been trusted advisors with me in my personal endeavors and future career plans. I value their support and counsel and hope to be able to continue our relationship for many years.

Special thanks should be mentioned as well for the associate dean for graduate students in the College of Engineering for the majority of my tenure at Drexel, Mun Choi. He was always a staunch supporter of mine and continued to encourage me throughout my studies at Drexel. Mun has moved on to become the dean of the College of Engineering at the University of Connecticut, but I still value his role in my Ph.D. studies.

I need to give another special thanks to Eric Perakslis who was instrumental to my early graduate work at Drexel. When I was just making the transition from a master's to a doctorate student Eric was able to extend a helping hand to me for support and mentorship. He was pivotal to me in a pivotal moment in my studies and for that I am truly grateful. Eric, I doubt that you will be working long enough for me to be your boss, but I'll do my best.

I wish to thank the other members of the Biomaterials and Drug Delivery Laboratory who have helped me over the years. Meredith Hans was always a generous source of advice, whether she wanted to be or not, and was a great help to making me a better researcher. I have enjoyed watching you succeed and am glad to call you my friend. Jennifer Vernengo and Noelle Comolli were with me as we all struggled through our early work as graduate students. It was a pleasure to have you as colleagues. I also wish to thank other members of the lab who have helped me including Koji Nakamura, Richard Pollard, Jonathan Thomas, Kara Spiller, Vanessa Vardon, Jason Coleman, Sam Laurencin, Karri Momyer, Michael Marks, and Erik Brewer.

I also wish to give special thanks to students who have worked directly with me during my and their time at Drexel. Becky Lownes was with me during the early stages

of the *in vivo* work that we first performed at Thomas Jefferson University. She was a joy to be with and I wish her the best. Lisa Leone helped me in my early work on the network characterization of P(MAA-g-EG) hydrogels. She was advanced for her years and I know that she will succeed in her endeavors. Kelsey Gold worked closely with me during more of the network characterization work and generated significant amounts of data that lead to some of the conclusion presented in this work. She was a diligent worker and her help was incredibly valuable. Finally Matthias Colomb worked with me in some of the first attempts to complete the insulin PEGylation. We did not achieve it together, but his help was well valued and I ended up being able to finish the work after he left.

I wish to acknowledge those who supported me financially during my graduate studies. First was my work at Centocor under the tutelage of Eric Perakslis. I wish to thank Dr. Robert Koerner who generated the Koerner Family Fellowship which supported me for one year. I also would like to thank the Nation Science Foundation Integrated Graduate Education and Research Traineeship (NSF-IGERT) which has supported me for the last 18 months. Finally, I would like to thank the National Institutes of Health, who has supported my research throughout my graduate work. They continue to fund valuable research and I hope that someday a better treatment for diabetes will be achieved.

Table of Contents

List of Tables	xi
List of Figures	xii
Abstract	xvi
1. CHAPTER 1: INTRODUCTION	1
1.1. References	3
2. CHAPTER 2: BACKGROUND	5
2.1. Diabetes	5
2.1.1. Type 1 Diabetes	6
2.1.2. Type 2 diabetes	7
2.2. Insulin	10
2.2.1. History of Insulin	10
2.2.2. Insulin Analogs	12
2.2.2.1 Fast-Acting Insulin Analogs	13
2.2.2.2. Long-Acting Insulin Analogs	14
2.2.2.3. Immunogenicity and Mitogenicity	15
2.3. Biological Role of Insulin	16
2.3.1. Insulin Production and Secretion	17
2.3.2. Effect of Insulin	18
2.3.2. Insulin Regulation	19
2.4. Insulin Therapy	20
2.5. The Diabetes Control and Complications Trial	21
2.6. Alternative Insulin Delivery Methods	22
2.6.1. Pulmonary Delivery of Insulin	23
2.6.2. Transdermal Delivery of Insulin	25
2.6.3. Nasal Delivery of Insulin	26
2.6.4. Other Delivery Routes for Insulin	27
2.6.5. Artificial Pancreas	28
2.7. Oral Insulin Delivery and its Challenges	30
2.7.1. Physiology of the Gastrointestinal Tract	31
2.7.1.1. Absorption in the Gastrointestinal Tract	34
2.7.1.2. Pathway for Orally Delivered Proteins	39

2.7.2.	Rationale for Oral Insulin Delivery	42
2.7.3.	Enzymatic Barrier	43
2.7.3.1.	Luminal Enzymes from Pancreatic and Hepatic Secretion	44
2.7.3.2.	The Brush-Border Membrane and Intracellular Enzymes	46
2.7.4.	Physical Barrier.....	48
2.8.	Approaches for Oral Insulin Delivery.....	49
2.8.1.	Enzyme Inhibitors.....	49
2.8.2.	Permeation Enhancers.....	50
2.8.3.	Prodrug Systems	52
2.8.4.	Active Transport and Receptor-Mediated Endocytosis	54
2.8.5.	Lipid Based Delivery Systems.....	57
2.9.	Polymeric Systems for Oral Insulin Delivery.....	59
2.9.1.	Micro- and Nanoparticles	59
2.9.2.	Biodegradable Systems.....	63
2.9.3.	Mucoadhesive Delivery Systems.....	65
2.10.	Hydrogels for Oral Protein Delivery.....	67
2.11.	Poly(methacrylic acid-g-ethylene glycol).....	69
2.12.	References.....	82
3.	CHAPTER 3: RESEARCH GOALS	106
4.	CHAPTER 4: SYNTHESIS AND NETWORK STRUCTURE CHARACTERIZATION OF P(MAA-g-EG) HYDROGELS.....	108
4.1.	Introduction.....	108
4.2.	Materials and Methods.....	110
4.2.1.	Materials	110
4.2.2.	Synthesis of P(MAA-g-EG) Hydrogels	110
4.2.3.	Hydrogel swelling.....	112
4.2.4.	Mechanical Testing.....	113
4.2.5.	Gel Permeation Chromatography	114
4.3.	Results and Discussion	115
4.3.1.	Hydrogel Synthesis	115
4.3.2.	P(MAA-g-EG) Swelling	116
4.3.3.	P(MAA-g-EG) Mechanical Testing.....	117
4.3.4.	P(MAA-g-EG) Gel Permeation Chromatography	118

4.3.5.	Network Modeling and Characterization.....	119
4.4.	Conclusions.....	121
4.5.	References.....	132
5.	CHAPTER 5: <i>IN VITRO</i> ELUCIDATION OF INSULIN UPTAKE AND RELEASE MECHANISM FROM P(MAA-g-EG) HYDROGELS.....	134
5.1.	Introduction.....	134
5.2.	Materials and Methods.....	136
5.2.1.	Materials	136
5.2.2.	Human Insulin Loading	137
5.2.3.	Insulin Glargine Loading.....	138
5.2.4.	Insulin Release Studies	139
5.2.5.	Insulin Glargine Release Studies	140
5.3.	Results and Discussion	140
5.3.1.	Human Insulin Loading	140
5.3.2.	Insulin Glargine Loading.....	141
5.3.3.	<i>In Vitro</i> Release Studies.....	142
5.3.3.1.	Human Insulin Release Studies	143
5.3.3.2.	Insulin Glargine Release Studies	145
5.3.3.3.	Insulin Release for Loosely Crosslinked Formulations	146
5.4.	Conclusions.....	147
5.5.	References.....	158
6.	CHAPTER 6: SYNTHESIS AND CHARACTERIZATION OF PEGYLATED INSULIN	160
6.1.	Introduction.....	160
6.2.	Materials and Methods.....	164
6.2.1.	Materials	164
6.2.2.	Synthesis of Di-BOC Insulin	165
6.2.3.	Recovery of Impure Diboc Treated Insulin	167
6.2.4.	Di-BOC Insulin PEGylation	168
6.2.5.	Di-BOC and PEGylated Insulin Characterization	168
6.2.5.1.	PEGylated Insulin Digestion.....	169
6.2.5.2.	MALDI-TOF Mass Spectroscopy.....	170
6.3.	Results and Discussion	171

6.3.1.	Synthesis of Di-BOC Insulin	171
6.3.2.	Purification of Di-BOC insulin.....	172
6.3.3.	Insulin PEGylation.....	175
6.3.4.	Characterization of PEGylated Insulin	177
6.3.4.1.	PEGylated Insulin Disulfide Reduction.....	177
6.3.4.2.	PEGylated Insulin Trypsin Digestion.....	178
6.4.	Conclusions.....	180
6.5.	References.....	200
7.	CHAPTER 7: <i>IN VITRO</i> AND <i>IN VIVO</i> TESTING OF PEGYLATED INSULIN WITH P(MAA-g-EG) HYDROGELS.....	203
7.1.	Introduction.....	203
7.2.	Materials and Methods.....	205
7.2.1.	Materials	205
7.2.2.	Synthesis of P(MAA-g-EG) Hydrogels.....	206
7.2.3.	PEGylated Insulin Loading and Release.....	206
7.2.4.	<i>In Vivo</i> Determination of PEGylated Insulin Bioactivity	207
7.2.5.	<i>In Situ</i> Testing of P(MAA-g-EG) Hydrogels.....	209
7.2.6.	Glucose and Insulin Determination	212
7.2.7.	Statistics	213
7.3.	Results and Discussion	213
7.3.1.	PEGylated Insulin Loading.....	213
7.3.2.	Bioactivity and PK/PD for IV Administration.....	215
7.3.3.	Bioactivity and PK/PD for SC Administration.....	219
7.3.4.	<i>In Vivo</i> Effect of a High Dose of Insulin and PEGylated Insulin	222
7.3.5.	<i>In Situ</i> Testing.....	223
7.4.	Conclusions.....	226
7.5.	References.....	242
8.	CHAPTER 8: CONCLUSIONS AND RECOMMENDATIONS FOR FUTURE WORK.....	244
8.1.	Conclusions.....	244
8.2.	Recommendations for Future Work.....	247
8.3.	References.....	251
9.	CHAPTER 9: VITA.....	252

List of Tables

Table 4.1 Formulations of polymerization conditions for the series of P(MAA-g-EG) hydrogels considered. Changes expected in the hydrogel network are indicated by the blue arrow.....	122
Table 4.2. The effective molecular weight of P(MAA-g-EG) chains in the absence of covalent crosslinks determined by GPC (\pm S.D., n = 3).....	123
Table 5.1. A comparison between native human insulin and insulin glargine	149
Table 5.2. Average insulin incorporation efficiency percentages for all P(MAA-g-EG) hydrogel formulations (\pm S.D., n = 3).....	150
Table 5.3. Average incorporation efficiencies for insulin glargine loading in four P(MAA-g-EG) hydrogel formulations \pm standard deviation (n = 3)	151
Table 7.1. PK/PD summary of IV and SC administration of insulin and PEGylated insulin at 1.0 IU/kg to healthy male Sprague Dawley rats	231

List of Figures

Figure 2.1. The amino acid sequence of native human insulin.....	72
Figure 2.2. Metabolic and catabolic processes involving glucose.....	73
Figure 2.3. Schematic of the entire human gastrointestinal tract.....	74
Figure 2.4. The intestinal epithelium	75
Figure 2.5. Transepithelial pathways for protein drugs from the intestinal lumen to the bloodstream. (1) Pinocytosis (2) paracellular transport (3) receptor-mediated transcytosis (4) active transport (5) passive transcellular transport.....	76
Figure 2.6. Structure of the tight junction in epithelial cells	77
Figure 2.7. Lipid based systems for oral protein delivery: (a) micelle and (b) liposome	78
Figure 2.8. Polymer based nanoparticle designs: (a) nanosphere from spray drying, (b) nanosphere from double emulsion, and (c) nanocapsule.....	79
Figure 2.9. Simplified diagram of a drug contained within a hydrogel network indicating the network mesh size, ξ , and the average molecular weight between crosslinks, \overline{M}_e	80
Figure 2.10. Interpolymer bonds between PMAA and PEG	81
Figure 4.1. Schematic of p(MAA-g-EG) hydrogel and its pH dependent swelling behavior.....	124
Figure 4.2. Hydrogel density determination using the buoyancy technique.....	125
Figure 4.3. Experimental setup for tensile testing of hydrated hydrogel strips in a custom made water bath at 37°C.	126
Figure 4.4. FTIR-ATR spectra of a polymerized, hydrated P(MAA-g-EG) hydrogel sample.....	127
Figure 4.5. Equilibrium polymer volume fraction for two P(MAA-g-EG) hydrogel formulations polymerized with 50 wt% monomer following 48 hours of swelling in PBS (\pm S.D., n = 3).....	128
Figure 4.6. Normalized tensile moduli for two P(MAA-g-EG) hydrogel formulations polymerized with 50 wt% monomer following 48 hours of swelling in PBS (\pm S.D., n = 3).....	129
Figure 4.7. (a) The modeled average effective molecular weight between crosslinks, \overline{M}_e , and (b) network correlation length, ξ , for two P(MAA-g-EG) hydrogel formulations polymerized with 50 wt% monomer (\pm S.D., n = 3).....	130
Figure 4.8. The modeled network correlation length, or mesh size, ξ , for all formulations tested in swelling and tensile studies.....	131

Figure 5.1. RP-HPLC absorbance at 214 nm of native human insulin standard (top) and human insulin following uptake and release from an ILP sample (bottom).....	152
Figure 5.2. Total absorbance spectra for (a) native human insulin standard and (b) human insulin following uptake and release from an ILP sample.....	153
Figure 5.3. Release of insulin from ILP samples of P(MAA-g-EG) formulations (a) 0.75/66 and (b) 2.0/66 into PBS at various pH levels (+ S.D., n = 3).....	154
Figure 5.4. Fractional insulin release following 3 hours of dissolution in PBS at 37°C (+ S.D., n = 3).....	155
Figure 5.5. Fractional insulin glargine release following 3 hours of dissolution in PBS at 37°C (+ S.D., n = 3).....	156
Figure 5.6. Release of insulin from ILP samples of P(MAA-g-EG) formulations 0.75/33 (closed symbols) and 0.375/50 (open symbols) into PBS at various pH levels (\pm S.D., n = 3).....	157
Figure 6.1. Amino acid sequence for human insulin with digestion pathways indicated.....	182
Figure 6.2. Space filled, three dimensional image of an insulin monomer (White = insulin receptor binding site, Red = GlyA1, Orange = LysB29, Green = PheB1).....	183
Figure 6.3. RP-HPLC absorbance at 214 nm for (a) insulin (b) crude diboc treated insulin (unpurified) and (c) purified di-BOC _{LysB29,GlyA1} insulin.....	184
Figure 6.4. FPLC elution profile of crude diboc treated insulin using cation exchange chromatography with absorbance at 280 nm.	185
Figure 6.5. RP-HPLC stacked plot of fractions collected from FPLC elution with absorbance at 214 nm.....	186
Figure 6.6. MALDI-TOF MS for fractions collected from FPLC separation of crude diboc treated insulin species	187
Figure 6.7. RP-HPLC spectra of recovered insulin following removal of BOC groups as compared to an insulin standard with absorbance at 214 nm.	188
Figure 6.8. RP-HPLC total absorbance spectrum of (a) recovered insulin following removal of BOC groups and (b) native insulin standard.....	189
Figure 6.9. RP-HPLC spectra of recovered insulin following removal of BOC groups as compared to a crude diboc treated insulin sample prior to purification.....	190
Figure 6.10. RP-HPLC spectra of recovered insulin treated a second time with diboc as compared to a first pass crude diboc treated insulin.....	191
Figure 6.11. MALDI-TOF MS of a physical mixture of di-BOC insulin and mPEG-SPA with a 2500:1 molar ratio of DHB to analyte.....	192

Figure 6.12. MALDI-TOF MS of PEGylated di-BOC insulin prior to eliminating unreacted components with a 2500:1 molar ratio of sinapic acid to analyte	193
Figure 6.13. Cation exchange elution profile of PEGylated insulin following removal of the BOC groups	194
Figure 6.14. Close up view of MALDI-TOF MS of purified PEGylated insulin following removal of BOC protecting groups	195
Figure 6.15. Reaction of iodoacetamide with a cysteine residue on insulin.....	196
Figure 6.16. MALDI-TOF MS spectra of the A-chain of PEGylated insulin following disulfide reduction and alkylation with DTT and iodoacetamide	197
Figure 6.17. MALDI-TOF MS spectra of the B-chain of PEGylated insulin following disulfide reduction and alkylation with DTT and iodoacetamide	198
Figure 6.18. MALDI-TOF MS spectrum for the trypsin digested PEGylated insulin sample	199
Figure 7.1. Loading efficiencies for regular human insulin and PEGylated insulin in P(MAA-g-EG) hydrogels with MAA/EG monomer ratios of 1/1 or 3/2 (+ S.D., ** $p < 0.01$, * $p < 0.5$).....	232
Figure 7.2. Insulin loaded polymer (ILP) and PEGylated insulin loaded polymer (PILP) release from P(MAA-g-EG) hydrogels with a MAA:EG monomer ratio of 3:2 following 3 hours of dissolution in PBS at 37 °C (+ S. D., n = 3).....	233
Figure 7.3. Insulin and PEGylated insulin plasma concentrations following IV and SC injection of 1.0 IU/kg in rats (+ S. D., n = 6).....	234
Figure 7.4. Zoom in of insulin and PEGylated insulin plasma concentrations in healthy male Sprague Dawley following IV injection of 1.0 IU/kg in rats (+ S.D., n = 6)	235
Figure 7.5.(a) Blood glucose levels and (b) normalized blood glucose levels of healthy male Sprague Dawley rats following IV administration of 1.0 IU/kg of insulin and PEGylated insulin (- S.D., n = 6).....	236
Figure 7.6. Insulin and PEGylated insulin plasma concentrations following SC injection of 1.0 IU/kg in healthy male Sprague Dawley rats (+ S. D., n = 6).....	237
Figure 7.8. (a) Blood glucose levels and (b) normalized blood glucose levels of healthy male Sprague Dawley rats following SC administration of 1.0 IU/kg of insulin and PEGylated insulin (- S.D., n = 6).....	238
Figure 7.8. Blood glucose levels of healthy male Sprague Dawley rats following SC administration of 4.0 IU/kg of insulin and PEGylated insulin (- S.D., n = 4).....	239
Figure 7.9. Insulin and PEGylated insulin plasma concentrations following <i>in situ</i> administration of solutions or protein loaded polymers to the duodenum of male Sprague Dawley rats at 20.0 IU/kg (+ S.D., n = 6).....	240

Figure 7.10. Normalized blood glucose levels of healthy male Sprague Dawley rats following <i>in situ</i> administration of 20.0 IU/kg of insulin and PEGylated insulin solutions and insulin and PEGylated insulin loaded polymers (- S.D., n = 4-6).....	241
--	-----

Abstract

Synthesis, characterization, and application of polyethylene glycol modified insulin for oral delivery using complexation hydrogels

Anthony D. Tuesca

Anthony M. Lowman, Ph.D.

Therapeutic proteins and peptides represent a major area of research in current pharmaceutical and biotechnology companies. Due to their inherent instability, the vast majority of these drugs require parenteral administration. Such is the case for as many as 6 million patients in the United States who use insulin in the treatment of diabetes mellitus. Oral insulin delivery would be a highly desirable alternative method of administration, though it continues to be an elusive target due to the enzymatic digestion of insulin and low levels of absorption from the gastrointestinal tract. Hydrogel polymers have shown promise as potential carriers for oral insulin delivery. In particular, a pH responsive hydrogel composed of poly(methacrylic acid-g-polyethylene glycol), P(MAA-g-EG), has shown the ability to protect insulin from enzymes in the gastric environment and release in small intestines. It was also able to induce a hypoglycemic effect *in vivo* when delivered to isolated ileal segments in rats. However, this material has not shown similar potential for oral protein delivery of other model drugs. To date, the unique interaction between P(MAA-g-EG) and insulin, which give it such potential for oral delivery, are not completely understood.

The focus of this research is to investigate how P(MAA-g-EG) hydrogels interact with insulin and to improve upon current designs for oral insulin delivery. An attempt is made to correlate the structure and chemistry of the hydrogel to its interaction with insulin over the pH range exhibited by the gastrointestinal tract *in vitro*. Further

insight is gained by observing the interaction of the hydrogel with insulin-like proteins including insulin glargine, an insulin analog, and polyethylene glycol (PEG) modified insulin. The PEG-insulin conjugate is synthesized and characterized to maintain the bioactivity of the protein, which is confirmed *in vivo* using intravenous and subcutaneous administration in rats. Finally, the proposed system is tested using an *in vivo* model in Sprague Dawley rats and related to the potential application of P(MAA-g-EG) to deliver insulin and PEG modified insulin for the treatment of diabetes.

CHAPTER 1: INTRODUCTION

Therapeutic proteins and peptides represent a major area of research in current pharmaceutical and biotechnology companies. In an editorial by Dr. E. Prosser of Trinity College in Dublin it was noted that 38 of the top 100 drugs are proteins or peptides, however only one of those drugs are available as an oral medication [1]. Generally therapeutic proteins and peptides require parenteral administration. Significant research efforts have been made investigating oral protein delivery because of the ease of administration, ability to avoid the pain of injections, leading to higher patient compliance, and elimination of infection as a potential side effect. However, little success has been achieved for oral protein delivery primarily due to the enzymatic degradation of proteins and low levels of transport across the epithelial layer of the gastrointestinal tract [2-4].

One promising approach to oral protein delivery is through the use of hydrogels. These materials have unique biomimetic properties which allow them to be applied to a number of drug delivery applications [5]. Of particular interest are dynamic hydrogels which can respond to changes in their environment. One class of environmentally responsive hydrogels reacts to the pH of their surroundings. They offer promise for oral protein delivery due to the pH shift which occurs in the gastrointestinal tract [6]. One particular pH responsive hydrogel for this application is poly(methacrylic acid-g-ethylene glycol), P(MAA-g-EG), which has been investigated primarily with insulin. Previous research with this material has shown that it has the ability to protect insulin from enzymatic degradation in the gastric environment and release it in the intestinal environment [7-10]. In doing so, this material has the potential to deliver insulin orally

and become a new method to treat diabetes. It induced a hypoglycemic effect in rats when delivered to ileal segments *in vivo* [9, 11]. Additional work has shown that P(MAA-g-EG) has other beneficial characteristics for oral insulin delivery including mucoadhesion [12, 13], enzyme inhibition [14], and permeation enhancement of the intestinal epithelium [15]. Most of this work, however, has strictly investigated the macromolecular behavior of the material and its potential as an insulin oral delivery device.

The focus of this research is to investigate how P(MAA-g-EG) hydrogels interact with insulin. An attempt is made to correlate the structure and chemistry of the hydrogel to its interaction with insulin over the pH range exhibited by the gastrointestinal tract *in vitro*. In doing so, the unique potential for oral insulin delivery using this material may be more accurately defined. Further insight can be gained by comparing the interaction of P(MAA-g-EG) with insulin to that of similar proteins with small but distinct changes in structure or chemistry. In this work, insulin glargine, an insulin analog, and polyethylene glycol (PEG) modified insulin are also investigated with the hydrogel. The PEG-insulin conjugate is synthesized in a controlled manner such that the bioactivity of the protein is maintained. Finally, the proposed system is tested using an *in vivo* model in Sprague Dawley rats and related to the potential application of P(MAA-g-EG) to deliver insulin and PEG modified insulin for the treatment of diabetes.

1.1. References

1. Sinha, V.R. and R. Kumria, *Microbially triggered drug delivery to the colon*. Eur J Pharm Sci, 2003. **18**(1): p. 3-18.
2. Sood, A. and R. Panchagnula, *Peroral route: an opportunity for protein and peptide drug delivery*. Chem Rev, 2001. **101**(11): p. 3275-303.
3. Wang, W., *Oral protein drug delivery*. J Drug Target, 1996. **4**(4): p. 195-232.
4. Still, J.G., *Development of oral insulin: progress and current status*. Diabetes Metab Res Rev, 2002. **18**(Suppl 1): p. S29-S37.
5. Peppas, N.A., et al., *Physicochemical foundations and structural design of hydrogels in medicine and biology*. Annu Rev Biomed Eng, 2000. **2**: p. 9-29.
6. Barrett, K.E., *Gastrointestinal Physiology*. 2006, New York: McGraw-Hill.
7. Perakslis, E., A. Tunesca, and A. Lowman, *Complexation hydrogels for oral protein delivery: an in vitro assessment of the insulin transport-enhancing effects following dissolution in simulated digestive fluids*. J Biomater Sci Polym Ed, 2007. **18**(12): p. 1475-90.
8. Morishita, M., et al., *Elucidation of the mechanism of incorporation of insulin in controlled release systems based on complexation polymers*. J Control Release, 2002. **81**(1-2): p. 25-32.
9. Nakamura, K., et al., *Oral insulin delivery using P(MAA-g-EG) hydrogels: effects of network morphology on insulin delivery characteristics*. J Control Release, 2004. **95**(3): p. 589-99.
10. Lowman, A.M., et al., *Oral delivery of insulin using pH-responsive complexation gels*. J Pharm Sci, 1999. **88**(9): p. 933-7.
11. Morishita, M., et al., *Mucosal insulin delivery systems based on complexation polymer hydrogels: effect of particle size on insulin enteral absorption*. J Control Release, 2004. **97**(1): p. 115-24.
12. Goto, T., et al., *Gastrointestinal transit and mucoadhesive characteristics of complexation hydrogels in rats*. Journal of Pharmaceutical Sciences, 2006. **95**(2): p. 462-469.

13. Peppas, N.A. and J.J. Sahlin, *Hydrogels as mucoadhesive and bioadhesive materials: a review*. *Biomaterials*, 1996. **17**(16): p. 1553-61.
14. Kavimandan, N.J., E. Losi, and N.A. Peppas, *Novel delivery system based on complexation hydrogels as delivery vehicles for insulin-transferrin conjugates*. *Biomaterials*, 2006. **27**(20): p. 3846-54.
15. Ichikawa, H. and N.A. Peppas, *Novel complexation hydrogels for oral peptide delivery: in vitro evaluation of their cytocompatibility and insulin-transport enhancing effects using Caco-2 cell monolayers*. *J Biomed Mater Res A*, 2003. **67**(2): p. 609-17.

CHAPTER 2: BACKGROUND

2.1. Diabetes

Diabetes mellitus is a disease in which the body does not produce or properly use insulin [1-3]. Insulin is a protein which is required for the cellular uptake of circulating glucose into most tissues in the body. The central identifying feature of diabetes mellitus is a chronic and substantial elevation of the circulating blood glucose concentration. In addition to blood glucose concentration, glycosylated hemoglobin (Hb_{A1c}) is used to measure blood glucose levels over a long period of time. Healthy levels are considered to be 70-150 mg/dl for blood glucose and < 7 % for Hb_{A1c}. The chronic effects of diabetes contribute to medical problems such as eye disease, neuropathy, cardiovascular disease, gastrointestinal disorders, kidney disease, impaired sexual function, bone and rheumatic disorders, endocrine diseases, central nervous system problems, and psychological and psychiatric conditions [1]. The population of Americans diagnosed with diabetes represented 4.9% of the total population in 1990. Currently, diabetes currently affects approximately 20.8 million people in the United States, 7 % of the total population [4]. Much of this increase over the last 18 years was due in large part to increased frequency of diagnosis, however, the growth of the diabetic population has reached epidemic levels. It is currently the fifth leading cause of death in the U.S., and the estimated total cost of diabetes in the U.S. increased from \$98 billion in 1997 to \$132 billion in 2002 [5]. Diabetes is generally separated into two major categories: insulin dependent diabetes mellitus (IDDM), or Type 1 diabetes, and non-insulin dependent diabetes mellitus (NIDDM), or Type 2 diabetes. Another significant type of diabetes is gestational diabetes, which affects about 4 % of pregnant women in the U.S. [6].

Gestational diabetes represents only a small population of people diagnosed with diabetes, and the effects generally subside after childbirth, so it will not be discussed in this work.

2.1.1. Type 1 Diabetes

Type 1 diabetes, previously referred to as juvenile onset diabetes, is an autoimmune disease in which the body attacks the pancreatic β -cells which produce insulin [1]. Those suffering from Type 1 diabetes are unable to produce insulin. Without treatment with insulin, Type 1 diabetics experience acute effects of the disease such as ketoacidosis, a condition wherein the body begins to burn fat and muscle tissues for energy causing the release of ketone bodies into the bloodstream. Ketoacidosis is extremely taxing on the kidneys and endothelial cells in the capillaries and eyes, causing extreme damage to those tissues and leading to kidney failure, blindness, and amputation of tissues of the extremities [1]. Type 1 diabetes affects about 5-10 % of diabetic patients.

Almost exclusively, the treatment for Type 1 diabetes is insulin therapy. This treatment requires self-monitoring of blood glucose levels and intermittent insulin administration. Generally insulin is taken subcutaneously in the form of an injection or an infusion. Insulin therapy will be discussed in more detail later in this chapter. The only other treatment for Type 1 diabetes is transplantation of pancreatic tissue, more specifically cells known as the islets of Langerhans, harvested from deceased donors. The first attempt for transplantation of pancreatic tissue was performed by Ballinger and Lacy in 1972 [7]. In this study, the transplant successfully reversed the effects streptozotocin induced diabetes in rats. Significant progress in this approach has occurred in the last 35

years [8-11], and islet transplant has the theoretical potential to completely reverse the effects of Type 1 diabetes. Insulin independence rates of transplant recipients after 1 year have been reported as high as 80% [12]. Islet transplantation has not yet achieved widespread practice, however, due to the very high immune response and tissue rejection caused by the transplanted tissue. This effect occurs with all islet recipients mandating administration of immunosuppressant drugs for the lifetime of the individual. The side effects of these drugs greatly increase the risk of infection, sickness, and death of the individual. Due to the high risk, this treatment is generally only considered for individuals also suffering from renal failure who receive concomitant kidney transplants.

2.1.2. Type 2 diabetes

Type 2 diabetes, previously referred to as adult onset diabetes, is generally caused by a combination of low production of insulin from the pancreas and insulin resistance in the tissues that require insulin. It is by far the most common type of diabetes affecting approximately 90 % of diabetic patients [13]. The effects of Type 2 diabetes are not as acute as Type 1 and there are even many people who are unaware that they have the disease. Type 2 diabetics still produce some insulin which significantly reduces the possibility of ketoacidosis, although the risk is still much higher than a non-diabetic person. The population of diabetics is increasing to epidemic proportions due primarily to the rapid increase in Type 2 diabetes. By a large margin, the leading cause of Type 2 diabetes is obesity [14, 15] In fact, of the patients with Type 2 diabetes, as many as 80-90 % are overweight or obese [16]. Other factors which have significant impact on the likelihood of developing Type 2 diabetes are age, race, and genetic disposition. The

prevalence of Type 2 diabetes increases dramatically for all races with advancing age. Americans between the ages of 45-55 are four times more likely to have Type 2 diabetes than those between 20-44 [17]. Of the major racial populations in the U.S., non-Hispanic whites have the lowest incidence of diabetes, while Hispanics have the highest. The racial group with the highest frequency of diabetes is the Pima Indian, with roughly 50 % of the population between 30-64 years old being diagnosed with one form of diabetes [18]. Because one cannot change their age, race, or genetics, the most important factor for the prevention of Type 2 diabetes is obesity.

The most important epidemiological approach to Type 2 diabetes is prevention. In most cases, Type 2 diabetes can be controlled by diet and exercise. Because the leading cause of the disease is obesity, controlling one's weight is critical. The key feature of diet for those diagnosed or at risk of developing Type 2 diabetes is controlling the caloric and carbohydrate intake [19]. Smoking also increases the likelihood in the development of the disease. Interestingly, some behaviors or habits which are often considered bad for health have caused a reduction in the risk of developing diabetes. Studies have shown that increased coffee consumption decreases the risk for Type 2 diabetes [20]. Also, moderate alcohol consumption (1-3 drinks per day) has been linked in improved insulin sensitivity and reduced circulating insulin levels, a sign of insulin resistance [20]. For many people, however, changing these environmental factors is not enough. For those patients who require additional treatment a variety of pharmacological options for Type 2 diabetes are available.

According to data from the CDC in 2003, 11.6 million adults with diabetes were taking some type of medication for their diabetes with 9.5 million taking some form of

oral medication [21]. There are a wide variety of drugs for the treatment of Type 2 diabetes which are distinguished as: sulphonylureas, meglitinides, α -glucosidase inhibitors, biguanidines, thiazolidinediones, dipeptidyl peptidase-4 (DPP-4) inhibitors, and glucagon-like peptide 1 (GLP1) antagonists [22, 23]. Sulphonylureas and meglitinides induce increased insulin production by closing ATP-sensitive (K_{ATP}) potassium channels in the pancreatic β -cells [24, 25]. The secretion of insulin occurs in response in the β -cells' attempt to re-equilibrate osmotic pressure and transmembrane potential within the cells. Drugs which are α -glucosidase inhibitors reduce the enzymatic cleavage of complex carbohydrates into lower molecular weight absorbable sugars at the brush border of the intestines, thus slowing the absorption of carbohydrates and reducing postprandial hyperglycemia [26]. The pharmacodynamic mode of action of biguanidines is not exactly understood, however they have been shown to reduce gluconeogenesis in the liver, reducing the level of endogenous glucose in the blood [27]. Thiazolidinediones induce a hypoglycemic effect by binding peroxisome proliferators-activated receptors, or PPARs, which stimulates carbohydrate metabolism [28]. This reduces the insulin resistance of the affected tissues, although the side effects of bone mass loss and increased heart problems may cause this type of drug to be discontinued in regular use [29, 30]. Both DPP-4 inhibitor and GLP1 antagonist drugs have similar modes of action: to increase the biological effect of GLP1, which increases the release of insulin as well as inhibits glucagon release [31, 32].

While these drugs are currently in clinical use, they all rely on some level of endogenous insulin production and sensitivity to be effective. Recently, there has been a swelling of support for increased administration of insulin to treat Type 2 diabetes and

currently as many as 30 % of Type 2 diabetics take insulin [33]. The American Diabetes Association has stated that intensive insulin therapy in addition to comprehensive self-management training should become the standard therapy in all diabetic patients [34]. There have also been several reviews which suggest implementing insulin therapy for Type 2 diabetics much earlier than is currently practiced [35-37], especially because those with Type 2 diabetes generally have difficulty maintaining healthy Hb_{A1c} levels with only diet, exercise, oral hypoglycemic agents, or combinations of the three.

2.2. Insulin

The discovery of insulin is one of the greatest discoveries of modern medical history. Its effect on the livelihood of individuals with diabetes was profound even in its earliest stages. It is by far the most studied protein in history and it was the first ever naturally produced protein to have its amino acid sequence determined, a feat for which Frederick Sanger won the Nobel Prize in Chemistry in 1958 [38-44]. Currently insulin and insulin analogs are available as several different polypeptide sequences with varying biological effects. Details of the history, physiology, use and delivery of insulin are given in the following sections.

2.2.1. History of Insulin

In 1869, a German medical student name Paul Langerhans discovered islet cells in the pancreas which are now know as the islet of Langerhans [45]. Unfortunately he died before their significance was discovered. Two fellow German researchers, Joseph von Mering and Oscar Minkowski, discovered that the removal of the islet of Langerhans

from dogs induced a diabetic state [46]. It was this discovery that led researchers to believe that these cells were involved in more than just digestion and damage to them induced diabetes. This work preceded that of Frederick Banting and his assistant Charles Best from the University of Toronto, however the pair is generally credited for the discovery of insulin [45, 47, 48]. Their work was performed in the lab of John Macleod and it was Macleod and Banting who received the Nobel Prize in 1923 for the discovery of insulin. Originally called “isletin”, it was first harvested from the pancreas of dogs and when given to de-pancreatized dogs caused a glucose lowering effect [3]. The group had significant difficulty purifying the pancreatic extract and enlisted the help of biochemist James Collip. With his help, the purification improved vastly and human trials produced immediate improvement in diabetic patients. The first patient to receive the extracts was Leonard Thompson at the age of 14 [45, 47]. He went on to live a relatively healthy life until dying of pneumonia at age 27. The demand for insulin quickly surpassed the ability of the group to produce it and Eli Lilly Pharmaceutical Company was contracted to produce insulin [49]. Another researcher from the University of Copenhagen, August Krogh, met with the research group at the University of Toronto in 1922. Upon his return to Denmark he founded the Nordisk Insulin Company [49]. The two companies are still the leading producers of insulin world wide.

The production of insulin has progressed greatly since its discovery. It originally depended largely on purification from extract produced in animals. In 1936, the first extended action version of insulin was produced as protamine insulin by Nordisk [49]. Ten years later, Nordisk produced Neutral Protamine Hagedorn (NPH) insulin which had a more extended effect and higher stability than protamine insulin [48]. In

1953, another type of long-acting insulin, Lente® insulin, was produced [49]. This formulation stabilized the hexameric form of insulin with the addition of zinc, reducing its rate of absorption into the bloodstream [49]. The variety of insulin products formulated for longer modes of action allowed diabetics greater flexibility in the self-administration of the medicines. The major breakthrough occurred in 1982 when Eli Lilly & Company produced the first synthetic insulin, made by recombinant DNA modification of *E. coli*, under the brand name Humilin® [50]. Because it did not require the use of animal extracts, vastly more quantities of the protein could be produced. Once the ability to produce insulin by synthetic means became common practice, it opened up a world of opportunity for new types of insulin to be produced with small variations in the amino acid sequence. These insulin variations are known as insulin analogs.

2.2.2. Insulin Analogs

Insulin analogs are synthetically produced variations of insulin which have a different amino acid sequence than that of native human insulin. A diagram of the amino acid sequence of native human insulin is given in Figure 2.1. In all cases, insulin analogs vary from this structure. When delivered subcutaneously, normal insulin has an onset of action of 30-60 minutes, a peak at 2.5-5 hours, and a duration of effect of 5-8 hours [51]. This profile of action poorly matches that of endogenous insulin secretion. Similar to formulator insulin variations, insulin analogs change the timing and duration for the effect of insulin and they are separated accordingly.

2.2.2.1 Fast-Acting Insulin Analogs

Fast-acting insulin analogs were designed to give more freedom to the diabetic patient such that they could administer insulin near mealtime. The first insulin analog to become available to clinicians was insulin lispro [52]. In insulin lispro the two residues in the B-chain of insulin are substituted for one another, the lysine at position 29 and the proline at position 28. The change causes a reduced tendency of the analog to self-associate into dimers by 200-300 times [53]. Because insulin is only biologically active as a monomer, the hypoglycemic effect of insulin lispro is more rapid than that of native insulin which exhibits some self-associative behavior. Another fast-acting insulin analog is insulin aspart in which the B-chain of insulin is again modified. In insulin aspart the proline at position 28 is replaced with an aspartic acid residue [52, 54]. The effect is similar to that of insulin lispro in terms of reducing self-association of the protein. Both analogs induce hypoglycemic behavior more rapidly than normal human insulin when administered subcutaneously and are often used in clinical practice [52-54]. Insulin glulisine is a third fast-acting insulin analog and has only been available as a pharmaceutical drug since 2004 [55]. Insulin glulisine has substitutions in the B-chain where glutamate replaces lysine at the 29th position and lysine replaces asparagine at the 3rd position. This analog exhibits improved monomer stability, reduced self-association, and an increased rate of absorption while maintaining an unaltered affinity for the insulin receptor [56]. In improving both monomer stability and absorption rate, insulin glulisine appears to have the most rapid rate of onset and clearance with similar biological activity of these three fast-acting insulin analogs [57].

Another early insulin analog, and one that did not succeed, is insulin Asp(B10). This insulin analog replaced a histidine with an aspartic acid at the B10 residue of insulin. It exhibited twice the absorption rate of regular insulin making it valuable as a potential drug. However, the clinical failure was due to the modified tertiary structure of the protein, which affected its pharmacodynamic behavior [52]. It exhibited an increased affinity for the insulin receptor in cells, inducing increased mitogenic activity and a dose-dependent increase in the incidence of adenocarcinomas in laboratory animals [58].

2.2.2.2. Long-Acting Insulin Analogs

Long-acting insulin analogs were originally designed due to the need of diabetics to maintain a healthy blood glucose levels throughout the night. Regular human insulin has a duration of roughly four hours, so a diabetic patient using it had to interrupt their sleep in order to maintain normal glucose levels [49]. While the extended action of insulin formulations such as NPH and Lente® insulin improved the treatment of diabetes, their action did not mimic the natural secretion of basal insulin levels, and these formulations are now considered to be intermediate-acting insulin formulations. Only within the last 5 years have long-acting insulin analogs become available in the U.S. Aventis began selling insulin glargine in the United States in 2003 under the brand name Lantus® [48]. Insulin glargine varies from native human insulin by the replacement of an asparagine at position A21 with glycine and the addition of two arginine residues at the C-terminus of the B-chain [51]. These changes cause the isoelectric point to shift from 5.4 for native insulin to 6.7 for insulin glargine. The effect of this shift is that the solubility of insulin glargine is greatly reduced at neutral pH levels. The formulation of

Lantus® is mixed in a solution with a pH of approximately 4.0, under which conditions the insulin glargine is completely solubilized. Upon injection and a return to neutral pH levels, insulin glargine precipitates causing a subcutaneous insulin depot. The analog is then slowly released from this depot, giving insulin glargine its long-acting effect [51, 54]. Another long-acting insulin analog is insulin detemir, which was approved by the FDA for use in the United States in 2006 under the brand name Levemir® [59, 60]. Insulin detemir is altered from native insulin by the removal of the threonine B30 residue and attachment of a C14 fatty acid chain (myristic acid) onto the lysine B29 [59]. Insulin detemir has a protracted effect because it forms hexamers and reversibly binds to albumin, causing it to be slowly absorbed into the bloodstream from the site of injection [48, 60]. In a head-to-head comparison of these two long-acting insulin analogs, insulin glargine had a longer hypoglycemic effect than insulin detemir and the median time for the end of action was 24 hours for insulin glargine versus 17.5 hours for insulin detemir [61]. Nonetheless, both analogs have significantly better pharmacokinetic and pharmacodynamic effects than traditional long-acting insulin formulations such as NPH [51, 59].

2.2.2.3. Immunogenicity and Mitogenicity

When changing the molecular structure of insulin from its natural state, it is vital to consider the potential for alterations in the immune response to those changes. As described previously, one early insulin analog with modification at the aspartic acid at the B10 residue was intended to provide a fast-acting insulin effect, however the change also caused a significant increase in the mitogenicity of that analog [58]. In a study performed

by Kurtzhals et. al. [62] the binding of several insulin analogs to the insulin growth factor 1 (IGF-1) receptor and the insulin receptor was measured and correlated to the metabolic and mitogenic potential. When compared to regular insulin, insulin lispro, insulin aspart, and insulin glargine had minimal change in binding to the insulin receptor, whereas insulin detemir was significantly lower. Each of the analogs had similar or increased dissociation rates from the insulin receptor, which is correlated to a reduced mitogenic behavior [63]. Thus, these results are important to determine primarily the metabolic potential of the individual analogs. Another important consideration for insulin analogs is that increased binding to the IGF-1 receptor has been attributed to increased mitogenicity and growth of human mammary epithelial cells [64]. The binding to IGF-1 of the insulin aspart was similar to that of native human insulin. Insulin lispro and insulin glargine had 1.5 and 6.5 fold increases in binding affinity to the IGF-1 receptor, respectively, whereas insulin detemir was more than 5 times lower than regular insulin. While this result implies that insulin glargine would induce a significantly greater mitogenic response, when tested in cultured human skeletal muscle cells no additional mitogenic effects were seen with insulin glargine [65]. The impacts of these findings are unclear and the long term effects of insulin analogs will continue to be an important point for their use in the treatment of diabetes.

2.3. Biological Role of Insulin

Insulin is composed of two polypeptide chains and has a molecular weight of 5808 Da. The two chains are connected to one another by two disulfide bonds as seen in Figure 2.1. It is produced and secreted from the β -cells in the islets of Langerhans in the

pancreas. The primary role of insulin is to facilitate the transport of glucose from the bloodstream to cells in the body. This is only the simplified explanation of the biological role of insulin, though, and a more detailed description follows.

2.3.1. Insulin Production and Secretion

In a non-diabetic person, insulin is first synthesized in the β -cells of the pancreas as a 110 amino acid chain called preproinsulin [1]. This polypeptide includes every amino acid of regular insulin. Upon translocation through the endoplasmic reticulum, a 24-peptide sequence at the N-terminus of preproinsulin is cleaved and protein becomes proinsulin. The tertiary structure of proinsulin folds and forms the three disulfide bonds which are present in insulin [1]. Proinsulin is then converted to insulin upon secretion at which point four basic amino acids are individually removed and a 21 peptide sequence known as the connector peptide, or C-peptide, is cleaved and secreted along with insulin [1]. A small amount of proinsulin is also released, but primarily equimolar quantities of insulin and C-peptide are released into the bloodstream.

The secretion of insulin is a carefully regulated process which is meant to maintain healthy levels of blood glucose in the bloodstream during periods of both feeding and fasting. The principal mediator of insulin secretion is the plasma concentration of glucose. Insulin release is also promoted by gastrointestinal inhibitory peptide (GIP), glucagon-like peptide 1 (GLP-1), gastrin, secretin, cholecystokinin, vasoactive intestinal peptide, gastrin-releasing peptide, and enteroglucagon [47]. Glucose stimulates insulin secretion by depolarizing the β -cells of the pancreas. It enters the β -cells facilitated by the GLUT2 transporter. Because GLUT2 is a passive transporter, the

rate of glucose uptake into β -cells is directly dependent on its plasma concentration. The same transporter is responsible for glucose release from hepatocytes when glycogen is broken down in the liver [66]. The glucose is phosphorylated and the increase in ATP inhibits the ATP-sensitive K^+ channel. In response, the voltage sensitive Ca^{2+} ion channel is opened to repolarize the cells. The increased intracellular concentration of Ca^{2+} induces insulin secretion [47].

2.3.2. Effect of Insulin

Plasma insulin concentrations are often measured in biological units. One international unit (IU) of insulin is 6 nmol, equivalent to 34.8 μ g [67]. For healthy adults, insulin concentrations vary between 5-15 μ IU/ml (30-90 pmol/l) for basal levels and 60-90 μ IU/ml (360-540 pmol/l) for postprandial levels [34]. Circulating insulin binds to the insulin receptor, which is present in many tissues but primarily in liver, muscle, and adipose tissues. Signals from the insulin receptor initiate the translocation of intracellular vesicles rich with GLUT4 transporters which fuse with the plasma membrane of the cells and are exposed to the extracellular surface [47]. Similarly to the GLUT2 transporter, GLUT4 increases the diffusion of glucose into the cytosol of cells. Upon translocation, glucose can be used by the cells for energy via glycolysis or stored as glycogen or triglycerides [3]. In times of fasting, the breakdown of the glycogen and triglyceride stores maintains cell energy levels.

In addition to glucose transport, insulin has several other significant roles in metabolic homeostasis. It stimulates the uptake of amino acids and synthesis of proteins in muscle tissues, regulates gene transcription, increases glycogen and fatty acid

synthesis, and inhibits the breakdown of glycogen, fat, and protein for energy [47]. Another very important process influenced by insulin is the hepatic production and release of glucose. In times of fasting, when plasma insulin concentrations are low, the liver synthesizes glucose from its glycogen stores through glycogenolysis and from other non-sugar substrates such as pyruvate through gluconeogenesis [3]. When insulin levels increase after a meal, these processes are reversed. A diagram of these processes and their relation to insulin is shown in Figure 2.2. Increased levels of insulin in the hepatic portal vein, which carries blood from the digestive tract to the liver, effectively eliminate endogenous glucose production by the liver [68]. Insulin action in the liver has a rapid onset and corresponding rapid recovery. Diabetics, however, often exhibit an insulin resistance in the liver and do not stop producing glucose, even when circulating levels are above normal. This leads to the primary identifying feature of diabetes: a chronic and substantial elevation of the circulating blood glucose concentration [1].

2.3.2. Insulin Regulation

The half life of insulin in the bloodstream is relatively short with a $t_{1/2}$ of only 5-6 minutes [47]. Its degradation occurs primarily in liver, kidney, and muscle tissues [69]. Roughly 50 % of insulin which is released into the portal vein, the route of insulin secretion, is destroyed by the liver and never reaches general circulation. Insulin is also removed from the plasma through renal clearance. Some insulin degradation occurs in peripheral tissues following internalization into the cells, but this accounts for only a small amount of insulin elimination. The natural process of regulating insulin concentration is important because when injected subcutaneously, insulin first enters the

general circulation, thus having its initial effect on peripheral tissues. This does not mimic the natural process of insulin secretion and the biological effect is different. The implications of these changes are discussed below.

2.4. Insulin Therapy

There are several different treatments for diabetes, depending on the type and severity of the disease. Insulin therapy remains as the most rigorous and physiological treatment for diabetes and is the only option for patients suffering from Type 1 diabetes. Current insulin administration is parenteral, generally performed by subcutaneous injection or continuous subcutaneous insulin infusion (CSII). While insulin production and insulin analog technology have made parenteral delivery much more effective, this method of treatment has remained relatively unchanged since insulin was first used clinically in 1923 [70]. Several studies have been performed examining the effectiveness of current insulin therapy, the most important of which was the Diabetes Control and Complications Trial (DCCT), which is discussed in the following section [71-74]. For each study, the majority of patients exhibited improved but still non-physiological glycemic control. This is largely due to the subcutaneous pathway that insulin is delivered. When injected, insulin enters the circulatory system from the periphery and has the largest effect on muscle and adipose tissues. These tissues have a delayed onset to insulin and a sustained duration of action [75]. In healthy individuals, insulin produced by the β -cells in the pancreas is released into the portal circulation in response to the presence of glucose and its effect on peripheral tissues occurs after first pass hepatic

clearance [47]. Nonetheless, insulin therapy based on subcutaneous insulin delivery remains the primary means of treatment for diabetes.

Insulin therapy by multiple daily injections (MDI) attempts to mimic the natural production of insulin in response to blood glucose levels. Prior to insulin analogs, normal insulin or insulin formulations were used, but they poorly matched normal glucose control [76]. Since they have become available more recently, MDI now uses a combination of long and short acting insulin analogs. Short-acting analogs are taken immediately prior to meals and can more closely mimic the postprandial spikes in insulin concentration in response to increase blood glucose levels. Long-acting analogs are taken each morning to mimic the basal insulin release from the pancreas. As an alternative to intermittent dosing CSII can be used and is currently used by as many as 20% of Type 1 diabetics [76-80]. Similar to the MDI approach, CSII requires constant monitoring of blood glucose levels. It uses a pump to deliver insulin subcutaneously from a small solution reservoir to a small port, generally into the patient's abdomen. Because it can deliver insulin slowly or in a bolus, it more closely resembles the pharmacokinetics of natural insulin production. However, because the insulin is still delivered subcutaneously, the mode of action in the body is not physiological.

2.5. The Diabetes Control and Complications Trial

In 1993 a monumental clinical study was concluded based on data collected for 10 years on the effects and treatments of Type 1 diabetes [74]. The study was conducted by the National Institute of Diabetes and Digestive and Kidney Diseases (NIDDK) and incorporated findings from 1,441 volunteers from 29 medical centers in the U.S. and

Canada. At the time, the body of work collected from the 10-year study was the most comprehensive on diabetes performed to date and its findings drastically altered the clinical treatment of Type 1 diabetes. The DCCT generated several critical results based on the comparison between conventional insulin therapy consisting of one or two daily injections of regular insulin to intensive insulin therapy requiring smaller, more frequent injections, at least three per day, and frequent monitoring of glucose levels. These results indicated that significant reductions in retinopathy, nephropathy, and neuropathy in patients with Type 1 diabetes were observed in patients who used intensive insulin therapy versus that of conventional therapy [74, 76]. While the results were widely regarded as elementary to many people, the thorough and incontrovertible evidence of the study altered the mindset for physicians, educators, and insurance companies that by aggressively treating diabetes, the chronic long-term effects can be greatly reduced in addition to the acute effects.

2.6. Alternative Insulin Delivery Methods

In general, all peptide and protein drugs must be administered subcutaneously or intravenously. Since the discovery of insulin, many non-invasive methods of insulin delivery have been thoroughly investigated. However, to date, no feasible alternative modes of delivery have achieved enough success to replace subcutaneous administration. Current delivery by injection is taxing on the patient who must continuously monitor their blood glucose and self-administer insulin. Non-compliance to this dosing regimen is common. Also, because it is challenging, treatment with insulin is often seen as a last resort for Type 2 diabetics even though data suggests that early prescription is beneficial

[34]. The investigation of alternative routes for insulin delivery is driven by the desire to simplify the administration of insulin and potentially reduce the levels of non-compliance currently seen with insulin therapy. The greatest challenge for all approaches to oral insulin delivery is achieving a high bioavailability when compared with subcutaneous delivery. The following discussion reviews the different delivery routes considered for delivery and their benefits and drawbacks.

2.6.1. Pulmonary Delivery of Insulin

Pulmonary insulin has significant potential as an alternative route for insulin delivery. The rate of insulin absorption and onset, however, makes it only applicable to replace postprandial insulin requirements not basal insulin requirements. Nonetheless, the potential to replace all but a single basal insulin injection have made it very appealing to diabetic patients and studies have shown that many would prefer pulmonary insulin to injection [81, 82]. To date, it is the most successful alternative to subcutaneous injection for insulin is the pulmonary route, and in 2006, an inhaled dry powder insulin formulation from Nektar and Pfizer was approved by the FDA for the treatment of diabetes under the name Exubera® [82, 83].

The delivery of insulin to the lungs has several distinct advantages. The lungs have a large surface area (100-140 m²), have a relatively high permeability, and are highly vascular [84, 85]. Each of these factors contributes significantly to the rapid absorption of insulin from the lungs. Insulin can be absorbed efficiently without the addition of absorption enhancers or enzyme inhibitors, so side effects generally associated with such treatments are non-existent. For the greatest amount of absorption

into the bloodstream, inhaled insulin should reach the alveolar or deep lung areas. The optimal particle size is 1.5-2.5 μm ; larger particles are largely deposited in the upper lungs, while smaller particles are mostly exhaled [82, 84, 85]. The pharmacokinetics of this delivery system shows a more rapid onset of insulin action and more rapid clearance than that of subcutaneous injection of regular human insulin. With the addition of a small amount of chelating agent or absorption enhancer the rate of absorbance and onset is faster even than current short-acting insulin analogs, though toxicity is a concern [86]. When absorbed from the lungs, insulin enters the circulation bypassing the first-pass hepatic clearance, giving it a slightly longer pharmacodynamic profile than endogenous insulin [87].

The major drawbacks to pulmonary insulin delivery are that the bioavailability is still only 9-22 % that of subcutaneously injected insulin and that improper inhalation technique can cause large variations in administration, causing potentially dangerous administration levels [84]. Because of the lower bioavailability, large quantities of insulin are required when compared to injection, making inhalable insulin significantly more expensive. Due to these drawbacks, heavy criticism of current products for pulmonary insulin delivery has been experienced and new products are being developed. In fact, as of October 17, 2007, Pfizer announced that it will no longer produce or market Exubera because it failed to gain acceptance among patients and physicians [88]. Efforts still continue in the development of an improved type of inhalable insulin delivery system.

2.6.2. Transdermal Delivery of Insulin

Transdermal insulin delivery would allow similar insulin absorption as current subcutaneous delivery without the pain associated with injection. The major challenges are that the skin is relatively impermeable to large, hydrophilic molecules such as insulin due primarily to the intracellular lipid layer of the stratum corneum (SC) [85]. One approach to transdermal delivery is through the use of micro or nanoneedles. They can permeate the skin in the same fashion as a standard needle with very low levels of associated pain. The direct disruption of the SC greatly increases the permeability of insulin and has been reported to have negligible pain [89]. A significant hypoglycemic response has been seen in tests with diabetic hairless rats in which the microneedles were inserted to puncture the skin and then an insulin solution was applied at the site of treatment [90]. A second approach to transdermal delivery is iontophoresis which uses electrical charge to disrupt the SC and propel insulin into the skin. This technique generally required pretreatment of the delivery site and still only delivered very little insulin into the bloodstream [85, 91]. Low-frequency ultrasound, or sonophoresis, has also been explored as a method for transdermal insulin delivery. This technique uses sound waves to disrupt the SC thus increasing the permeability of insulin. In a study performed with pigs, a drop in blood glucose was evident; however it required 60 minutes of treatment, an unreasonably long time for a patient to try to use this method [92]. Photomechanical waves or laser-generated stress has also been investigated for transdermal insulin delivery [93]. A hypoglycemic response was exhibited in tests with diabetic rats, but similarly to sonophoretic approaches, it required a long time to dose. Each technique for transdermal insulin delivery has had only limited success. All

approaches require extended exposure to topical insulin solutions and the variability in dosing and occurrence of skin irritation make it unlikely that transdermal insulin delivery will become standard practice.

2.6.3. Nasal Delivery of Insulin

The delivery of insulin to the nasal cavity has been investigated due to its convenience, large absorptive surface, and high vascularity [94]. Drug absorption by the nasal mucosa is generally rapid and directly enters the systemic circulation, bypassing the first-pass hepatic clearance. However the low absorption of insulin, mucociliary clearance, and presence of proteolytic enzymes make this approach challenging [85, 94]. The major approaches to nasal delivery use permeation enhancers, mucoadhesive materials, enzyme inhibitors, or a combination of these methods. Permeation enhancers have a tendency to damage the nasal mucosa and may present a significant challenge for any long-term use of nasally delivered insulin. Nonetheless, studies in which insulin formulations were delivered along with didecanoly-L- α -phosphatidylcholine (DDPC), an absorption enhancer, had bioavailabilities of 8.3-13.2 % compared to intravenous injection [95]. The hypoglycemic effect in these studies had lower variability and faster onset than subcutaneous injection. Another popular approach to nasal insulin delivery is through the use of chitosan, a positively charged polysaccharide [96-98]. The study by Dyer et. al. used chitosan in solution, as a dry powder, and grafted to nanoparticles to deliver insulin. Each approach succeeded in producing a hypoglycemic effect *in vivo*, with the highest bioavailability of 17.0 % for insulin delivered with chitosan powder [98]. Enzyme inhibitors have also been investigated for nasal insulin delivery, though the

degree of absorption of insulin does not exceed that of other absorption enhancing methods [94]. Nasal insulin delivery has significant promise; but higher bioavailability levels are necessary for it to succeed in becoming a standard practice.

2.6.4. Other Delivery Routes for Insulin

Other routes of delivery for insulin that have been investigated are rectal, ocular, vaginal, buccal, and oral. A number of studies evaluating rectal insulin delivery systems have been performed due to the lack of enzymatic degradation. However, low absorption (4-10 %) persists and it does not seem to represent an acceptable alternative route [85]. Both ocular [99] and vaginal [100] insulin delivery similarly have achieved only limited absorption levels and severe local adverse reactions indicate that they offer little opportunity for insulin delivery [85, 101]. Buccal or sublingual delivery systems have generated a significant amount of attention due to the ease of administration, low proteolytic activity, and high vascularization [102-105]. The challenges include the thick, multilayered structure of the buccal and sublingual mucosa and the constant flow of saliva. A Canadian company specializing in buccal drug delivery, Genex, currently produces Oral-Lyn™ which delivers insulin via the buccal route [106]. The product is only intended for those who have pre-diabetes or Type 2 diabetes as an insulin therapy to slow the progression of the disease. For each of these routes investigated designs use nanoparticles, permeation enhancers, mucoadhesion, or a combination of these to overcome these barriers. Of the routes discussed in this section, oral insulin delivery has generated the largest body of research. A review of oral insulin will be discussed later in this chapter.

2.6.5. Artificial Pancreas

One other major area of research for insulin delivery is the development of an artificial pancreas. The premise behind the artificial pancreas is that it would be able to dose insulin to a patient in response to endogenous glucose levels. The first approach is to have an insulin pump connected to a real-time glucose monitoring system in a feedback control loop. The benefit of this design is that it can use pump technology currently being used for CSII therapy. Alternatively, implantable pumps have been investigated for future designs [107]. The largest challenge to this type of artificial pancreas is maintaining rapid, accurate, and consistent monitoring of the endogenous blood glucose levels which can provide continuous or near-continuous glucose determination [107, 108]. Most glucose monitors use optical or electrochemical changes induced by glucose in the presence of immobilized glucose oxidase as the means of detection [108-112]. Traditional implanted sensor designs require direct contact with whole blood using intravenous catheters. Newer monitoring techniques use interstitial fluid to detect glucose. These sensors generally require multiple daily calibrations using whole blood from finger prick samples due to potential changes in enzymatic activity in the sensor and build up of tissue from a foreign body response [107, 113]. An alternative glucose monitor uses the optical characteristics of a synthetic hydrogel receptor called phenylboronic acid [114]. The measurement of glucose is based on the swelling of the hydrogel material in response to glucose concentration which imparts a change in the modulation of light diffracted through the material. The benefit of this material is that the binding of glucose is completely reversible (as opposed to glucose oxidase which converts glucose to gluconic acid) and the sensitivity is generally maintained longer than

traditional glucose monitors. However, the measurements are highly sensitive to interstitial pH and the rate of change is rather slow compared to conventional glucose meters.

A second type of artificial pancreas is referred to as a bio-hybrid or bio-artificial pancreas. This design utilizes natural pancreatic β -cells which are encapsulated in some sort of semi-permeable membrane such that glucose and insulin can diffuse through it, but the cells are protected from immunological detection and destruction [115-117]. The premise is that following implantation the natural function of pancreatic β -cells has a more intricate action than what is currently modeled by artificial means. Direct transplantation of pancreatic tissue requires the use of immune suppressive drugs for the remaining lifetime of the individual. Immunoisolation of the cells would remove this treatment, the major drawback of current pancreas transplant methods. Bio-hybrid pancreas designs can be either intravascular or extravascular. Intravascular systems are grafted directly to a blood vessel similar to the way that natural tissues may be. However, decreased insulin secretion with time due to cell death and surgical risk of implantation and extrication are major drawbacks [117]. Extravascular systems avoid the risks of intravascular because they are implanted into tissue without direct access to the bloodstream. However, there is a delay in the response of the cells due to diffusive restrictions of glucose in the interstitial fluids. Also, over time the fibrous encapsulation of the implant further reduces the flux of glucose and pancreatic secretions into and out of the bio-hybrid pancreas [115, 117].

A third approach utilizes glucose-responsive biomaterials as the platform of the artificial pancreas. In most cases the biomaterial responds to glucose by biodegradation

[118], by swelling changes [119, 120], competitive binding of glucose for glycosylated insulin on concanavalin A [121, 122], or by sol-gel transition [123] such that insulin trapped in the material is released. These approaches are promising when performed *in vitro*, but their *in vivo* applications have had limited success. The designs are inherently limited for long-term use because they cannot be replenished. Only intermittent administration of a bioresorbable, glucose-responsive material could be applicable for this approach, though significant challenges still exist.

2.7. Oral Insulin Delivery and its Challenges

The growth of the development of protein and peptide drugs has increased significantly in recent years due to the ability to create them using recombinant techniques. In general these drugs require parenteral delivery, as is currently the case for insulin. Oral delivery is perhaps the most enticing alternative to parenteral delivery due to the general acceptance of orally administered drugs. However, oral delivery arguably represents the most challenging route of insulin delivery and it continues to be the “holy grail” of insulin therapy. These challenges are due primarily to proteolytic degradation and limited absorption of insulin in the gastrointestinal tract. Overcoming each of these enzymatic and physical barriers has been investigated using a multitude of approaches. The following sections will discuss the pathway, potential benefits, challenges, and approaches related to the oral delivery of insulin.

2.7.1. Physiology of the Gastrointestinal Tract

In order to design an approach to orally delivered insulin, the physiology of the gastrointestinal (GI) tract should be well understood. A drawing of the entire human GI tract can be seen in Figure 2.3. Sequentially, the GI tract includes the mouth, esophagus, stomach, duodenum, jejunum, ileum, colon, rectum, and anus. It exists primarily to transport water and nutrients into the body. Most nutrients required for human are present as solid material composed of macromolecules, which makes them nearly impermeable across cell membranes. Therefore, the function of the GI tract is to physically and chemically break down food in a process generically referred to as digestion [124]. The absorption of digested material from the GI tract varies widely and is dependent on the physiochemical characteristics of the material. The rate of nutrient absorption can vary greatly depending on whether it is hydrophobic or hydrophilic, or if it has a specific mechanism for facilitated or active transport into the bloodstream [125]. The efficiency of nutrient absorption is quite high and there is significant excess capacity of surface area and enzymatic activity in the GI tract. This was crucial for the survival of humans in ancient times when food may not have been plentiful. However, in modern times, especially in developed nations, this efficient nutrient absorption may contribute significantly to high rates of obesity [125]. The GI tract also serves an important role for excretion from the body. This is important not only for non-absorbable foods, but also for materials which cannot exit the body through alternative means. The critical characteristic of the GI tract is the defensive structure of the tissues. The GI tract exists as a single tube with an inner (apical) surface that is in continuity with the outside of the body, making it a potential pathway for toxic or invading molecules, viruses, or bacteria

can enter the body [126]. For drug delivery, this easy access to the GI tract is exploited to administer therapeutic molecules. However, the physiology of the GI tract has several layers of resistance to uncontrolled absorption that persist throughout its entirety such as: polarized epithelial cells joined by tight junctions, a mucosal boundary layer, and the largest concentration of lymphocytes in the body.

The epithelial cells in the GI tract, collectively referred to as the epithelium, form a single cell thick membrane which represents the first layer encountered by an ingested material. It is at this layer that the where the distinction is made for absorption or rejection of nutrients. The epithelial cells are polarized, distinguishing between the apical and basolateral (blood-side) membranes. The surface area of the epithelium is greatly increased by the structure of these cells as seen in Figure 2.4. They are folded into many finger-like projections of the tissue called villi [125]. The villi are approximately 0.6-1.0 mm in length, 0.2-0.4 mm wide, and spaced approximately 15-40 μm apart [127]. This makes the surface of the GI tract appear to be rough and folded. On a smaller scale, the apical surface of these individual epithelial cells is covered with projections of the cell membrane called microvilli which are approximately 1-2 μm long, 50-100 nm wide, and spaced 18-24 nm apart [124, 128].

Beneath the epithelium, on the basolateral side, is the basement membrane which lies atop the lamina propria and muscularis mucosa. The lamina propria contains the majority of the nerve endings and blood vessels and the muscularis mucosa controls villi movement. These layers, along with the epithelium, make up what is referred to as the mucosa [124, 125]. Beneath the mucosa is a grouping of nervous tissue meant to carry information to and from the GI tract called the submucosa. Beneath the submucosa

are several layers of muscle tissue oriented either around or along the GI tract which is meant to either squeeze the diameter of the GI tube or propel its contents along, depending on the muscular orientation.

Movement of the GI is controlled by the enteric nervous system based on the signals generated by chemoreceptors and mechanoreceptors and is not voluntarily controlled [126]. There are several different types of digestive tube movements present in the GI tract. Peristalsis is the forward propulsion of luminal contents by a controlled wave of muscle contractions [124, 126]. Segmentation is a type of tube movement in which a simultaneous contraction of non-adjacent areas of the digestive tube occurs. This generally happens exclusively in the small intestines and the purpose is to mix the chyme with digestive enzymes as it is moved back and forth [124]. Mass peristalsis is the simultaneous contraction of several adjacent segments of the intestine and is usually associated with bowel movements. All motor movements of the contents of the GI tract are lubricated by a large amount of mucus and saliva. Glandular secretion of saliva produces between 1 and 1.5 liters each day [126]. Further down the GI tract, mucosal secretions cover the epithelium. The composition of the secretions changes from the stomach to the small intestines and the large intestines, but in all cases it is composed of a mixture of water, glycoproteins, and digestive enzymes. This mucus serves several purposes: it lubricates the lining of the GI tract, prevents the majority of diffusion of macromolecules to the surface of the epithelium prior to digestion, provides a concentrated digestive surface near sites of absorption, and provides a concentrated boundary layer for the transport of signals to and from the epithelium [126].

2.7.1.1. Absorption in the Gastrointestinal Tract

For many years research on the transport of proteins and peptides from the GI tract was focused exclusively on short peptide chains of one, two, or three amino acids. More recently, however, whole proteins have been found to enter intestinal epithelial cells. Absorption of proteins and peptides across the epithelial layer of the GI tract can take place through several different pathways as seen in Figure 2.5: paracellular transport, active transport, receptor-mediated endocytosis, diffusive transport, and pinocytosis [129]. Paracellular transport is the movement of a drug or solute between adjacent cells to cross the epithelial membrane. Passive transcellular transport is the movement of a drug or solute through a cell or cell membrane from the apical to basolateral side, or vice versa. Receptor-mediated transport is a process through which a ligand is internalized from the extracellular fluids by endocytosis following its binding to a receptor on the cell surface [130]. Pinocytosis is a type of non-specific endocytosis in which extracellular fluids and incorporated solutes are internalized by pinching off a section of the plasma membrane [131, 132]. The resulting endosome then fuses with lysosomes and the contents are degraded by intracellular enzymes. Pinocytosis is non-specific in that it not initiated by a ligand from the extracellular fluids. It represents a very small amount of protein absorption in intestinal epithelial cells and will not be discussed in detail [129].

Paracellular transport of proteins between epithelial cells occurs most often when the intercellular connection between the two cells is disrupted. The strong connection between epithelial cells is stabilized by a number of different types of bonds as is seen in Figure 2.6. Tight junctions (TJ), or zona occludens, are the closest intercellular bond to the apical surface of epithelial cells and are the first barrier to

paracellular transport. They are also the least permeable membrane for paracellular transport of proteins because they generally exclude all solutes with a molecular radius greater than 11-15 Å [133, 134]. Tight junctions are formed by several transmembrane proteins which connect intercellularly to one another between cells in the extracellular space. Their intracellular domains bind to the actin filaments which constitute the cell cytoskeleton. The transmembrane proteins present in TJs are occludin, claudin, and junctional adhesion molecule (JAM) [135, 136]. The concentration of highly hydrophobic residues in the extracellular regions of these bonds suggests that hydrophobic interactions stabilize the tight junctions [137]. Intracellular proteins associated with TJs are Zona Occludens (ZO) 1, 2, and 3, which are part of the family of proteins referred to as the Membrane Associated Guanine Kinases (MAGUK). The ZO proteins bind to the transmembrane proteins through the interaction of a PDZ binding motif which is present on both proteins [138]. Both ZO-2 and ZO-3 form dimers with ZO-1, but not with each other. The ZO-1 and ZO-2 proteins are the F-actin binding proteins which allow them to connect the intercellular bonds formed by transmembrane proteins with the actin-based cytoskeleton of the epithelial cells [138, 139]. Paracellular transport through the TJ is the primary pathway for the absorption of hydrophilic proteins from the GI tract which have very low absorption and lack active transport mechanisms, such as insulin. In recent years, modulation of the TJs has been investigated with some success as will be discussed later.

Other intercellular bonds exist between epithelial cells which can inhibit paracellular transport. Adherens junctions (AJ), located just beneath the TJs, form intercellular bonds in a circumferential pattern around epithelial cells [137, 138]. Their

function is not as clear as that of TJs because the cell membranes are 15-20 nm apart at AJs, compared to only 1.1-1.5 nm at TJs. They likely contribute to strengthening TJs and may serve a regulatory function for coordinating multicellular processes [138]. Desmosomes represent another form of intercellular bonds in epithelial cells. They are located medially on the intercellular surfaces between adjacent epithelial cells and their purpose is to strengthen the physical connection between adjacent cells providing mechanical strength to tissues [140]. They do so without preventing the passage of solutes through the extracellular space between epithelial cells. Desmosomes are formed by the desmosome filament complex, which forms a fibrous connection of desmosomal adhesion molecules connected to the cytoskeletal filaments of the cells. One other connection between cells in the epithelium is gap junctions. They are small, reinforced openings connecting the cytosol of adjacent cells which provide a portal to electrical current, ions, and small molecules [141]. They are primarily used for signaling and are neither a barrier to paracellular transport nor a source of significant physical strength between epithelial cells. Adherins junctions, desmosomes, and gap junctions are all important to the function and maintenance of the epithelial cell layer, but because the most restricting feature for protein transport is the tight junctions, paracellular drug delivery research generally focuses on tight junctions and their temporary modification.

Active transport is a mechanism of transepithelial transport coupled to an exergonic process such as the movement of ions or breakdown of ATP. In the epithelial cells of the intestine actively transport molecules include amino acids, oligopeptides, bile acids, water-soluble vitamins, monocarboxylic acids, phosphate, and carbohydrates [142]. Each of these materials exists as part of the lumen of the intestine due to the

digestion of food or from exocrine releases of the pancreas, liver, or endothelium. The transporters have potential to provide a pathway for peptide and protein absorption across the epithelial wall of the intestine [143-148]. One oligopeptide transporter in particular, PepT1, has been thoroughly investigated and due to its broad substrate specificity and high level of expression in the small intestine. It has been utilized to increase the intestinal absorption of peptide-mimetic molecules such as β -lactam antibiotics, angiotensin converting enzyme inhibitors, the antiviral drug valacyclovir, and the anticancer drug bestatin [149]. Transporters for bile acids are also of great interest because they are the largest molecules which are actively transported from the GI tract and represent transport capacities of as high as 10-20 g/day with > 95 % absorption efficiency [133, 150-153]. While results of conjugated drug transfer across epithelial cells using either PepT1 or bile acid transporters is promising, most of the work has been performed with very short peptide chains only. Transport of large peptides and proteins through these channels will most likely not be possible.

Receptor-mediated endocytosis is an active transport mechanism in which a ligand initiates the endocytosis of the ligand-receptor complex along with a small amount of extracellular fluids [66]. The endocytotic vesicle is generally much smaller than that of pinocytotic vesicles, but protein uptake by receptor-mediated endocytosis occurs much more frequently and represents roughly 100-1000 times that of non-specific pinocytosis [154]. The internalized vesicle, also referred to as an endosome, follows a number of different pathways depending on the signal cascade initiated by the active receptor [155]. The endosome can fuse with intracellular lysosomes and be degraded by enzymes. Alternatively, the ligand can be disassociated from its receptor in the endosome such that

the receptor returns to the cell surface and the ligand is not degraded but incorporated by the cell. A third outcome is that the ligand is unidirectionally transported across the epithelial cell through a process called transcytosis. This is of particular interest for the purposes of protein delivery by oral delivery because it has the potential to actively transport large molecules across the epithelium of the intestine in tact and specifically release it into the bloodstream. Only a few receptor-mediated transcellular transport mechanisms have been identified [155]. Immunoglobulins in the neonatal intestine actively transport maternal antibodies through this method. More applicable for drug delivery are vitamin B₁₂, transferrin, dietary lectins, viruses, various bacteria, and certain toxins which enter epithelial cells via receptor-mediated endocytosis. In the case of viruses, bacteria, and toxins, the end result of internalization is infection and apoptosis of the cell. Vitamin B₁₂, transferrin, and dietary lectins, however, all are absorbed by the epithelium to be utilized by the body. Macromolecular and even nanoparticle drug delivery via receptor-mediated endocytosis is a promising route for oral protein delivery and significant research efforts have been made to investigate its potential [155-158].

Another means of absorption in the GI tract is via diffusive transport. There are two theoretical pathways of diffusive transport across epithelial cells: paracellular and transcellular. Diffusive paracellular transport is the movement of a molecule along the lipid bilayer of the cell membrane. In order to follow this path, the diffusing solute must be highly lipophilic and roughly 4 Å in size, so this is generally not considered a reasonable pathway for proteins [129]. Transcellular diffusive transport is the movement of a molecule through and across the cell membrane. The factors that influence transcellular diffusive transport are molecule size and lipophilicity. It generally occurs

when a highly hydrophobic regions of a protein or attached fatty acid chain is inserted into the cell membrane. Macromolecular proteins such as insulin, however, are generally too large to easily diffuse across cell membranes and this route of absorption has a low efficiency.

2.7.1.2. Pathway for Orally Delivered Proteins

The pathway for ingested food and the physiological response of the GI tract is well understood and characterized. After food is chewed and swallowed, it enters the stomach from the esophagus through one of two sphincters on either side of the stomach. The lower esophageal sphincter is at the union of the esophagus and the stomach. It is this muscle that keeps acidic stomach contents from flowing backward into the esophagus; the failure of it to do so is what leads to acid reflux. Once in the stomach, orally administered food or drugs are mixed and churned with gastric fluids until gastric emptying.

Gastric emptying occurs in a controlled fashion according to signals received by the stomach. Under normal circumstances, the stomach empties about 200 kcal/h into the small intestines, although this can vary significantly [125]. Therefore, the stomach can serve the function of a mixer or homogenizer as well as a reservoir for yet to be digested foods. The emptying of the stomach is controlled by the pyloric sphincter, or pylorus [159]. This is a muscle which surrounds the opening from the stomach to the duodenum. When the stomach is filled with a meal, the muscle is contracted, restricting the flow of particles greater than 1-2 mm in size to the duodenum [125]. The residence time of an orally delivered meal depends directly on the amount and type of food detected by the

stomach. A larger meal of solid food requires significantly longer than a liquid or highly hydrated foods. The signals for gastric emptying are believed to be related to the 5-hydroxytryptamine (5-HT) receptors where 5-HT₁ receptors reduce it and 5-HT₃ receptors induce it [160]. There are some drugs and chemicals which affect gastric emptying. Nitric oxide has been reported to induce gastric emptying while certain opioids reduce it [125]. Synthetic drugs can also induce gastric emptying and are sometimes utilized when GI motility is reduced such as occurs in gastroparesis [161]. The transfer of chyme from the stomach to the intestine is critical for GI function because the majority of absorption of nutrients and water occurs in the small intestine.

The small intestine is referred as such due to its relatively smaller diameter when compared to the large intestine. In reality, however, the small intestine has a much larger surface area due to its length (~20 ft.) compared to the large intestine (~4.5 ft.) and the high concentration of folds in the tissue [128]. It also plays a much larger role in nutrient absorption than the large intestine [125]. The small intestine is separated into three sections: duodenum, jejunum, and ileum, descending from the stomach to the large intestine. The duodenum is the most proximal region of the small intestine and also the shortest at roughly 12 inches long. The remainder of the small intestine is composed of the jejunum (~8 ft.) and ileum (~12 ft.) [128]. Because the small intestine represents the majority of absorption of the GI tract, it is critical for orally administered drugs. It is also the location of the majority of potential active and receptor-mediated transport pathways for oral protein delivery. The ileum contains a unique concentration of lymphatic tissues concentrated into groups called Peyer's patches. Lymphocytes lie directly beneath a follicle-associated epithelium (FAE) that is different than the majority of the epithelial

membrane in the small intestine. The FAE contains a high amount of M-cells which express only minimal mucosal covering, limited microvilli, and increased luminal absorption by pinocytosis [162-164]. These cells offer unique absorption pathways for oral vaccine delivery as well as proteins which can exist in the lymphatic system. Because of the vast array and high level of absorption mechanisms, most research investigating the oral delivery of proteins focuses on improving the absorption of therapeutic proteins in the small intestine.

The large intestine, also referred to as the colon, is the final length of the GI tract prior to excretion. Its general purpose is to serve as a storage area for waste material and absorption of excess water [125]. Several drug delivery techniques target colonic uptake of proteins because of the significant reduction in proteolytic enzymes or to treat local diseases such as irritable bowel syndrome, Crohn's disease, colorectal cancer, amebiasis, and ulcerative colitis [165-168]. Other benefits of colonic protein delivery are the increased response of the epithelium to absorption enhancers, increased lymphoid tissue for delivery of antibodies to the immune system, and sustained residence time for absorption. The colon is inhabited by 400-500 types of bacterial microflora which have a total live population of 10^{14} organisms compared to 10^{13} eukaryotic cells in the human body [168]. The digestive behavior of these bacteria contributes to the metabolism and absorption of carbohydrates and proteins. One of the primary digestion products in the large intestines are short chain fatty acids, which are readily absorbed by transporters in the large intestine. Other peptide and amino acid transporters are also present in the large intestine such as the PepT1 transporter.

2.7.2. Rationale for Oral Insulin Delivery

Oral insulin delivery would provide an easy and convenient method of delivery and likely improve patient compliance, a large issue for current parenteral delivery [85]. With an easy administration method, doctors and patients would likely be more inclined to start insulin therapy before the disease becomes advanced or use it for Type 2 diabetics who often resist starting intensive insulin therapy [37]. Detractors cite low bioavailability, potentially high cost and high protein requirement, potential side effects, and poor reproducibility as significant difficulties which make oral insulin delivery unlikely for the future [169]. So what are the potential benefits for oral insulin delivery which justify its continued and growing research?

When nutrients are absorbed from the gastrointestinal tract, primarily in the small intestines, they immediately enter the portal circulation and undergo first-hepatic pass metabolism [126]. For many drugs, bypassing first-pass metabolism is desired to reduce the clearance of the drug from the bloodstream. For insulin, however, this delivery route would mimic the physiological pathway of endogenous insulin produced from the pancreas [68]. In the postprandial state, the interaction of insulin and glucose with the liver is the most critical for maintaining euglycemic levels [170]. First of all, in a healthy individual, the majority of ingested glucose is taken up by splanchnic tissue (the liver) [68]. In order to do so, insulin must be bound to the surface receptors in the liver. Following oral delivery, the first potential site for insulin action is in the liver. Second, the presence of insulin at these receptors is critical to initiate glycogenesis and glycolysis, and inhibit gluconeogenesis and glycogenolysis. Each of these processes are important steps in maintaining healthy circulating glucose concentrations. A schematic of the action

of insulin on glucose can be seen in Figure 2.2. Third, the sensitivity of the liver is much greater than that of muscle tissues and it responds very quickly to the presence of insulin [68]. Thus, a more rapid hypoglycemic effect is seen from insulin in the portal vein than from insulin delivered parenterally reducing the risk of postprandial hyperglycemia. Fourth, the residence time of insulin on insulin receptors in the liver is significantly less than that of muscle and adipose tissues [171]. This reduces the risk of sustained hypoglycemia induced by extended hyperinsulinemic reactivity in peripheral tissues. Finally, one of the most common problem among Type 2 diabetics is insulin resistance in the liver [172]. These patients require high insulin levels ($\sim 100 \mu\text{U/ml}$) in the portal circulation to affect hepatic glucose production [173]. Insulin concentrations at this level can be safely utilized by the liver, but if circulating plasma insulin concentrations were that high in the general circulation, as would be the case for subcutaneously delivered insulin, a severe hypoglycemic episode would occur. Therefore, orally administered insulin has the potential to treat both Type 1 and Type 2 diabetics in a pharmacokinetic route similar to that of native endogenous insulin production.

2.7.3. Enzymatic Barrier

For oral delivery of traditional small molecule pharmaceuticals, the largest concern is digestion in the stomach and bond cleavage due to very low pH. For macromolecules, the presence of lipases and peptidases represent serious challenges in maintaining the integrity of the molecular structure. Proteins delivered orally are digested into smaller peptides or individual amino acids prior to their absorption primarily by pepsin in the stomach and pancreatic enzymes such as trypsin, α -chymotrypsin, and

elastase in the small intestine [174]. In the stomach, the primary materials secreted by the stomach are mucus, hydrochloric acid (HCl), intrinsic factor, pepsinogen, and a group of regulatory peptides which stimulate gastric secretion upon the ingestion of food [125, 126, 175]. The mixture of food and secretions is referred to as chyme. The most important of these gastric secretions to orally delivered drugs are HCl and pepsinogen, which is enzymatically converted to pepsin in the presence of HCl. The low pH of the stomach can induce the hydrolytic breakdown of several different ingested species. Additionally pepsin, which is most active at low pH levels and deactivated at $\text{pH} > 5$, can cleave the amino bond of phenylalanine, tryptophane, and tyrosine amino acid residues [66]. Further digestion of food and drugs takes place further down the GI tract as described in the following section.

2.7.3.1. Lumenal Enzymes from Pancreatic and Hepatic Secretion

Pancreatic and hepatic secretions into the lumen of the intestine are critical for natural digestion. Understanding their role in metabolism is critical to design an oral delivery method for insulin. While endocrine secretions of the pancreas are important for controlling circulating insulin and glucose levels, exocrine pancreatic secretions into the GI tract are critical for normal digestive function. This secretion into the duodenum imparts an array of changes on the chyme of the small intestine. The most important of these secreted substances for digestion are the pancreatic proteases including: trypsin, α -chymotrypsin, elastase, carboxypeptidase A, and carboxypeptidase B [174]. Also generated and release from the pancreas are amylolytic enzymes, lipases, nucleases, and secretory modulating species [125].

The release of pancreatic and hepatic secretions into the duodenum is controlled by the hepatopancreatic sphincter. The stimulus for the opening and closing of the port is dependent on a hormone called cholecystokinin, or CCK [124, 126]. Cholecystokinin is synthesized and stored in the endocrine cells in the duodenum. It triggers contracting the gall bladder, relaxing of the hepatopancreatic sphincter, and slow gastric motility and emptying, thus giving duodenal enzymes more time to digest the chyme before sending it lower in the intestine [125]. The release of CCK is modulated according to competitive binding of the CCK-releasing peptide (CCK-RP) which is normally present in the lumen of the duodenum. In the absence of food, trypsin digests CCK-RP rapidly and it cannot initiate CCK release. When food is present, however, CCK-RP is not digested as rapidly, it triggers CCK release which in turn initiates exocrine hepatic and pancreatic secretion into the duodenum.

Pancreatic enzymes represent a very large challenge to any macromolecular drug entering the duodenum in the chyme from the stomach. Without some way of resisting degradation, the digestion of proteins, starches, or nucleotides is likely to take place to a large degree due to these enzymes. One other important chemical which is released by pancreatic secretion is bicarbonate ion. Ductular cells line the ducts of the pancreas which concentrate its exocrine products. When they are stimulated they also transport bicarbonate ions into the pancreatic juice as it passes along the ducts, making it highly alkaline. When combined with the acidic chyme exiting the stomach upon secretion, it has a neutralizing effect which occurs over a very short length of the GI tract [125]. The neutralization of the chyme is critical because the activity of the five major

pancreatic peptidases is optimal at pH ~ 7 [174]. This rapid pH change can also be exploited for potential routes of oral protein delivery.

Concomitant to the release of pancreatic material is the bile produced from the liver. Bile is a lipid rich solution produced by the liver which facilitates the elimination of hydrophobic substrates from the body as well as promoting the absorption of long-chain fatty acids and fat soluble vitamins [125]. It consists of micelles formed from the combination of bile salts with phosphatidylcholine. The two main hepatic ducts transport bile the liver to the gall bladder which serves as a reservoir until it can be secreted [124]. The common bile duct then connects the gall bladder to the pancreatic duct at the outlet to the duodenum at the hepatopancreatic sphincter. The effect of bile on peptide and protein drug delivery is primarily for the absorption of lipophilic materials such as lipids and lipoproteins. Their presence is important for the delivery of hydrophobic proteins and peptide drugs but is not applicable to insulin. Transport mechanisms of bile salts can also be utilized for protein drug delivery.

2.7.3.2. The Brush-Border Membrane and Intracellular Enzymes

The second important groups of enzymes that are part of the enzymatic barrier to oral insulin delivery are those which are located along the absorptive pathway of orally delivered drugs. These enzymes are located in three sub-cellular locations in epithelial cells: the brush-border, the cytoplasm, and the lysosomes [176]. The primary degradation of proteins in sub-cellular regions of epithelial cells occurs on their apical surface by brush-border enzymes. The brush-border is the surface of composed of the microvilli of epithelial cells covered with the mucous/glycocalyx layer which consists of mucous,

glycoproteins, and enzymes. In all pathways for protein absorption following oral administration the drug must pass through the brush-border region of the epithelium. Brush-border enzymes include amino-exopeptidases, carboxy-exopeptidases, and endopeptidases which cleave bonds and the N-terminus, C-terminus, and at particular internal sites of amino acid chains, respectively [174, 176]. They range in specificity, but in concert they have the potential to degrade whole proteins to short peptide sequences. They tend to be anchored to the cell membrane by a hydrophobic anchor with a large extracellular hydrophilic component responsible for the enzymatic activity of the protein [176]. Not all orally delivered proteins are equally susceptible to hydrolysis by brush-border enzymes, however. Insulin, for instance, exhibits very limited degradation after 24 hours of exposure to brush-border enzymes [177]. The presence of proline in the amino acid sequence may be critical to the digestion of proteins by brush-border enzymes in the intestines. Several dietary proteins contain large amounts of proline and their efficient degradation is important for healthy GI function [176].

Cytoplasmic enzymes tend to be ubiquitous in nature and are intended to hydrolyze di- and tripeptides which are absorbed by surface transporters [178]. These enzymes are not active toward large peptide molecules and do not present a significant source of protein degradation. Lysosomal proteases mostly consist of cathepsins, exo- and endopeptidases which can degrade proteins upon their incorporation into the lysosome [179].

2.7.4. Physical Barrier

The second major challenge to oral insulin delivery is the physical barrier of the intestinal epithelium. A thick mucous/glycocalyx layer covers the luminal side of the intestines which serves several functions to GI function. Water can account for up to 95 % of the weight of this layer with the remainder being composed of glycoproteins, proteoglycans, glycolipids, and inorganic salts [180, 181]. The mucous and glycocalyx layers have thicknesses of 5-10 and 0.1-0.5 μm , respectively. One function is to protect the apical epithelial surface from microbial and foreign materials. The mucous/glycocalyx layer also lubricates the lumen of the intestine to facilitate the movement of chyme. For protein drug delivery, the most important feature of the mucous/glycocalyx layers is the reduced access to the surface of epithelial cells. The diffusion rate of large molecules greater than approximately 5000 Da is severely reduced by the mucous and glycocalyx [133]. Larger molecules may not be effectively degraded by brush-border enzymes and this layer keeps the majority of them in the lumen where they can be degraded by pancreatic peptidases. On the other hand, the mucous layer on epithelial cells can also be exploited for drug delivery as will be discussed later. Another important feature of the physical barrier is the impermeability of the epithelial layer to protein transport. The reason for this feature is defensive in nature to exclude other macromolecular species such as bacteria and viruses which may enter the GI tract. The structure of the epithelial layer is discussed previously in this chapter. Overcoming the physical barrier is an important factor for oral insulin delivery.

2.8. Approaches for Oral Insulin Delivery

Researchers have investigated a plethora of methods in attempts to deliver insulin orally. Generally the techniques attempt to address one or both the enzymatic barrier and the physical barrier of the GI tract. Common approaches to overcome the enzymatic barrier include enzyme inhibitors [174, 182, 183], prodrug strategies [133, 184, 185], and protein encapsulation [186-188]. Approaches for overcoming the physical barrier include carrier-mediated uptake [144, 189-191], receptor-mediated transcytosis [132, 142, 192], and permeation enhancement [134, 137, 193]. Often times, efforts to modify the absorption of the protein drugs through enzymatic or physical modification are coupled with polymeric delivery vehicles which improve the targeting of these techniques. Each approach has various degrees of success; however none have been able to create high levels of bioactivity to make oral protein delivery a reality. The following is a brief review of methods and results achieved in attempts to deliver insulin and other proteins orally.

2.8.1. Enzyme Inhibitors

Inhibiting the action of enzymes greatly reduces the loss of proteins in the gastric and intestinal environments. There are two main considerations for enzyme inhibition. First, the multitude of enzymes in the lumen, brush-border, and intracellular environments make a single approach difficult. Second, by altering the proteolytic activity of the GI tract, natural digestive processes are modified which may induce significant side effects. The enzymatic barrier for the oral absorption of individual proteins varies from one to another because certain enzymes may or may not readily

degrade them. The enzymes of the GI tract are well characterized, so a systematic evaluation of the degradation of each therapeutic protein can be performed *in vitro* and *in vivo* [183]. Discovery of the individual enzymatic barrier for a single protein allows for the use of specialized protein inhibitors which are intended to only disrupt the activity of particular enzymes. Examples of enzyme inhibitors include pepsinostreptin, aprotinin, chymastatin, elastatinal, EDTA, chitosan-EDTA, soybean or basic pancreatic trypsin inhibitor, amastatin, puromycin, bestatin, phosphinic acid dipeptide analogues, and enterostatin [133, 183, 194, 195]. Often enzyme inhibitors are co-administered or maintained in close proximity to the protein to be delivered. In a study performed by Plate et. al., a delivery system including pancreatic and soybean trypsin inhibitor immobilized into polymers was able to maintain high insulin retention levels in the presence of trypsin, α -chymotrypsin, and elastase [196]. Another approach utilized citric acid and aminopeptidase inhibitor as protease inhibitors release concomitantly with a model peptide drug [174]. A similar design used aprotinin as the enzyme inhibitor [194]. Other approaches to use enzyme inhibitors do so by covalently attaching them to the protein thus using a combination of enzyme inhibition and prodrug strategies to address the enzyme barrier [197-199].

2.8.2. Permeation Enhancers

With the exception of proteins that are transported across the epithelial cell membrane by active or receptor-mediated transport, hydrophilic proteins generally must be absorbed through paracellular pathways. Several small peptide drugs are believed to be absorbed by this route including octreotide, vasopressin analogue desmopressin, and

thyrotropin releasing hormone [200]. Most proteins, however, are too large and too hydrophilic to be readily absorbed through the TJ of epithelial cells. Paracellular transport can be increased in the intestine through the use of permeation or absorption enhancing materials. Generally, these chemicals disrupt the TJ of the epithelial cell layer which constitutes the largest barrier to passive paracellular drug absorption [193]. Three primary mechanisms have been identified to increase transport through the TJ of epithelial layers: membrane perturbation by interaction with membrane lipids or proteins, decreasing the non-protein thiol content in the membrane, and complexation of extracellular Ca^{2+} ions which facilitate TJ formation [133]. A wide variety of intestinal absorption enhancers have been investigated including bile salts, dimethyl- β -cyclodextrin, chitosan, hydrochloride, sodium lauryl sulfate, nafamostat, bacitracin, capric acid, taurodeoxycholic acid, glycyrrhizic acid, and zona occludens toxin [138, 195, 201-204].

Often the paracellular absorption enhancers are used in addition to enzyme inhibitors. Two studies by Takeyama et. al. and Komada et. al. demonstrated that enzymatic insulin degradation was inhibited by the absorption enhancer nafamostat [205, 206]. Radwan et. al. demonstrated a similar result with glycyrrhizic acid [204]. A variation of permeation enhancers involves covalent attachment of the therapeutic molecule to the delivery agent through prodrug strategies. Clement et. al. demonstrated that the covalent attachment of a 7-9 unit length of polyethylene glycol and a hydrophilic hexyl alkyl chain to the lysine B29 residue of insulin to form hexyl insulin monoconjugate-2 (HIM2) increased the enzymatic resistance of insulin as well as increasing its permeation across a modeled intestinal epithelium using Caco-2 cells [207].

When disrupting the TJ of intestinal epithelial cells care must be taken to only cause minimal and reversible loss of the TJ for increased drug transport as extended opening greatly increases the potential for paracellular transport of other large species such as viruses, bacteria, mycoplasma, and E-Coli [138, 208]. Several disease states are directly or partially induced by loss of TJ integrity such as Crohn's disease, ankylosing spondylitis, Type 1 diabetes, and certain types of cancer [208]. Therefore, increased paracellular transport via tight junction modulation offers potential for increased protein uptake from the GI tract, but problems may be encountered in chronic diseases which require long-term and frequent dosing.

2.8.3. Prodrug Systems

Prodrugs are pharmacological substances which are modified from their normal form such that they have a different molecular structure which alters the biological action of the substance [133, 209]. Insulin analogs are sometimes referred to as insulin prodrugs. Prodrugs can also involve the covalent conjugation of a chemical species to the drug which directly alters its absorption, distribution, metabolism, and excretion (ADME) behavior [210]. Prodrugs have been investigated for use with both traditional and protein and peptide drugs for many parenteral and non-parenteral delivery methods [133, 211-216]. Specifically for oral delivery of insulin, prodrug strategies generally attempt to address one or both the enzymatic and physical barriers of the intestinal epithelium. Prodrugs differ from traditional enzyme inhibitors and permeation enhancers because their action is immediately concentrated in close proximity to the therapeutic protein due to covalent modification. In some cases this modification is reversible such that upon

exposure to luminal, brush-border, or intracellular enzymes the prodrug is reduced to the native form of the substance. Other protein prodrugs maintain the integrity of the covalent modification even in the presence of enzymes. Common approaches involving prodrugs for oral delivery include modifying the N-terminus or C-terminus of proteins such that they can't be degraded by amino- or carboxypeptidases, conjugating actively transported compounds, reducing immunogenicity of the protein, or reducing hepatic and renal clearance. Two research groups have used prodrug strategies on the platelet fibrinogen receptor antagonist (GP IIb/IIIa) such that its absorption increased up to 20 times that of the parent peptide [211, 217]. Prodrugs utilizing single amino acid modifications have exhibited increased intestinal permeability for L- α -methyldopa and bisphosphonates [216]. Sinha et. al. utilize a prodrug strategy to target drug delivery to the colon [168]. By conjugation with bonds which are specifically cleaved by the microflora of the large intestine, release of the biologically active substrate could be exclusively targeted to the colon. Not all investigated prodrug strategies have succeeded, however. Work by Kondo et. al. indicated that while the oral absorption of an ester-type prodrug GP IIb/IIIa was increased in mice, the efflux was also increased negating the increased absorption rates [214].

Another type of protein prodrug involves the conjugation of polyethylene glycol (PEG). The conjugation of PEG, also known as PEGylation, has been shown to reduce enzymatic degradation, increase circulation time, and increase the solubility of therapeutic protein and peptide drugs [218-222]. PEGylation has been studied with many drugs such as: adenosine deamidase, bovine liver catalase, uricase, collagen, human growth hormone, nerve growth factor, trypsin, and insulin [223]. PEG is highly

biocompatible, has been found to be nontoxic, and is approved by the U.S. FDA for use in drugs, foods, and cosmetics [224]. It is a readily available polymer species and can be made in many different forms including single chains, branched chains, dendrimers and star polymers. The molecular weights are easily controlled to various lengths from only three or four repeat units to molecular weights well over 1 million Da. Further, the chemistry of the end groups for PEG is easily modified to make it reactive toward any one of a number of species. Because of these benefits, PEGylated proteins have garnered significant interest in recent research. In fact, several PEGylated proteins have been commercialized including granulocyte colony stimulating factor, alpha interferon 2b and 2a, and human growth hormone [225].

2.8.4. Active Transport and Receptor-Mediated Endocytosis

Facilitated absorption by active transport and receptor-mediated endocytotic pathways are other promising techniques for oral protein delivery. As discussed above, transmembrane transporters are primarily utilized for peptide or peptidometric drugs which low molecular weights (<1000 Da). Large proteins generally cannot be absorbed using these transporters. Therefore, absorption by receptor-mediated endocytosis is more often investigated to increase the absorption of perorally administered proteins [184, 226, 227]. This mechanism usually requires conjugation of the ligand to the protein either directly or using a spacer to ensure endocytosis of the therapeutic substance. Many endocytosed materials, however, directly shuttle the endosome to digestive lysosomes for hydrolysis of the ligand and/or receptor [132]. Some ligands exist which specifically induce the unidirectional transcytosis of endocytosed material from apical to basolateral

membranes of intestinal epithelial cells. The two which have been most investigated are transferrin and cobalamin (Vitamin B₁₂).

Transferrin (Tf) is an iron transporting glycoprotein with a molecular weight of ~82 kDa which is expressed primarily in the mucosa of the GI tract. It is relatively stable in the GI environment and digestion of the protein by α -chymotrypsin does not affect the biological action of the protein with its receptor [156]. It has a high binding affinity for iron which induces the binding of Tf with the transferrin receptor (TfR) on epithelial cells [155, 156]. The Tf-TfR complex is then internalized by endocytosis of a clathrin coated pit formed by the concentration of activated TfR receptors [66]. The endosome then is transcytosed to the basolateral side of the epithelial cell at which point the ligand is released along with iron into the bloodstream. Several groups have investigated the potential for oral delivery of Tf-conjugated insulin to the bloodstream [156, 192, 228, 229]. Each study exhibited increased transport of insulin across *in vitro* models of the intestinal epithelium using Caco-2 cells. Xia et. al. [228] and Lim et. al. [156] also showed a hypoglycemic effect of Tf-insulin conjugated insulin following oral administration to streptozotocin-induced diabetic rats.

Another receptor-mediated material investigated for oral insulin delivery is cobalamin, or vitamin B₁₂ (VB₁₂). It is a naturally occurring vitamin normally bound to food in the regular human diet. The process of VB₁₂ absorption in the intestine is well established [175, 230-233]. Upon digestion by gastric enzymes, VB₁₂ is released from food and is bound to haptocorrin (HC), a naturally secreted protein present in the saliva [234]. After passing the bile duct in the duodenum, HC bound to VB₁₂ is degraded in the intestinal lumen by trypsin and α -chymotrypsin. Free VB₁₂ is then bound to intrinsic

factor (IF), a glycoprotein weighing ~ 45 kDa which is secreted in the stomach [232, 235]. The binding of IF to VB_{12} is blocked in the stomach by HC, but IF has a much higher binding affinity for VB_{12} than degraded HC and replaces it in the duodenum by competitive binding. The IF- VB_{12} travels down to the intestinal tract with minimal loss where it can be actively endocytosed after binding to the intrinsic factor receptor (IFR). The distribution of IFR varies along the small intestine with the majority residing in the lower jejunum and ileum [230, 233]. Once inside the epithelial cell, the IF- VB_{12} complex is broken down by an unknown method and VB_{12} is exocytosed bound to transcobalamin II (TC II), a basolateral exocrine receptor of epithelial cells [236]. Typically, the endosome formed during endocytosis is about 200 nm in diameter [155]. Such a large space could easily accommodate the ligand as well as any drug complex that may be attached to it.

Russell-Jones et. al. have shown that it is possible to covalently attach VB_{12} to several different peptides and hormones [155, 237]. In doing so, they were able to significantly increase the transport of covalently attached erythropoietin and granulocyte-colony stimulating factor across the intestinal epithelium of rats. One major limitation of utilizing VB_{12} as a vehicle for oral protein delivery is the natural saturability of the transport mechanism. Generally, the amount of VB_{12} in the human diet exceeds the biological need 4-fold [175]. Prodrugs of VB_{12} -conjugates and the IF- VB_{12} -conjugate exhibit a reduced binding affinity for IF and IFR, respectively [236]. Competitive binding of this material would greatly reduce the amount of VB_{12} prodrugs which would be absorbed without significant changes in diet. Also, only about 1 mg of VB_{12} is absorbed

daily, so potency of the drug is critical. Nonetheless, exploiting this pathway for oral protein delivery is a promising alternative to parenteral delivery.

2.8.5. Lipid Based Delivery Systems

Another commonly investigated system to overcome the barriers to oral protein delivery is lipid based delivery systems. These designs use lipids, bile salts, cholesterol, or a combination thereof to encapsulate a protein in one of several 3-dimensional configurations. By separating the orally delivered protein from the surrounding environment by a lipid layer, the enzymatic degradation is greatly reduced. The design of lipid based systems attempt to utilize the natural tendency of the amphiphilic molecules to coalesce in an organized manner. The most common designs investigated are micelles and liposomes (a.k.a. vesicles). These two approaches are easily distinguished from one another based on the organization of the lipids as seen in Figure 2.7. This organization is based on the hydrophobic/hydrophilic interaction of the molecules in aqueous environments. Micelles are spherical collections of lipids in which the hydrophilic head of the lipid forms the exterior shell of the sphere and the internal phase consists of the hydrophobic chains [66]. This system is a unilamellar design because there is only a single layer of lipids required to stabilize the structure. Liposomes are bilamellar spherical organizations of lipids in which a lipid bilayer forms around an aqueous core [130]. The structure of the shell of a liposome is similar to that of the lipid bilayer of cell membranes. In oral protein delivery, the most important distinction between the two designs is the contents of the center of the sphere. The center of a micelle is highly hydrophobic in nature whereas the center of a liposome is aqueous, thus each design can

only be used for the corresponding type of protein drug. Micelles are typically used for the delivery of hydrophobic drugs, but since most protein and peptide drugs are hydrophilic, they are infrequently used.

Liposomal delivery of proteins to the GI tract has been investigated by a number of research groups due to their aqueous core and similarity to the cell membrane [238-240]. Several critical findings were similar throughout these studies. The primary method of absorption was found to be pinocytosis in the Peyer's patches primarily located in the ileum. The Peyer's patches have high concentrations of absorptive M-cells. Absorption in M-cells has been reported to increase with increasing hydrophobicity [241], making liposomes ideal candidates. As the size of the liposomes increased, their absorption efficiencies and the bioavailability of the model drug both decreased. Therefore, the smallest possible size liposome would be desired. However, because liposomes are bilamellar, they are difficult to make and stabilize in sizes as small as that of micelles. Two major obstacles to oral protein delivery using liposomes are their instability in the GI tract and their tendency to leak their contents due to the transient nature of the lipid bilayer [129]. The instability of liposomes is due to several factors. First, their structure is only maintained to a great deal in dilute aqueous environments. When concentrated, liposomes have a tendency to aggregate and in the process may become too large to be absorbed in the Peyer's patches. Second, the outer lipid bilayer may be disrupted by the presence of bile salts and lipases present in the GI tract [242]. Even if only briefly compromised the stability of the liposome can easily be lost. A 26 % loss of insulin incorporated in a model liposome was exhibited when it was stored at 4 °C for 3 days [243]. This leakiness would make accurate dosing difficult because protein

content would be unknown even after only 3 days. Nonetheless, liposomes continue to be actively investigated [244] due to their high level of absorption from Peyer's patches. Much work is also being done in a liposome-mimetic polymer particle as will be discussed below.

2.9. Polymeric Systems for Oral Insulin Delivery

Over the last 30 years, a very large body of work has been generated investigating the potential of polymeric delivery systems for oral protein delivery. These polymeric systems attempt to address the challenges of the GI tract through various methods. All techniques protect the protein from proteolytic enzymes in the GI tract and/or facilitate the uptake of the protein. There are a number of delivery designs using polymers including micro- and nanoparticles, biodegradable systems, bioadhesive systems, and hydrogels. Each of these designs has the common feature of entrapping or encapsulating the protein. The most-significant benefits to using polymers for oral protein delivery are their customizability, low cost, and high availability. Because the amount of research for all designs and proteins is so large, the discussion of polymeric oral protein delivery systems in this work will focus on insulin.

2.9.1. Micro- and Nanoparticles

Polymeric particles to encapsulate insulin have been designed on both the micrometer and nanometer scale. The structures of these particles vary significantly based on the incorporation mechanism used. They can be broadly separated into two groups: micro- or nanocapsules and micro- or nanospheres. Capsules utilize a body-and-

shell design in which the drug is contained within the center of a particle which is surrounded by a polymeric shell. Spheres do not have this feature and the distribution of the polymers and drug can be dispersed throughout the particle. A diagram of the common designs of polymeric capsules and spheres is shown in Figure 2.8. The polymeric particle design is a good method in addressing a few barriers to oral protein delivery. First, by physically separating the protein from the chyme of the GI tract, luminal enzymes cannot attack the protein until it is released from the particle. Second, the transport of a single micro- or nanoparticle to the bloodstream represents the transport of many individual protein molecules.

The most common design for micro- or nanocapsules has similar structural designs as liposomes utilizing hydrophilic-hydrophobic-hydrophilic tri-block copolymers to associate into the bilamellar structure. Xiong et. al used a more complicated design utilizing a block copolymer with polylactic acid (PLA), polyethylene oxide (PEO), and polypropylene (PPO) in a PLA-PEO-PPO-PEO-PLA configuration to make polymeric vesicles of 30-100 nm [245]. The reason for the complexity of the block copolymer is that the center PEO-PPO-PEO tri-block copolymer is a commercial ready, FDA approved polymer sold under the brand name Pluronic®. The stability of these nanoparticles is greater than that of liposomes and the size of the particles can be controlled based on the molecular weight of the PLA hydrophilic blocks [245]. The PLA groups slowly degrade by hydrolytic degradation allowing for timed release of the drug release following oral dosing [246]. The polymeric vesicles were loaded with insulin by forming them in an insulin solution. The indirect method of loading was only able to incorporate 0.08 wt% of available insulin into the nanoparticles [247]. When these nanoparticles were delivered to

diabetic mice a hypoglycemic was exhibited for 24 hours indicating that insulin could be protected from enzymatic attack and still be absorbed as the biologically active protein [247]. However, the dosing levels in this study were at least 100-fold greater than that of subcutaneous injection of insulin, so the bioavailability of the protein remained very low. Another polymeric particle design was used by Furtado et. al. to make insulin containing microcapsules from a block copolymer of fumaric anhydride (FA) and sebacic anhydride (SA) [248]. They used a phase inversion technique which is used for the entrapment of a hydrophilic drug within a hydrophobic polymer shell [249]. A solution of insulin was added in a 1:100 volume ratio to a solution of 20:80 p(FA:SA) in petroleum ether while stirring. The spontaneous separation of the insulin-containing aqueous phase occurred and was stabilized by the p(FA:SA). The microparticles formed by this technique were quite stable and exhibited insulin release for at least 12 days [250]. The oral dosing of these particles, however, resulted in only minimal hypoglycemic effect in rats and dogs even at dosing levels of 250 IU/kg. This low bioavailability is most likely due to the slow rate of insulin release, the non-specific rate of release, and the large size of the particles expected to be transported across the intestinal epithelium.

Polymeric particles as micro- or nanospheres can have two different constructions as seen in Figure 2.8. The most common particle synthesis method investigated utilizes a double emulsion technique. This technique, also referred to as a water-in-oil-in-water or W/O/W, first encapsulates protein in an aqueous solution within a non-aqueous solvent containing an emulsifier. The combination generally agitated such that the emulsion generates individual particles of nanometer dimensions. This first emulsion is then added to an aqueous phase containing a second emulsifier, often

polyvinyl alcohol (PVA). The non-aqueous solvent then evaporates at the water/air interface. After separating the particles from the emulsion solution, the particles consist of a solid hydrophobic polymer particle which contains one or more pockets of drug containing emulsions. Many W/O/W particles use hydrophobic polymers which degrade slowly for extended release *in vivo*. The W/O/W technique was used by Damgé et. al. for the oral delivery of insulin using poly(ϵ -caprolactone) (PCL) as the hydrophobic block and poly(methacrylic acid) (PMMA) as the hydrophilic block [186]. The second emulsion was stabilized by PVA. The oral delivery of these particles to diabetic rats caused a sustained hypoglycemic effect for 8 hours. Again in these particles the dosing was quite high (50 or 100 IU/kg) for orally dosed rats indicating that the transport of insulin from the GI tract to the bloodstream was inefficient. A second polymeric sphere design utilizes spray drying techniques to create a drug containing particle. Briefly, an aqueous drug solution is dispersed in a non-aqueous polymer solution. The mixture is heated and nebulized in a spray such that both solvents rapidly evaporate leaving only the drug and polymer. This approach rarely creates particles of less than 5 μm , though, so it is rarely used in oral insulin delivery research [187].

Each of the two designs for micro- or nanoparticles described above is useful in protecting proteins from luminal enzymes. However, the number of particles which reach the bloodstream is low because of the inefficient, non-specific means of transport from the GI tract. To address this issue, a nanoparticle design which has vitamin B₁₂ (VB₁₂) conjugated to its surface has been investigated [251]. The absorption of the nanoparticle was mediated by the transcytosis of VB₁₂ from the GI tract. By utilizing a nanoparticle design many insulin molecules can be transferred to the bloodstream for each VB₁₂

ligand-receptor transport. The in vivo results for these particles caused a hypoglycemic effect in diabetic rats at doses of 10 and 20 IU/kg, the lowest doses of the nanoparticle designs discussed, and bioavailability as high as 29.4 % compared to subcutaneous injection [252]. This design seems promising, however the processing of the particles and insulin loading is an incredibly cumbersome process and would be very difficult to scale up to commercial scale.

The additional challenge of overcoming the physical barrier for absorption has not been adequately researched with polymer particles to give a thorough discussion on approaches. Many polymeric micro- or nanoparticle research contends that the uptake of the particles from the GI tract via pinocytosis is sufficient for drug transport. The dosing levels, however, had to be at least 100-fold greater than that of subcutaneous dosing. The approach using VB₁₂ is restricted by the very small amount of VB₁₂ normally absorbed from the GI tract, competitive binding of the receptors with native VB₁₂, and difficult processing of the particles. For these reasons, investigators have spent much more time researching other polymeric materials for oral protein delivery.

2.9.2. Biodegradable Systems

Polymeric materials have been developed and investigated for oral protein delivery which has unique properties of degradation when exposed to the GI tract. The earliest designs of biodegradable polymers were based on degradation of the polymer bonds based on the amount of time it was exposed to particular environments. An example of a time-based biodegradable polymer is a copolymer of poly(lactic acid) (PLA) with poly(glycolic acid) (PGA) [253-257]. Both polymers are hydrophobic and

can be used to make micro- or nanoparticles using methods described previously. More importantly, however, is the fact that the polymer bonds of each polymer are cleaved by hydrolysis. The bonds for PGA are degraded more quickly than that of PLA. The use of a copolymer allows for customization of the rate of degradation. These particles have been investigated somewhat for oral protein delivery systems, but the degradation times are generally quite long and unless the particle is absorbed in its entirety, much of the orally delivered dose would be passed before the drug is released.

Other types of investigated biodegradable polymers for oral protein delivery are polysaccharides. Some of the most common polysaccharides researched are dextran and chitosan because they are well characterized, easily customizable, plentiful, and highly biocompatible. Dextran is a polysaccharide derived from glucose and chitosan is commercially produced from chitin, a material found in the exoskeleton of shellfish. The degradation of the particles is based on the natural digestion of polysaccharides by the GI tract. Sarmiento et. al. used dextran sulfate with chitosan to make biodegradable nanoparticles for oral insulin delivery [258]. These particles exhibited the ability to maintain high insulin content through the stomach and release it in the small intestine in the presence of amylolytic enzymes [258]. A hypoglycemic response was seen following oral dosing of 50 or 100 IU/kg to diabetic rats from particles loaded with just over 2 wt% insulin. Similar to other designs, the dosing levels were quite high, though significant bioavailability was observed (5.6 %) due to the extended action of the hypoglycemic effect versus subcutaneous injection [259].

Another biodegradable polymer investigated for oral protein delivery is Eudragit® [260]. This material is made from poly(methacrylic acid) and can be used to

encapsulate many different materials. Its applicability for oral protein delivery lies in the fact that poly(methacrylic acid) is a weak acid with a pKa of ~ 4.8 [261]. When exposed to pH environments below this pH, the polymer is hydrophobic and insoluble in chyme. When in environments above this pH, the polymer is hydrophilic and soluble due to loss of hydrogen on the carboxylic acid side group. This pH dependent solubility can be utilized with Eudragit for oral protein delivery because of the large shift in pH that occurs in the duodenum. A Eudragit coated particle or pill will be impermeable to water and luminal enzymes in the gastric environment. Upon exposure to the near neutral environment of the small intestine it dissolves and releases its contents. Several research groups have used Eudragit as a coating for protein delivery designs to ensure that they do not release their contents in the stomach [201, 260, 262]. This approach is good because it can ensure that gastric and early pancreatic enzymes do not degrade the orally delivered protein, but the transport of the protein across the intestinal epithelium is not increased when using Eudragit alone.

2.9.3. Mucoadhesive Delivery Systems

Another technique being investigated for enhanced transepithelial transport of proteins is the use of mucoadhesive polymers [263-265]. These materials preferentially bind to the mucus layer covering the epithelial cells. This is beneficial for oral protein delivery because it brings the protein within close proximity to the epithelial layer that it needs to cross in order to be absorbed into the bloodstream. Mucoadhesive polymers should also increase the residence time of the delivery system in the GI tract. If the protein is protected from enzymatic degradation, this could improve the percentage of

drug which reaches the bloodstream by reducing loss from fecal elimination. There are several theories of mucoadhesion which are used to describe the interaction [181]. Electronic theory suggests that the cause of binding is electron transfer between adhering surfaces causing the formation of an electrical double layer at their interface. Wetting theory states that the strength of a mucoadhesive bond is related to the surface energies of the two interacting surfaces. Absorption theory attributes mucoadhesion to van der Waal's forces. Diffusion theory describes the interdiffusion of polymer chains with the glycoproteins in mucus layers. Mechanical theory attributes mucoadhesion to the surface tension of the water and its penetration into irregularities in the surface of the binding material. Fracture theory relates the adhesive strength to the forces required to separate the two surfaces. This theory is different because it assumes fracture at the interface, when in fact the loss of mucoadhesion is generally due to loss of the cohesion of the mucus.

The most commonly investigated mucoadhesive polymers include chitosan, poly(acrylic acid), poly(methacrylic acid), sodium alginate, and cellulose derivatives [181]. Several studies have used only mucoadhesion to promote the absorption of proteins [263, 264, 266]. One approach by Whitehead et. al. utilized unidirectional release from mucoadhesive patches to significantly improve the bioavailability of insulin when placed *in situ* in the intestine of rats [263]. Other approaches use mucoadhesive polymers in concert with other materials investigated for oral protein delivery to improve the absorption of the protein. Combination of protease inhibitors with mucoadhesive polymers can address parts of both the enzymatic and physical barriers [196]. Alternatively, some mucoadhesive polymers can provide enzyme inhibition and/or

permeation enhancement through indirect modulation of the immediate surroundings [267]. The long-term effects of mucoadhesive materials are not yet determined. Concerns over potential buildup in the GI tract or toxicity must be addressed in future work with these materials.

2.10. Hydrogels for Oral Protein Delivery

Hydrogels are defined as water-swollen, crosslinked polymer structure produced by the reaction of one or more monomers [268]. In comparison to other synthetic biomaterials, they are widely considered to most closely resemble living tissue because of their high water content and soft texture [269]. Their consistency can range from nearly liquid materials that can flow through syringes to rubbery material with the stiffness of tissues such as cartilage and tendons. Their crosslinks can be stabilized by physical, covalent, ionic, hydrogen bonds, or ligand-receptor bonds. Because of their unique properties, their potential use is wide reaching for biomedical and drug delivery applications [269-273].

The use of hydrogel systems for drug delivery has been investigated for over 40 years. They can be classified based on the nature of the polymer or side chain, the nature of the crosslinking, the physical structure of the network, natural or synthetic sources, and being composed of one or more monomers. The wide variety of materials which can be used to make hydrogels adds to their potential use for numerous applications. They can absorb up to thousands of times their dry weight in water and the swelling of these materials is a critical feature in their applicability for delivery of hydrophilic proteins [272]. When a hydrogel imbibes water, it can also incorporate solutes in that water, such

as proteins, into the polymeric network of the gel. In doing so, the hydrogel can be used as a delivery vehicle for these loaded proteins. Understanding the movement of water and soluble drugs into and out of hydrogels is based largely on their swelling characteristics.

The swelling behavior of a hydrogel is mostly defined by the chemical nature of the polymer. As a hydrogel becomes more swollen there is an increased transport of water and drug through the polymer network [274]. A simplified picture of a hydrogel can be seen in Figure 2.9. The important parameters for hydrogel swelling are based on the density of the crosslinks and the polymer chain length in between those crosslinks. This length can be expressed as the average molecular weight between crosslinks, \overline{M}_c , or as the network correlation length or mesh size, ξ . The determination of each of these parameters is dependent on the swelling, polymerization, ionization, and number and type of crosslinks within the hydrogel. An explanation for one type of hydrogel is described in Chapter 4 and a very good review of hydrogel theory can be found in the reference by Brannon-Peppas [268].

The swelling of some hydrogels is dependent not only on the intrinsic nature of the polymer, but on that of the surroundings also. Environmentally responsive hydrogels exhibit changes in swelling characteristics based on the conditions of the surroundings. They can be dependent on temperature, light, pH, ionic strength, pressure, electric current, or the presence of particular species such as glucose [275]. Of particular interest to oral protein delivery are pH-sensitive hydrogels. In a similar fashion as that of Eudragit, pH sensitive hydrogels can restrict release of encapsulated protein in the stomach due to the low pH levels and allow its release in the neutral environment of the small and large intestines. Several different pH responsive hydrogels have been

investigated for oral protein delivery [269, 275-277]. In addition to environmentally responsive swelling characteristics, hydrogels can also be formulated to be mucoadhesive, permeation enhancers, or enzyme inhibitors [272].

2.11. Poly(methacrylic acid-g-ethylene glycol)

A copolymer of poly(methacrylic acid) (PMAA) and poly(ethylene glycol) (PEG) has generated much of the research on oral protein delivery using pH responsive hydrogels, in particular for insulin delivery. In studies of uncrosslinked PMAA and PEG chains in solution, the two polymers were observed to complex to one another in acidic media while in neutral media the complexation did not occur [278]. The interpolymer association was deemed to be due to the hydrogen bonding between the protonated carboxylic acid group of PMAA and the ether groups in PEG. The weak acid PMAA polymer has a pKa of ~ 4.8 . In solutions at pH levels below the pKa, PMAA is protonated and can form these hydrogen bonds. In solutions at pH levels above the pKa, PMAA becomes deprotonated and negatively charged. The hydrogen bonds formed between PMAA and PEG are then lost. This bond formation behavior is depicted in Figure 2.10. These results were later confirmed by Osada and Sato who also found that the complexation was disrupted in the presence of methanol and ethanol [279]. Hydrogels consisting of the two polymers have been made using PMAA as the backbone with PEG grafts polymerized into the PMAA backbone. This has been done by utilizing pre-made PEG chains with one terminal methacrylate group which can react with the propagating PMAA chain. The polymers are covalently crosslinked to form an insoluble polymer matrix by introducing short PEG chains with methacrylate groups at each end. In doing

so, hydrogels of P(MAA-g-EG) can be highly swollen in the presence of water, but never dissociate such that the polymers are completely dissolved.

This material forms a copolymer network with water-filled nanopores which exhibits reversible, pH-dependent swelling behavior [271, 280-286]. The swelling occurs in a similar fashion as that seen for the two non-crosslinked polymers in solution. At low pH levels ($\text{pH} < 4$) the network complexes due to hydrogen bonds between the PMAA backbone and the pendant PEG ether groups. This complexation causes both macroscopic and microscopic changes to the hydrogel. At low pH levels the network collapses, making the hydrogel shrink and become stiffer. The polymer mesh size is reduced when P(MAA-g-EG) hydrogels are in the complexed state because of the hydrogen bonds which form temporary crosslinks in addition to the covalent crosslinks. In this complexed state, the hydrogel is unable to imbibe much fluid and solute transport through the network is severely limited [281, 286]. Upon exposure to more neutral environments ($\text{pH} > 6$), the PMAA backbone becomes deprotonated and the hydrogen bonds between PMAA and PEG are lost. Additionally, the PMAA groups become negatively charged causing the hydrogel to swell due to ionic repulsion.

The use of P(MAA-g-EG) hydrogel for oral insulin delivery has shown significant promise *in vitro* and *in vivo* [282, 285, 287-292]. A high loading efficiency with insulin has been observed for P(MAA-g-EG) [293, 294]. Further, when highly complexed, P(MAA-g-EG) has exhibited high retention of insulin in low pH solutions [294]. The high loading efficiency and retention was most pronounced when the ratio of MAA:EG monomer groups was 1:1. In this ratio the complexation of the hydrogel was most pronounced [281, 286]. Another important factor for P(MAA-g-EG) is that the

transition between swelling states occurs over a pH range that is relevant for oral drug delivery, between the pH of the stomach (pH ~ 1-2) and the small intestine and colon (pH ~ 6.4-7.2) [125]. In the acidic environment of the stomach the network collapses, trapping insulin. In the neutral environment of the lower intestine (pH ~ 6.4-7.2) the network swells, allowing insulin release. *In vitro* studies with the hydrogel have shown its ability to protect insulin from enzymatic degradation in a simulated gastric environment [292]. When exposed to an intestinal environment, the swelling of the hydrogel allows insulin release [284-286, 292]. This behavior allows insulin to be released in areas of the small intestine where enzymatic activity is significantly lower. Additionally, when the hydrogel is in the intestinal environment, it has exhibited the ability to reduce enzymatic activity of several intestinal enzymes due in large part to steric hindrance of local enzymes and reduction of extracellular calcium ion, which is necessary for luminal peptidases [284]. By reducing the degradation of insulin in both the complexed and uncomplexed state, the enzymatic barrier to oral insulin delivery is greatly lessened by P(MAA-g-EG). The hydrogel has also exhibited mucoadhesive characteristics [264, 287, 295] which provides localized release of insulin at the apical membrane of the intestinal epithelium. Another key feature of P(MAA-g-EG) for oral insulin delivery is its binding of extracellular calcium ions by the hydrogel. This can temporarily and reversibly disrupt the tight junctions of the intestinal enterocyte, promoting the absorption of insulin across the epithelial layer [286]. Thus, P(MAA-g-EG) can address both the enzymatic and the physical barriers to oral insulin delivery.

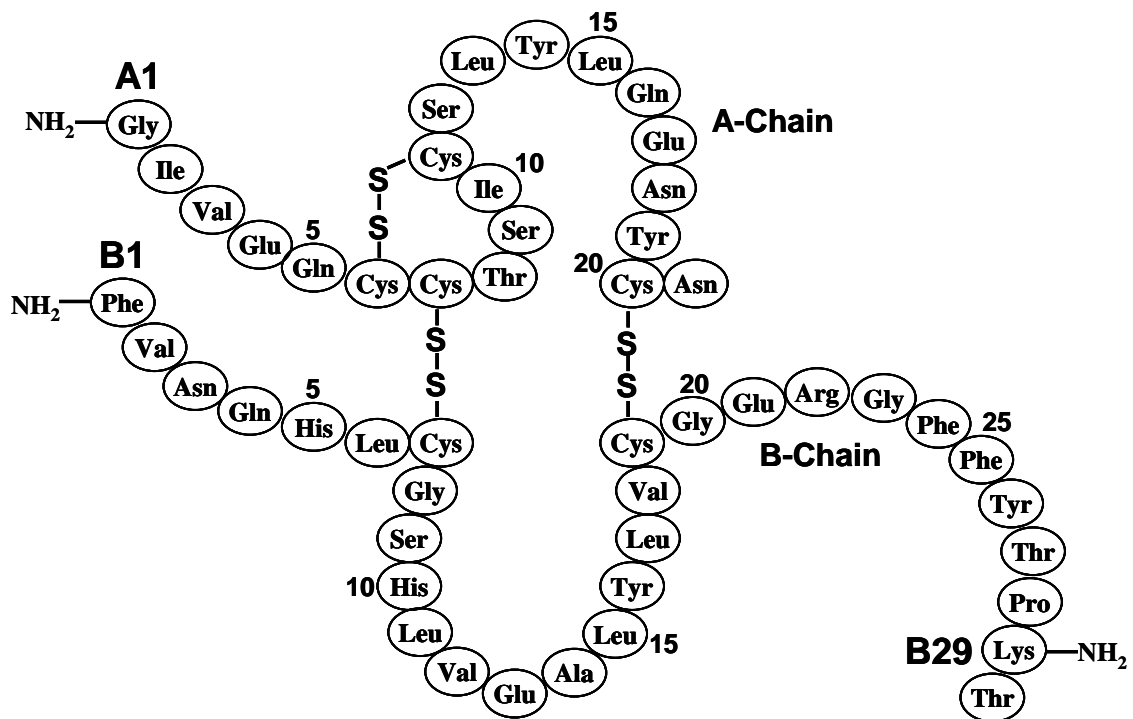


Figure 2.1. The amino acid sequence of native human insulin

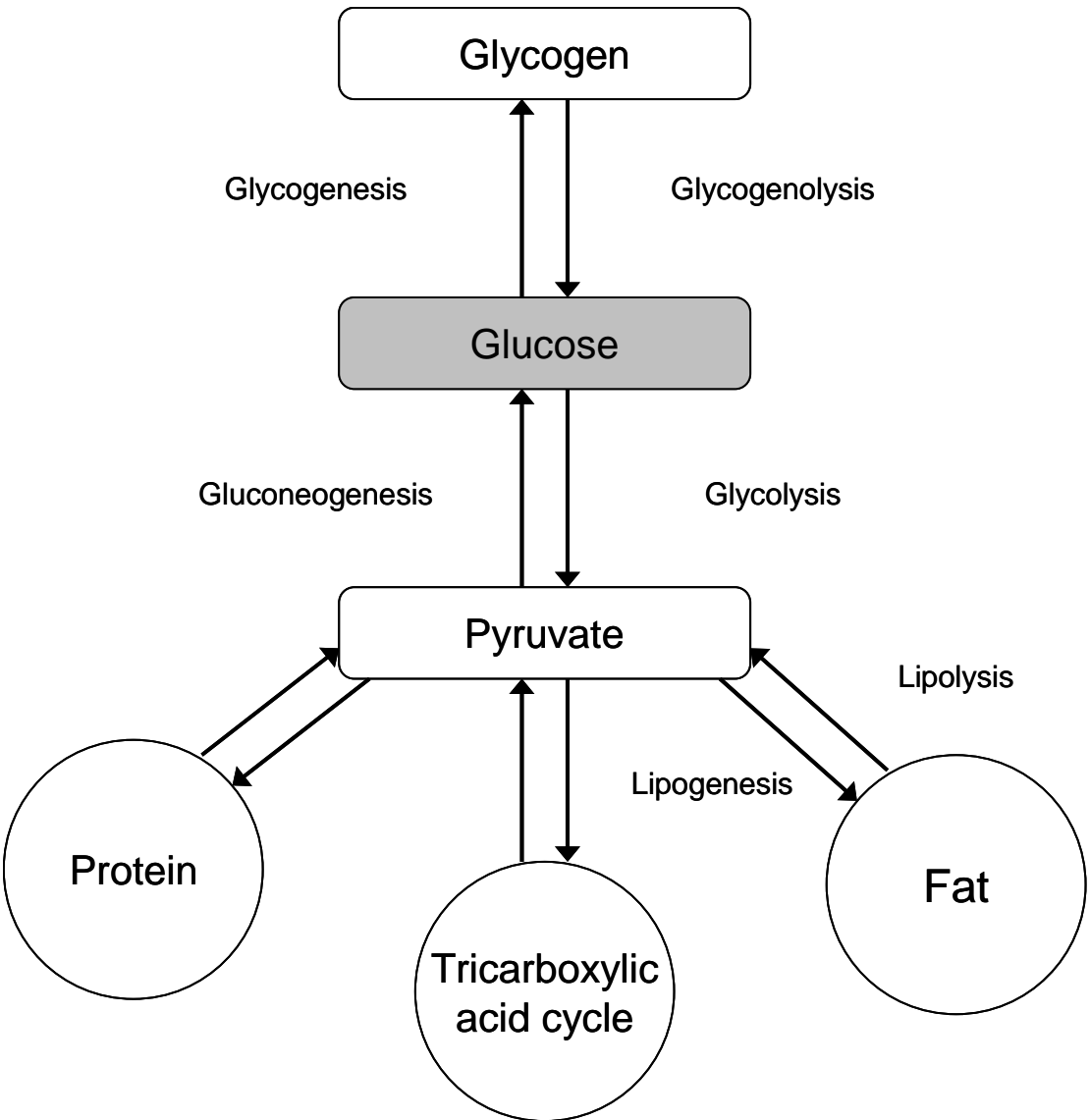


Figure 2.2. Metabolic and catabolic processes involving glucose

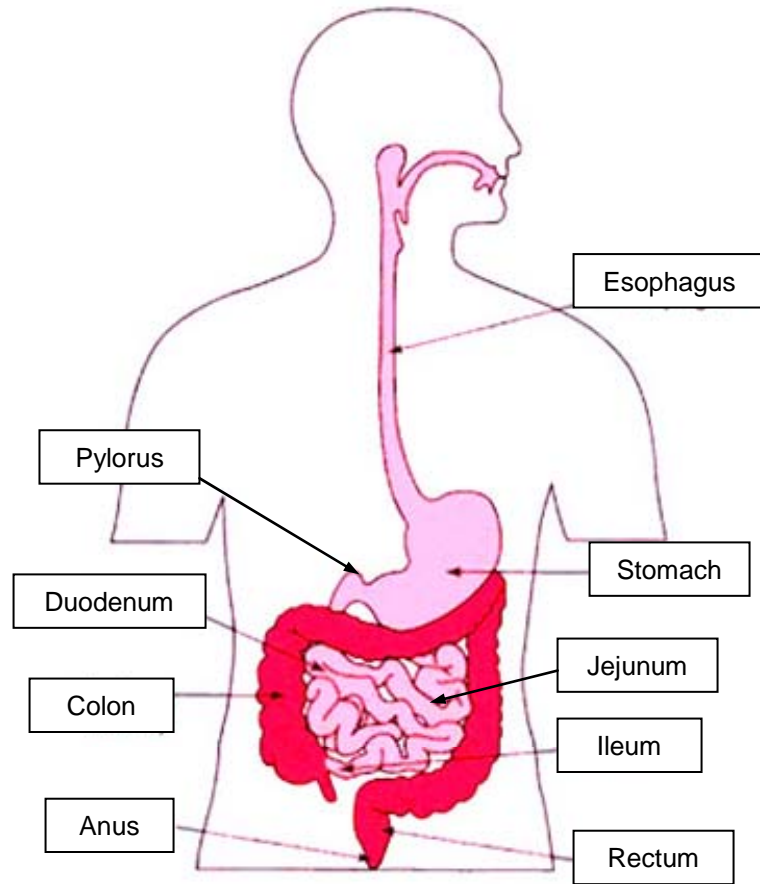


Figure 2.3. Schematic of the entire human gastrointestinal tract

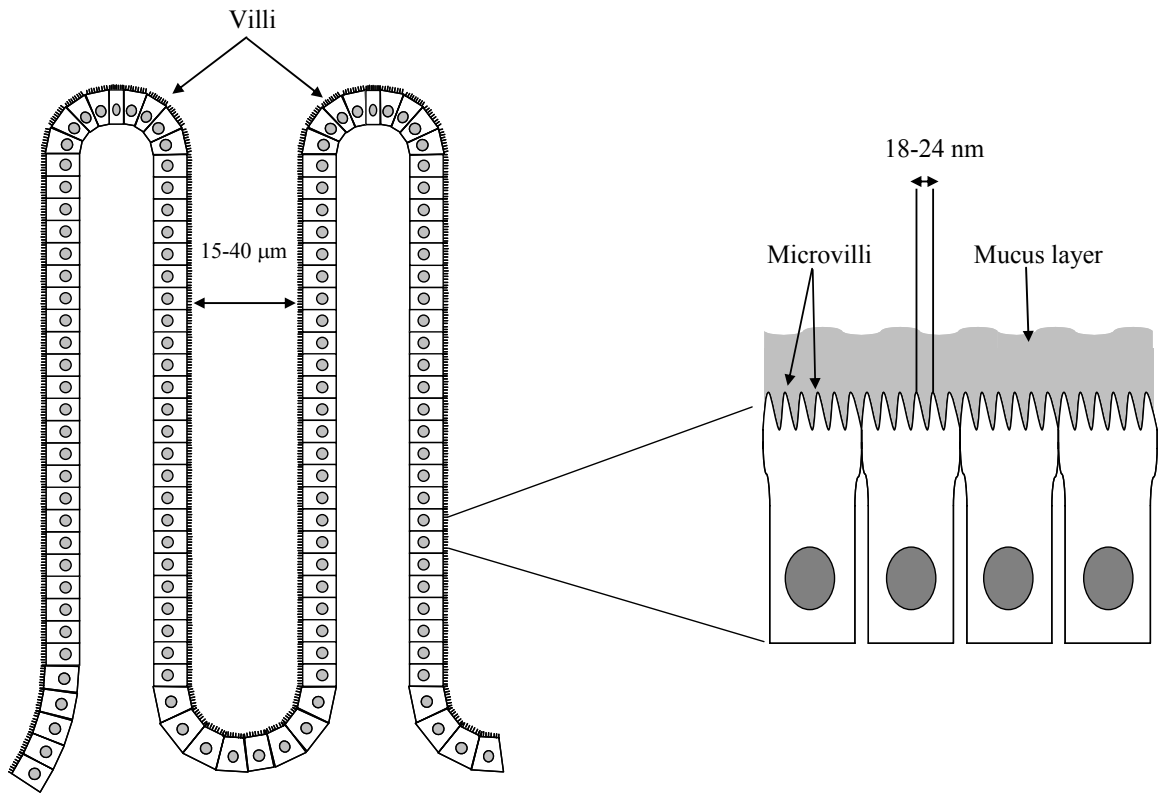


Figure 2.4. The intestinal epithelium

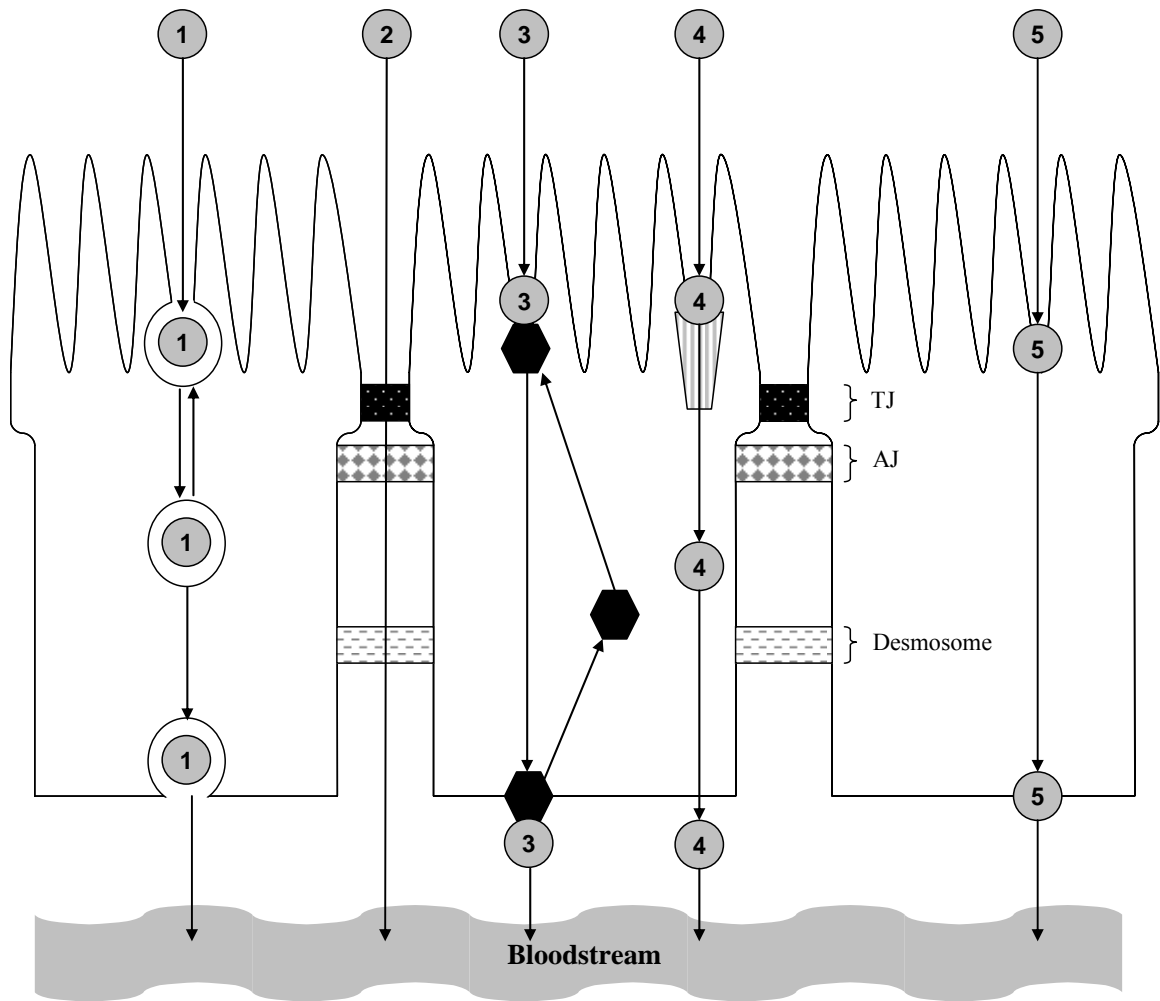


Figure 2.5. Transepithelial pathways for protein drugs from the intestinal lumen to the bloodstream: (1) pinocytosis (2) paracellular transport (3) receptor-mediated transcytosis (4) active transport (5) passive transcellular transport

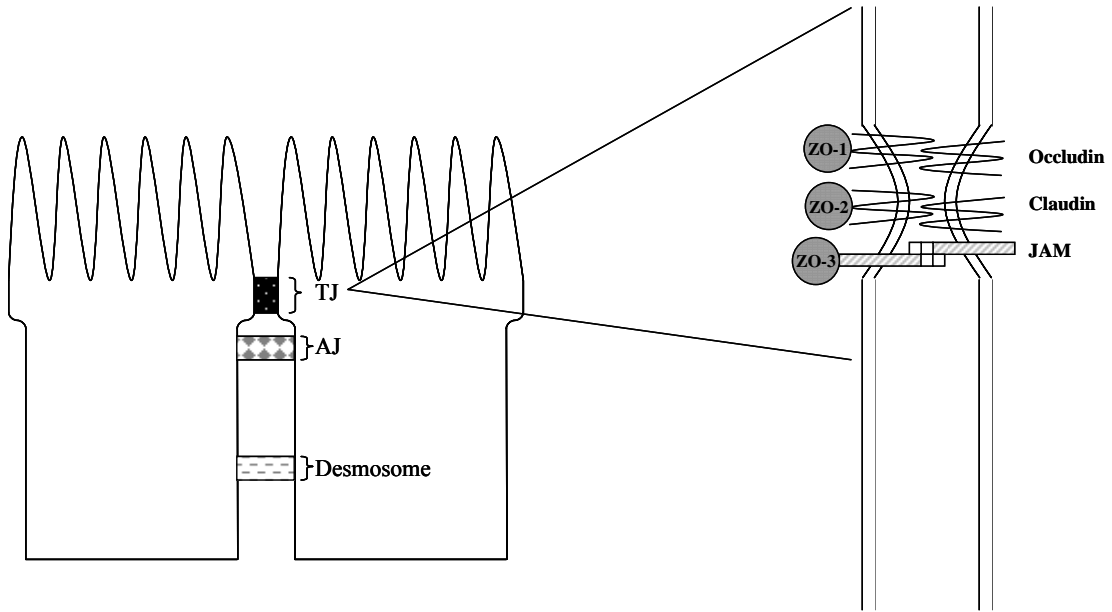


Figure 2.6. Structure of the tight junction in epithelial cells

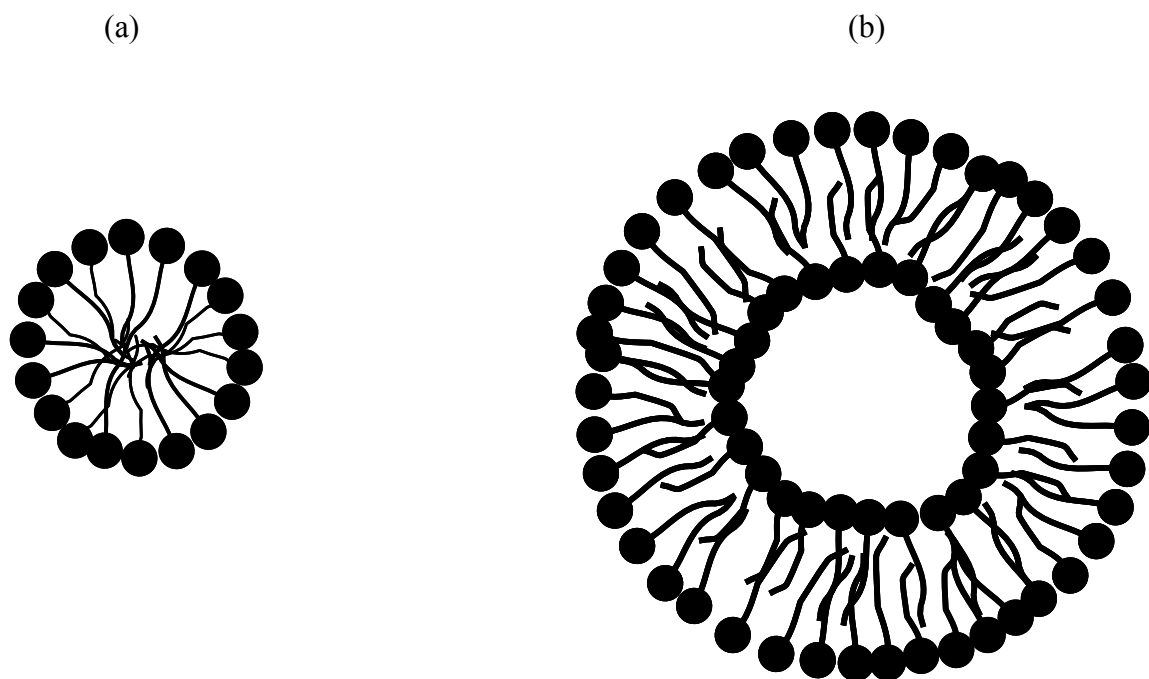


Figure 2.7. Lipid based systems for oral protein delivery: (a) micelle and (b) liposome

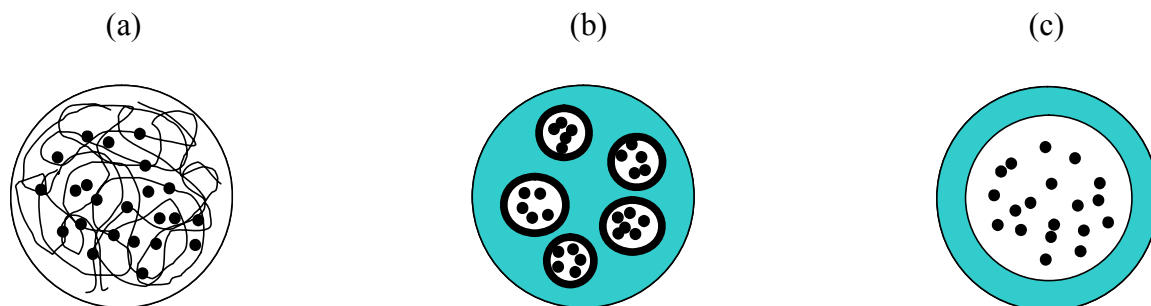


Figure 2.8. Polymer based nanoparticle designs: (a) nanoparticle from spray drying, (b) nanoparticle from double emulsion, and (c) nanocapsule

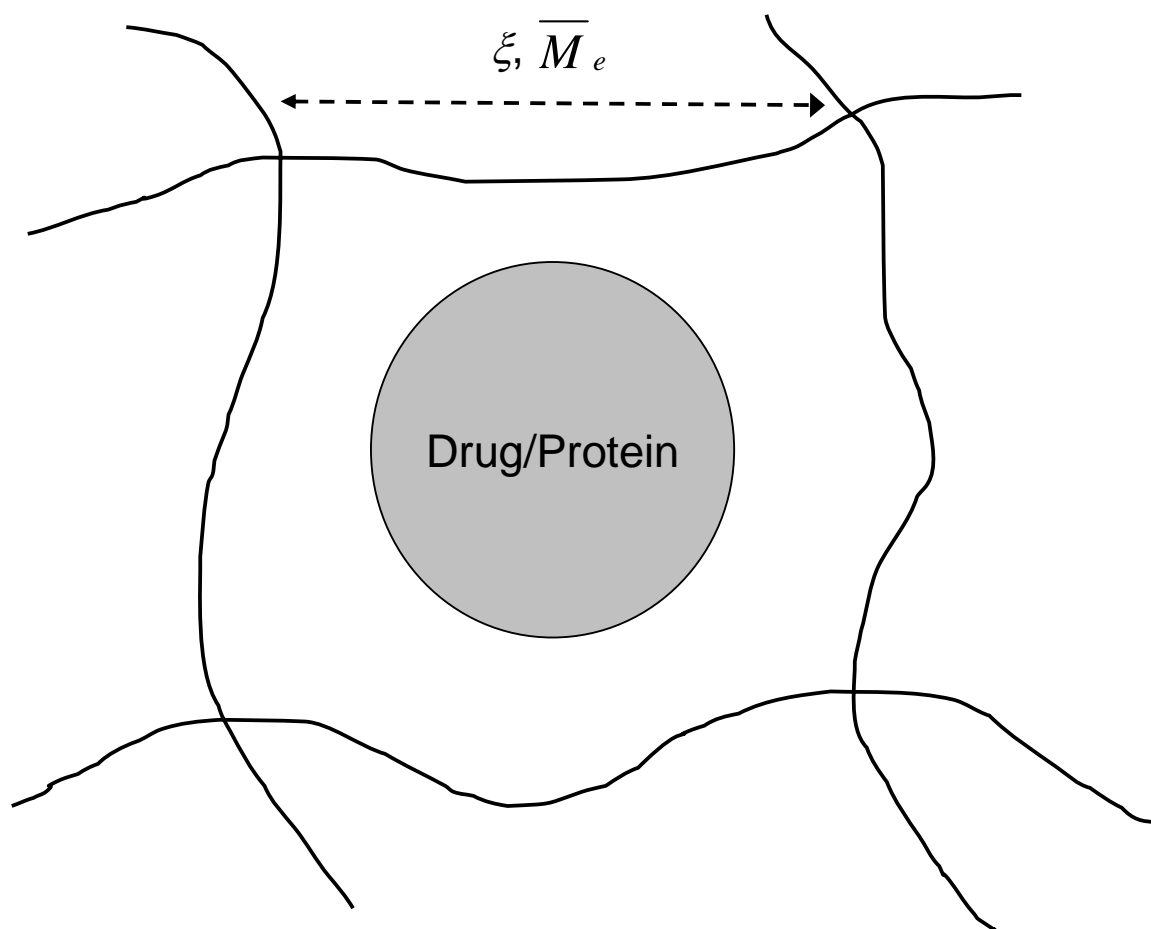


Figure 2.9. Simplified diagram of a drug contained within a hydrogel network indicating the network mesh size, ξ , and the average molecular weight between crosslinks, \overline{M}_e

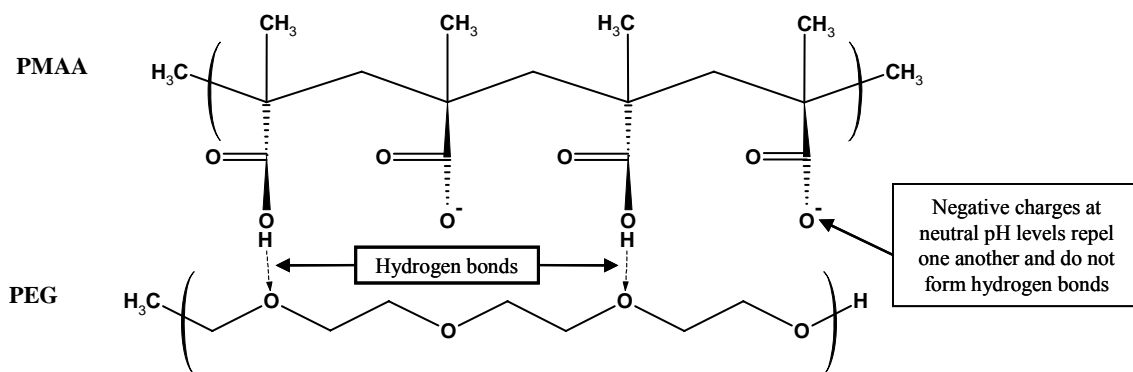


Figure 2.10. Interpolymer bonds between PMAA and PEG

2.12. References

1. Pickup, J.C. and G. Williams, Eds., *Textbook of Diabetes*. 2 ed. Vol. 1. 1997, Malden, MA: Blackwell Science Ltd.
2. Clark, M., *Understanding Diabetes*. 2004, Hoboken, NJ: John Wiley & Sons, Ltd.
3. Dean, L., McIntyre, J., *The Genetic Landscape of Diabetes*. 2004, National Institute of Diabetes and Digestive and Kidney Disease.
4. Mokdad, A.H., et al., *Prevalence of obesity, diabetes, and obesity-related health risk factors, 2001*. *Jama*, 2003. **289**(1): p. 76-9.
5. *National diabetes fact sheet: general information and national estimates on diabetes in the United States, 2003. Rev. ed.* 2003, Centers for Disease Control and Prevention, U.S. Department of Health and Human Services: Atlanta, GA.
6. *Gestational Diabetes*. 2007, American Diabetes Association.
7. Ballinger, W.F. and P.E. Lacy, *Transplantation of intact pancreatic islets in rats*. *Surgery*, 1972. **72**(2): p. 175-86.
8. Dafoe, D.C. and L.E. Ratner, *Pancreatico-renal composite transplant: a new technique designed to decrease pancreatic graft thrombosis*. *Clin Transplant*, 2005. **19**(5): p. 690-3.
9. Sansalone, C.V., et al., *Surgical complications are the main cause of pancreatic allograft loss in pancreas-kidney transplant recipients*. *Transplant Proc*, 2005. **37**(6): p. 2651-3.
10. Ricordi, C., *Islet transplantation: a brave new world*. *Diabetes*, 2003. **52**(7): p. 1595-603.
11. Fiorina, P. and A. Secchi, *Pancreatic islet cell transplant for treatment of diabetes*. *Endocrinol Metab Clin North Am*, 2007. **36**(4): p. 999-1013; ix.
12. Noguchi, H., et al., *Immunosuppression for islet transplantation*. *Acta Med Okayama*, 2006. **60**(2): p. 71-6.
13. Harris, M.I., *Summary*, in *Diabetes in America, 2nd Edition*, M.I. Harris, Editor. 1995, National Institutes of Health: Bethesda, MD.

14. Weber, J., *Changing Epidemiology of Obesity - Implications for Diabetes*, in *Obesity and Diabetes*, A.H. Barnett, Kumar, Sudesh, Editor. 2004, John Wiley & Sons, Ltd: Hoboken, NJ.
15. Kenny, S.J., Aubert, R. E., Geiss, L. S., *Prevalence and Incidence of Non-Insulin-Dependent Diabetes Mellitus*, in *Diabetes in America, 2nd Edition*, M.I. Harris, Editor. 1995, The National Institutes of Health: Bethesda, MD.
16. Astrup, A. and N. Finer, *Redefining type 2 diabetes: 'diabesity' or 'obesity dependent diabetes mellitus'?* *Obes Rev*, 2000. **1**(2): p. 57-9.
17. Finucane, P., Popplewell, P., *Diabetes Mellitus and Impaired Glucose Regulation in Old Age: The Scale of the Problem*, in *Diabetes in Old Age, 2nd Edition*, P. Finucane, Sinclair, A. J., Editor. 2001, John Wiley & Sons Ltd.: Hoboken, NJ.
18. Rewers, M., Hamman, R. F., *Risk Factors for Non-Insulin-Dependent Diabetes Mellitus*, in *Diabetes in America, 2nd Edition*, M.I. Harris, Editor. 1995, The National Institutes of Health: Bethesda, MD.
19. Powers, M., *American Dietetic Association Guide to Eating Right When You Have Diabetes*. 2003, Hoboken, NJ: John Wiley & Sons, Inc.
20. Tupper, T. and G. Gopalakrishnan, *Prevention of diabetes development in those with the metabolic syndrome*. *Med Clin North Am*, 2007. **91**(6): p. 1091-105, viii-ix.
21. *Number of Adults with Diabetes by Diabetes Medication Status, United States, 1997–2003*. 2002, Centers for Disease Control and Prevention.
22. Scemons, D., *Are you up-to-date on diabetes medications?* *Nursing*, 2007. **37**(7): p. 45-9; quiz 49-50.
23. Umpierrez, G.E., et al., *Diabetes mellitus in the Hispanic/Latino population: an increasing health care challenge in the United States*. *Am J Med Sci*, 2007. **334**(4): p. 274-82.
24. Black, C., et al., *Meglitinide analogues for type 2 diabetes mellitus*. *Cochrane Database Syst Rev*, 2007(2): p. CD004654.
25. Rambiritch, V., P. Naidoo, and N. Butkow, *Dose-response relationships of sulfonylureas: will doubling the dose double the response?* *South Med J*, 2007. **100**(11): p. 1132-6.

26. Servey, J.T., *Alpha-glucosidase inhibitors may reduce the risk of type 2 diabetes*. Am Fam Physician, 2007. **76**(3): p. 374-5.
27. Stumvoll, M., et al., *Metabolic effects of metformin in non-insulin-dependent diabetes mellitus*. N Engl J Med, 1995. **333**(9): p. 550-4.
28. Chaudhry, J., et al., *Antihyperglycemic effect of a new thiazolidinedione analogue and its role in ameliorating oxidative stress in alloxan-induced diabetic rats*. Life Sci, 2007. **80**(12): p. 1135-42.
29. Schwartz, A.V. and D.E. Sellmeyer, *Effect of thiazolidinediones on skeletal health in women with Type 2 diabetes*. Expert Opin Drug Saf, 2008. **7**(1): p. 69-78.
30. Eurich, D.T., et al., *Benefits and harms of antidiabetic agents in patients with diabetes and heart failure: systematic review*. Bmj, 2007. **335**(7618): p. 497.
31. O'Farrell, A.M., et al., *Pharmacokinetic and pharmacodynamic assessments of the dipeptidyl peptidase-4 inhibitor PHX1149: double-blind, placebo-controlled, single- and multiple-dose studies in healthy subjects*. Clin Ther, 2007. **29**(8): p. 1692-705.
32. Yamazaki, K., et al., *Comparison of efficacies of a dipeptidyl peptidase IV inhibitor and alpha-glucosidase inhibitors in oral carbohydrate and meal tolerance tests and the effects of their combination in mice*. J Pharmacol Sci, 2007. **104**(1): p. 29-38.
33. Saudek, C.D., Rubin, Richard R., Shump, Cynthia S., *Johns Hopkins Guide to Diabetes : For Today and Tomorrow*. 1997, Baltimore, MD: The Johns Hopkins University Press.
34. Nolte, M.S., Karam, John H., *Pancreatic Hormones & Antidiabetic Drugs*, in *Basic and Clinical Pharmacology, 10th Edition*, B.G. Katzung, Editor. 2007, McGraw-Hill: New York.
35. Haas, L.B., *Optimizing insulin use in type 2 diabetes: role of basal and prandial insulin in long-term care facilities*. J Am Med Dir Assoc, 2007. **8**(8): p. 502-10.
36. Spellman, C.W., *Insulin therapy for maximal glycemic control in type 2 diabetes mellitus*. J Am Osteopath Assoc, 2007. **107**(7): p. 260-9.
37. Campos, C., *Treating the whole patient for optimal management of type 2 diabetes: considerations for insulin therapy*. South Med J, 2007. **100**(8): p. 804-11.

38. Sanger, F. and H. Tuppy, *The amino-acid sequence in the phenylalanyl chain of insulin. I. The identification of lower peptides from partial hydrolysates*. Biochem J, 1951. **49**(4): p. 463-81.
39. Sanger, F., E.O. Thompson, and R. Kitai, *The amide groups of insulin*. Biochem J, 1955. **59**(3): p. 509-18.
40. Sanger, F., L.F. Smith, and R. Kitai, *The disulphide bridges of insulin*. Biochem J, 1954. **58**(330th Meeting): p. vi-vii.
41. Sanger, F. and E.O. Thompson, *The amino-acid sequence in the glycyl chain of insulin. II. The investigation of peptides from enzymic hydrolysates*. Biochem J, 1953. **53**(3): p. 366-74.
42. Sanger, F. and E.O. Thompson, *The amino-acid sequence in the glycyl chain of insulin. I. The identification of lower peptides from partial hydrolysates*. Biochem J, 1953. **53**(3): p. 353-66.
43. Sanger, F. and E.O. Thompson, *The amino-acid sequence in the glycyl chain of insulin*. Biochem J, 1952. **52**(1): p. iii.
44. Sanger, F. and H. Tuppy, *The amino-acid sequence in the phenylalanyl chain of insulin. 2. The investigation of peptides from enzymic hydrolysates*. Biochem J, 1951. **49**(4): p. 481-90.
45. King, K.M. and G. Rubin, *A history of diabetes: from antiquity to discovering insulin*. Br J Nurs, 2003. **12**(18): p. 1091-5.
46. Bliss, M., *The Discovery of Insulin*. 1982, Edinburgh, England: Paul Harris Publishing.
47. Davis, S.N., *Insulin, Oral Hypoglycemic Agents, and the Pharmacology of the Endocrine Pancreas*, in *Goodman and Gilman's - The Pharmacological Basis of Therapeutics, 11 ed.*, L.L. Brunton, Ed., Editor. 2006, McGraw-Hill.
48. Heller, S., P. Kozlovski, and P. Kurtzhals, *Insulin's 85th anniversary--An enduring medical miracle*. Diabetes Res Clin Pract, 2007. **78**(2): p. 149-58.
49. King, K.M., *A history of insulin: from discovery to modern alternatives*. Br J Nurs, 2003. **12**(19): p. 1137-41.
50. Ladisch, M.R. and K.L. Kohlmann, *Recombinant human insulin*. Biotechnol Prog, 1992. **8**(6): p. 469-78.

51. Bell, D.S., *Insulin therapy in diabetes mellitus: how can the currently available injectable insulins be most prudently and efficaciously utilised?* *Drugs*, 2007. **67**(13): p. 1813-27.
52. Vajo, Z. and W.C. Duckworth, *Genetically engineered insulin analogs: diabetes in the new millenium*. *Pharmacol Rev*, 2000. **52**(1): p. 1-9.
53. Brange, J. and A. Volund, *Insulin analogs with improved pharmacokinetic profiles*. *Adv Drug Deliv Rev*, 1999. **35**(2-3): p. 307-335.
54. Oiknine, R., M. Bernbaum, and A.D. Mooradian, *A critical appraisal of the role of insulin analogues in the management of diabetes mellitus*. *Drugs*, 2005. **65**(3): p. 325-40.
55. *Aventis receives FDA approval of its rapid-acting insulin analogue Apidra*. 2007, Aventis Pharmaceuticals Inc.
56. Robinson, D.M. and K. Wellington, *Insulin glulisine*. *Drugs*, 2006. **66**(6): p. 861-9.
57. Heise, T., et al., *Insulin glulisine: a faster onset of action compared with insulin lispro*. *Diabetes Obes Metab*, 2007. **9**(5): p. 746-53.
58. Drejer, K., *The bioactivity of insulin analogues from in vitro receptor binding to in vivo glucose uptake*. *Diabetes Metab Rev*, 1992. **8**(3): p. 259-85.
59. Goldman-Levine, J.D. and K.W. Lee, *Insulin detemir--a new basal insulin analog*. *Ann Pharmacother*, 2005. **39**(3): p. 502-7.
60. Russell-Jones, D.L., *Insulin detemir and basal insulin therapy*. *Endocrinol Metab Clin North Am*, 2007. **36 Suppl 1**: p. 7-13.
61. Porcellati, F., et al., *Comparison of pharmacokinetics and dynamics of the long-acting insulin analogs glargine and detemir at steady state in type 1 diabetes: a double-blind, randomized, crossover study*. *Diabetes Care*, 2007. **30**(10): p. 2447-52.
62. Kurtzhals, P., et al., *Correlations of receptor binding and metabolic and mitogenic potencies of insulin analogs designed for clinical use*. *Diabetes*, 2000. **49**(6): p. 999-1005.

63. Hansen, B.F., et al., *Sustained signalling from the insulin receptor after stimulation with insulin analogues exhibiting increased mitogenic potency*. *Biochem J*, 1996. **315 (Pt 1)**: p. 271-9.
64. Slieker, L.J., et al., *Modifications in the B10 and B26-30 regions of the B chain of human insulin alter affinity for the human IGF-I receptor more than for the insulin receptor*. *Diabetologia*, 1997. **40 Suppl 2**: p. S54-61.
65. Ciaraldi, T.P., et al., *Effects of the long-acting insulin analog insulin glargine on cultured human skeletal muscle cells: comparisons to insulin and IGF-I*. *J Clin Endocrinol Metab*, 2001. **86(12)**: p. 5838-47.
66. Nelson, D.L., Cox, M. M., *Lehninger Principles of Biochemistry, 3rd Edition*. 2000, New York: Worth Publishers.
67. Volund, A., *Conversion of insulin units to SI units*. *Am J Clin Nutr*, 1993. **58(5)**: p. 714-5.
68. Arbit, E., *The physiological rationale for oral insulin administration*. *Diabetes Technol Ther*, 2004. **6(4)**: p. 510-7.
69. Duckworth, W.C., R.G. Bennett, and F.G. Hamel, *Insulin degradation: progress and potential*. *Endocr Rev*, 1998. **19(5)**: p. 608-24.
70. Bliss, M., *Resurrections in Toronto: the emergence of insulin*. *Horm Res*, 2005. **64 Suppl 2**: p. 98-102.
71. Hayward, R.A., et al., *Starting insulin therapy in patients with type 2 diabetes: effectiveness, complications, and resource utilization*. *Jama*, 1997. **278(20)**: p. 1663-9.
72. Harris, M.I., et al., *Racial and ethnic differences in glycemic control of adults with type 2 diabetes*. *Diabetes Care*, 1999. **22(3)**: p. 403-8.
73. Turner, R.C., et al., *Glycemic control with diet, sulfonylurea, metformin, or insulin in patients with type 2 diabetes mellitus: progressive requirement for multiple therapies (UKPDS 49)*. *UK Prospective Diabetes Study (UKPDS) Group*. *Jama*, 1999. **281(21)**: p. 2005-12.
74. DCCT, *The effect of intensive treatment of diabetes on the development and progression of long-term complications in insulin-dependent diabetes mellitus*. *N Engl J Med*, 1993. **329(14)**: p. 977-86.

75. Cherrington, A.D., et al., *Physiological consequences of phasic insulin release in the normal animal*. Diabetes, 2002. **51 Suppl 1**: p. S103-8.
76. Jeandidier, N. and S. Boivin, *Current status and future prospects of parenteral insulin regimens, strategies and delivery systems for diabetes treatment*. Adv Drug Deliv Rev, 1999. **35**(2-3): p. 179-198.
77. Norgaard, K., *A nationwide study of continuous subcutaneous insulin infusion (CSII) in Denmark*. Diabet Med, 2003. **20**(4): p. 307-11.
78. Thompson, J.S. and W.C. Duckworth, *Insulin pumps and glucose regulation*. World J Surg, 2001. **25**(4): p. 523-6.
79. White, R.D., *Insulin pump therapy (continuous subcutaneous insulin infusion)*. Prim Care, 2007. **34**(4): p. 845-71.
80. Lee, S.W., R. Im, and R. Magbual, *Current perspectives on the use of continuous subcutaneous insulin infusion in the acute care setting and overview of therapy*. Crit Care Nurs Q, 2004. **27**(2): p. 172-84.
81. Royle, P., et al., *Inhaled insulin in diabetes mellitus*. Cochrane Database Syst Rev, 2004(3): p. CD003890.
82. Setter, S.M., et al., *Inhaled dry powder insulin for the treatment of diabetes mellitus*. Clin Ther, 2007. **29**(5): p. 795-813.
83. Crotty, S. and S.L. Reynolds, *The new insulins*. Pediatr Emerg Care, 2007. **23**(12): p. 903-5; quiz 906-7.
84. Patton, J.S., J.G. Bukar, and M.A. Eldon, *Clinical pharmacokinetics and pharmacodynamics of inhaled insulin*. Clin Pharmacokinet, 2004. **43**(12): p. 781-801.
85. Owens, D.R., B. Zinman, and G. Bolli, *Alternative routes of insulin delivery*. Diabet Med, 2003. **20**(11): p. 886-98.
86. Hussain, A. and F. Ahsan, *State of insulin self-association does not affect its absorption from the pulmonary route*. Eur J Pharm Sci, 2005. **25**(2-3): p. 289-98.
87. Brain, J.D., *Inhalation, deposition, and fate of insulin and other therapeutic proteins*. Diabetes Technol Ther, 2007. **9 Suppl 1**: p. S4-S15.
88. Simons, J., *How the Exubera Debacle Hurts Pfizer*, in Fortune. 2007.

89. Kaushik, S., et al., *Lack of pain associated with microfabricated microneedles*. *Anesth Analg*, 2001. **92**(2): p. 502-4.
90. Martanto, W., et al., *Transdermal delivery of insulin using microneedles in vivo*. *Pharm Res*, 2004. **21**(6): p. 947-52.
91. Kanikkannan, N., J. Singh, and P. Ramarao, *Transdermal iontophoretic delivery of bovine insulin and monomeric human insulin analogue*. *J Control Release*, 1999. **59**(1): p. 99-105.
92. Park, E.J., J. Werner, and N.B. Smith, *Ultrasound mediated transdermal insulin delivery in pigs using a lightweight transducer*. *Pharm Res*, 2007. **24**(7): p. 1396-401.
93. Lee, S., et al., *Photomechanical transdermal delivery of insulin in vivo*. *Lasers Surg Med*, 2001. **28**(3): p. 282-5.
94. Hinchcliffe, M. and L. Illum, *Intranasal insulin delivery and therapy*. *Adv Drug Deliv Rev*, 1999. **35**(2-3): p. 199-234.
95. Pontiroli, A.E., *Peptide hormones: Review of current and emerging uses by nasal delivery*. *Adv Drug Deliv Rev*, 1998. **29**(1-2): p. 81-87.
96. Zhang, X., et al., *Nasal absorption enhancement of insulin using PEG-grafted chitosan nanoparticles*. *Eur J Pharm Biopharm*, 2007.
97. Yu, S., et al., *Nasal insulin delivery in the chitosan solution: in vitro and in vivo studies*. *Int J Pharm*, 2004. **281**(1-2): p. 11-23.
98. Dyer, A.M., et al., *Nasal delivery of insulin using novel chitosan based formulations: a comparative study in two animal models between simple chitosan formulations and chitosan nanoparticles*. *Pharm Res*, 2002. **19**(7): p. 998-1008.
99. Lee, Y.C. and S.H. Yalkowsky, *Ocular devices for the controlled systemic delivery of insulin: in vitro and in vivo dissolution*. *Int J Pharm*, 1999. **181**(1): p. 71-7.
100. Degim, Z., et al., *Rectal and vaginal administration of insulin-chitosan formulations: an experimental study in rabbits*. *J Drug Target*, 2005. **13**(10): p. 563-72.
101. Lee, Y.C., et al., *Review on the systemic delivery of insulin via the ocular route*. *Int J Pharm*, 2002. **233**(1-2): p. 1-18.

102. Senel, S. and A.A. Hincal, *Drug permeation enhancement via buccal route: possibilities and limitations*. J Control Release, 2001. **72**(1-3): p. 133-44.
103. Junginger, H.E., J.A. Hoogstraate, and J.C. Verhoef, *Recent advances in buccal drug delivery and absorption--in vitro and in vivo studies*. J Control Release, 1999. **62**(1-2): p. 149-59.
104. Luo, Y., et al., *Study on a nanoparticle system for buccal delivery of insulin*. Conf Proc IEEE Eng Med Biol Soc, 2005. **5**: p. 4842-5.
105. Pozzilli, P., et al., *Biokinetics of buccal spray insulin in patients with type 1 diabetes*. Metabolism, 2005. **54**(7): p. 930-4.
106. Generex, *Oral-lyn product information*. 2008, <http://www.generex.com/products/oral-lyn/>.
107. Hanazaki, K., Y. Nose, and F.C. Brunnicardi, *Artificial endocrine pancreas*. J Am Coll Surg, 2001. **193**(3): p. 310-22.
108. Lim, M.W. and T.P. Fan, *A "pancreatic tooth" design best accommodates the limitations of current artificial pancreas technology*. Med Hypotheses, 2007. **69**(4): p. 741-5.
109. Tohda, K. and M. Gratzl, *A microscopic, continuous, optical monitor for interstitial electrolytes and glucose*. Chemphyschem, 2003. **4**(2): p. 155-60.
110. Woderer, S., et al., *Continuous glucose monitoring in interstitial fluid using glucose oxidase-based sensor compared to established blood glucose measurement in rats*. Anal Chim Acta, 2007. **581**(1): p. 7-12.
111. Wentholt, I.M., et al., *Comparison of a needle-type and a microdialysis continuous glucose monitor in type 1 diabetic patients*. Diabetes Care, 2005. **28**(12): p. 2871-6.
112. Kono, T., et al., *Pancreatic polypeptide administration reduces insulin requirements of artificial pancreas in pancreatectomized dogs*. Artif Organs, 2005. **29**(1): p. 83-7.
113. Ratner, B.D., Hoffman, A. S., Schoen, F. J., Lemons, J. E., *Biomaterials Science*. 1996, San Diego: Academic Press.
114. Worsley, G.J., et al., *Continuous blood glucose monitoring with a thin-film optical sensor*. Clin Chem, 2007. **53**(10): p. 1820-6.

115. Silva, A.I., et al., *An overview on the development of a bio-artificial pancreas as a treatment of insulin-dependent diabetes mellitus*. Med Res Rev, 2006. **26**(2): p. 181-222.
116. Hirotani, S., et al., *A bio-artificial endocrine pancreas for the treatment of diabetes*. Transplant Proc, 1998. **30**(2): p. 485-9.
117. Hou, Q.P. and Y.H. Bae, *Biohybrid artificial pancreas based on macrocapsule device*. Adv Drug Deliv Rev, 1999. **35**(2-3): p. 271-287.
118. Kashyap, N., et al., *Design and evaluation of biodegradable, biosensitive in situ gelling system for pulsatile delivery of insulin*. Biomaterials, 2007. **28**(11): p. 2051-60.
119. Miyata, T., et al., *Preparation of reversibly glucose-responsive hydrogels by covalent immobilization of lectin in polymer networks having pendant glucose*. J Biomater Sci Polym Ed, 2004. **15**(9): p. 1085-98.
120. Matsumoto, A., R. Yoshida, and K. Kataoka, *Glucose-responsive polymer gel bearing phenylborate derivative as a glucose-sensing moiety operating at the physiological pH*. Biomacromolecules, 2004. **5**(3): p. 1038-45.
121. Liu, F., et al., *Glucose-induced release of glycosylpoly(ethylene glycol) insulin bound to a soluble conjugate of concanavalin A*. Bioconj Chem, 1997. **8**(5): p. 664-72.
122. Cheng, S.Y., J. Gross, and A. Sambanis, *Hybrid pancreatic tissue substitute consisting of recombinant insulin-secreting cells and glucose-responsive material*. Biotechnol Bioeng, 2004. **87**(7): p. 863-73.
123. Kim, J.J. and K. Park, *Modulated insulin delivery from glucose-sensitive hydrogel dosage forms*. J Control Release, 2001. **77**(1-2): p. 39-47.
124. Layman, D.P., *Physiology Demystified*. 2004, Blacklick, OH: McGraw-Hill.
125. Barrett, K.E., *Gastrointestinal Physiology*. 2006, New York: McGraw-Hill.
126. Pasley, J.N., *USMLE Road Map: Physiology*. 2003, New York: McGraw-Hill.
127. Goldberg, H.I., et al., *In vivo demonstration of small intestinal villi in dogs and monkeys using radiographic magnification*. Radiology, 1982. **142**(1): p. 53-8.
128. Netter, F.H., *Netter's Atlas of the Human Body*. 2006, Hauppauge, NY: Barrons.

129. Wang, W., *Oral protein drug delivery*. J Drug Target, 1996. **4**(4): p. 195-232.
130. Saltzman, W.M., *Drug Delivery: Engineering Principles for Drug Therapy*. 2001, Oxford: Oxford University Press.
131. Beck, F. and R.M. Williams, *Pinocytosis in the neonate mammalian small intestine*. J Anat, 1969. **104**(Pt 1): p. 174-5.
132. Liu, J. and J.I. Shapiro, *Endocytosis and signal transduction: basic science update*. Biol Res Nurs, 2003. **5**(2): p. 117-28.
133. Sood, A. and R. Panchagnula, *Peroral route: an opportunity for protein and peptide drug delivery*. Chem Rev, 2001. **101**(11): p. 3275-303.
134. Salama, N.N., N.D. Eddington, and A. Fasano, *Tight junction modulation and its relationship to drug delivery*. Adv Drug Deliv Rev, 2006. **58**(1): p. 15-28.
135. Puthenedam, M., et al., *Modulation of tight junction barrier function by outer membrane proteins of enteropathogenic Escherichia coli: role of F-actin and junctional adhesion molecule-1*. Cell Biol Int, 2007. **31**(8): p. 836-44.
136. Lapiere, L.A., *The molecular structure of the tight junction*. Adv Drug Deliv Rev, 2000. **41**(3): p. 255-64.
137. Anderson, J.M. and C.M. Van Itallie, *Tight junctions and the molecular basis for regulation of paracellular permeability*. Am J Physiol, 1995. **269**(4 Pt 1): p. G467-75.
138. Miyoshi, J. and Y. Takai, *Molecular perspective on tight-junction assembly and epithelial polarity*. Adv Drug Deliv Rev, 2005. **57**(6): p. 815-55.
139. Nusrat, A., et al., *Tight junctions are membrane microdomains*. J Cell Sci, 2000. **113** (Pt 10): p. 1771-81.
140. Garrod, D. and M. Chidgey, *Desmosome structure, composition and function*. Biochim Biophys Acta, 2007.
141. Larsen, W.J., *Biological implications of gap junction structure, distribution and composition: a review*. Tissue Cell, 1983. **15**(5): p. 645-71.
142. Tsuji, A. and I. Tamai, *Carrier-mediated intestinal transport of drugs*. Pharm Res, 1996. **13**(7): p. 963-77.

143. Kunta, J.R. and P.J. Sinko, *Intestinal drug transporters: in vivo function and clinical importance*. *Curr Drug Metab*, 2004. **5**(1): p. 109-24.
144. Thwaites, D.T. and C.M. Anderson, *H⁺-coupled nutrient, micronutrient and drug transporters in the mammalian small intestine*. *Exp Physiol*, 2007. **92**(4): p. 603-19.
145. Terada, T. and K. Inui, *Gene expression and regulation of drug transporters in the intestine and kidney*. *Biochem Pharmacol*, 2007. **73**(3): p. 440-9.
146. Terada, T. and K. Inui, *Peptide transporters: structure, function, regulation and application for drug delivery*. *Curr Drug Metab*, 2004. **5**(1): p. 85-94.
147. Rubio-Aliaga, I. and H. Daniel, *Mammalian peptide transporters as targets for drug delivery*. *Trends Pharmacol Sci*, 2002. **23**(9): p. 434-40.
148. Maubon, N., et al., *Analysis of drug transporter expression in human intestinal Caco-2 cells by real-time PCR*. *Fundam Clin Pharmacol*, 2007. **21**(6): p. 659-63.
149. Nozawa, T., et al., *Enhanced intestinal absorption of drugs by activation of peptide transporter PEPT1 using proton-releasing polymer*. *J Pharm Sci*, 2003. **92**(11): p. 2208-16.
150. Swaan, P.W., et al., *Enhanced transepithelial transport of peptides by conjugation to cholic acid*. *Bioconjug Chem*, 1997. **8**(4): p. 520-5.
151. Kramer, W., Gunther, W., Enhnen, A., Eugen, F., Hoffman, A., Neckermann, G., Gerrit, S., Urmann, M., *Modified bile acids as carriers for peptides and drugs*. *J Control Release*, 1997. **46**(1-2): p. 17-30.
152. Kamath, A.V., I.M. Darling, and M.E. Morris, *Choline uptake in human intestinal Caco-2 cells is carrier-mediated*. *J Nutr*, 2003. **133**(8): p. 2607-11.
153. Alrefai, W.A. and R.K. Gill, *Bile acid transporters: structure, function, regulation and pathophysiological implications*. *Pharm Res*, 2007. **24**(10): p. 1803-23.
154. Steinman, R.M., et al., *Endocytosis and the recycling of plasma membrane*. *J Cell Biol*, 1983. **96**(1): p. 1-27.
155. Russell-Jones, G.J., *The potential use of receptor-mediated endocytosis for oral drug delivery*. *Adv Drug Deliv Rev*, 2001. **46**(1-3): p. 59-73.

156. Lim, C.J. and W.C. Shen, *Comparison of monomeric and oligomeric transferrin as potential carrier in oral delivery of protein drugs*. J Control Release, 2005. **106**(3): p. 273-86.
157. Kavimandan, N.J., et al., *Synthesis and characterization of insulin-transferrin conjugates*. Bioconjugate Chemistry, 2006. **17**(6): p. 1376-1384.
158. Russell-Jones, G.J., L. Arthur, and H. Walker, *Vitamin B12-mediated transport of nanoparticles across Caco-2 cells*. Int J Pharm, 1999. **179**(2): p. 247-55.
159. Camilleri, M., et al., *Human gastric emptying and colonic filling of solids characterized by a new method*. Am J Physiol, 1989. **257**(2 Pt 1): p. G284-90.
160. Smith, A.J., et al., *5-Hydroxytryptamine contributes significantly to a reflex pathway by which the duodenal mucosa protects itself from gastric acid injury*. Faseb J, 2006. **20**(14): p. 2486-95.
161. Decktor, D.L., et al., *Effect of metoclopramide, bethanechol and the cholecystokinin receptor antagonist, L-364,718, on gastric emptying in the rat*. Eur J Pharmacol, 1988. **147**(2): p. 313-6.
162. Higgins, L.M., et al., *In vivo phage display to identify M cell-targeting ligands*. Pharm Res, 2004. **21**(4): p. 695-705.
163. Brayden, D.J. and A.W. Baird, *Apical membrane receptors on intestinal M cells: potential targets for vaccine delivery*. Adv Drug Deliv Rev, 2004. **56**(6): p. 721-6.
164. Brayden, D.J., Jepson, M. A., Baird, A. W., *Intestinal Peyer's patch M cells and oral vaccine targeting*. Drug Discov Today, 2005. **10**(17): p. 1145-1157.
165. Yang, L., J.S. Chu, and J.A. Fix, *Colon-specific drug delivery: new approaches and in vitro/in vivo evaluation*. Int J Pharm, 2002. **235**(1-2): p. 1-15.
166. Tozaki, H., et al., *Chitosan capsules for colon-specific drug delivery: improvement of insulin absorption from the rat colon*. J Pharm Sci, 1997. **86**(9): p. 1016-21.
167. Chourasia, M.K. and S.K. Jain, *Pharmaceutical approaches to colon targeted drug delivery systems*. J Pharm Pharm Sci, 2003. **6**(1): p. 33-66.
168. Sinha, V.R. and R. Kumria, *Microbially triggered drug delivery to the colon*. Eur J Pharm Sci, 2003. **18**(1): p. 3-18.

169. Brange, J., Langkjaer, L., *Insulin Formulation & Delivery*, in *Protein Delivery: Physical Systems*, L.M. Sanders, Editor. 1997, Kluswer Academic Publishers: Hingham, MA.
170. Ferrannini, E., et al., *The role of fractional glucose extraction in the regulation of splanchnic glucose metabolism in normal and diabetic man*. *Metabolism*, 1980. **29**(1): p. 28-35.
171. Moore, M.C., A.D. Cherrington, and D.H. Wasserman, *Regulation of hepatic and peripheral glucose disposal*. *Best Pract Res Clin Endocrinol Metab*, 2003. **17**(3): p. 343-64.
172. Lebovitz, H.E. and M.A. Banerji, *Treatment of insulin resistance in diabetes mellitus*. *Eur J Pharmacol*, 2004. **490**(1-3): p. 135-46.
173. Nathan, D.M., *Clinical practice. Initial management of glycemia in type 2 diabetes mellitus*. *N Engl J Med*, 2002. **347**(17): p. 1342-9.
174. Langguth, P., et al., *The challenge of proteolytic enzymes in intestinal peptide delivery*. *Journal of Controlled Release*, 1997. **46**(1-2): p. 39-57.
175. Festen, H.P., *Intrinsic factor secretion and cobalamin absorption. Physiology and pathophysiology in the gastrointestinal tract*. *Scand J Gastroenterol Suppl*, 1991. **188**: p. 1-7.
176. Erickson, R.H., *Peptide Metabolism at Brush-Border Membranes*, in *Peptide-based drug design, controlling transport and metabolism*, M.D.a.G.L.A. Taylor, Editor. 1995, American Chemical Society: Washington, DC. p. 23-45.
177. Stephenson, S.L. and A.J. Kenny, *Metabolism of neuropeptides. Hydrolysis of the angiotensins, bradykinin, substance P and oxytocin by pig kidney microvillar membranes*. *Biochem J*, 1987. **241**(1): p. 237-47.
178. Peters, T.J., *The subcellular localization of di- and tri-peptide hydrolase activity in guinea-pig small intestine*. *Biochem J*, 1970. **120**(1): p. 195-203.
179. Ciechanover, A., *Intracellular protein degradation: from a vague idea thru the lysosome and the ubiquitin-proteasome system and onto human diseases and drug targeting*. *Exp Biol Med (Maywood)*, 2006. **231**(7): p. 1197-211.
180. Morishita, M., et al., *In situ ileal absorption of insulin in rats: effects of hyaluronidase pretreatment diminishing the mucous/glycocalyx layers*. *Pharm Res*, 2004. **21**(2): p. 309-16.

181. Smart, J.D., *The basics and underlying mechanisms of mucoadhesion*. Adv Drug Deliv Rev, 2005. **57**(11): p. 1556-68.
182. Shah, R.B., A. Palamakula, and M.A. Khan, *Cytotoxicity evaluation of enzyme inhibitors and absorption enhancers in Caco-2 cells for oral delivery of salmon calcitonin*. J Pharm Sci, 2004. **93**(4): p. 1070-82.
183. Bernkop-Schnurch, A., *The use of inhibitory agents to overcome the enzymatic barrier to perorally administered therapeutic peptides and proteins*. J Control Release, 1998. **52**(1-2): p. 1-16.
184. Steffansen, B., et al., *Intestinal solute carriers: an overview of trends and strategies for improving oral drug absorption*. Eur J Pharm Sci, 2004. **21**(1): p. 3-16.
185. Han, H.K. and G.L. Amidon, *Targeted prodrug design to optimize drug delivery*. AAPS PharmSci, 2000. **2**(1): p. E6.
186. Damgé, C., P. Maincent, and N. Ubrich, *Oral delivery of insulin associated to polymeric nanoparticles in diabetic rats*. J Control Release, 2007. **117**(2): p. 163-170.
187. Delie, F. and M.J. Blanco-Prieto, *Polymeric particulates to improve oral bioavailability of peptide drugs*. Molecules, 2005. **10**: p. 65-80.
188. Leobandung, W., et al., *Preparation of stable insulin-loaded nanospheres of poly(ethylene glycol) macromers and N-isopropyl acrylamide*. J Control Release, 2002. **80**(1-3): p. 357-63.
189. Pang, K.S., *Modeling of intestinal drug absorption: roles of transporters and metabolic enzymes (for the Gillette Review Series)*. Drug Metab Dispos, 2003. **31**(12): p. 1507-19.
190. Foster, N. and B.H. Hirst, *Exploiting receptor biology for oral vaccination with biodegradable particulates*. Adv Drug Deliv Rev, 2005. **57**(3): p. 431-50.
191. Ronnestad, I., et al., *Oligopeptide transporter PepT1 in Atlantic cod (Gadus morhua L.): cloning, tissue expression and comparative aspects*. J Exp Biol, 2007. **210**(Pt 22): p. 3883-96.
192. Shah, D. and W.C. Shen, *Transcellular delivery of an insulin-transferrin conjugate in enterocyte-like Caco-2 cells*. J Pharm Sci, 1996. **85**(12): p. 1306-11.

193. Salamat-Miller, N. and T.P. Johnston, *Current strategies used to enhance the paracellular transport of therapeutic polypeptides across the intestinal epithelium*. Int J Pharm, 2005. **294**(1-2): p. 201-16.
194. Larionova, N.V., et al., *Biodegradable cross-linked starch/protein microcapsules containing proteinase inhibitor for oral protein administration*. Int J Pharm, 1999. **189**(2): p. 171-8.
195. Hussain, A., et al., *Absorption enhancers in pulmonary protein delivery*. J Control Release, 2004. **94**(1): p. 15-24.
196. Plate, N.A., et al., *Mucoadhesive polymers with immobilized proteinase inhibitors for oral administration of protein drugs*. Biomaterials, 2002. **23**(7): p. 1673-7.
197. Marschutz, M.K. and A. Bernkop-Schnurch, *Oral peptide drug delivery: polymer-inhibitor conjugates protecting insulin from enzymatic degradation in vitro*. Biomaterials, 2000. **21**(14): p. 1499-507.
198. Bernkop-Schnurch, A. and A. Scerbe-Saiko, *Synthesis and in vitro evaluation of chitosan-EDTA-protease-inhibitor conjugates which might be useful in oral delivery of peptides and proteins*. Pharm Res, 1998. **15**(2): p. 263-9.
199. Bernkop-Schnurch, A., A. Krauland, and C. Valenta, *Development and in vitro evaluation of a drug delivery system based on chitosan-EDTA BBI conjugate*. J Drug Target, 1998. **6**(3): p. 207-14.
200. Pauletti, G.M., Gangwar, S., Knipp, G. T., Nerurkar, M. M., Okumu, F. W., Tamura, K. Siahaan, T. J., Borchardt, R. T., *Structural requirements for intestinal absorption of peptide drugs*. J Control Release, 1996. **41**(1-2): p. 3-17.
201. Hosny, E.A., H.I. Al-Shora, and M.M. Elmazar, *Oral delivery of insulin from enteric-coated capsules containing sodium salicylate: effect on relative hypoglycemia of diabetic beagle dogs*. Int J Pharm, 2002. **237**(1-2): p. 71-6.
202. Uchida, T., et al., *Preparation and characterization of insulin-loaded acrylic hydrogels containing absorption enhancers*. Chem Pharm Bull (Tokyo), 2001. **49**(10): p. 1261-6.
203. Shah, P., et al., *Modulation of ganciclovir intestinal absorption in presence of absorption enhancers*. J Pharm Sci, 2007. **96**(10): p. 2710-22.

204. Radwan, M.A. and H.Y. Aboul-Enein, *The effect of absorption enhancers on the initial degradation kinetics of insulin by alpha-chymotrypsin*. Int J Pharm, 2001. **217**(1-2): p. 111-20.
205. Komada, F., K. Okumura, and R. Hori, *Fate of porcine and human insulin at the subcutaneous injection site. II. In vitro degradation of insulins in the subcutaneous tissue of the rat*. J Pharmacobiodyn, 1985. **8**(1): p. 33-40.
206. Takeyama, M., et al., *Enhanced bioavailability of subcutaneously injected insulin by pretreatment with ointment containing protease inhibitors*. Pharm Res, 1991. **8**(1): p. 60-4.
207. Clement, S., et al., *Oral insulin product hexyl-insulin monoconjugate 2 (HIM2) in type 1 diabetes mellitus: the glucose stabilization effects of HIM2*. Diabetes Technol Ther, 2002. **4**(4): p. 459-66.
208. Cereijido, M., et al., *New diseases derived or associated with the tight junction*. Arch Med Res, 2007. **38**(5): p. 465-78.
209. Garnett, M.C., *Targeted drug conjugates: principles and progress*. Adv Drug Deliv Rev, 2001. **53**(2): p. 171-216.
210. Hou, T., et al., *ADME evaluation in drug discovery. 6. Can oral bioavailability in humans be effectively predicted by simple molecular property-based rules?* J Chem Inf Model, 2007. **47**(2): p. 460-3.
211. Saitoh, H. and B.J. Aungst, *Prodrug and analog approaches to improving the intestinal absorption of a cyclic peptide, GPIIb/IIIa receptor antagonist*. Pharm Res, 1997. **14**(8): p. 1026-9.
212. Biessen, E.A., et al., *Design of a targeted peptide nucleic acid prodrug to inhibit hepatic human microsomal triglyceride transfer protein expression in hepatocytes*. Bioconjug Chem, 2002. **13**(2): p. 295-302.
213. Sharma, S.K., et al., *Sustained tumor regression of human colorectal cancer xenografts using a multifunctional mannosylated fusion protein in antibody-directed enzyme prodrug therapy*. Clin Cancer Res, 2005. **11**(2 Pt 1): p. 814-25.
214. Kondo, C., et al., *Lack of improvement of oral absorption of ME3277 by prodrug formation is ascribed to the intestinal efflux mediated by breast cancer resistant protein (BCRP/ABCG2)*. Pharm Res, 2005. **22**(4): p. 613-8.

215. Pauletti, G.M., et al., *Improvement of oral peptide bioavailability: Peptidomimetics and prodrug strategies*. *Advanced Drug Delivery Reviews*, 1997. **27**(2-3): p. 235-256.
216. Ezra, A., et al., *A peptide prodrug approach for improving bisphosphonate oral absorption*. *J Med Chem*, 2000. **43**(20): p. 3641-52.
217. Weller, T., et al., *Orally active fibrinogen receptor antagonists. 2. Amidoximes as prodrugs of amidines*. *J Med Chem*, 1996. **39**(16): p. 3139-47.
218. Veronese, F.M., *Peptide and protein PEGylation: a review of problems and solutions*. *Biomaterials*, 2001. **22**(5): p. 405-17.
219. Veronese, F.M. and G. Pasut, *PEGylation, successful approach to drug delivery*. *Drug Discov Today*, 2005. **10**(21): p. 1451-8.
220. Roberts, M.J., M.D. Bentley, and J.M. Harris, *Chemistry for peptide and protein PEGylation*. *Adv Drug Deliv Rev*, 2002. **54**(4): p. 459-76.
221. Greenwald, R.B., et al., *Effective drug delivery by PEGylated drug conjugates*. *Adv Drug Deliv Rev*, 2003. **55**(2): p. 217-50.
222. Bailon, P. and W. Berthold, *Polyethylene glycol-conjugated pharmaceutical proteins*. *Pharmaceutical Science & Technology Today*, 1998. **1**(8): p. 352-356.
223. Hinds, K.D. and S.W. Kim, *Effects of PEG conjugation on insulin properties*. *Adv Drug Deliv Rev*, 2002. **54**(4): p. 505-30.
224. Fuertges, F. and A. Abuchowski, *The Clinical Efficacy of Poly(Ethylene Glycol)-Modified Proteins*. *Journal of Controlled Release*, 1990. **11**(1-3): p. 139-148.
225. Veronese, F.M. and J.M. Harris, *Introduction and overview of peptide and protein pegylation*. *Adv Drug Deliv Rev*, 2002. **54**(4): p. 453-6.
226. Stoll, B.R., et al., *A mechanistic analysis of carrier-mediated oral delivery of protein therapeutics*. *J Control Release*, 2000. **64**(1-3): p. 217-28.
227. Valuev, L.I., et al., *A biospecific polymeric carrier for polypeptide drugs*. *Russian Chem Bull, Int Ed.*, 2004. **53**(11): p. 2611-2616.
228. Xia, C.Q., J. Wang, and W.C. Shen, *Hypoglycemic effect of insulin-transferrin conjugate in streptozotocin-induced diabetic rats*. *J Pharmacol Exp Ther*, 2000. **295**(2): p. 594-600.

229. Kavimandan, N.J., E. Losi, and N.A. Peppas, *Novel delivery system based on complexation hydrogels as delivery vehicles for insulin-transferrin conjugates*. *Biomaterials*, 2006. **27**(20): p. 3846-54.
230. Booth, C.C., et al., *The site of absorption and tissue distribution of orally administered ⁵⁶Co-labelled vitamin B12 in the rat*. *Br J Haematol*, 1957. **3**(3): p. 253-61.
231. Seetharam, B. and D.H. Alpers, *Cellular uptake of cobalamin*. *Nutr Rev*, 1985. **43**(4): p. 97-102.
232. Seetharam, B., et al., *Normal and abnormal physiology of intrinsic factor mediated absorption of cobalamin (vitamin B12)*. *Indian J Biochem Biophys*, 1991. **28**(5-6): p. 324-30.
233. Hagedorn, C.H. and D.H. Alpers, *Distribution of intrinsic factor-vitamin B12 receptors in human intestine*. *Gastroenterology*, 1977. **73**(5): p. 1019-22.
234. Russell-Jones, G.J., *Oral delivery of therapeutic proteins and peptides by the vitamin B12 uptake system*, in *Peptide based drug design: Controlling transport and metabolism*, M.D.a.G.L.A. Taylor, Editor. 1995, American Chemical Society: Washington, D.C.
235. Seetharam, B., et al., *Intestinal uptake and release of cobalamin complexed with rat intrinsic factor*. *Am J Physiol*, 1985. **248**(3 Pt 1): p. G326-31.
236. Alsenz, J., et al., *Oral absorption of peptides through the cobalamin (vitamin B12) pathway in the rat intestine*. *Pharm Res*, 2000. **17**(7): p. 825-32.
237. Russell-Jones, G.J., *Oral delivery of therapeutic proteins and peptides by the vitamin B12 uptake system*, in *Peptide-Based Drug Design: Controlling Transport and Metabolism*, G.L. Amidon, Editor. 1995, American Chemical Society: Washington, D.C. p. 181-198.
238. DiBiase, M.D., Morrel, E. M., *Oral Delivery of Microencapsulated Proteins*, in *Protein Delivery: Physiacal Systems*, L.M. Sanders, Editor. 1997, Kluwer Academic Publishers: Hingham, MA.
239. Martin, C., et al., *Cholesterol-bile salt vesicles as potential delivery vehicles for drug and vaccine delivery*. *Int J Pharm*, 2005. **298**(2): p. 339-43.
240. Zasadzinski, J.A., *Novel approaches to lipid based drug delivery*. *Biomaterials*, 1997. **2**(3): p. 345-349.

241. Eldridge, J.H., Hammond, C. J., Meubroek, J. A., Staas, J. K., Gilley, R. M., Tice, T. R., *Controlled vaccine release in the gut associated lymphoid tissues: orally administered biodegradable microspheres target the Peyer's patches*. J Control Release, 1990. **11**(205-214).
242. Patel, H.M., *Transcytosis of drug carriers carrying peptides across epithelial barriers*. Biochem Soc Trans, 1989. **17**(5): p. 940-2.
243. Arrieta-Molero, J.F., et al., *Orally administered liposome-entrapped insulin in diabetic animals. A critical assessment*. Horm Res, 1982. **16**(4): p. 249-56.
244. Degim, I.T., et al., *Oral administration of liposomal insulin*. J Nanosci Nanotechnol, 2006. **6**(9-10): p. 2945-9.
245. Xiong, X.Y., Tam, K. C., *Synthesis and aggregation behavior of Pluronic F127/poly(lactic acid) block copolymers in aqueous solutions*. Macromolecules, 2003. **36**(26): p. 9979-9985.
246. Xiong, X.Y., Tam, K. C., *Hydrolytic degradation of Pluronic F127/poly(lactic acid) block copolymer nanoparticles*. Macromolecules, 2004. **37**(9): p. 3425-3430.
247. Xiong, X.Y., et al., *Vesicles from Pluronic/poly(lactic acid) block copolymers as new carriers for oral insulin delivery*. J Control Release, 2007. **120**(1-2): p. 11-7.
248. Furtado, S., et al., *Oral delivery of insulin loaded poly(fumaric-co-sebacic) anhydride microspheres*. Int J Pharm, 2008. **347**(1-2): p. 149-55.
249. Mathiowitz, E., et al., *Biologically erodable microspheres as potential oral drug delivery systems*. Nature, 1997. **386**(6623): p. 410-4.
250. Furtado, S., et al., *Subcutaneous delivery of insulin loaded poly(fumaric-co-sebacic anhydride) microspheres to type I diabetic rats*. Eur J Pharm Biopharm, 2006. **63**(2): p. 229-36.
251. Chalasani, K.B., et al., *A novel vitamin B12-nanosphere conjugate carrier system for peroral delivery of insulin*. J Control Release, 2007. **117**(3): p. 421-9.
252. Chalasani, K.B., et al., *Effective oral delivery of insulin in animal models using vitamin B12-coated dextran nanoparticles*. J Control Release, 2007. **122**(2): p. 141-50.

253. Carino, G.P., J.S. Jacob, and E. Mathiowitz, *Nanosphere based oral insulin delivery*. J Control Release, 2000. **65**(1-2): p. 261-9.
254. Cui, F.D., et al., *Preparation of insulin loaded PLGA-Hp55 nanoparticles for oral delivery*. J Pharm Sci, 2007. **96**(2): p. 421-7.
255. Kwon, Y.M., et al., *In situ study of insulin aggregation induced by water-organic solvent interface*. Pharm Res, 2001. **18**(12): p. 1754-9.
256. Li, Y.-P., et al., *PEGylated PLGA nanoparticles as protein carriers: synthesis, preparation and biodistribution in rats*. Journal of controlled release, 2001. **71**: p. 203-211.
257. Sahana, D.K., et al., *PLGA nanoparticles for oral delivery of hydrophobic drugs: Influence of organic solvent on nanoparticle formation and release behavior In Vitro and In Vivo using estradiol as a model drug*. J Pharm Sci, 2007.
258. Sarmiento, B., et al., *Development and characterization of new insulin containing polysaccharide nanoparticles*. Colloids Surf B Biointerfaces, 2006. **53**(2): p. 193-202.
259. Sarmiento, B., et al., *Oral bioavailability of insulin contained in polysaccharide nanoparticles*. Biomacromolecules, 2007. **8**(10): p. 3054-60.
260. Jain, D., D.K. Majumdar, and A.K. Panda, *Insulin loaded eudragit L100 microspheres for oral delivery: preliminary in vitro studies*. J Biomater Appl, 2006. **21**(2): p. 195-211.
261. Brandrup, J., Immergut, E. H., Grulke, E. A., Abe, A., Bloch, D. R., ed. *Polymer Handbook (4th Edition)*. 4 ed. 1999, John Wiley & Sons.
262. Jain, D., A.K. Panda, and D.K. Majumdar, *Eudragit S100 entrapped insulin microspheres for oral delivery*. AAPS PharmSciTech, 2005. **6**(1): p. E100-7.
263. Whitehead, K., Z. Shen, and S. Mitragotri, *Oral delivery of macromolecules using intestinal patches: applications for insulin delivery*. J Control Release, 2004. **98**(1): p. 37-45.
264. Sahlin, J.J. and N.A. Peppas, *Enhanced hydrogel adhesion by polymer interdiffusion: use of linear poly(ethylene glycol) as an adhesion promoter*. J Biomater Sci Polym Ed, 1997. **8**(6): p. 421-36.

265. Goto, T., et al., *Gastrointestinal transit and mucoadhesive characteristics of complexation hydrogels in rats*. Journal of Pharmaceutical Sciences, 2006. **95**(2): p. 462-469.
266. Krauland, A.H., D. Guggi, and A. Bernkop-Schnurch, *Oral insulin delivery: the potential of thiolated chitosan-insulin tablets on non-diabetic rats*. J Control Release, 2004. **95**(3): p. 547-55.
267. Lee, Y.H., et al., *Impact of regional intestinal pH modulation on absorption of peptide drugs: oral absorption studies of salmon calcitonin in beagle dogs*. Pharm Res, 1999. **16**(8): p. 1233-9.
268. Brannon-Peppas, L. and R.S. Harland, *Absorbent Polymer Technology*. 1990, New York: Elsevier Science Publishers. 278.
269. Gupta, P., K. Vermani, and S. Garg, *Hydrogels: from controlled release to pH-responsive drug delivery*. Drug Discov Today, 2002. **7**(10): p. 569-79.
270. Lowman, A.M. and N.A. Peppas, *Hydrogels*, in *Encyclopedia of Controlled Drug Delivery*, E. Mathiowitz, Editor. 1999, John Wiley & Sons. p. 397-418.
271. Peppas, N.A., et al., *Hydrogels in pharmaceutical formulations*. Eur J Pharm Biopharm, 2000. **50**(1): p. 27-46.
272. Hoffman, A.S., *Hydrogels for biomedical applications*. Adv Drug Deliv Rev, 2002. **54**(1): p. 3-12.
273. Peppas, N.A., et al., *Physicochemical foundations and structural design of hydrogels in medicine and biology*. Annu Rev Biomed Eng, 2000. **2**: p. 9-29.
274. Peppas, N.A., *Controlling Protein Diffusion in Hydrogels*, in *Trends and Future Perspectives in Peptide and Protein Drug Delivery*, V.H. Lee, Hashida, M., Mizushima, Y., Editor. 1995, CRC Press: Boca Raton, FL. p. 23-37.
275. Qiu, Y. and K. Park, *Environment-sensitive hydrogels for drug delivery*. Adv Drug Deliv Rev, 2001. **53**(3): p. 321-39.
276. Podual, K., F.J. Doyle, 3rd, and N.A. Peppas, *Dynamic behavior of glucose oxidase-containing microparticles of poly(ethylene glycol)-grafted cationic hydrogels in an environment of changing pH*. Biomaterials, 2000. **21**(14): p. 1439-50.

277. Mahkam, M., *Using pH-sensitive hydrogels containing cubane as a crosslinking agent for oral delivery of insulin*. J Biomed Mater Res B Appl Biomater, 2005. **75**(1): p. 108-12.
278. Antipina, A.D., Baranovsky, V. Y., Papisov, I. M., Kabanov, V. A., *Equilibrium peculiarities in the complexing of polymeric acids with polyethylene glycol*. Vysokomol. Soyed., 1972. **A14**: p. 941-949.
279. Osada, Y., Sato, M., *Thermal equilibrium of the intermacromolecular complexes of polycarboxylic acids realized by cooperative hydrogen bonding*. J Poly Sci, Poly Let Ed, 1976. **14**: p. 129-134.
280. Lowman, A.M., et al., *Oral delivery of insulin using pH-responsive complexation gels*. J Pharm Sci, 1999. **88**(9): p. 933-7.
281. Lowman, A.M. and N.A. Peppas, *Analysis of the complexation/decomplexation phenomena in graft copolymer networks*. Macromolecules, 1997. **30**(17): p. 4959-4965.
282. Peppas, N.A., *Devices based on intelligent biopolymers for oral protein delivery*. Int J Pharm, 2004. **277**(1-2): p. 11-7.
283. Peppas, N.A., et al., *Poly(ethylene glycol)-containing hydrogels in drug delivery*. J Control Release, 1999. **62**(1-2): p. 81-7.
284. Yamagata, T., et al., *Characterization of insulin protection properties of complexation hydrogels in gastric and intestinal enzyme fluids*. J Control Release, 2006. **112**(3): p. 343-9.
285. Kim, B. and N.A. Peppas, *In vitro release behavior and stability of insulin in complexation hydrogels as oral drug delivery carriers*. Int J Pharm, 2003. **266**(1-2): p. 29-37.
286. Madsen, F. and N.A. Peppas, *Complexation graft copolymer networks: swelling properties, calcium binding and proteolytic enzyme inhibition*. Biomaterials, 1999. **20**(18): p. 1701-8.
287. Morishita, M., et al., *Mucosal insulin delivery systems based on complexation polymer hydrogels: effect of particle size on insulin enteral absorption*. J Control Release, 2004. **97**(1): p. 115-24.

288. Peppas, N.A. and N.J. Kavimandan, *Nanoscale analysis of protein and peptide absorption: insulin absorption using complexation and pH-sensitive hydrogels as delivery vehicles*. Eur J Pharm Sci, 2006. **29**(3-4): p. 183-97.
289. Ichikawa, H. and N.A. Peppas, *Novel complexation hydrogels for oral peptide delivery: in vitro evaluation of their cytocompatibility and insulin-transport enhancing effects using Caco-2 cell monolayers*. J Biomed Mater Res A, 2003. **67**(2): p. 609-17.
290. Besheer, A., et al., *Loading and mobility of spin-labeled insulin in physiologically responsive complexation hydrogels intended for oral administration*. J Control Release, 2006. **111**(1-2): p. 73-80.
291. Morishita, M., et al., *Novel oral insulin delivery systems based on complexation polymer hydrogels: single and multiple administration studies in type 1 and 2 diabetic rats*. J Control Release, 2006. **110**(3): p. 587-94.
292. Perakslis, E., A. Tuesca, and A. Lowman, *Complexation hydrogels for oral protein delivery: an in vitro assessment of the insulin transport-enhancing effects following dissolution in simulated digestive fluids*. J Biomater Sci Polym Ed, 2007. **18**(12): p. 1475-90.
293. Nakamura, K., et al., *Oral insulin delivery using P(MAA-g-EG) hydrogels: effects of network morphology on insulin delivery characteristics*. J Control Release, 2004. **95**(3): p. 589-99.
294. Morishita, M., et al., *Elucidation of the mechanism of incorporation of insulin in controlled release systems based on complexation polymers*. J Control Release, 2002. **81**(1-2): p. 25-32.
295. Peppas, N.A. and J.J. Sahlin, *Hydrogels as mucoadhesive and bioadhesive materials: a review*. Biomaterials, 1996. **17**(16): p. 1553-61.

CHAPTER 3: RESEARCH GOALS

The overall goal of this research is to investigate the potential for oral insulin delivery using complexation hydrogels composed of poly(methacrylic acid – g – ethylene glycol) (P(MAA-g-EG)) hydrogels. Previous work with this material has clearly identified its potential application for oral insulin delivery, but several specific characteristics of the material remain unknown. Insulin has been unique in this preceding work in its ability to be incorporated in the hydrogel network with very high efficiency when compared to other proteins or dextrans. One of the most important aspects of this work is to investigate the interaction between insulin and P(MAA-g-EG). In doing so, the network characteristics of the hydrogel are determined and correlated to the *in vitro* behavior with insulin.

Additionally, the application of P(MAA-g-EG) loaded with insulin and insulin conjugated with polyethylene glycol (PEG) is investigated *in vivo* in rats. The purpose of the investigation with a PEG modified insulin species is two-fold: to investigate how it affects the protein-hydrogel interaction in support of earlier work and to improve the potential application *in vivo* against the enzymatic barrier in the GI tract. The specific aims of this work are:

Specific Aim # 1: To synthesize a series of P(MAA-g-EG) hydrogels, modifying and characterizing the network properties by altering the amount of difunctional PEG and monomer concentration present during polymerization

Specific Aim # 2: To perform loading and release studies from each polymer formulation with regular human insulin and insulin glargine to examine the mechanism of insulin uptake and release from P(MAA-g-EG) hydrogels *in vitro*

Specific Aim # 3: To synthesize, purify, and characterize a site-specific PheB1 mono-substituted PEG-insulin conjugate

Specific Aim # 4: To examine the *in vitro* and *in vivo* behavior of the PEGylated insulin with P(MAA-g-EG) hydrogels

CHAPTER 4: SYNTHESIS AND NETWORK STRUCTURE CHARACTERIZATION OF P(MAA-g-EG) HYDROGELS

4.1. Introduction

Hydrogels hold significant promise for protein and peptide drug delivery. The biocompatibility of both synthetic and natural hydrogels is due to their ability to imbibe large amounts of water. When used for the delivery of water soluble drugs the motility of the water through the hydrogel is paramount for determining the effectiveness of the delivery system. The relationship between hydrogel pore size and the size of the water borne drug is very important. For rigid materials, the diffusion of a solute is greatly inhibited moving through pores with diameters less than one order of magnitude greater than that of the dynamic radius of the diffusing solute [1]. In the case of hydrogels, however, such scaling relationships are less easily determined due to the movement of the hydrated polymer chains. In a model described by Peppas [2], the diffusion rate of a protein through a hydrogel decreases dramatically as the ratio of protein size to pore size increases. In order to evaluate the feasibility of using P(MAA-g-EG) hydrogels for insulin delivery, it is important to understand the properties of the structure of the polymer network.

The most important parameters defining the network structure of swollen hydrogels are the polymer volume fraction in the swollen state, $\nu_{2,s}$, average effective molecular weight of the polymer chain between crosslinks, \overline{M}_e , and network correlation length, or mesh size, ξ [3]. Mesh size is used to describe hydrogels with a crosslinked polymer backbone and is synonymous with pore size. A more detailed discussion of the calculations used to determine these values is provided in the discussion of this chapter.

The relationship between the hydrogel network characteristics and drug size is represented in Figure 4.1. In the case of P(MAA-g-EG) hydrogels, the network mesh size changes in response to the pH of the solution. At neutral pH levels the hydrogel swells to a great degree due to the lack of interpolymer complexation. Under these conditions, the MAA repeat units of the hydrogel backbone are negatively charged causing them to repel one another and they cannot form hydrogen bonds with the grafted PEG chains. In this state, the mesh size is sufficiently large to allow insulin to diffuse into and out of the network with minimal restriction. In acidic solutions, the hydrogel collapses into a highly complexed state. This is due to the protonation of the MAA repeat units of the hydrogel backbone which allows them to form hydrogen bonds with PEG as well as with other MAA groups. These hydrogen bonds form temporary crosslinks in addition to the covalent crosslinks introduced by difunctional PEG chains. Under these conditions, insulin release is severely reduced due to the drastic reduction in the network mesh size. P(MAA-g-EG) hydrogels with an equimolar ratio of ethylene glycol to methacrylic acid have exhibited the highest levels of interpolymer complexation due to hydrogen bonding between the two copolymers [4-6]. The same hydrogels repeatedly exhibited the highest efficiency of insulin retention [7, 8]. While each of these behaviors has been investigated, no attempt has been made to correlate the two. Therefore, in this work a series of P(MAA-g-EG) hydrogel formulations were polymerized and the network characteristics were determined for a range of pH levels relevant for oral insulin delivery. Additionally, modifications were made to the polymerization environment to impart network variation on the hydrogel formulations. By changing the amount of difunctional PEG or the

monomer weight fraction present during polymerization, the number and distribution of covalent crosslinks in the network was altered, irrespective of environmental pH.

4.2. Materials and Methods

4.2.1. Materials

Methacrylic acid (MAA), dimethoxy propyl acetophenone (DMPA), Sigmacote® and ethanol were purchased from Sigma-Aldrich Chemical Co. (St. Louis, MO). In this study, quinone inhibitors in MAA monomer were removed by passing it through a column packed with DE-HIBIT 200 (Polysciences, Inc., Warrington, PA). Methacrylate terminated poly(ethylene glycol) monomethacrylate monomethyl ether 1000 (PEGMA), and polyethylene glycol dimethacrylate 200 (PEGDMA) were purchased from Polysciences Inc. (Warrington, PA). The term crosslinker is used interchangeably for PEGDMA because its incorporation into the hydrogel imparts the covalently bonded crosslinks formed in the network. All chemicals were at least reagent grade.

4.2.2. Synthesis of P(MAA-g-EG) Hydrogels

Hydrogels of P(MAA-g-EG) were prepared by free-radical photopolymerization of MAA and PEGMA 1000. The MAA and PEGMA were mixed to yield a 1:1 ratio of MAA:EG units in the gel. The amount of EG units was assumed to be 22.7 moles per mole of PEGMA based on a molecular weight of the PEG chain of 1000 Da. Difunctional PEGDMA was then added to the solution in varying mol% based on the number of moles

of PEGDMA/total moles monomer (MAA and EG) in solution, as listed in Table 4.1. The mol% of PEGDMA investigated were 0.375, 0.75, 1.25, and 2.0 mol%. The monomers and crosslinker were placed into a 50 wt% mixture of ethanol in DI water and allowed to fully dissolve while stirring at 350 rpm for 30 minutes. The concentrations of the monomers were varied in this solution to alter the polymerization of the hydrogel by wt% (total weight of monomers/total weight of monomers and solvents), also described in Table 4.1. The wt% used for this study were 33, 50, and 66 wt%. The purpose of varying the mol% of PEGDMA and wt% of monomer was to alter the intrinsic crosslink density in the P(MAA-g-EG) formulations.

A photoinitiator, DMPA, was used in the amount of 1 wt% of the monomers. The solution was stirred for approximately 15 minutes to ensure complete dissolution of the initiator. Nitrogen was gently bubbled through the solution to remove dissolved oxygen, a free radical scavenger, for 15 minutes. The reaction solution was pipetted between glass slides spaced 0.8 mm apart with Teflon spacers. The glass slides were previously treated with Sigmacote, a material which forms a thin covalently bonded coating on glassware to reduce its surface energy and making it water repellent. This minimized the hydrogel adhesion to the surface of the glass slides. Photopolymerization was initiated by UV light (Ultracure 100, Efos Inc. Buffalo, NY) at 1 mW/cm^2 at 365 nm and allowed to react for 35 min. The polymerized hydrogel films were removed from the glass plates and rinsed for 1 week with deionized (DI) water (changed daily) to remove any unreacted monomer and remaining solvent. To ensure complete reaction of the monomers in the hydrogel, several samples were analyzed by Attenuated Total Reflectance – Fourier Transform Infrared spectroscopy (ATR-FTIR) measurements on a

Nicolet 560 (Madison, WI). The sample was examined as a hydrated hydrogel on a zinc selenide (ZnSe) crystal. The scanning resolution was set to 1 cm^{-1} with a total of 128 scans per sample.

4.2.3. Hydrogel swelling

Swelling experiments were performed to measure the volume fractions of the polymer and water in the hydrogel. Discs with diameters of 14 mm were cut from the hydrogel films following the rinsing in DI water. The discs were then dried under vacuum for 2 days. The dried hydrogel discs were weighed in air and heptane to determine dry polymer volume using the buoyancy technique [8]. The experimental setup can be seen in Figure 4.2. The weight of the hydrogel is taken in a cup suspended above the heptane, then while completely submerged in heptane. The volume of the disc is determined according to the following equation:

$$\text{Volume} = \frac{\text{Disc weight in heptane} - \text{Disc weight in air}}{\rho_{\text{heptane}}} \quad (\text{Eqn. 4.1})$$

The density of heptane at room temperature is 0.684 g/ml. Each disc was then isolated and placed into 20 mL of a phosphate buffered saline (PBS) solution adjusted to a specific pH. Ten pH levels were used at pH = 2.2, 2.7, 3.16, 3.71, 4.2, 4.7, 5.2, 5.6, 6.2, and 6.8. These values encompass the pH levels defined by the U.S. Pharmacopeia for gastric fluids at pH = 2.2 and for intestinal fluids at pH = 6.8 [9]. Each disc was allowed to swell over 48 hours, changing the buffer after 4 and 24 hours. The volume of the swollen disc was measured after swelling for 4, 24 and 48 hours. The polymer volume fraction of the hydrogel could be found by comparing the dry polymer volume to that of

the swollen polymer volume, assuming that any difference in volume was due to imbibed water, according to equation 4.2.

$$v_{2,s} = \frac{\text{volume of dry polymer}}{\text{volume of swollen gel}} = \frac{V_p}{V_{gel}} = \frac{1}{Q} \quad (\text{Eqn. 4.2})$$

4.2.4. Mechanical Testing

Rubber elasticity experiments were conducted to characterize the network structure of the swollen hydrogel. The rinsed hydrogel films were cut into strips roughly 5 mm wide and a minimum of 30 mm long. These hydrogel strips were then swollen in PBS buffers at the same pH levels used for swelling experiments. They were allowed to swell for 48 hours, refreshing the buffer after 24 hours. The swollen sample dimensions were then measured with calipers prior to testing the tensile stress with a gauge length of 20 mm. Each strip was stretched up to 15% strain at 10% strain per minute using an automated materials tensile testing system with a 5 N load cell (Instron Model 4442, Park Ridge, IL). The samples were tested at 37°C submerged in PBS at the same pH of the swelling buffer. A custom-made testing apparatus was used which made the effects of buoyancy negligible. A diagram of the setup can be seen in Figure 4.3. The reservoir buffer is maintained at 37 °C in a vacuum flask which is sealed and connected to the water bath by an air tight seal. This way the buffer from the water bath can be removed between samples using a vacuum created by the 3-way bulb so the temperature of the buffer can reach equilibrium at 37 °C and the hydrogel sample can be changed. The water bath itself is a tube which slides up and down the lower testing arm along a water tight washer to allow access to the grips which hold the sample in place.

4.2.5. Gel Permeation Chromatography

The number average molecular weight of the linear polymer chains in the absence of crosslinks, \overline{M}_n , was determined using gel permeation chromatography (GPC). The polymers were synthesized by the same procedure described for P(MAA-g-EG) hydrogels, except that all PEGDMA 200 was omitted to prevent covalent crosslinking of the polymers. After photopolymerization, the polymer was present as a highly viscous solution. These samples were not technically hydrogels, because at this point there were no crosslinks present in the polymer. Each solution was dispersed at a concentration of 1 mg/ml polymer in PBS based on the initial polymer fraction of the solution and dissolved overnight at 80°C. Once in solution, the samples were injected onto a Waters Ultrahydrogel Linear® column (Milford, MA) in PBS at pH = 7.4 with an isocratic flow of 0.7 mL/min. The eluent from the column was passed through a Waters 410 refractive index detector (Milford, MA). The unknown values for \overline{M}_n of the P(MAA-g-EG) samples were determined by comparing to PEG standards with known molecular weight and polydispersity indices. Because the backbone of the samples are MAA, the values measured were adjusted based on the discrepancy found when running MAA standards of known molecular weight and polydispersity as experimental samples against the PEG standards.

4.3. Results and Discussion

4.3.1. Hydrogel Synthesis

The FTIR spectrum of a polymerized P(MAA-g-EG) hydrogel is shown in Figure 4.4. Each of the hydrogel formulations exhibited a similar ATR-FTIR spectrum. The spectrum clearly exhibits the most prominent peaks of the copolymer with stretching at 2923, 1695, and 1082 cm^{-1} , indicative of C-H, COOH, and C-O bonds, respectively. Absent is the stretching at 1490-1680 cm^{-1} , which would be exhibited if unsaturated carbon-carbon double bonds were present from unreacted methacrylate groups. These results were taken after rinsing the hydrogel samples for 7 days in DI water. If any unreacted monomers were present after polymerization, this spectrum indicates that they were effectively removed by this washing method.

The hydrogel polymerized with 0.375 mol% PEGDMA and 33 wt% monomer had such low mechanical strength that films could not be removed from the mold without destroying them, so they were discarded. The hydrogels with 0.75 mol% PEGDMA and 33 wt% monomer and 0.375 mol% PEGDMA and 50 wt% monomer could be removed from the molds and used for insulin loading and release studies; however, they did not have enough mechanical integrity to be tested for swelling and mechanical data without destroying the hydrogel. The other 9 formulations were tested to the full extent of this study. The macroscopic behavior of the three samples described above is indicative that they did, in fact, have the lowest crosslink density, as was expected and presented in Table 4.1. Future references to individual hydrogel formulations use the numbers for the mol% of PEGDMA and wt% monomer represented as a ratio (e.g. 0.375/50).

4.3.2. P(MAA-g-EG) Swelling

The value of $\nu_{2,s}$, the equilibrium polymer volume fraction of the swollen gel, and its inverse, Q , the equilibrium volume swelling ratio, is determined through equilibrium swelling experiments according to equation 4.2. These swelling measurements are indicative of the molecular changes occurring in the P(MAA-g-EG) hydrogel. Each hydrogel formulation exhibited the expected pH responsive swelling behavior. The values for $\nu_{2,s}$ decreased with increasing pH. The results for two sample formulations can be seen in Figure 4.5. These formulations were polymerized with 0.75 or 2.0 mol% PEGDMA with 66 wt% monomer and are referred to as 0.75/66 and 2.0/66.

The largest change in $\nu_{2,s}$ for these two samples occurred when the pH of the PBS was between 5.6 and 6.2. Each tested P(MAA-g-EG) formulation exhibit a similar pH dependent transition in the same range (data not shown). The inflection points of the curves indicate that the pKa of the hydrogel is roughly 5.8-6.0. This is dissimilar from previously reported values of the pKa of P(MAA-g-EG) hydrogels at pH = 4.8 [10, 11], which are based on the referenced value for the pKa of MAA. Some investigators concluded that the pKa of this material is at pH = 4.8 [8]. Others report findings that more closely match those presented in this study for pKa [6, 7, 12]. There is one particular difference in technique that could account for this variation. The hydrogel discs in this study were allowed to swell for 48 hours prior to determining the “equilibrium” swelling. In this study the hydrated discs may not have actually achieved equilibrium in the 48 hours allotted. Some previous methods measured the volume of each disc every 24 hours until it changed by less than 5 % over a 48 hour period, such that the samples were actually at equilibrium. With that in mind, the reason that the hydrogels were only

swollen for 48 hours in this work is due to the intended application of the material for oral insulin delivery. Upon oral ingestion, the residence time of food in the stomach of humans is generally only 2-4 hours prior to gastric emptying into the small intestine [13, 14]. The 48 hour swelling is roughly the amount of time that an ingested sample would remain within the entire gastrointestinal tract. Therefore, all hydrogel swelling was performed for only 48 hours.

4.3.3. P(MAA-g-EG) Mechanical Testing

The hydrogel mechanical testing exhibited similar characteristics as that of the swelling studies. For all formulations of P(MAA-g-EG) examined, the values for the normalized tensile modulus decreased with increasing pH. The results from two sample formulations are shown in Figure 4.6. The normalized tensile modulus, G , is described by the following equation:

$$G = \frac{\tau}{\alpha - 1/\alpha^2} \nu_{2,s}^{1/3} \quad (\text{Eqn. 4.3})$$

The value for G is the same as the left side of Equation 4.4 multiplied by the equilibrium volume swelling ratio of the polymer ($\nu_{2,s}$) raised to the 1/3 power. This additional value normalizes the tensile stress based on the amount of polymer present based on swelling results in the one dimensional direction of the strain [15]. For the two results in Figure 4.6, the greatest drop in G occurs between pH of 5.2 and 6.2. This transition point was seen for all formulations indicating the loss of interpolymer complexation between MAA and PEG chains with increasing pH across the pKa of the material. These results corroborate the swelling tests which exhibited a large change in behavior over the same pH range.

4.3.4. P(MAA-g-EG) Gel Permeation Chromatography

This marks the first time in the investigation of P(MAA-g-EG) hydrogels in our lab that the values for \overline{M}_n were determined experimentally using GPC. Previous characterization used theoretical calculations based on the polymerization kinetics described [8, 16]. By directly measuring the value for \overline{M}_n using experimental techniques a more accurate model for the network properties of P(MAA-g-EG) hydrogels can be created.

The results of the values found for the average molecular weight of the polymer in the absence of covalent crosslinks, \overline{M}_n , can be seen in Table 4.2. The values were a significantly higher than those previously reported based on theoretical calculations [6]. The molecular weights of the samples were measured against PEG standards and then adjusted based on PMAA standards run as unknown samples against the same PEG standards. All subsequent calculations requiring values for \overline{M}_n used the average values listed in Table 4.2. The difference is given as the percentage decrease from the experimentally determined values for \overline{M}_n .

The theoretical calculations for \overline{M}_n make several assumptions which most likely account for the difference between experimental and theoretical values. Most importantly, theoretical values assume that the free radical polymerization is for a linear polymer chain. The polymer chains are linear, but the presence of the PEG grafts introduced by PEGMA significantly increases the actual molecular weight of the polymer chain. As the weight fraction of the monomers in solution decreases, the average

molecular weight also decreases and the effect of the PEG grafts becomes more prominent as shown by the higher variance from theoretical calculations.

4.3.5. Network Modeling and Characterization

By combining the results of the swelling, mechanical, and GPC testing, the network properties of P(MAA-g-EG) hydrogels can be modeled. The determination of \overline{M}_e and ξ is described by Peppas and Merrell [17] in a model based on Flory's theory of rubber elasticity [18]. The value for \overline{M}_e is found from the following equation:

$$\frac{\tau}{(\alpha - 1/\alpha^2)} = RT\rho_{2,r} \left(\frac{1}{\overline{M}_e} - \frac{2}{\overline{M}_n} \right) \left(\frac{\nu_{2,s}}{\nu_{2,r}} \right)^{1/3} \quad (\text{Eqn. 4.4})$$

where τ is the tensile stress, $\rho_{2,r}$ is the density of the gel in the relaxed state, α is the normalized elongation of the sample,

$$\alpha = \frac{(l - l_o)}{l_o} \quad (\text{Eqn. 4.5})$$

$\nu_{2,r}$ is the polymer volume fraction of the gel in the relaxed state, R is the ideal gas constant, and \overline{M}_n is the average molecular weight of linear polymer chains in the absence of a crosslinker. The values for $\nu_{2,r}$ were assumed to be 0.33, 0.5 and 0.67 for polymers made with 33, 50, and 67 wt% monomers, respectively. The mesh size of the polymer network is calculated using the value determined for \overline{M}_e as,

$$\xi = l\nu_{2,s}^{-1/3} \left(\frac{2C_n\overline{M}_e}{M_o} \right)^{1/2} \quad (\text{Eqn. 4.6})$$

in which C_n is the Flory characteristic ratio (PMAA = 14.6) [19], l is the carbon-carbon chain length (1.54 Å), and M_o is the molecular weight of the polymeric repeat unit.

Methacrylic acid was used as the monomer for this calculation because it is the backbone of P(MAA-g-EG) hydrogels. The mesh size is the simplest way to represent the structure of the hydrogel. For environmentally responsive hydrogels, the values of the characteristics used to describe the hydrogel change in response to the conditions of their surroundings. The amount of crosslinking in the hydrogel depends on both the covalent crosslinks and temporary hydrogen bond stabilized crosslinks. When highly complexed at low pH, the values of \overline{M}_e and ξ are the lowest observed for each formulation due to the addition of the temporary crosslinks. When these bonds are lost at neutral pH levels, the values for \overline{M}_e and ξ are the highest for each formulation and are only dependent on the covalent crosslinks.

Results for the effective molecular weight between crosslinks and the mesh size of two sample formulations are shown in Figure 4.7. These two formulations exhibit a pH dependent increase for both \overline{M}_e and ξ with the largest change occurring between pH of 5.6 and 6.2. This again suggests that the pKa of the P(MAA-g-EG) hydrogels is 5.8-6.0. The two formulations have average network mesh sizes of 8 and 10 nm at pH \leq 4.7 for the samples polymerized with 2.0 and 0.75 mol% PEGDMA, respectively. The mesh sizes increased to 16 and 19 nm at pH = 6.8 with the greatest increase occurring between pH = 5.6 and 6.2 for the same formulations. The values of ξ for all formulations are represented in Figure 4.8. While the differences in swelling and mechanical characteristics were significantly affected by changes in the hydrogel formulations, this was not apparent for ξ . The reason for this is that the values for ξ are dependent on $\nu_{2,s}$ to the $-1/3$ power and τ to the $1/2$ power. Therefore, changes in these values have a reduced

effect on ξ , which may be important when considering the use of this hydrogel for oral insulin delivery.

4.4. Conclusions

A total of eleven P(MAA-g-EG) hydrogel formulations were polymerized using UV light initiated polymerization. The polymerization was confirmed using ATR-FTIR following a 7 day rinsing process. Of the eleven formulations, nine were tested for hydrogel swelling and mechanical properties. The hydrogels exhibited pH responsive swelling in which they were minimally swollen by PBS buffer below pH = 5.2 and highly swollen above pH = 6.2. The values for $\nu_{2,s}$ represent this swelling behavior. The apparent pKa of the material was 5.8-6.0 based on the inflection point of the chart for $\nu_{2,s}$. The normalized tensile moduli also exhibited a pH dependent decrease in value as the pH of the swelling buffer was increased through the apparent pKa of the hydrogel. The values for \overline{M}_n determined by GPC were significantly larger than theoretical values used in previous investigations. Using the results from each of these experiments, \overline{M}_e and ξ were calculated. In the same fashion as the swelling and mechanical data, the values for \overline{M}_e and ξ increased with increasing pH and exhibited a similar transition point based on pH. However, the characteristic length scale of the hydrogel mesh size did not vary greatly between each formulation.

Table 4.1. Formulations of polymerization conditions for the series of P(MAA-g-EG) hydrogels considered. Changes expected in the hydrogel network are indicated by the blue arrow.

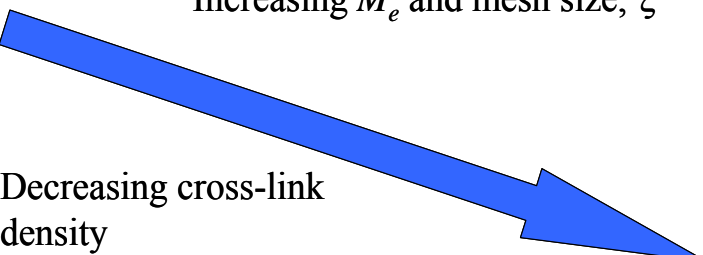
		Monomer fraction (wt%)		
		66 wt%	50 wt%	33 wt%
PEGDMA (200) (mol%)	2.00%	 <p>Increasing M_e and mesh size, ξ</p> <p>Decreasing cross-link density</p>		
	1.25%			
	0.75%			
	0.375%			

Table 4.2. The effective molecular weight of P(MAA-g-EG) chains in the absence of covalent crosslinks determined by GPC (\pm S.D., n = 3)

Monomer fraction	Experimental	Theoretical	% difference
66 wt%	24930 \pm 1160	16334	34.50%
50 wt%	19370 \pm 330	11550	40.40%
33 wt%	16150 \pm 750	8168	49.40%

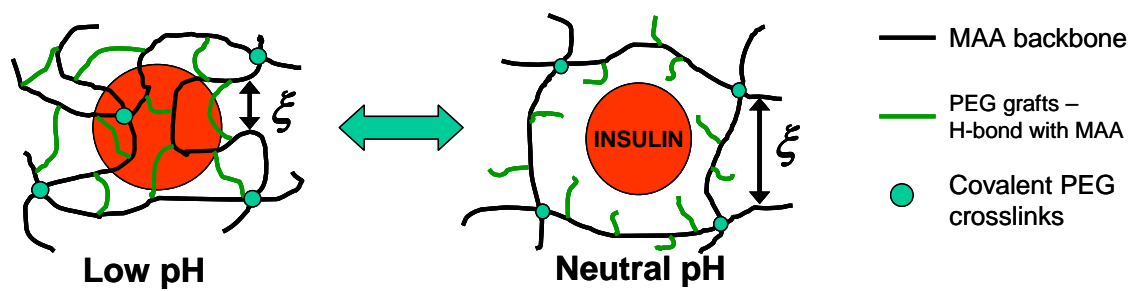


Figure 4.1. Schematic of p(MAA-g-EG) hydrogel and its pH dependent swelling behavior

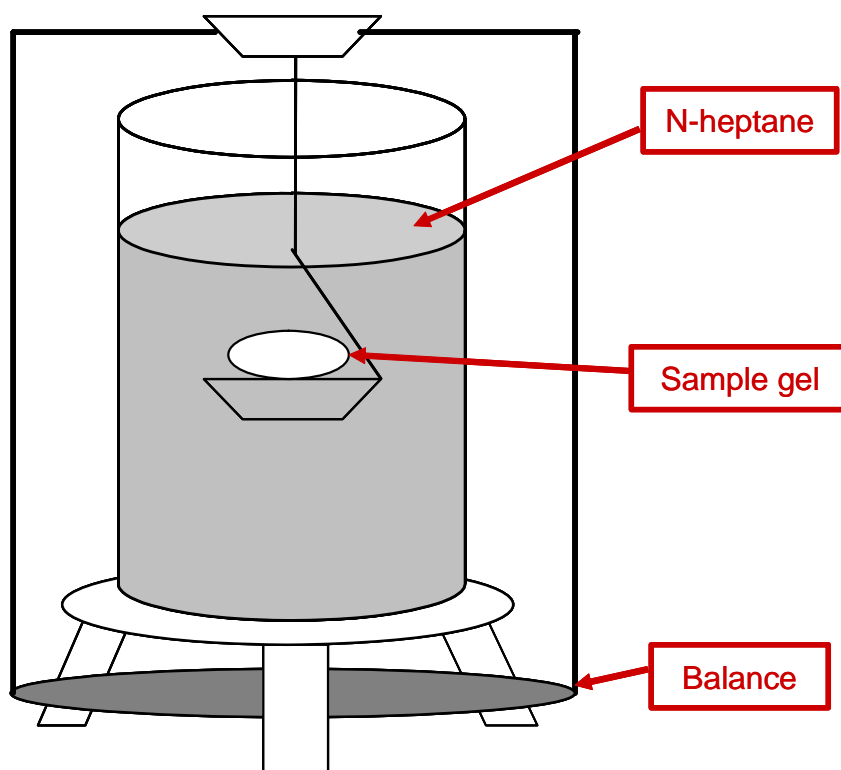


Figure 4.2. Hydrogel density determination using the buoyancy technique

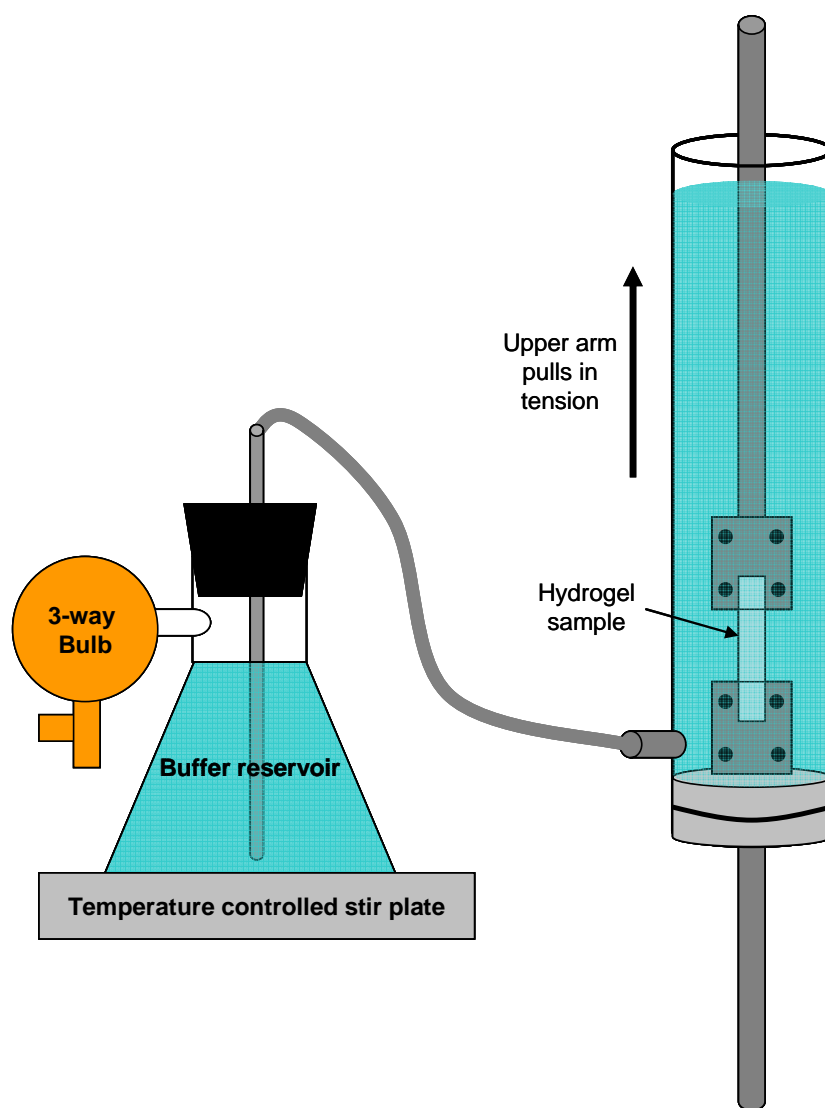


Figure 4.3. Experimental setup for tensile testing of hydrated hydrogel strips in a custom made water bath at 37°C.

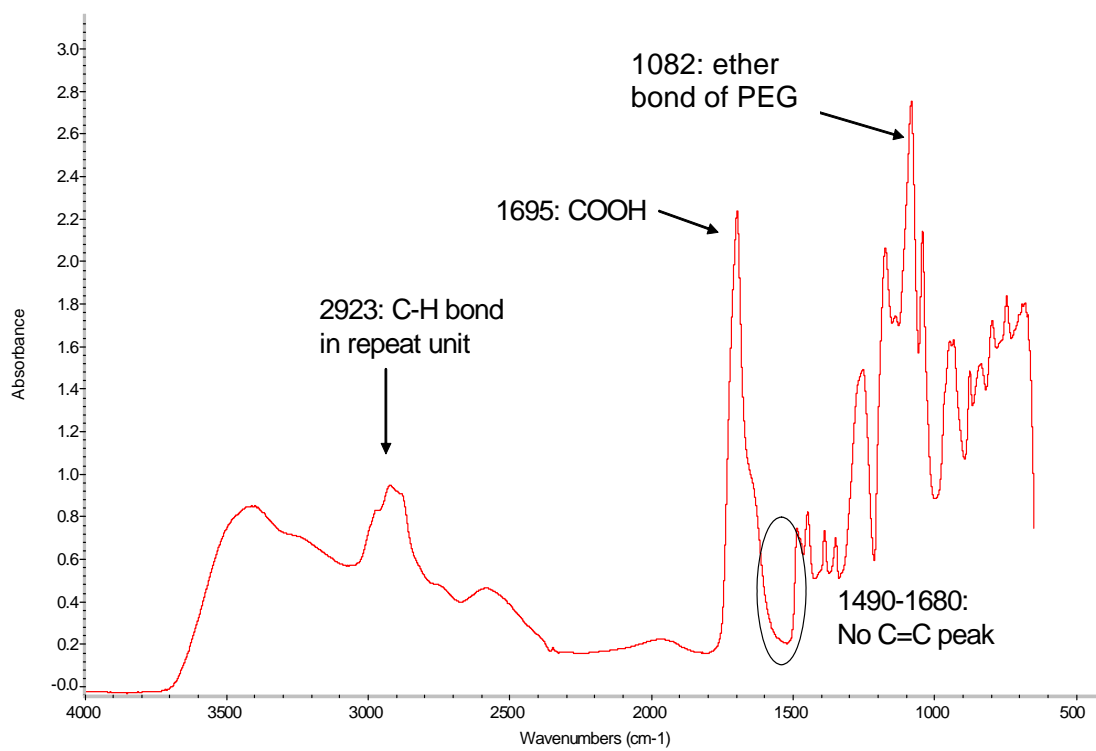


Figure 4.4. FTIR-ATR spectra of a polymerized, hydrated P(MAA-g-EG) hydrogel sample

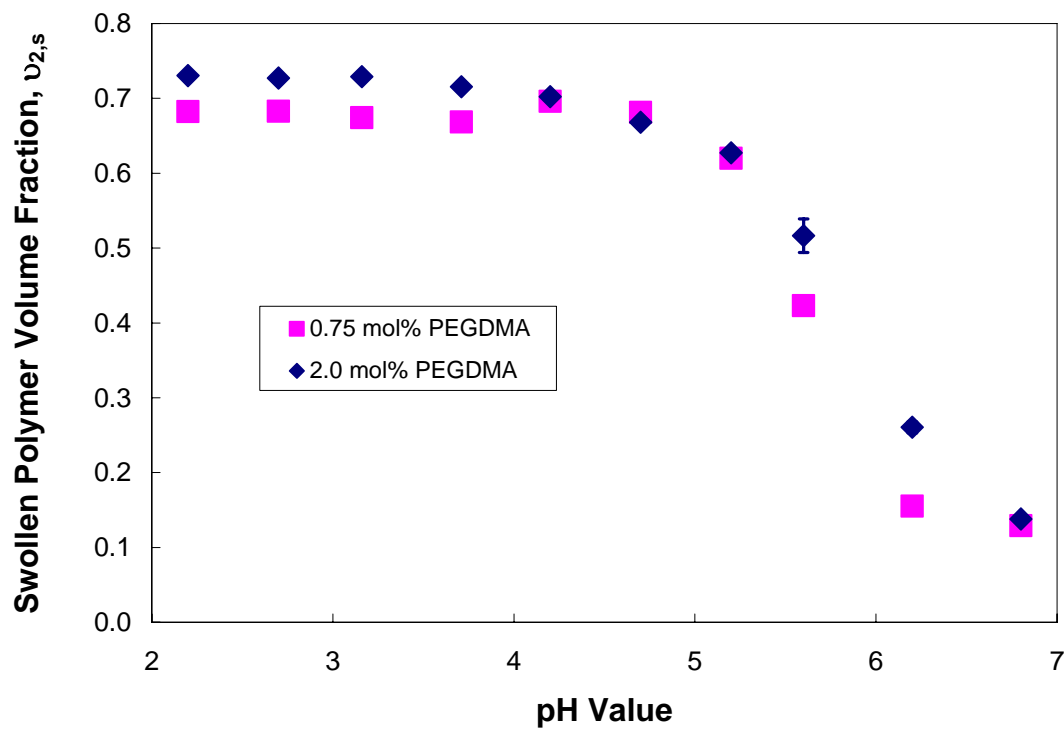


Figure 4.5. Equilibrium polymer volume fraction for two P(MAA-g-EG) hydrogel formulations polymerized with 50 wt% monomer following 48 hours of swelling in PBS (\pm S.D., $n = 3$)

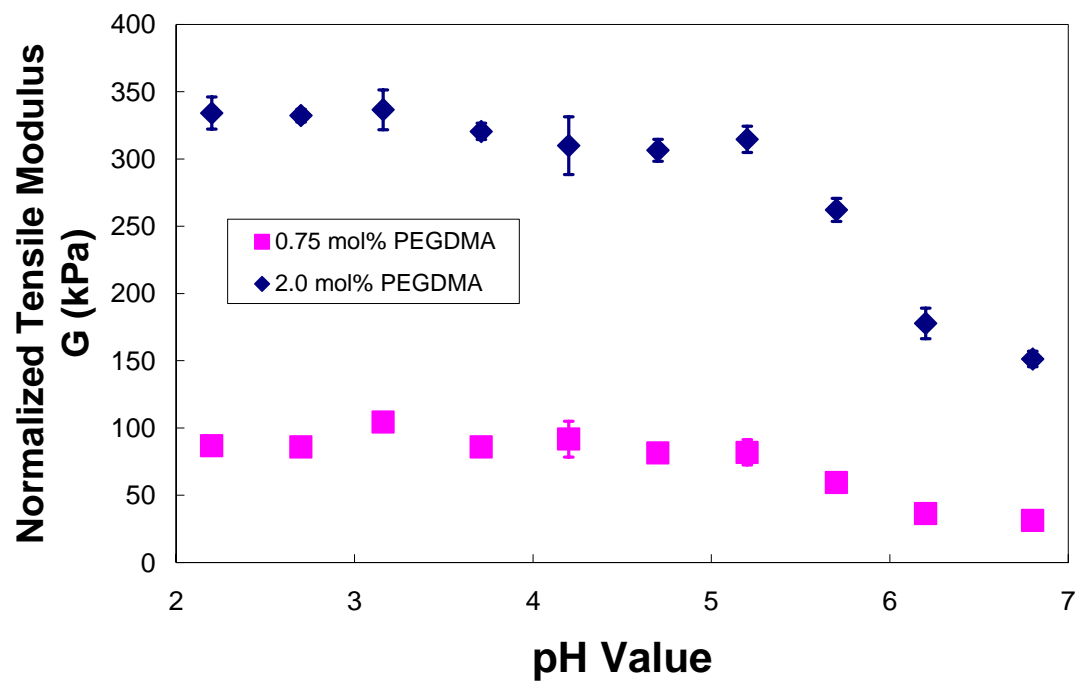


Figure 4.6. Normalized tensile moduli for two P(MAA-g-EG) hydrogel formulations polymerized with 50 wt% monomer following 48 hours of swelling in PBS (\pm S.D., $n = 3$)

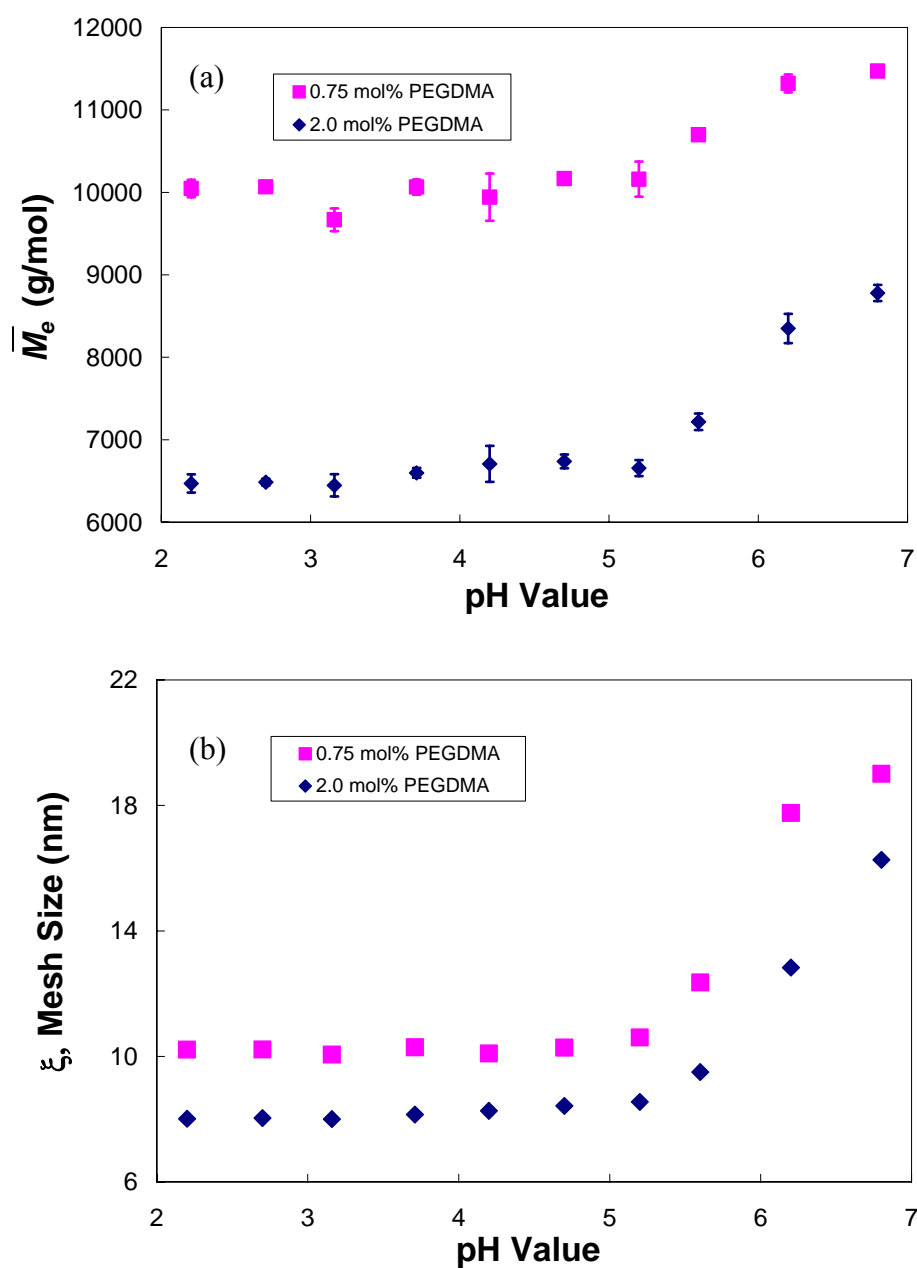


Figure 4.7. (a) The modeled average effective molecular weight between crosslinks, \bar{M}_e , and (b) network correlation length, ξ , for two P(MAA-g-EG) hydrogel formulations polymerized with 50 wt% monomer (\pm S.D., $n = 3$)

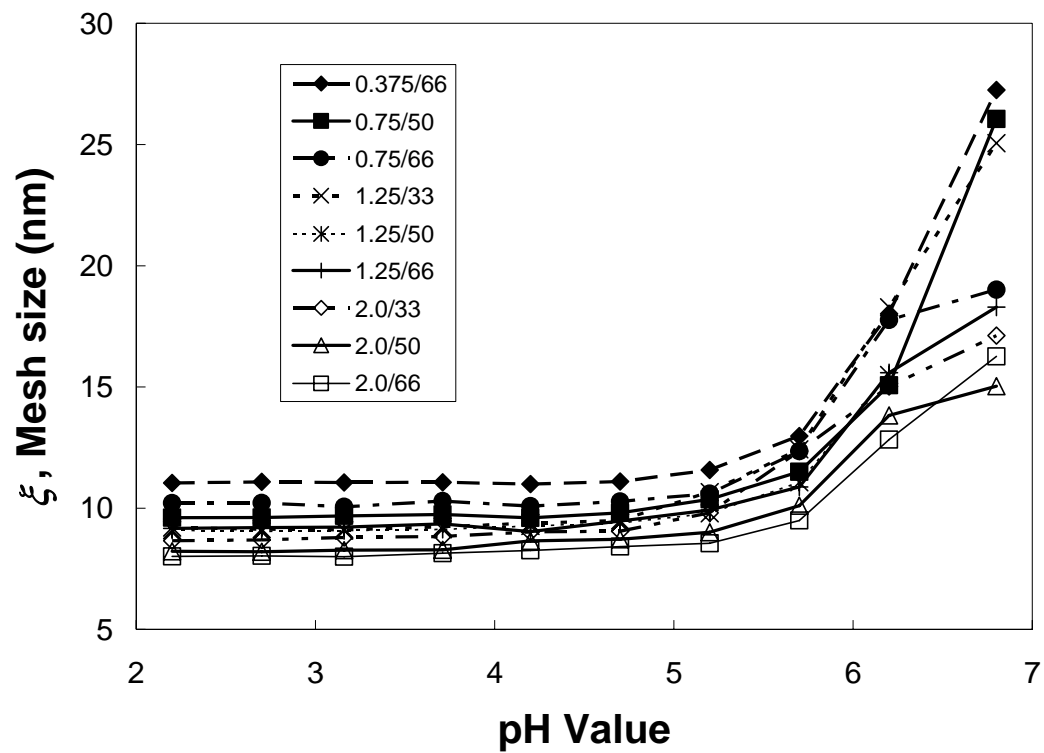


Figure 4.8. The modeled network correlation length, or mesh size, ξ , for all formulations tested in swelling and tensile studies

4.5. References

1. Kathawalla, I.A. and J.L. Anderson, *Pore size effects on diffusion of polystyrene in dilute solution*. Ind Eng Chem Res, 1988. **27**: p. 866-871.
2. Peppas, N.A., *Controlling Protein Diffusion in Hydrogels*, in *Trends and Future Perspectives in Peptide and Protein Drug Delivery*, V.H. Lee, Hashida, M., Mizushima, Y., Editor. 1995, CRC Press: Boca Raton, FL. p. 23-37.
3. Lowman, A.M. and N.A. Peppas, *Hydrogels*, in *Encyclopedia of Controlled Drug Delivery*, E. Mathiowitz, Editor. 1999, John Wiley & Sons. p. 397-418.
4. Peppas, N.A., et al., *Physicochemical foundations and structural design of hydrogels in medicine and biology*. Annu Rev Biomed Eng, 2000. **2**: p. 9-29.
5. Morishita, M., et al., *Elucidation of the mechanism of incorporation of insulin in controlled release systems based on complexation polymers*. J Control Release, 2002. **81**(1-2): p. 25-32.
6. Nakamura, K., et al., *Oral insulin delivery using P(MAA-g-EG) hydrogels: effects of network morphology on insulin delivery characteristics*. J Control Release, 2004. **95**(3): p. 589-99.
7. Madsen, F. and N.A. Peppas, *Complexation graft copolymer networks: swelling properties, calcium binding and proteolytic enzyme inhibition*. Biomaterials, 1999. **20**(18): p. 1701-8.
8. Lowman, A.M. and N.A. Peppas, *Analysis of the complexation/decomplexation phenomena in graft copolymer networks*. Macromolecules, 1997. **30**(17): p. 4959-4965.
9. *The United States Pharmacopeia. The National Formulary*. 20 ed. 1995, Rockville, MD: United States Pharmacopeial Convention, Inc.
10. Peppas, N.A. and N.J. Kavimandan, *Nanoscale analysis of protein and peptide absorption: insulin absorption using complexation and pH-sensitive hydrogels as delivery vehicles*. Eur J Pharm Sci, 2006. **29**(3-4): p. 183-97.
11. Blanchette, J. and N.A. Peppas, *Cellular evaluation of oral chemotherapy carriers*. J Biomed Mater Res A, 2005. **72A**(4): p. 381-8.

12. Lopez, J.E. and N.A. Peppas, *Effect of poly (ethylene glycol) molecular weight and microparticle size on oral insulin delivery from P(MAA-g-EG) microparticles*. Drug Dev Ind Pharm, 2004. **30**(5): p. 497-504.
13. Proano, M., et al., *Transit of solids through the human colon: regional quantification in the unprepared bowel*. Am J Physiol, 1990. **258**(6 Pt 1): p. G856-62.
14. Camilleri, M., et al., *Human gastric emptying and colonic filling of solids characterized by a new method*. Am J Physiol, 1989. **257**(2 Pt 1): p. G284-90.
15. Treloar, R.G., *The Physics of Rubber Elasticity, 2nd Edition*. 1958, Oxford: Oxford University Press.
16. Odian, G., *Principles of Polymerization, 4th Edition*. 2004, New York: John Wiley & Sons.
17. Peppas, N.A. and E.W. Merrill, *Crosslinked poly(vinyl Alcohol) hydrogels as swollen elastic networks*. Journal of applied polymer science, 1977. **21**(7): p. 1763-1770.
18. Flory, P.J., *Principles of Polymer Chemistry*. 1953, Cornell, NY: Cornell University Press. 688.
19. Brandrup, J., Immergut, E. H., Grulke, E. A., Abe, A., Bloch, D. R., ed. *Polymer Handbook (4th Edition)*. 4 ed. 1999, John Wiley & Sons.

CHAPTER 5: *IN VITRO* ELUCIDATION OF INSULIN UPTAKE AND RELEASE MECHANISM FROM P(MAA-g-EG) HYDROGELS

5.1. Introduction

Many studies have investigated the effectiveness for oral insulin delivery with P(MAA-g-EG) hydrogels based on the *in vitro* behavior of insulin release. While the first of these studies were performed nearly 10 years ago [1, 2], each subsequent study has repeated much of the same proof: insulin can be efficiently maintained within the hydrogel at low pH levels ($\text{pH} < 3.2$) and released upon exposure to neutral pH levels ($\text{pH} > 6.5$) [3-10]. This pH responsive behavior is the primary reason that P(MAA-g-EG) has potential for oral insulin delivery. However, none of these studies make any attempt to correlate the hydrogel network properties, namely the network mesh size, to the ability of the material to control insulin release. With the large body of research concerning this hydrogel, this information may be critical to be able to optimize the drug delivery system for insulin, as well as other potential protein and peptide drugs.

As discussed in the conclusions of the preceding chapter, the network mesh size exhibited pH responsive changes with an apparent pK_a of P(MAA-g-EG) at 5.8-6.0. The changes in the mesh size, however, were not as profound as expected and do not adequately explain the *in vitro* behavior which has been seen with these hydrogels. The hydrodynamic radius of insulin is between 1.3-2.7 nm, depending on its quaternary structure [11-13]. The hydrogel network mesh size is more than one order of magnitude larger than the hydrodynamic radius of insulin when completely uncomplexed at $\text{pH} = 6.8$, allowing it to be released from the network. However, the network mesh size is also significantly larger than insulin at $\text{pH} \leq 4.7$ for all of the P(MAA-g-EG) formulations

tested. According to the hydrogel diffusion model reported by Peppas [14], when the characteristic ratio of the hydrodynamic radius of insulin divided by the radius of the pore (referred to here as mesh size) is 0.25, the diffusion rate should be roughly 20% that of free diffusion in solution. Based on these values, insulin should be released to a great extent even when these hydrogels are highly complexed at pH levels below the pKa of the material. However, reported insulin retention efficiencies in P(MAA-g-EG) hydrogels remain near 100%, much higher than what is expected based on the network mesh size. This retention was not nearly as efficient for alternative model drugs [15]. This suggests that diffusion rates may only be partially responsible for insulin loading and release, and additional factors may be important to understand the *in vitro* behavior of the hydrogel with insulin.

A greater understanding of the interaction between insulin and P(MAA-g-EG) hydrogels can be achieved by carefully examining the differences between native insulin and other protein drugs. Insulin glargine is an insulin analog in which a glycine replaces the native asparagine residue at the A21 residue and two arginine residues are attached to the C-terminus of the B chain [16]. This has the effect of shifting the isoelectric point (pI) of the molecule to from 5.2 for native human insulin to 6.7 for insulin glargine, making it the least soluble near neutral conditions. In solutions at pH levels below the pI, the protein is protonated and has a slight positive charge; in solutions at pH levels above the pI, the protein is deprotonated and has a slight negative charge. The purpose of this modification for clinical use is to make the protein crystallize following a subcutaneous bolus injection. The insulin glargine slowly dissolves into the bloodstream by zero order kinetics giving a very steady baseline level of insulin for at least 24 hours [16]. It is

currently produced by Sanofi-Aventis under the trade name Lantus®. For the purposes of this study, the shift in the pI allows the study of two insulin species with different ionization characteristics. If ionic interactions are the leading cause for insulin uptake and release from P(MAA-g-EG) then a difference in release profiles should be apparent between the pI levels of the two proteins. The major benefit of comparing insulin glargine to human insulin is that they are nearly identical with the one major difference of isoelectric point. They have nearly identical tertiary structure, they have nearly the same molecular weight and hydrodynamic radius, and since insulin glargine is derived from human insulin the changes were considered negligible for the purposes of this study. A side by side comparison of the two proteins is given in Table 5.1.

The focus of this work was to examine the loading and release characteristics of insulin and insulin glargine with P(MAA-g-EG) using *in vitro* techniques. By combining these results with those of the network characteristics determined in Chapter 4, the threshold for insulin release should be able to be determined as a function of mesh size. Alternatively, if other interactions between P(MAA-g-EG) hydrogels and insulin are the driving cause for uptake and release of insulin from the hydrogel, that should also be apparent.

5.2. Materials and Methods

5.2.1. Materials

Phosphate buffered saline (PBS), Sigmacote® ammonium bicarbonate (NH_4HCO_3), and acetonitrile were purchased from Sigma Aldrich (St. Louis, MO).

Spectrapor® 6 dialysis tubing was purchased from Fisher Scientific (Hampton, NH). Recombinant human insulin was purchased from Seracare Diagnostics (Milford, MA). Insulin glargine was purified from the pharmaceutical preparation of Lantus®, which was purchased from Sanofi Aventis (Bridgewater, NJ).

5.2.2. Human Insulin Loading

Insulin loading studies with recombinant human insulin were performed with all 11 formulations of P(MAA-g-EG) described in Chapter 4 to make insulin loaded polymer (ILP) samples. Rinsed hydrogel films were dried under vacuum and then crushed into a fine powder first using a mill grinder followed by manual grinding with a mortar and pestle. The powder was passed through a sieve with a mesh size of 45 μm with gentle mixing. Hydrogel particles of this size exhibited the greatest amount of insulin absorption *in vivo* following ileal administration in rats [3].

All of the glassware used for insulin loading was treated with Sigmacote® to prevent insulin adsorption on the glass wall. An insulin solution with a concentration of 500 $\mu\text{g/mL}$ in PBS at $\text{pH} = 7.4$ was prepared. The crushed P(MAA-g-EG) particles (140 mg) were dispersed into 20 mL of the human insulin solution at 37°C and stirred at 300 rpm. After 4 hours, 10 mL of 0.1M HCl was added to the solutions to collapse the hydrogel network. The collapsed hydrogel samples were recovered by filtration using filter paper with a 0.6 μm pore size and rinsed with 50 mL of 0.1 M HCl and 50 mL of DI-water to remove any surface bound protein. Each sample was then frozen and lyophilized to remove residual water. Samples were kept at -20°C until needed.

The total weight of insulin present was calculated using the concentration and the total volume of solution. Insulin incorporation efficiency was determined based on the ratio of insulin remaining in the wash solutions to the initial insulin in the loading solution. The weight fraction of insulin in a given ILP batch was then calculated based on the total amount of insulin loaded according to equation 5.1.

$$\text{ILP loading \%} = \frac{\text{mg insulin loaded}}{\text{mg polymer} + \text{mg insulin loaded}} \times 100\% \quad (\text{Eqn. 5.1})$$

Aliquots of 0.2 ml of solution were taken using a 1 ml syringe with a 0.45 μm filter. In order to determine the insulin concentration in solution, reversed phase high performance liquid chromatography (RP-HPLC) was used. A mixture of water (mobile phase A) and acetonitrile (mobile phase B) with 0.1 % TFA (v/v) was used as the mobile phase on a Waters Spherisorb® C8 column (5 μm , 4.6 x 250 mm). Samples of 50 μl were injected to Waters 2695 separations module equipped with a 996 Photodiode Array detector (Milford, MA) at a 1 mL/min. A gradient from 35-65 % mobile phase B was run for 30 minutes. Concentrations were determined based on the area under the curve compared to insulin standards with detection at 214 nm. Average elution time was 6.5 minutes.

5.2.3. Insulin Glargine Loading

Prior to working with insulin glargine, it had to be isolated from the pharmacological preparation which included glycerol, zinc, m-cresol, and insulin glargine. Purification was performed by dialysis using a regenerated cellulose membrane with a molecular weight cutoff (MWCO) of 3500 Da against 0.01M NH_4HCO_3 for 2 days. The protein crashed out of solution at the neutral pH and all other solutes were

removed. The dialysate was changed 3 times daily. The crystalline protein was removed from the dialysis membrane, frozen and lyophilized.

The insulin glargine loading studies were performed using the lyophilized powder to make glargine insulin loaded polymer (GILP) in a similar method as regular human insulin loaded polymer samples. However, because the pI of insulin glargine is so close to the loading pH for native human insulin (pH = 7.4), the loading solution was maintained at pH = 9.5. The rest of the loading protocol remained the same as that for native human insulin. For the study with insulin glargine, only 4 hydrogel formulations were considered due to limited availability of the protein. The formulations considered were 0.75/33, 0.75/66, 2.0/33, and 2.0/66 where ratio indicates the mol% of PEGDMA/monomer weight% present during polymerization. These formulations were chosen because they represent a wide variation in crosslink density of P(MAA-g-EG) hydrogels. Insulin glargine concentrations were determined using RP-HPLC using the same mobile phases as that for native insulin with a gradient from 40-55 %B over 25 minutes at a flow rate of 0.8 mL/min. The areas of the peaks with detection at 214 nm were compared with insulin glargine standards with an average elution time of 13 minutes.

5.2.4. Insulin Release Studies

Release studies for human insulin were performed using jars treated with Sigmacote® to minimize insulin absorption. For each P(MAA-g-EG) formulation, 10 mg of ILP was dispersed into 20 mL PBS at 37 °C at pH = 2.7, 3.7, 4.7, 5.6, and 6.8. The solutions were stirred at 300 rpm and 0.2 mL aliquots were withdrawn using a syringe

equipped with a 0.45 μm syringe filter at set time intervals. To maintain a constant release volume and ensure complete maintenance of polymer suspended in solution, the 0.2 ml samples were replaced with 0.2 ml of fresh PBS at the particular release pH by backflushing through the syringe filter. The protein concentration was determined using RP-HPLC as previously described, and insulin release was represented as the ratio of measured insulin release to the theoretical maximum insulin release.

5.2.5. Insulin Glargine Release Studies

Release studies for insulin glargine loaded polymer samples were performed using jars treated with Sigmacote®. The release studies with were performed at pH = 4.7, 5.6, 6.2, 6.8 and 7.4. In this range the ionization of the analog should be distinct from that of native human insulin. Additional release studies had to be performed with native insulin at pH = 6.2 to supplement to previous results. Insulin glargine concentrations were determined using RP-HPLC as previously described.

5.3. Results and Discussion

5.3.1. Human Insulin Loading

The average insulin loading efficiencies for each formulation of P(MAA-g-EG) considered are listed in Table 5.2. The values for insulin loading efficiency range from 42.7 to 84.9 % of insulin from solution which is loaded into the hydrogel. For each column and row of Table 5.2, the loading efficiencies increase with increasing monomer wt% or with increasing PEGDMA present during polymerization of the hydrogel

formulation, though some of the differences are statistically insignificant. This trend was exhibited for all formulations to varying extents.

The insulin loading efficiency of P(MAA-g-EG) tended to increase with increasing crosslink density. In comparing Tables 4.1 and 5.2, this is quite clear. These results indicate that the network structure of the hydrogel is important to the loading of insulin. In these tests, there was no apparent optimal crosslink density which appeared to maximize insulin loading; rather the greatest efficiency was obtained with the most highly crosslinked hydrogel formulation. The results of the insulin loading studies can be interpreted in two ways. The data suggests that there is a direct correlation between the network structure of P(MAA-g-EG) hydrogels and the amount of insulin which can be incorporated within the network. However, this does not explain why insulin is maintained within the hydrogel even when the network mesh size is significantly larger than the hydrodynamic radius of insulin. Alternatively, the data may suggest that higher crosslink density increases the interaction between insulin and P(MAA-g-EG). In doing so, an attractive force between the two efficiently binds the protein to the hydrogel. This would be a new result which could provide significant insight for future work with this material for oral insulin delivery.

5.3.2. Insulin Glargine Loading

Loading studies of insulin glargine were less extensive than those of human insulin due to the difficulty of obtaining significant amounts of the model protein. Four formulations were considered to cover a wide variety of crosslink densities. The formulations are listed in Table 5.3 with their respective average loading efficiencies.

Each hydrogel formulation exhibited varying loading efficiencies. The values ranged from 45.7 to 83.2 % of insulin glargine in the loading solution which was successfully incorporated into the hydrogels. Insulin glargine exhibited the same trend as human insulin in that the loading efficiencies increased with increasing monomer wt% and increasing mol% PEGDMA present during hydrogel polymerization. Again, the correlation between the network crosslink density and the loading of insulin glargine was apparent. This may give particularly meaningful results for this drug delivery system because insulin glargine is a variation of native insulin and therefore is inherently different in various characteristics. If the loading of insulin and insulin glargine is due to an interaction between the hydrogel and the protein, differences in the *in vitro* behavior should be seen. In either case, by carefully controlling the hydrogel characteristics, one can tailor the efficiency with which at least these two protein drugs can be loaded into P(MAA-g-EG) hydrogels.

5.3.3. *In Vitro* Release Studies

The release of human insulin from each insulin loaded polymer (ILP) formulation was first performed at pH = 2.7, 3.7, 4.7, 5.6, and 6.8. Based on the results, which are discussed below, a second *in vitro* study was performed with insulin glargine as well as insulin which focused more on the pH range which incorporates the ionic transition point of both the ionic hydrogel and the proteins. To do so, release studies were also performed at pH = 6.2.

5.3.3.1. Human Insulin Release Studies

The release of human insulin was performed for all 11 formulations of ILP. The insulin maintained its chemical structure as is indicated in Figures 5.1 and 5.2. The retention time remains the same (Figure 5.1) and total absorbance spectrum (Figure 5.2) for an insulin standard in PBS was identical to that of insulin following incorporation and release from a P(MAA-g-EG) sample. The smaller peak and absorbance for the insulin released from the ILP is simply due to the reduced concentration of the sample. The insulin control sample used was left at 37 °C for several days in a shaker bath to induce some aggregation. The absence of the aggregate peak in Figure 5.1 for insulin released from P(MAA-g-EG) indicated that insulin aggregation did not occur due to loading and release in the hydrogels. Figure 5.3 displays the fractional release of insulin from two formulations used for examples of insulin release and are the same ones used in Chapter 4: 0.75/66 and 2.0/66. The release of insulin is given as a fractional release based on the insulin incorporation efficiency of the tested sample. For both samples, the release of insulin does not exceed 20% until the pH of the release buffer is at 6.8. Nine of the eleven P(MAA-g-EG) formulations tested exhibited the same release behavior as the results for the examples shown in Figure 5.3. The two formulations that do not follow this trend are 0.375/50 and 0.75/33, which had significant release of insulin at pH = 5.6 as well as 6.8 over the three hour release study. These results will be discussed in more detail later.

The most intriguing part of the results presented in Figure 5.3 is how rapidly the transition is between insulin being maintained to a great extent within the hydrogel to insulin release based on pH. This is especially true when considering the results of the network structure characterization described in Chapter 4. While the mesh size of each of

these two hydrogels does change between pH = 5.6 and pH = 6.8, they only increase to roughly twice the size of the highly complexed state of the hydrogel at lower pH levels. If there were no attractive or repulsive forces between the protein and the hydrogel, a mesh size change of this order should only increase the diffusion of the drug through the hydrogel slightly. However, the release of insulin from these two hydrogels occurs almost instantaneously at pH = 6.8. This suggests that at pH = 6.8, insulin is driven out of the hydrogel by repulsive forces rather than simple diffusion.

When combined with the loading data, it appears that at pH levels below the pKa of the hydrogel, hydrogen bonds form between insulin and the hydrogel in a similar fashion as those responsible for its pH responsive swelling. Above the pKa of P(MAA-g-EG), the hydrogen bonds are lost allowing insulin release. This result suggests that the same weak interactions which occur between MAA and PEG in the hydrogel may contribute significantly to insulin loading and release behavior *in vitro* and are crucial to its potential for oral insulin delivery. However, this does not explain why insulin appears to be driven from the hydrogel. One important point to consider is the fact that all proteins exhibit polarization and ionization in response to environmental pH. In the case of insulin, its isoelectric point (pI) has been reported at pH = 5.2 [17]. Above this pH, insulin becomes more deprotonated causing it to behave as an anionic molecule. Therefore, when the pH of the release buffer is above the ionic transition point for both insulin and P(MAA-g-EG) both materials are negatively charged. This ionic repulsion is likely the reason for the rapid release of insulin at pH = 6.8.

To supplement the previous results, additional release studies were performed with four P(MAA-g-EG) hydrogel formulations which included release at pH = 6.2. With

this study, more information was gathered in the pH range which exhibits the largest change with respect to the interaction between the hydrogel and insulin. These results are shown in Figure 5.4. The pI of insulin and the pKa of P(MAA-g-EG) are displayed as vertical lines at pH = 5.2 and 5.8, respectively. Results at lower pH levels are omitted. The points represent the fractional release of insulin following 3 hours of dissolution in PBS at pH = 4.7, 5.6, 6.2, and 6.8. For three of the four formulations considered the release of insulin did not occur until the pH of the release buffer was above that of both the pI of insulin and the pKa of P(MAA-g-EG). Again, there is one exception to this rule with formulation 0.75/33. The results for this formulation are discussed later in this chapter. For the other three formulations considered, insulin release required that both the hydrogel and insulin were negatively charged for insulin release to exceed 20%. If this result is truly the behavior of this delivery system, and the result for formulation 0.75/33 is the exception to the rule, then this represents a significant step in understanding how the release of insulin from P(MAA-g-EG) hydrogels can be tailored to suit the needs of a pH dependent system for oral insulin delivery.

5.3.3.2. Insulin Glargine Release Studies

The four P(MAA-g-EG) formulations used for *in vitro* work with insulin glargine are listed in Table 5.3. Their release profiles are shown in Figure 5.5. The fractional release is shown as cumulative release following 3 hours of dissolution in PBS at pH = 4.7, 5.6, 6.2, 6.8, and 7.4. The highest pH sample was added for insulin glargine due to its elevated pI at 6.7 with respect to native human insulin [18]. The pI for insulin glargine and pKa for P(MAA-g-EG) are indicated on the graph. Insulin glargine provides

a unique perspective when considered with P(MAA-g-EG) hydrogels because its pI is at a higher pH than that of the hydrogel, as opposed to insulin, which was at a lower pH.

In contrast to insulin, the release of the insulin glargine did not exceed 20% until the release buffer was at pH = 6.2. If the release of the protein is driven by ionic repulsion, then it would not occur until both the protein and the hydrogel are negatively charged, at pH levels above the ionic transition points of both species. With insulin glargine, this is exactly what happened for the four formulations considered. Only when the PBS was at pH = 6.8, when insulin glargine carries a slight negative charge, did the majority of the protein come out of the hydrogel. In combination with the results for insulin release, these results strongly indicate that ionic repulsion is the driving force for the release of insulin and insulin glargine from P(MAA-g-EG) hydrogels.

5.3.3.3. Insulin Release for Loosely Crosslinked Formulations

The release of insulin from two P(MAA-g-EG) formulations did not follow the patterns which are discussed previously. The two formulations are 0.375/50 and 0.75/33. These two formulations were the most loosely crosslinked hydrogels of all those considered in this body of work. They exhibited the lowest loading efficiency and, because they were so delicate, could not be tested for network properties. Nonetheless, their *in vitro* behavior with insulin was unique from the other 9 formulations and they justify a more detailed analysis.

The release of both of these formulations is shown in Figure 5.6. Three pH levels are represented here: pH = 4.7, 5.6, and 6.8. At pH = 4.7 the release of insulin was highly restricted for the duration of the 3 hour test, the same result as that seen for all

other P(MAA-g-EG) hydrogels. Similarly, at pH = 6.8 nearly 100% of insulin was released within 5 minutes and the total amount released did not increase. At pH = 5.6, however, the release of insulin progressed over the duration of the test for both formulations. The curves for this release profile appear to be what would be expected if the release was controlled by diffusion. This is likely due to the low polymer volume fraction of these two formulations. With the very low crosslink density, these hydrogels rely very heavily on hydrogen bonds to maintain their integrity. As the pH is increased through the pKa of the hydrogel, and hydrogen bonding is lost, the volume fraction of the hydrogels could drop below 5%, which was the lowest value for $\nu_{2,s}$ seen in the swelling studies. In this case, interactions between the hydrogel and insulin would be significantly reduced and a release profile such as is seen in Figure 5.6 might be explained. The same behavior was not seen with insulin glargine at pH = 5.6, or even at pH = 6.2. This could be due to the fact that insulin glargine is much more strongly ionic in nature than native human insulin due to the addition of the arginine residues.

5.4. Conclusions

Insulin and insulin glargine were successfully loaded into various formulations of P(MAA-g-EG) hydrogels. For both insulin species, the loading efficiency increased with increasing crosslink density for the hydrogel. While this trend was clear, no optimum value was achieved which suggested a point of excessive crosslinking. The high efficiency of loading was not adequately explained by the characteristic mesh size with regard to diffusive limitations by the network. This indicated that insulin was bound within the hydrogel by attractive forces. The most likely bonds which could have formed

are hydrogen bonds which are also responsible for the complexation of the hydrogel at low pH levels.

Insulin and insulin glargine loaded hydrogels were suspended in PBS at various pH levels to measure the release of the protein. In general, the release of the protein did not exceed 20 % until the pH or the release buffer was above both the pKa of P(MAA-g-EG) and the pI of the incorporated insulin or insulin glargine, at which point the release occurred as a burst. Exceptions to this trend occurred for human insulin for the most loosely crosslinked formulations, but not for insulin glargine. These results lead to two major conclusions. First, the burst release of insulin at pH levels above the ionic transition points for the polymer and the protein indicated that insulin was propelled from the network due to ionic repulsion. Second, the apparent diffusive release of insulin at pH = 5.6 from the two most loosely crosslinked hydrogel formulations suggested that there was a critical polymer volume fraction necessary to effectively maintain the hydrogen bonds between P(MAA-g-EG) and insulin. At this point, however, these results are only an indication of this behavior and a thorough explanation for the interaction between P(MAA-g-EG) and protein drugs would require further investigation.

Table 5.1. A comparison between native human insulin and insulin glargine

	Human Insulin	Insulin Glargine
Molecular Weight (Da)	5808	6063
Structure Change	None	Glycine replaces AspA21 & two arginine residues at C-terminus of B chain
Isoelectric Point (pI)	5.2	6.7

Table 5.2. Average insulin incorporation efficiencies for all P(MAA-g-EG) hydrogel formulations (\pm S.D., n = 3)

PEGDMA (200) (mol%)	Monomer fraction (wt%)		
	33 wt%	50 wt%	66 wt%
0.375%	N/A	42.7 \pm 25.3	76.6 \pm 4.7
0.75%	52.7 \pm 7.0	76.7 \pm 2.2	77.8 \pm 0.3
1.25%	67.3 \pm 3.4	77.1 \pm 1.8	81.9 \pm 1.4
2.00%	75.2 \pm 3.6	82.0 \pm 2.1	84.9 \pm 0.9

Table 5.3. Average incorporation efficiencies for insulin glargine loading in four P(MAA-g-EG) hydrogel formulations (\pm S. D., n = 3)

PEGDMA (200) (mol%)	Monomer fraction (wt%)	
	33 wt%	66 wt%
0.750%	45.7	64.7
2.000%	61.9	83.2

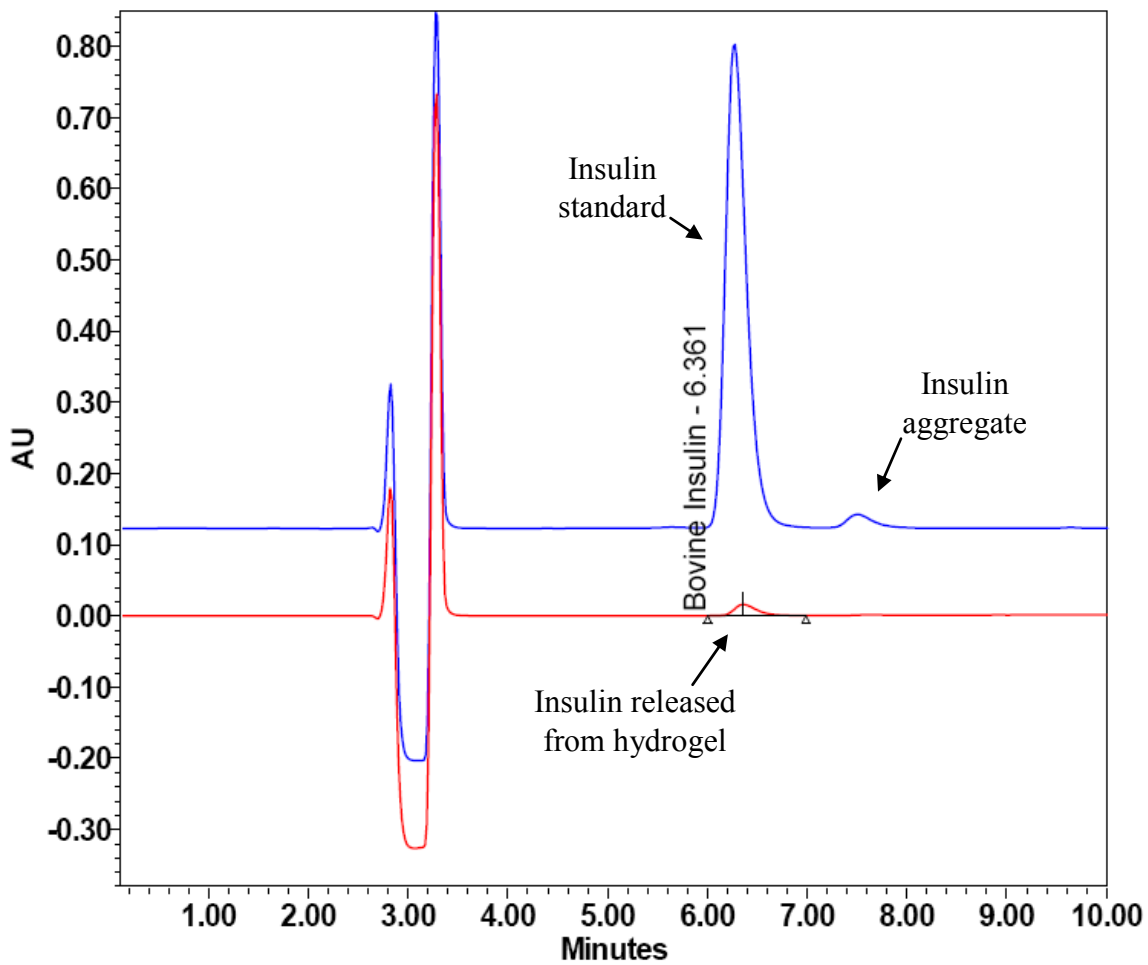


Figure 5.1. RP-HPLC absorbance at 214 nm of native human insulin standard with insulin aggregate (top) and human insulin following uptake and release from an ILP sample (bottom)

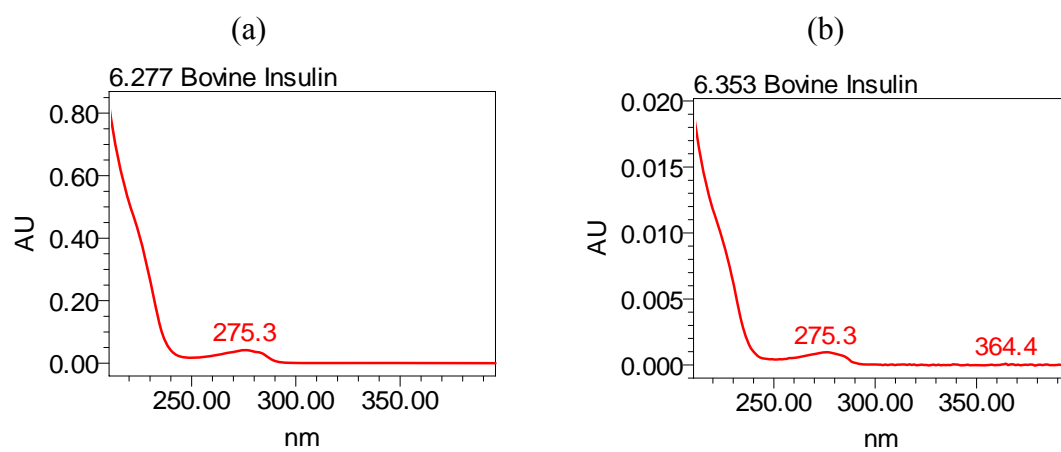


Figure 5.2. Total absorbance spectra for (a) native human insulin standard and (b) human insulin following uptake and release from an ILP sample

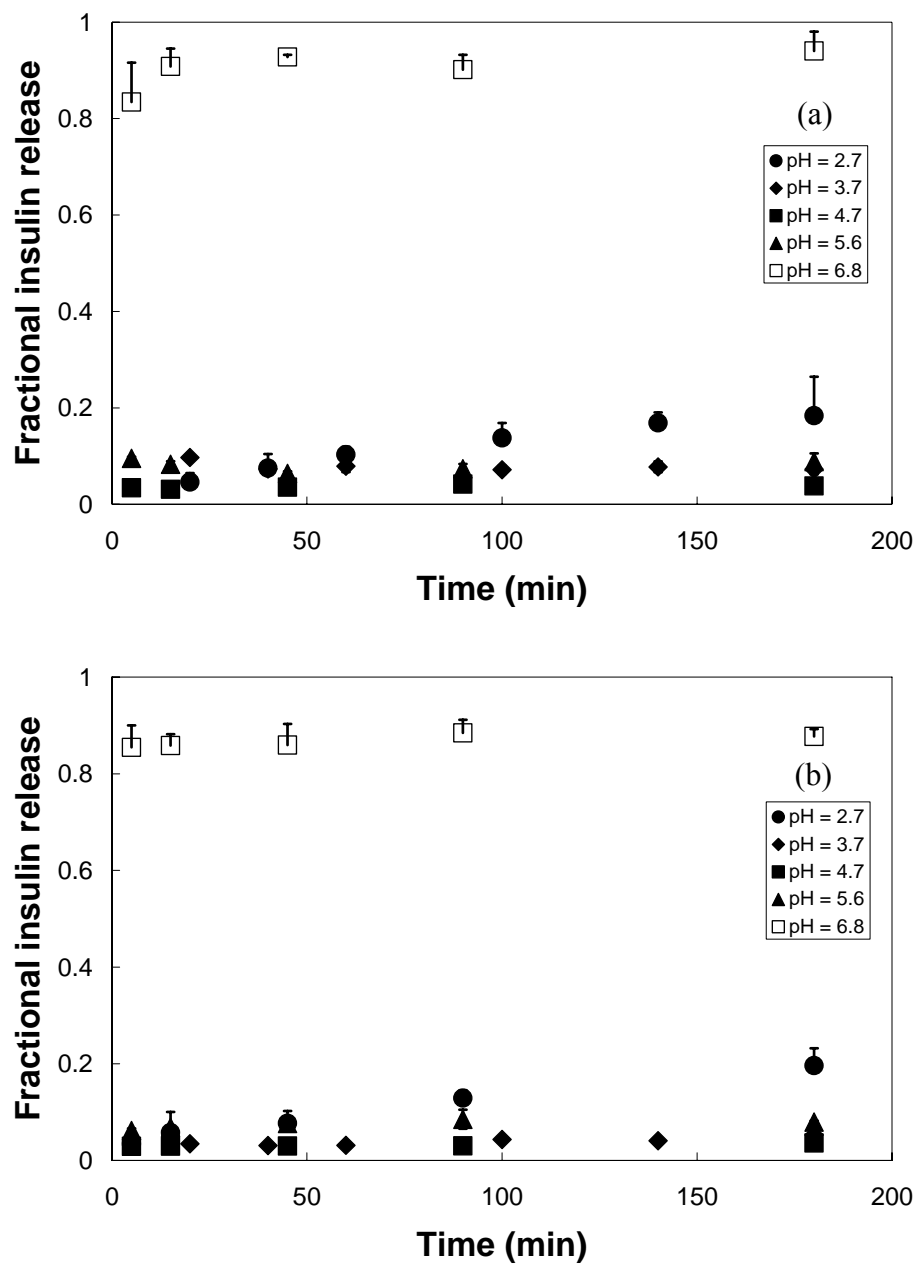


Figure 5.3. Release of insulin from ILP samples of P(MAA-g-EG) formulations (a) 0.75/66 and (b) 2.0/66 into PBS at various pH levels (+ S.D., n = 3)

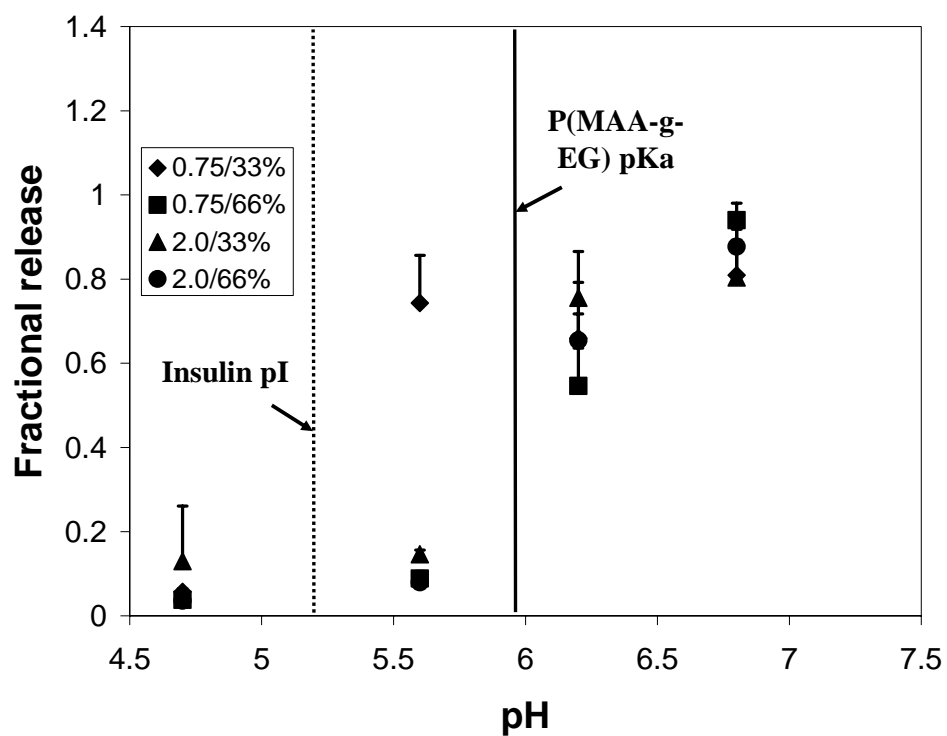


Figure 5.4. Fractional insulin release following 3 hours of dissolution in PBS at 37°C (+ S.D., n = 3)

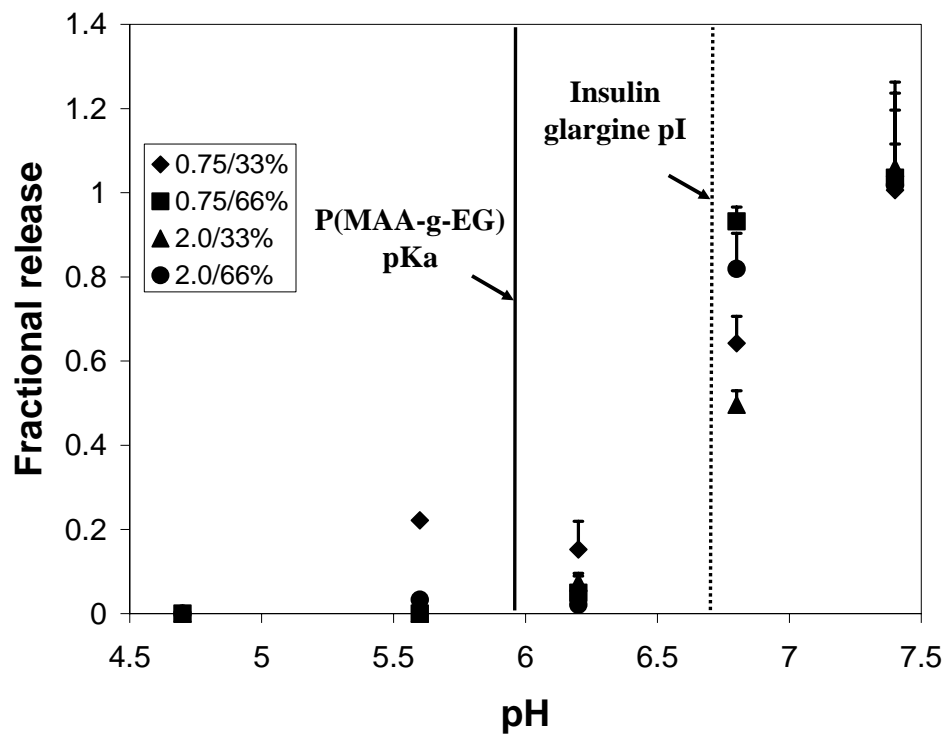


Figure 5.5. Fractional insulin glargine release following 3 hours of dissolution in PBS at 37°C (+ S.D., n = 3)

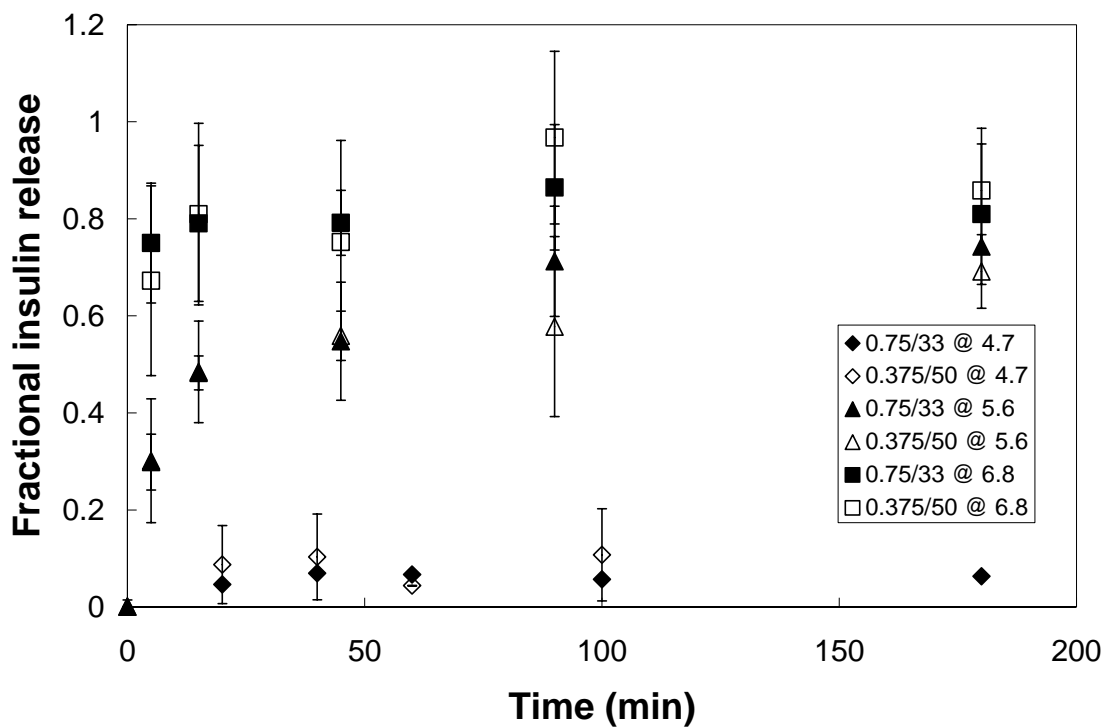


Figure 5.6. Release of insulin from ILP samples of P(MAA-g-EG) formulations 0.75/33 (closed symbols) and 0.375/50 (open symbols) into PBS at various pH levels (\pm S.D., $n = 3$)

5.5. References

1. Lowman, A.M., et al., *Oral delivery of insulin using pH-responsive complexation gels*. J Pharm Sci, 1999. **88**(9): p. 933-7.
2. Peppas, N.A., et al., *Poly(ethylene glycol)-containing hydrogels in drug delivery*. J Control Release, 1999. **62**(1-2): p. 81-7.
3. Morishita, M., et al., *Mucosal insulin delivery systems based on complexation polymer hydrogels: effect of particle size on insulin enteral absorption*. J Control Release, 2004. **97**(1): p. 115-24.
4. Peppas, N.A. and N.J. Kavimandan, *Nanoscale analysis of protein and peptide absorption: insulin absorption using complexation and pH-sensitive hydrogels as delivery vehicles*. Eur J Pharm Sci, 2006. **29**(3-4): p. 183-97.
5. Lopez, J.E. and N.A. Peppas, *Effect of poly (ethylene glycol) molecular weight and microparticle size on oral insulin delivery from P(MAA-g-EG) microparticles*. Drug Dev Ind Pharm, 2004. **30**(5): p. 497-504.
6. Ichikawa, H. and N.A. Peppas, *Novel complexation hydrogels for oral peptide delivery: in vitro evaluation of their cytocompatibility and insulin-transport enhancing effects using Caco-2 cell monolayers*. J Biomed Mater Res A, 2003. **67**(2): p. 609-17.
7. Besheer, A., et al., *Loading and mobility of spin-labeled insulin in physiologically responsive complexation hydrogels intended for oral administration*. J Control Release, 2006. **111**(1-2): p. 73-80.
8. Kim, B. and N.A. Peppas, *In vitro release behavior and stability of insulin in complexation hydrogels as oral drug delivery carriers*. Int J Pharm, 2003. **266**(1-2): p. 29-37.
9. Morishita, M., et al., *Elucidation of the mechanism of incorporation of insulin in controlled release systems based on complexation polymers*. J Control Release, 2002. **81**(1-2): p. 25-32.
10. Peppas, N.A., *Devices based on intelligent biopolymers for oral protein delivery*. Int J Pharm, 2004. **277**(1-2): p. 11-7.

11. Bromberg, L., J. Rashba-Step, and T. Scott, *Insulin particle formation in supersaturated aqueous solutions of poly(ethylene glycol)*. *Biophys J*, 2005. **89**(5): p. 3424-33.
12. Hamilton-Wessler, M., et al., *Mode of transcapillary transport of insulin and insulin analog NN304 in dog hindlimb: evidence for passive diffusion*. *Diabetes*, 2002. **51**(3): p. 574-82.
13. Sweiry, J.H. and G.E. Mann, *Pancreatic microvascular permeability in caerulein-induced acute pancreatitis*. *Am J Physiol*, 1991. **261**(4 Pt 1): p. G685-92.
14. Peppas, N.A., *Controlling Protein Diffusion in Hydrogels*, in *Trends and Future Perspectives in Peptide and Protein Drug Delivery*, V.H. Lee, Hashida, M., Mizushima, Y., Editor. 1995, CRC Press: Boca Raton, FL. p. 23-37.
15. Torres-Lugo, M., et al., *pH-Sensitive hydrogels as gastrointestinal tract absorption enhancers: transport mechanisms of salmon calcitonin and other model molecules using the Caco-2 cell model*. *Biotechnol Prog*, 2002. **18**(3): p. 612-6.
16. Porcellati, F., et al., *Comparison of pharmacokinetics and dynamics of the long-acting insulin analogs glargine and detemir at steady state in type 1 diabetes: a double-blind, randomized, crossover study*. *Diabetes Care*, 2007. **30**(10): p. 2447-52.
17. Roskamp, R.H. and G. Park, *Long-acting insulin analogs*. *Diabetes Care*, 1999. **22 Suppl 2**: p. B109-13.
18. Oiknine, R., M. Bernbaum, and A.D. Mooradian, *A critical appraisal of the role of insulin analogues in the management of diabetes mellitus*. *Drugs*, 2005. **65**(3): p. 325-40.

CHAPTER 6: SYNTHESIS AND CHARACTERIZATION OF PEGYLATED INSULIN

6.1. Introduction

One of the most difficult challenges to oral insulin delivery is maintaining the integrity of the protein against enzymatic degradation in the GI tract. In simulated testing, hydrogels of P(MAA-g-EG) have been able to successfully protect insulin through the most aggressive section of the stomach and duodenum to then release it in the jejunum [1-4]. Delivering insulin to the small intestine is important because of the lower enzymatic activity and the potential for absorption by the local tissues. These hydrogels exhibit additional characteristics which enhance their potential for oral insulin delivery. The mucoadhesive behavior of swollen P(MAA-g-EG) causes insulin to be released at the proposed site of absorption, near the apical surface of the epithelial cells in the small intestine which are covered by a thick mucous layer [5-7]. By releasing in this location insulin has a greater chance of absorption because it has shown low levels of enzymatic degradation in the presence of brush border peptidases [8]. Additionally, these hydrogels strongly bind Ca^{2+} ions from the intestinal lumen. This contributed to the reversible opening of the tight junctions between Caco-2 cells in an *in vitro* model of the intestinal epithelium as well as reduced the enzymatic activity of intestinal enzymes, which rely on extracellular Ca^{2+} to maintain their activity [9-12]. While all of these attributes of P(MAA-g-EG) benefit the design for oral insulin delivery, they are only significant when insulin is in close proximity to the hydrogel. Upon release, insulin may not immediately diffuse to the apical surface of the tissues in the intestine. Extended exposure to the GI tract, unless in the presence of P(MAA-g-EG), is likely to lead to the protein's eventual

enzymatic degradation by luminal enzymes. In order to improve the design of this delivery system and improve bioavailability of orally delivered insulin, the resistance of insulin to enzymatic degradation should be improved.

There are several approaches to reduce environmental enzymatic activity. Several groups have proposed the co-administration of enzyme inhibitors with an orally delivered protein [13-16]. However, considerably reducing enzymatic activity in the GI tract could greatly affect natural digestion and lead to complications such as poor nutrient absorption, diarrhea, or even malnutrition [16, 17]. In order to reduce the proteolytic degradation of insulin with minimal effect to natural digestion the changes must be localized near the protein. One method of making the protein resistant to enzymatic attack is through PEGylation, the covalent conjugation of polyethylene glycol (PEG) to the molecule.

PEGylation of proteins has several key benefits that are associated with the high biocompatibility of the polymer. PEGylation has been shown to decrease immunogenicity and antigenicity, improve solubility, and increase circulation time for proteins [18-20]. The most important effect for oral protein delivery is the reduced enzymatic degradation of PEGylated proteins [18-21]. The steric hindrance caused by the presence of PEG decreases the accessibility of proteolytic enzymes to sites for degradation on the polypeptide. For many proteins PEGylation can occur at many different locations on the protein sequence by a number of various chemical reactions. In the case of insulin, however, there are few potential sites for conjugation and it must be targeted to very specific locations on the protein in order to maintain its biological activity.

In work performed by Lindsay and Shall [22] the three amino groups of insulin were individually acetylated: the N-termini of the A and B chains and the lysine in the 29th residue of the B chain. These sites will henceforth be referred to as GlyA1, PheB1, and LysB29 in this chapter. The amino acid sequence of insulin is given in Figure 6.1. Their study determined that upon modifying the GlyA1 residue that the bioactivity of insulin was significantly reduced. The bioactivity was maintained, however, after modification of the other two amino acids. Similar results were made by several studies performed by Baudys et. al. [23, 24] which showed that glycosylation with a low molecular weight glycoside at the GlyA1 residue reduced bioactivity. The same modification at PheB1 or LysB29 indicated full retention of bioactivity. For this reason, both the PheB1 and the LysB29 site have been targeted for insulin PEGylation in the past and there is still debate as to which location is more suitable.

In this study the PheB1 was targeted for a mono-substituted PEG-insulin conjugate for several reasons. First, even though both LysB29 and PheB1 can be modified without reducing bioactivity of insulin, the bioactivity of insulin was significantly reduced for di-substituted insulin species in which both LysB29 and PheB1 were PEGylated [23-25]. Second, while each site maintained similar biological activity levels, modification at the PheB1 site exhibited a greater reduction in the immunogenicity of the protein [26]. Third, PheB1 modification had a more pronounced effect on the stability of the protein when compared to LysB29 [23, 27]. Fourth, modifying the PheB1 residue eliminates the ability of the protein to self-associate into 6 member hexamers. Insulin is only reactive as a monomer and if it forms dimers or hexamers it must dissociate in order to bind to the insulin receptor. Modifying the LysB29 site stops the

monomer from forming dimers, however, hexamers can still occur in a Zn^{2+} stabilized formation. Finally, the location of the PheB1 residue in the tertiary structure of insulin is on the opposite side of the protein as that of the binding site. This is clear in a space-filled, 3-D rendering of the insulin monomer seen in Figure 6.2. In this figure, the white residues indicate the insulin receptor binding site, which includes GlyA1. The three highlighted residues are: GlyA1 (red), LysB29 (orange), and PheB1 (green). If the reduction in biological activity by PEG is due to steric hindrance, the modification of PheB1 should be less pronounced than LysB29 due to the relative proximity of LysB29 to the receptor binding site. The major argument for modifying the LysB29 residue is that the synthesis of LysB29 modified insulin is easier and generally has a higher yield than PheB1 modification. However, due to the reasons listed above, the PheB1 residue was targeted for this work.

The synthesis of PEGylated insulin has been achieved through a variety of ways. Until recently, however, most of those approaches did not attempt to target a particular amino acid for modification and relied on purification methods to separate the product mixtures. The technique used in this work was a modification of a protocol designed by Hinds et. al. which investigated insulin PEGylation with PEG groups of 750 and 2000 Da [27]. In this work, the molecular weight of the PEG group investigated is 5000 Da. The higher molecular weight should impart more of the beneficial effects of PEGylation on insulin, but it may cause a drop in bioactivity. This will be discussed and determined in Chapter 7.

In order to target the PheB1 amino acid for PEG conjugation the other two sites with free amine groups had to be eliminated as potential sites for conjugation. In order to

do so, the protein was pre-treated with di-*t*-butyl dicarbonate (diboc), which can reversibly react with the free amine groups of a protein [28]. This reaction attaches extremely hydrophobic *t*-butyl (BOC) groups to the amino acids with which it reacts. When the protection reaction is performed in dimethyl sulfoxide (DMSO) with triethylamine (TEA) the GlyA1 and LysB29 are more reactive than PheB1 [24]. Although PheB1 is less probable to be modified with a BOC group, this reaction produces a number of side products. This protection is reversible, however, and if the side products are separated from the desired product they should be able to be recycled for use in subsequent batches. After reacting with diboc and purifying the desired product, the reaction with an amine reactive mPEG species is isolated to the single remaining free amine group of insulin at PheB1. After PEGylation the BOC groups can be removed and a mono-substituted mPEG-insulin conjugate is produced. In this work, the synthesis of PheB1-mPEG-insulin is described and characterized.

6.2. Materials and Methods

6.2.1. Materials

Dimethyl sulfoxide (DMSO), triethylamine (TEA), trifluoroacetic acid (TFA) di-*tert*-butyl dicarbonate (diboc), acetonitrile ethanol amine, ethylenediaminetetraacetic acid (EDTA), tris, sodium chloride (NaCl), ammonium bicarbonate (NH₄HCO₃), hydrogen chloride (HCl), urea, dithiothreitol (DTT), 2,5-dihydroxybenzoic acid (DHB), sinapic acid, α -cyano-4-hydroxycinnamic acid (CHCA), iodoacetamide, ammonium hydroxide, and acetic acid were purchased from Sigma Aldrich (St. Louis, MO).

Spectrapor® 6 regenerated cellulose dialysis tubing was purchased from Fisher Scientific (Hampton, NH). Recombinant human insulin was purchased from Seracare Diagnostics (Milford, MA). mPEG succinimidyl propionate 5000 (mPEG-SPA) was purchased from Nektar Therapeutics (Huntsville, AL). Immobilized TPCK Trypsin was purchased from Pierce Chemical Company (Rockville, IL)

6.2.2. Synthesis of Di-BOC Insulin

In order to target insulin PEGylation to only the PheB1 amino acid, the native protein was first modified such that the PEG conjugation did not occur at two other potential amino acid residues, GlyA1 and LysB29. To do this a solution of 500 mg insulin was made in 9.5 ml of DMSO and 0.5 ml TEA. Another solution with 41 mg diboc was made in 0.5 ml DMSO. Insulin and diboc were reacted in a 1:2 stoichiometric molar ratio to increase the yield of the properly protected insulin intermediate. The reaction of insulin with diboc reversibly alkylates free amine groups with a BOC protecting group.

Once both reactants were completely dissolved, the solution with diboc was pipetted into the solution with insulin using a glass transfer pipette. A few drops of DMSO were then used to rinse the centrifuge vial with the solution originally containing diboc and added to the reaction solution. The solution was stirred at 60 rpm and the alkylation reaction was allowed to take place for 30 minutes at room temperature. After 30 minutes, 25 μ l of ethanol amine was added to the solution to quench any remaining unreacted diboc. The entire reaction mixture was then pipetted into 200 ml of acetone and 1 drop of 6 M HCl was added to initiate precipitation of the protein. The reaction vial was

rinsed with a small amount of acetone to ensure complete transfer of the reaction product. The precipitate was removed by filtration using a 0.22 mm PVDF filter paper under vacuum until dry. To be sure that no further protein was in solution, several drops of 6 M HCl was added to the recovered filtrate. If any further precipitation occurred the solution was filtered a second time. The precipitate and filter paper were then placed into 30 ml of DI water. A small amount of DI water was used to rinse the filtration funnel. After 30 minutes, the filter paper was removed, rinsed with water, and discarded. The remaining solution was then dialyzed against DI water in a 3500 MWCO membrane overnight to remove residual acetone, unreacted diboc, and ethanol amine.

The crude product from the reaction between diboc and native human insulin was purified using ion exchange chromatography (IEC), more specifically cation exchange chromatography. Urea and acetic acid was added to the solution recovered from dialysis to make a 7M urea and 1 M acetic acid solvent. This was the starting mobile phase of the IEC purification. When doing this, the total volume of the solution increased greatly, so the amount of urea and acetic acid necessary were based on an increase in volume of 50%. The purification was performed using Fast Protein Liquid Chromatography (FPLC) (GE Healthcare, Piscataway, NJ). A gradient elution profile was used with two mobile phases: buffer A contained 7M urea, 1M acetic acid, and 0.01 M NaCl, buffer B contained 7M urea, 1M acetic acid and 0.3M NaCl. The gradient was performed from 0 – 60 %B over 80 column volumes using either a SP FF 16/10 cation exchange column (GE Healthcare, Piscataway, NJ) at a flow rate of 2 ml/min for large volume samples or a Mono S 5/50 cation exchange column (GE Healthcare) at a flow rate of 0.7 ml/min for small volume samples. The column was then washed with 100 %B

and re-equilibrated with 100 %A prior to any additional injections. The elution was collected by a Frac-950 fraction collector in 14.5 ml fractions for the SP FF 16/10 column and 2 ml fractions for the Mono S 5/50 column. The elution profile from the column was measured by UV absorbance at 280 nm.

Characterization of each fraction was performed using RP-HPLC. The mobile phases were 0.1 % TFA in DI water as mobile phase A and 0.1 % TFA in acetonitrile as mobile phase B. Samples of 50 μ l were run through a Waters Spherisorb® C8 column (5 μ m, 4.6 x 250 mm) using a Waters 2695 separations module equipped with a 996 Photodiode Array detector (Milford, MA) at a 1 mL/min. A gradient from 35-65 % mobile phase B was run for 35 minutes. Purified fractions with greater than 90 % purity of di-BOC_{LysB29/GlyA1} insulin were then used for PEGylation. The remaining fractions were recycled as described below. All fractions were then dialyzed with a MWCO 3500 membrane against 0.01M NH₄HCO₃ for three days, changing the dialysate twice daily. The dialyzed fractions were then frozen overnight and lyophilized.

6.2.3. Recovery of Impure Diboc Treated Insulin

As a proof of concept, products collected from the FPLC purification of diboc treated insulin which were not deemed have two BOC groups or have sufficient purity for PEGylation were recycled. Any modification with BOC groups was removed from the product mixture by placing the lyophilized material in TFA at 0 °C for 90 minutes. The TFA was then diluted into 10 times the volume of DI water and dialyzed for 24 hours changing the dialysate three times. The recovered deprotected insulin product was then

frozen and lyophilized. This insulin was now simply regular human insulin and could be treated with diboc in a similar fashion as described above.

6.2.4. Di-BOC Insulin PEGylation

The purified di-BOC_{LysB29/GlyA1} insulin was reacted with mPEG-SPA to conjugate PEG to the PheB1 residue. Purified di-BOC_{LysB29/GlyA1} insulin powder was dissolved in 2 mL of DMSO containing 47.5 μ L TEA. A 3:1 molar excess of mPEG-SPA was added to the reaction solution, and the reaction was allowed to proceed for 24 hours at room temperature. The products were then diluted into 100 mL of DI water, dialyzed and lyophilized in the same fashion as section 6.2.2.

The lyophilized product was dissolved in TFA at 0°C for 90 minutes to remove the BOC protection groups from the newly formed PEGylated insulin. After 90 minutes, the TFA was diluted into 10 times the volume of DI water and dialyzed by the same fashion described above. The solution was purified to remove insulin and excess mPEG-SPA using IEC in the same fashion as described above. The elution was again collected and the peaks were dialyzed and lyophilized. The major peak corresponding to the PheB1-PEG-insulin conjugate was recovered and stored under nitrogen at -20°C until needed.

6.2.5. Di-BOC and PEGylated Insulin Characterization

Both di-BOC and PEGylated insulin were characterized to validate the method to create a PEG-insulin conjugate in which the modification is only present at the PheB1

residue. Two of digestion techniques were required to identify individual sites of modification and are described below.

6.2.5.1. PEGylated Insulin Digestion

In one of the digestion methods used to determine the site of PEGylation, the disulfide groups were reduced to separate the A and B chains of insulin (Figure 6.1). Two mg of PEGylated insulin was dissolved in 5 mL denaturation buffer of 7 M urea, 0.2 M tris, and 2 mM EDTA at pH = 8.5 in a screw-cap test tube. The solution was flushed with nitrogen and heated to 50 °C for 30 minutes in a water bath. A 50-fold molar excess of DTT over the number of moles of disulfide present in insulin was then added and allowed to react for 4 hours. This reaction cleaved any disulfide bonds present in the protein. To keep the disulfide bonds from reforming, a 100-fold molar excess of iodoacetamide over the number of moles of disulfide present in insulin was added after the 4 hour reduction reaction. The solution pH was measured immediately following the addition of iodoacetamide and a small amount of ammonium hydroxide was added to maintain the pH of the solution at 8.5. The reaction was then allowed to proceed for 20 minutes at room temperature in the dark. This was done to limit the conversion of liberated iodide ion to iodine which would react with tyrosine residues in the protein [29]. After treatment with DTT, a precipitate formed in the solution. Following the final step of this reaction process, the precipitate was removed by centrifugation and analysis of the liquid was possible. As will be described later for PEGylated insulin, the B chain remained in solution while the A chain crashed out.

The second digestion process with PEGylated insulin was performed using a gel immobilized trypsin kit. This digestion cleaved two bonds in the amino acid sequence of insulin as seen in Figure 6.1. Trypsin specifically cleaves the carboxyl side of arginine and lysine residues. This allowed the LysB29 residue to be separated from the other two potential sites for amine specific PEGylation of insulin. One mg of PEGylated insulin was dissolved in 0.5 ml of 0.1 M NH_4HCO_3 at pH = 8.0. A slurry of 0.25 ml of the gel immobilized TPCK trypsin was then added to the solution in a 1.5 ml centrifuge tube. The mixture was flushed with nitrogen, sealed, and incubated overnight on a rapidly shaking tray in an oven at 37 °C. The immobilized trypsin was then removed from solution by centrifugation and the supernatant was recovered which contained the degraded insulin conjugate. Combination of the two digestion techniques allowed for clear identification of modification at any one of the three potential conjugation sites.

6.2.5.2. MALDI-TOF Mass Spectroscopy

Matrix assisted laser desorption ionization/time of flight mass spectroscopy (MALDI-TOF MS) was used to characterize many of the modified insulin or degraded insulin species throughout this study. Most of the work was performed on a VG ToFSpec E MALDI-TOF (ThermoVG, Beverly, MA). Sinapic acid or DHB was used as the matrix for this instrument. Some of the final spectra shown in this report were processed using a Voyager DE Pro MALDI-TOF (Applied Biosystems, Foster City, CA). The matrix used for this instrument was CHCA.

A 2500:1 ratio of matrix to analyte was used for each run. The sample protein or peptide was dissolved into a 50 % acetonitrile solution in DI water with 0.1 % TFA. This

was done so that any samples collected from RP-HPLC elution could be tested without changing solvents. The analytes were then dispersed into a 0.05 M solution of the matrix with proper volumetric ratios to give a 2500:1 molar ratio. Because this solution did not dry quickly upon spotting on the MALDI-TOF plate, the plate was placed in an oven at 80 °C for about 5 minutes prior to spotting.

6.3. Results and Discussion

6.3.1. Synthesis of Di-BOC Insulin

For clarity, di-BOC_{LysB29/GlyA1}, insulin with BOC groups specifically at the LysB29 and GlyA1 residues, will henceforth be referred to as di-BOC insulin. This should be distinguished from diboc treated insulin which refers to insulin which has been reacted with di-*t*-butyl dicarbonate, but not purified.

Di-BOC insulin was synthesized and purified from recombinant human insulin. RP-HPLC spectra for insulin, diboc treated insulin, and purified di-BOC insulin can be seen in Figure 6.3. The later the peaks eluted, the more hydrophobic they were. A shift to the right in the elution profile indicated the attachment of BOC groups to the insulin molecule. The peaks for insulin, mono-BOC insulin, di-BOC insulin, and tri-BOC insulin eluted at approximately 9.2, 12.2, 15.1, and 21.2 minutes as shown in Figure 6.3b. Additional peaks correspond to alternative locations of the BOC group. The reactivity of the amine groups in insulin proceeds with LysB29 \geq GlyA1 > PheB1 when in the DMSO/TEA solution used in this study, so the alternative BOC locations should proceed accordingly [24]. The three major peaks in Figure 6.3b at 12.2, 15.1, and 21.2 minutes

corresponded to 13.40, 56.80, and 14.68 % of the total integrated area of the chromatogram. The peak of interest for di-BOC insulin was the major peak at 15.1 minutes, so the yield of the BOC protection was 56.8 %.

6.3.2. Purification of Di-BOC insulin

Individual peaks of the impure mixture were separated using cation exchange chromatography on an FPLC. The isolation of each peak had some loss due to peak overlap causing a reduction in overall product yield. However, the recycle and recovery of discarded diboc treated insulin was possible and could be used to greatly improve overall yield. A sample elution profile for the separation of individual peaks is in Figure 6.4. Fractions of 14.5 ml were collected throughout the elution. Because the separation was performed with cation exchange chromatography, the binding was dependent on the number of positively charged residues in the protein. The most highly substituted tri-BOC insulin eluted first followed by di-BOC insulin, mono-BOC insulin, and native insulin. This was the reverse of the elution order as seen with RP-HPLC. After collection, the purity of collected fractions was determined by RP-HPLC. A set of collected fractions can be seen in a single chromatogram in Figure 6.5. The profiles for fractions 3, 4, and 5 indicated samples with greater than 90 % purity of the major peak eluting at 17 minutes. This sample run was performed with a different batch of mobile phase which caused the slight shift seen between this di-BOC insulin sample retention time and that seen in Figure 6.3.

While the RP-HPLC and IEC retention times are indicative of the changes expected from the modification of insulin with BOC groups, further analysis should be

included to validate the results. The most pure samples collected for each of the major peaks eluted from the FPLC cation exchange were tested using MALDI-TOF MS. Each BOC modification adds 100 Da to the molecular weight of the protein. Figure 6.6 shows the molecular weight of each species. Each of the molecular weights were not exactly as expected due to variances in the calibration files used. The molecular weight shifts ranged from 95-102 Da added between samples, which corresponded very well with the addition of a single BOC group. The smaller peaks which were slightly heavier than the main peaks were due to associated salts which were present in small amounts in the sample solutions.

During the diboc insulin treatment and purification of process, the majority of product loss occurred. This was primarily due to the nature of the reaction which produced di-BOC_{LysB29/GlyA1} insulin as the major product, but also had several side products with BOC groups attached to other residues. Because the BOC modification was reversible, products deemed to be incorrectly modified or with low purity were recycled. The purpose of this exercise was a proof of concept that the overall yield could be improved through good chemical engineering techniques of recovery and recycling.

The fractions of the diboc treated insulin which were not used for PEGylation following FPLC separation were dialyzed, frozen, and lyophilized. This product mixture was then recycled to native insulin by removing the BOC groups in TFA and purifying the sample by dialysis. A RP-HPLC spectrum of the recovered native insulin against an insulin standard is given in Figure 6.7. The major single peak of insulin was mirrored by the recovered insulin. Figure 6.8 indicated that the total absorbance spectrum for the recovered insulin sample was exactly the same as that of the insulin standard. However, a

second peak at 13 minutes was also present in the recovered insulin which was absent in the control sample. In Figure 6.9, the recovered insulin absorbance at 214 nm is overlaid with a crude insulin sample from the initial diboc treatment. The peak for mono-BOC modified insulin correlated very well with the secondary peak of the recovered insulin indicating that a small portion of the mono-BOC insulin was not removed from insulin. The recycled insulin was then reacted with diboc to create a “second pass” diboc treated insulin. Figure 6.10 compares the first and second pass diboc treated insulin samples. The two samples corresponded exceptionally well in retention time and relative peak sizes and areas. This work proved that insulin treated with diboc could be recycled and reused to generate more of the intermediate product. If this process were to be scaled up or used on a more consistent basis, this method should be utilized to improve yield of PEGylated insulin.

This work shows definitively that the diboc modification worked to modify insulin with zero, one, two, or three BOC species. The majority of the reaction product was an insulin molecule with two BOC groups attached. The separation of individual species was successfully carried out using cation exchange chromatography. This indicated that the modification with BOC occurred at the free amine groups on insulin, which were positively charged in the mobile phase used for the ion exchange purification. Another result of this work is that the diboc treatment can be repeated with insulin in a way that impure products are recycled and reused. This could be used to greatly improve the yield of the diboc protection process.

6.3.3. Insulin PEGylation

Di-BOC insulin samples with greater than 90 % purity were reacted with mPEG-SPA to create PEGylated di-BOC insulin. The molecular weight of the mPEG-SPA was 5298 as determined by the manufacturer using gel permeation chromatography. A corresponding shift was seen in the molecular weight of the protein and was exhibited by several MALDI-TOF MS spectra which were used to characterize the reaction. Figure 6.11 shows a physical mixture of di-BOC insulin with mPEG-SPA with DHB as the matrix. The matrix was chosen for this scan because it was able to charge both proteins and polymers in a single scan. The PEG is easily distinguished by its distribution in molecular weight in a Gaussian distribution with its center around 5628 and repeat units of ethylene glycol of 44 Da, the molecular weight monomer. Figure 6.12 shows a MALDI-TOF spectrum following the reaction of di-BOC insulin with mPEG-SPA. In the absence of salts, the matrix used for this scan, sinapic acid, was only able to charge proteins. The peaks associated with mPEG-SPA shifted up to ~ 11600 Da with the same distribution as seen for PEG alone and maintained the 44 Da repeat units of the polymer. This indicated the conjugation of one PEG molecule to di-BOC insulin. Some residual di-BOC insulin was present because the sample had not yet been purified.

After conjugation, the BOC protecting groups on insulin were removed using TFA. The elimination of residual reactants was then performed using cation exchange chromatography. In order to improve the efficiency of sample retention, a series of small injections were run on the FPLC instead of a single large injection. The entire series of elution spectra are displayed in Figure 6.13 with absorbance at 280 nm. The peak occurring between 2 and 12 ml in the elution profile was due to excess PEG, which did

not bind to the column. The first major peak at ~ 38 ml was PEGylated insulin and the second peak at 52 ml was native insulin. It was evident from this chart that the purification method was very repeatable and each peak was easily distinguishable with minimal overlap. The fractions for PEGylated insulin were collected and dialyzed to remove salts and solvents present in the IEX mobile phase. The purified sample solution was then lyophilized and the recovered powder was stored at -20 °C under nitrogen until needed.

The purified sample of PheB1-PEGylated insulin was confirmed using MALDI-TOF MS. A close up view of the distribution for the PEGylated insulin can be seen in Figure 6.14. The center of the distribution for this scan was at 11381, almost exactly 200 Da lower than the center for the PEGylated di-BOC insulin in Figure 6.12. The drop in molecular weight was due to the loss of the two BOC protecting groups. The 44 Da molecular weight repeat unit was evident in this figure. MALDI-TOF scans in higher molecular weight ranges (data not shown) did not exhibit any peaks for PEGylated insulin which may have had two or three PEG conjugations.

The final yield of PEGylated insulin after each of these steps was 68.6 mg. Taking the increased molecular weight of the protein conjugate into account, this constituted a yield of 6.9 %. While this was quite low, there were several key factors which could be addressed to improve the yield of the process. The majority of the loss for producing PheB1 PEGylated insulin was in the first step of the diboc treatment. This reaction had a yield of 56.8 % of di-BOC insulin. As discussed above, the side products and impure di-BOC insulin could be recycled for use in a second batch of PEGylated insulin. If the process were to be scaled up or performed more regularly, recovering and

recycling these extra diboc treated insulin species would greatly improve the efficiency of this process. The remaining loss was likely due to handling of lyophilized powders, transfer of solutions, dialysis, IEC purification of the final product, and sampling throughout the process to analyze intermediate products.

6.3.4. Characterization of PEGylated Insulin

To this point, the conjugation of a single mPEG polymer chain on insulin has been proven. However, the site of conjugation must be determined to prove that the PheB1 was in fact the only site modified. In order to do so, each potential site for PEGylation must be distinguished from one another. For proteins and peptides, the easiest way to do this is to utilize enzymatic or chemical cleavage of discrete points in the protein. In this work two degradation techniques were used: disulfide reduction and trypsin digestion.

6.3.4.1. PEGylated Insulin Disulfide Reduction

By eliminating disulfide bonds between cysteine residues in insulin, the A and B chains of the protein were separated from one another (Figure 6.1). This separation isolates the two chains allowed elucidation of the site of PEGylation being on the A chain at the GlyA1 or on the B chain at either the PheB1 or LysB29 site. In order to keep disulfide bond from reforming, they were stabilized with iodoacetamide according to the reaction shown in Figure 6.15. This reaction added 58 Da at each cysteine residue which was reduced by DTT.

Following the reaction protocol described above, the retentate was analyzed using the Voyager DE Pro MALDI-TOF MS. In a scan between 1000-6000 Da, a strong peak was evident at 2634 Da, as shown in Figure 6.16. This corresponded well to the expected peak for the A-Chain without conjugation with mPEG-SPA, which has a molecular weight of 2615 Da. When the same sample was observed between 5000-15000 Da as shown in Figure 6.17, a molecular weight distribution was clear centered on 9036 Da. Since the matrix used for this analysis, CHCA, did not charge polymers in the absence of salts, the PEG must have been conjugated to a digested fragment of insulin. The molecular weight corresponded well to the expected mass if mPEG-SPA was conjugated to the B-chain of insulin, a distribution which would have been centered at 9174. If PEG was conjugated to the A-chain a similar distribution would be present centered at 8127, which was not evident in the MALDI-TOF spectra. These results confirm that the PEGylation of insulin took place at one of the two potential residues on the B-chain of insulin, PheB1 or LysB29, and not at the GlyA1 residue.

6.3.4.2. PEGylated Insulin Trypsin Digestion

The second method to determine the site of PEGylation for insulin was to digest the modified protein using trypsin. This method separated the two ends of the B chain and allowed for elucidation of which residue of the B chain was PEGylated. Trypsin specifically cleaves polypeptide bonds at the carboxyl side of lysine and arginine residues. For the case of insulin, the B-chain was cleaved at two locations indicated in Figure 6.1. This was relevant for PEGylated insulin because it isolated the LysB29 site from the other two residues which could be conjugated with amine reactive mPEG-SPA.

A MALDI-TOF MS spectrum for the mass range of 9000-13000 following the trypsin digestion is shown in Figure 6.18. The Voyager DE Pro MALDI-TOF MS with CHCA was used for this spectrum. There were two distinct peak distributions present. They exhibited the characteristic Gaussian distribution associated with PEG centered at 10591 and 11356 Da. The expected shift in the molecular weight of the PEGylated insulin due to the loss of the 8 peptide sequence at the C-terminus of the B-chain (GFFYTPKT) was 959 Da. The shift in the peaks seen in Figure 6.18 indicated a shift of approximately 765 Da. This was most likely due to the significant amount of crossover of the two distributions near the center of the lower molecular weight, shifting the peak to the right. The only other peaks seen from this sample were due to the protein being doubly charged thus giving it a measured molecular weight distribution centered at 5654 (not shown), roughly to $\frac{1}{2}$ the molecular weight of the major peak at 11356. No other peaks were observed from this sample so the spectrum was truncated. These results corresponded very well to digested and undigested PEGylated insulin if the site for PEG conjugation was on either the GlyA1 or the PheB1, but not on the LysB29. Since the site of PEGylation was determined to not be present at the GlyA1 from disulfide digestion, this work confirms that the mPEG-SPA is conjugated exclusively to the PheB1 residue of insulin. These results are the clearest representation of this site-specific, mono-conjugation of PEG to the PheB1 residue of insulin to date, and the methods used should be employed by others who wish to target specific residues for conjugation with insulin using this or other techniques.

One interesting result that can be indirectly inferred from this data was the fact that less than half of the PEGylated protein was degraded by trypsin, even after the

digestion was performed for more than 3 times the recommended amount, due to the reduction of enzymatic proteolysis caused by PEGylation. This was a good indication that the covalent attachment of PEG to insulin would significantly increase the residence time of insulin in the intestinal milieu, increasing its opportunity for absorption across the intestinal epithelium.

6.4. Conclusions

The work presented in this chapter clearly displayed the successful PEGylation of insulin. The modification was specifically targeted to the PheB1 residue by reacting insulin with diboc prior to conjugation with PEG. The reaction products from diboc treatment included a mixture of mono-BOC, di-BOC, tri-BOC, and native human insulin, 56.8 % of which was the primary di-BOC_{LysB29/GlyA1} peak. The crude mixture was characterized using RP-HPLC. The di-BOC_{LysB29/GlyA1} was purified using cation exchange chromatography. MALDI-TOF MS analysis of all of the fractions collected from the IEX purification indicated the presence of zero, one, two, or three BOC groups attached to insulin for individual elution peaks, confirming the results of the RP-HPLC characterization. Approximately 80 % of the purified di-BOC sample was present with ≥ 90 % purity and was isolated for reaction with mPEG-SPA 5000. Thus, 45.6 % of the initial amount of insulin treated with diboc was used for PEGylation. As a proof of concept, the remaining diboc treated insulin was recycled and returned insulin to its native state. The recycled insulin was reacted again with diboc. The recycled insulin and second pass diboc treated insulin products corresponded very well with controls of native human insulin and first-pass crude product of diboc treated insulin, respectively. This

indicated that this technique could be used to significantly improve yield of the intermediate di-BOC insulin.

Purified di-BOC insulin was reacted with a molar excess of mPEG-SPA 5000. The BOC groups were then removed and the conjugate was purified using IEC to produce the PheB1-mPEG-insulin conjugate. PEGylated insulin was characterized using a series of protein digestion methods in conjunction with MALDI-TOF MS. By process of elimination, the PheB1 residue was confirmed as the only site of PEG conjugation. Additionally, the difficulty in degrading insulin with trypsin indicated the improved enzymatic resistance of PEGylated insulin.

The final yield of PEGylated insulin was 6.9%. Several changes and improvements of the process are possible for future production including: minimal sampling of intermediate steps, improved purification resolution, increased PEGylation reaction yield from di-BOC insulin, and especially recycling of reaction by-products for both the diboc and the PEGylation reactions.

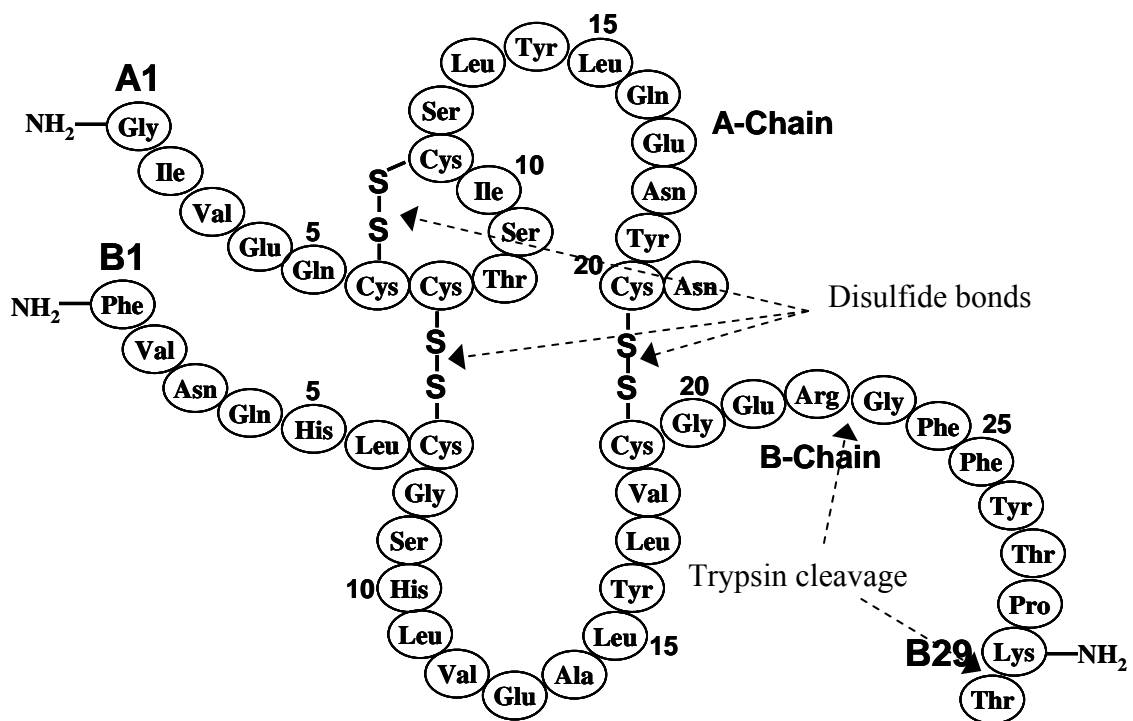


Figure 6.1. Amino acid sequence for human insulin with digestion pathways indicated

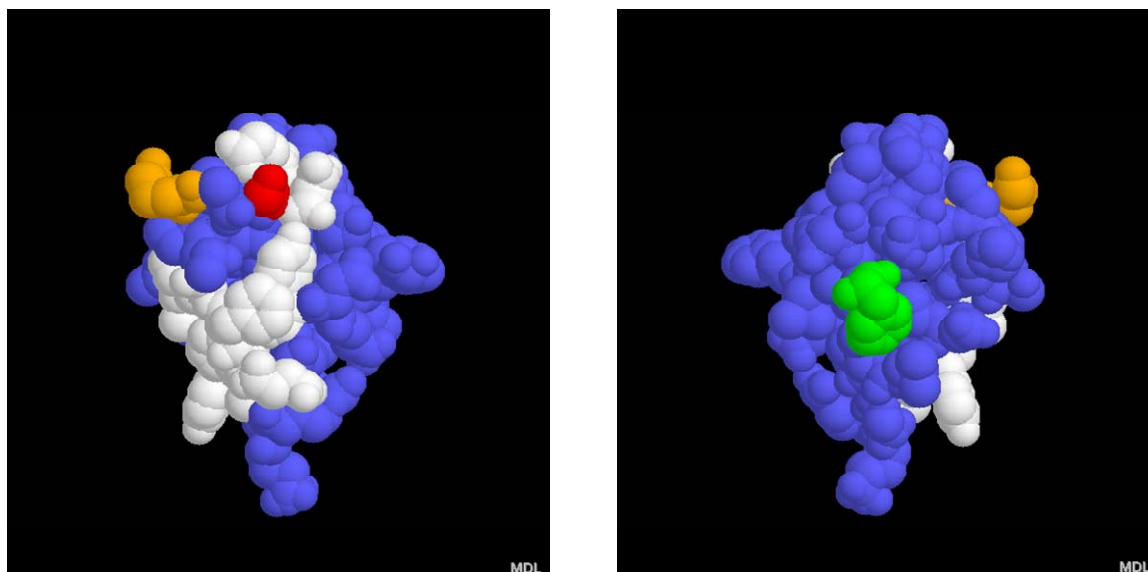


Figure 6.2. Space filled, three dimensional image of an insulin monomer (White = insulin receptor binding site, Red = GlyA1, Orange = LysB29, Green = PheB1)

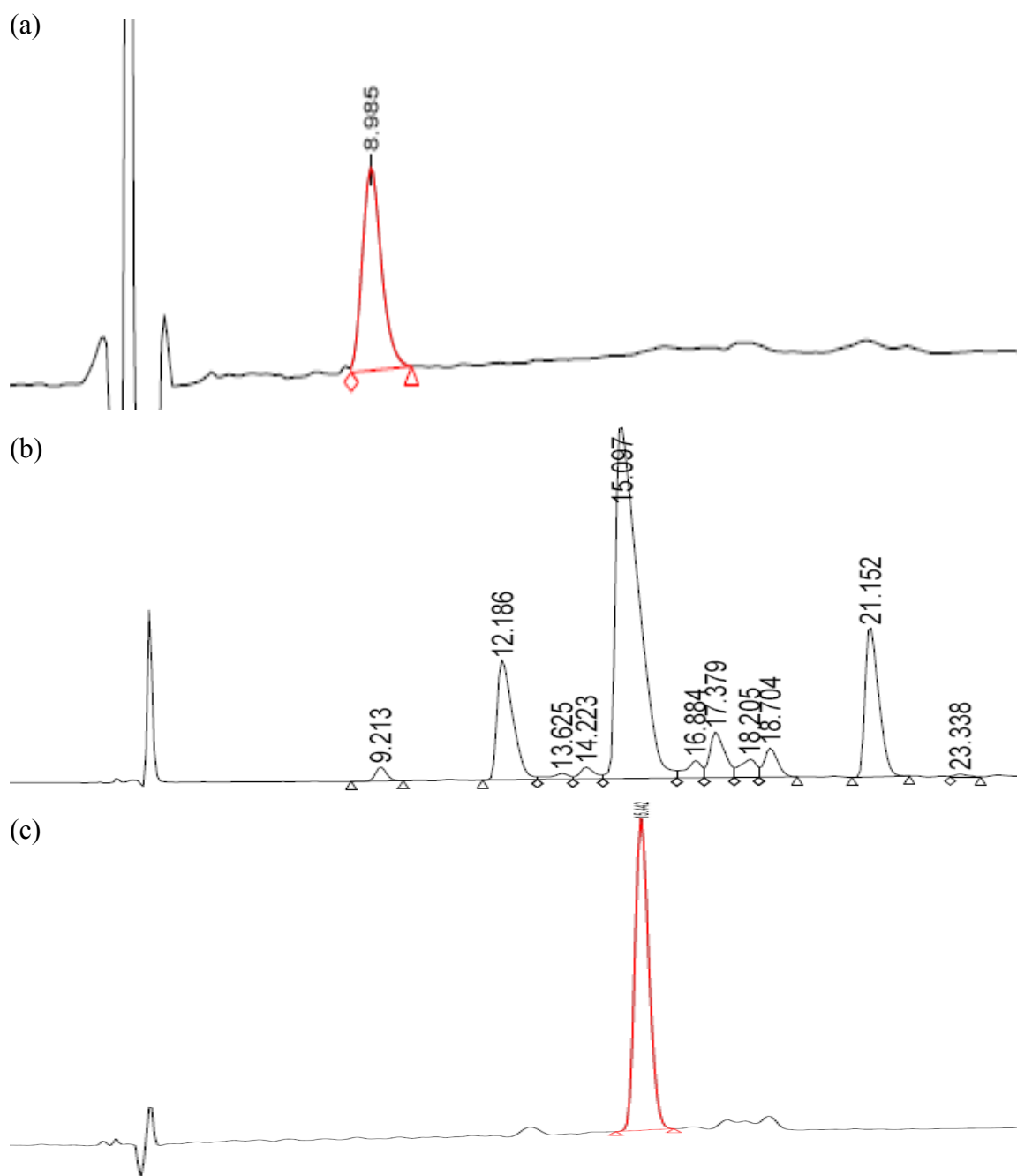


Figure 6.3. RP-HPLC absorbance at 214 nm for (a) insulin (b) crude diboc treated insulin (unpurified) and (c) purified di-BOC_{LysB29/GlyA1} insulin

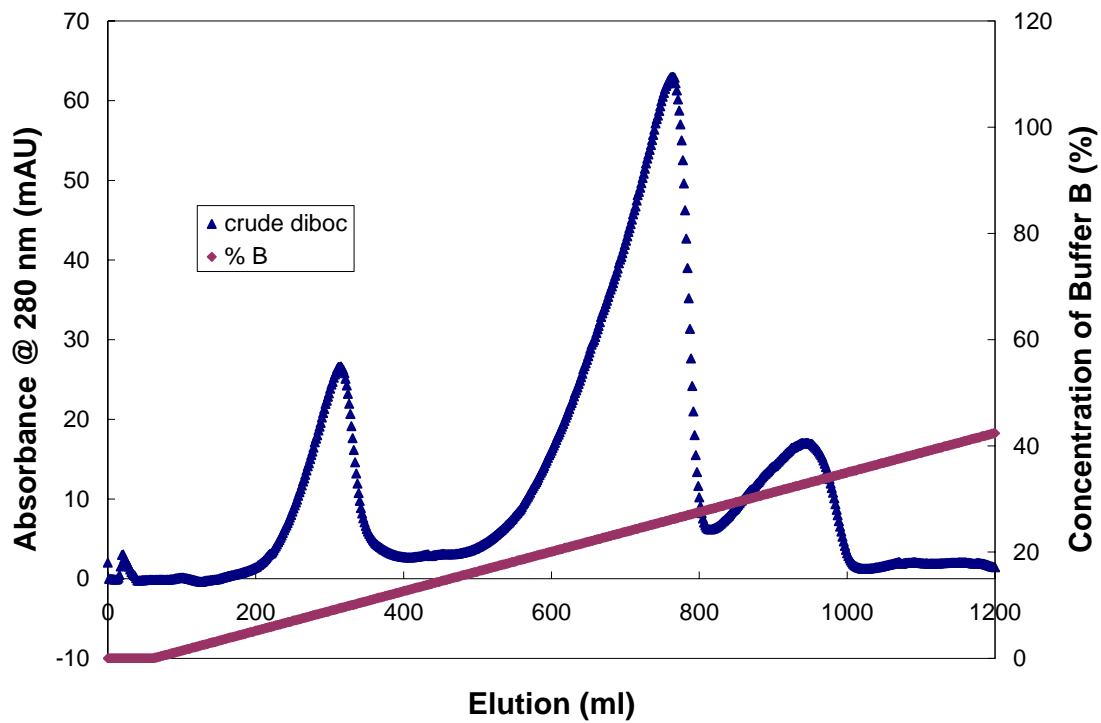


Figure 6.4. FPLC elution profile of crude diboc treated insulin using cation exchange chromatography with absorbance at 280 nm.

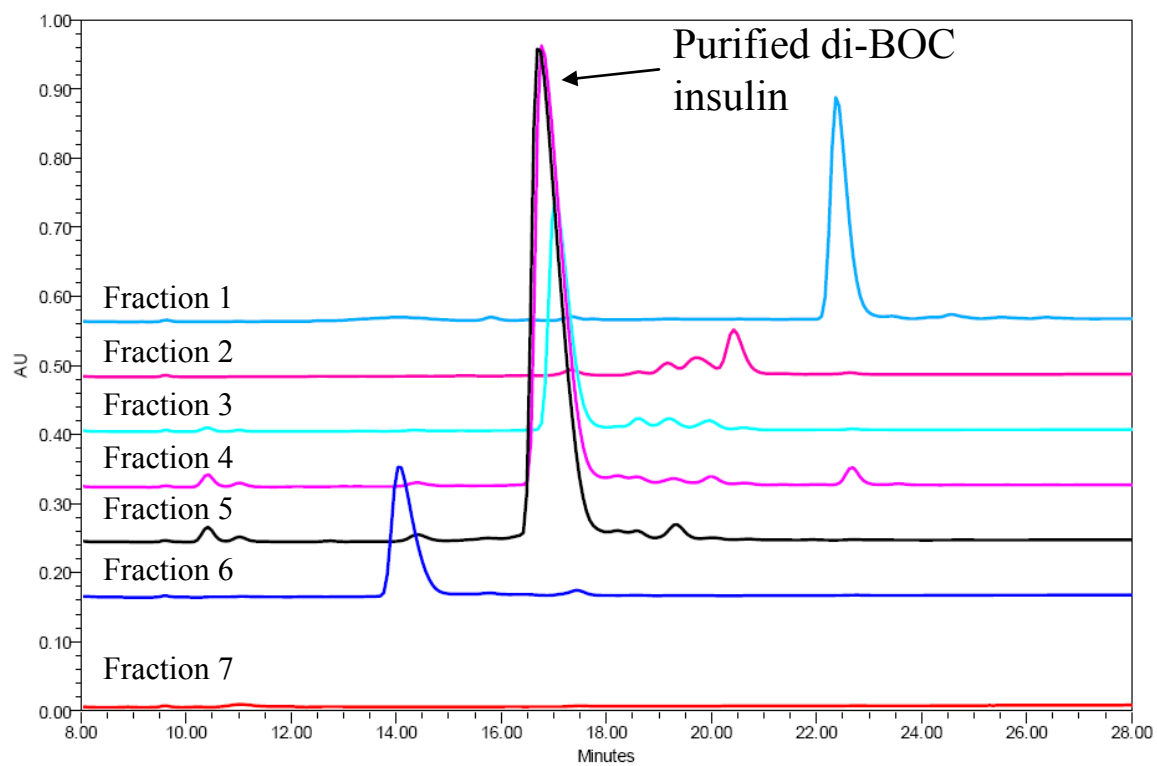


Figure 6.5. RP-HPLC stacked plot of fractions collected from FPLC elution with absorbance at 214 nm

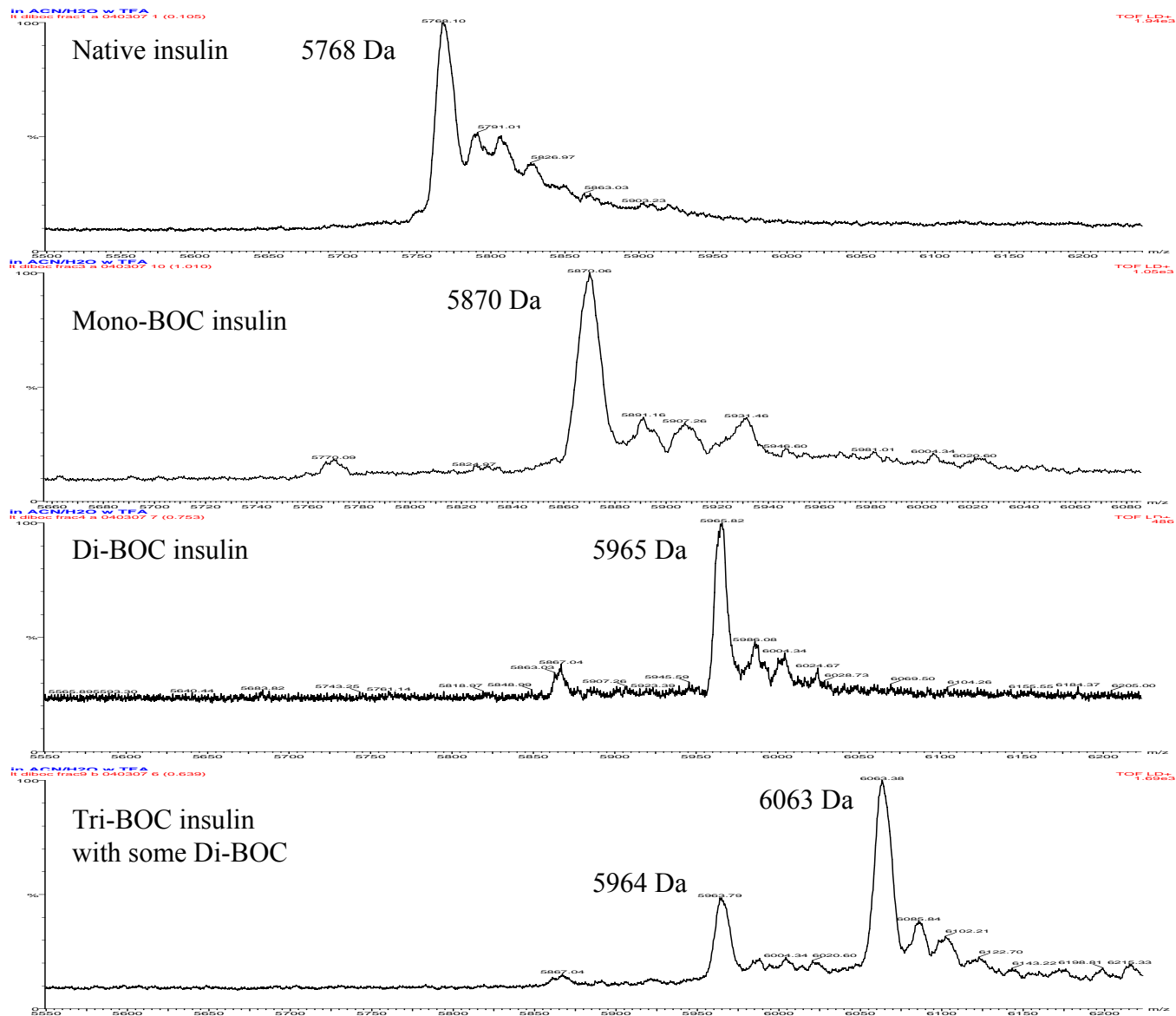


Figure 6.6. MALDI-TOF MS for fractions collected from FPLC separation of crude diboc treated insulin species

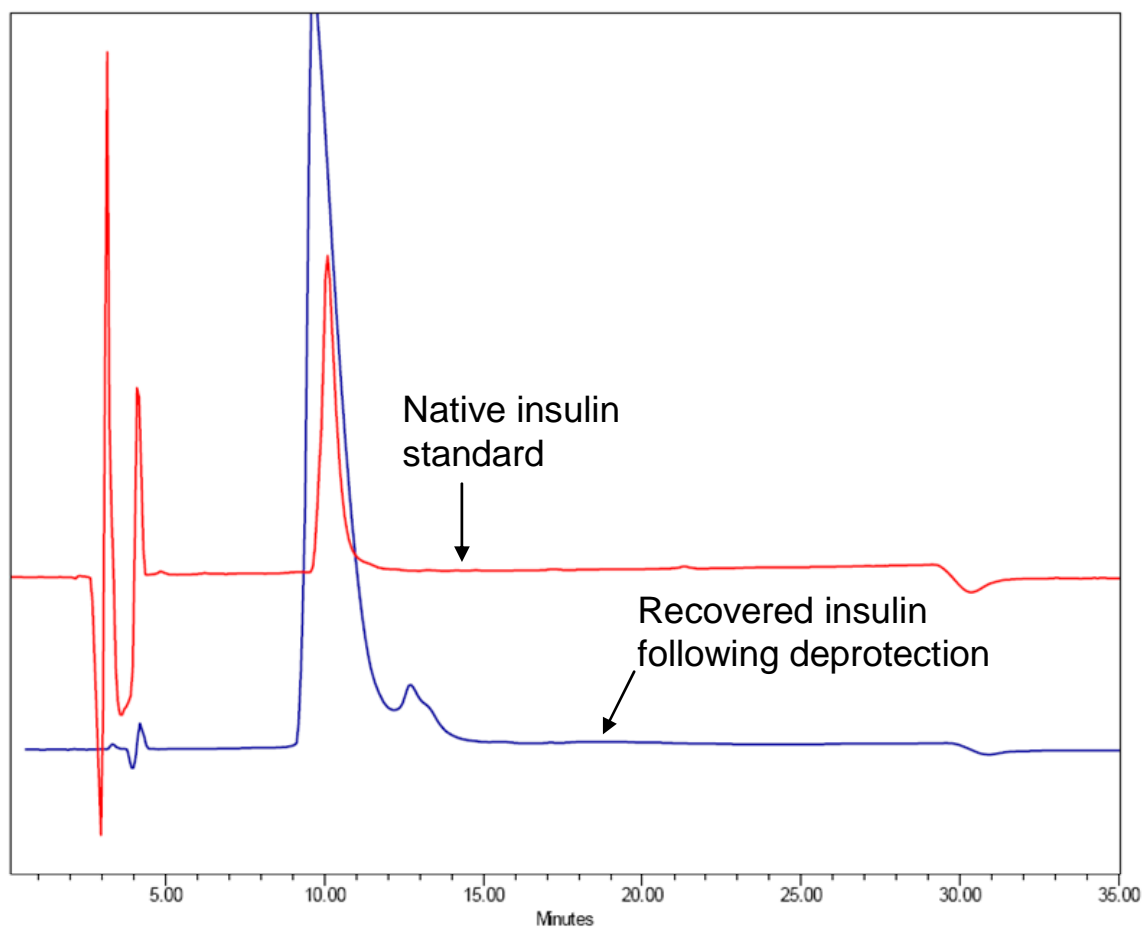


Figure 6.7. RP-HPLC spectra of recovered insulin following removal of BOC groups as compared to an insulin standard with absorbance at 214 nm.

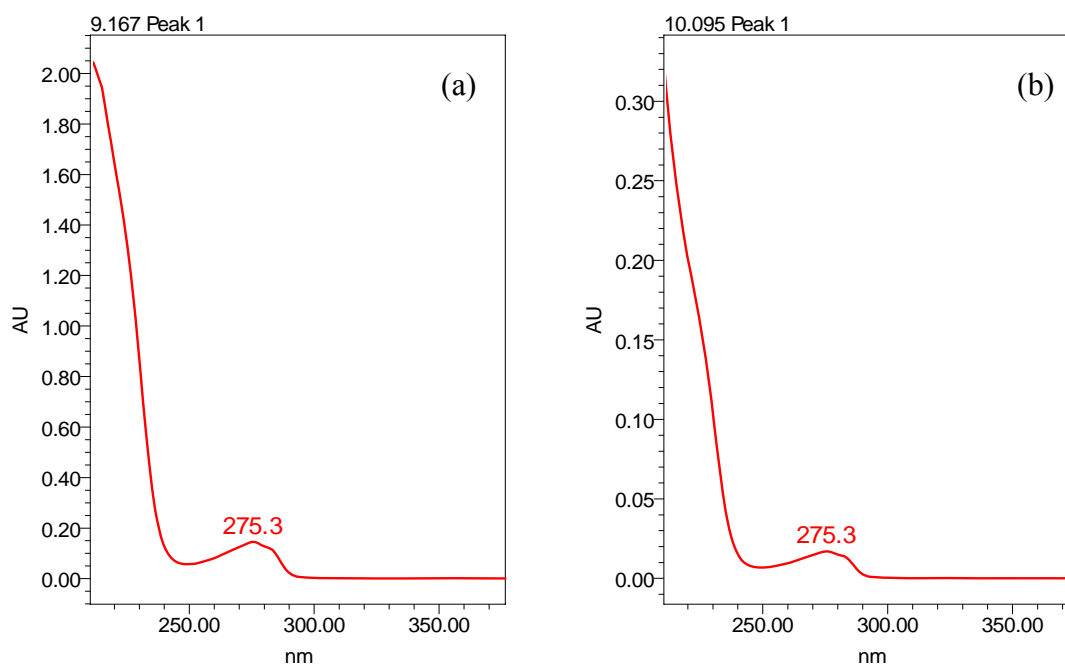


Figure 6.8. RP-HPLC total absorbance spectrum of (a) recovered insulin following removal of BOC groups and (b) native insulin standard

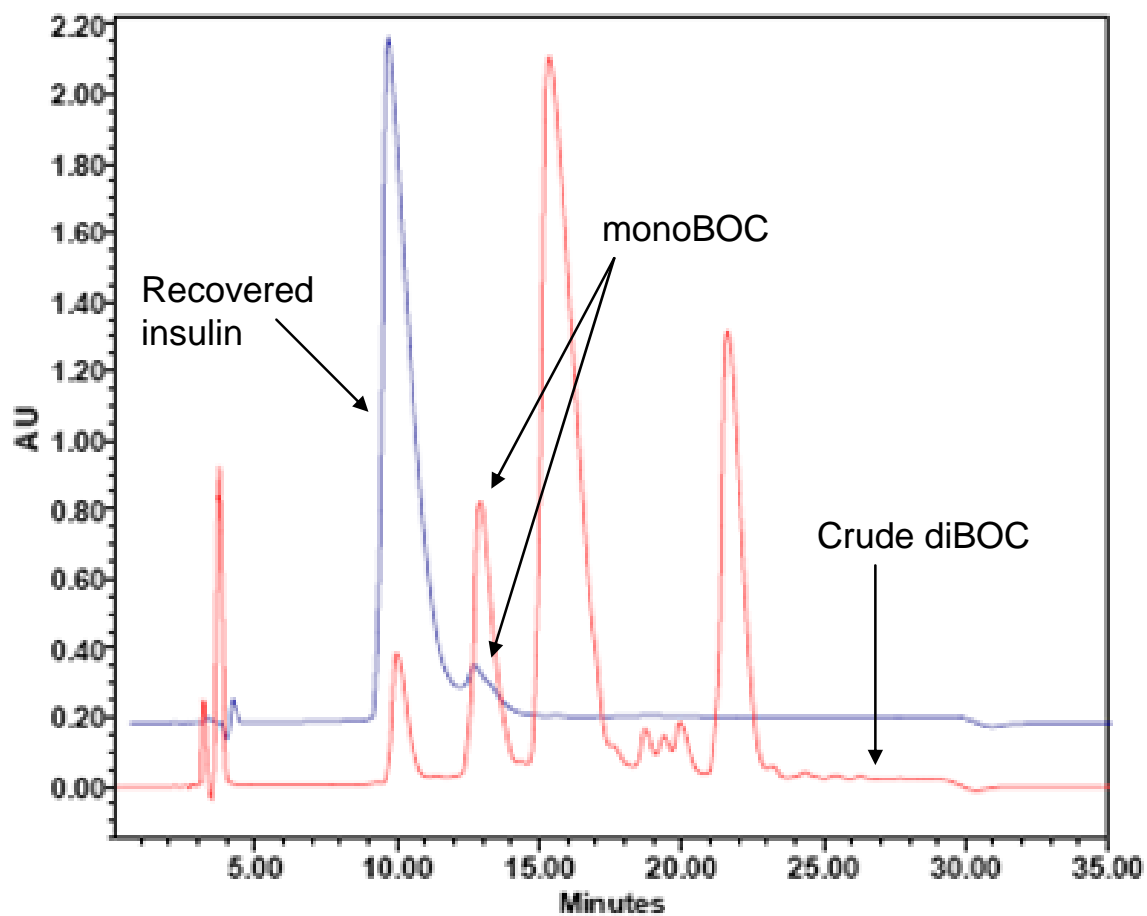


Figure 6.9. RP-HPLC spectra of recovered insulin following removal of BOC groups as compared to a crude diboc treated insulin sample prior to purification

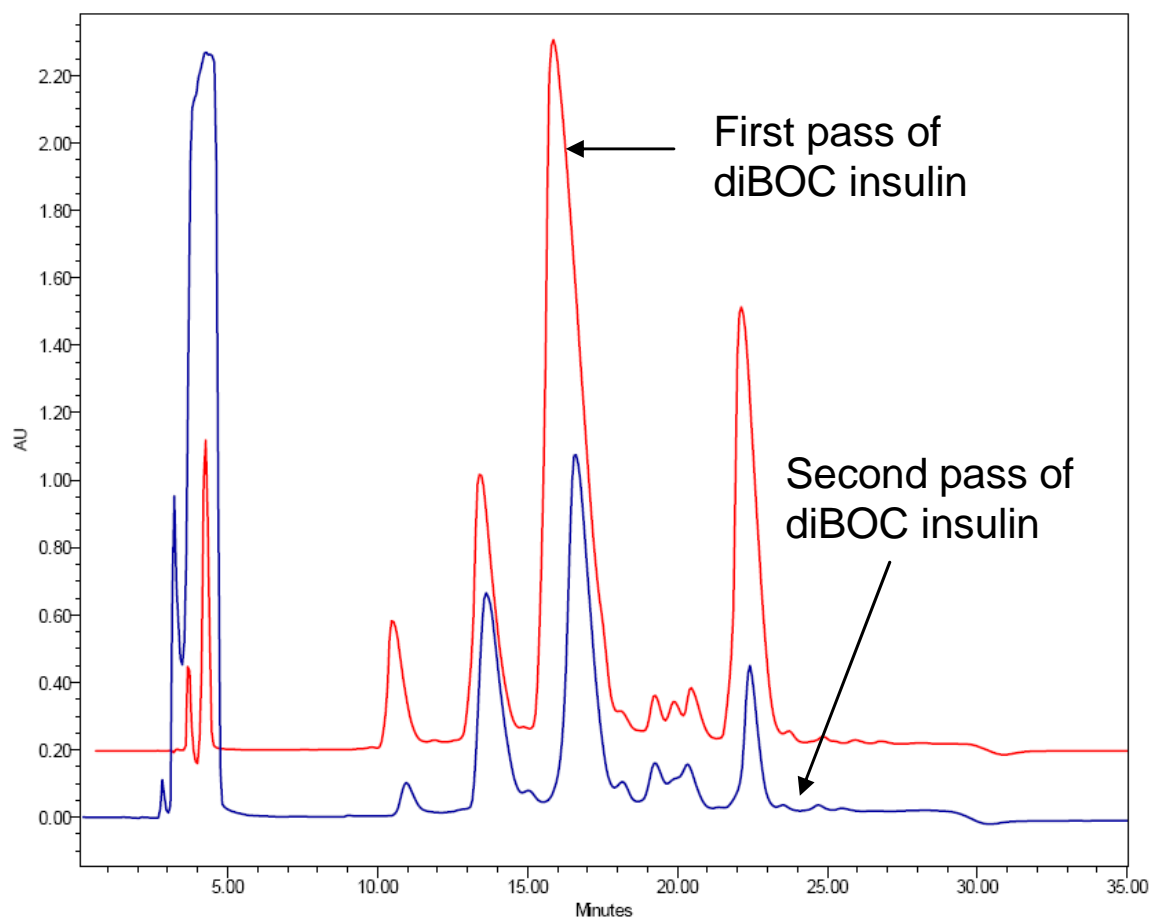


Figure 6.10. RP-HPLC spectra of recovered insulin treated a second time with diboc as compared to a first pass crude diboc treated insulin

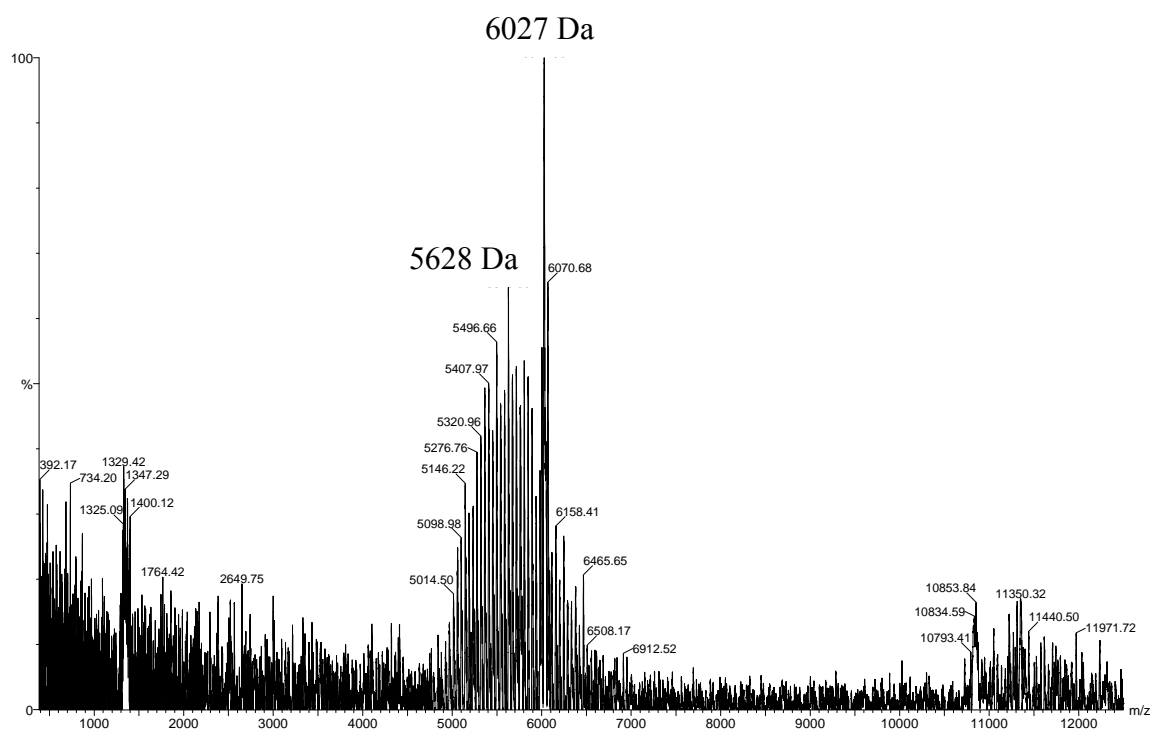


Figure 6.11. MALDI-TOF MS of a physical mixture of di-BOC insulin and mPEG-SPA with a 2500:1 molar ratio of DHB to analyte

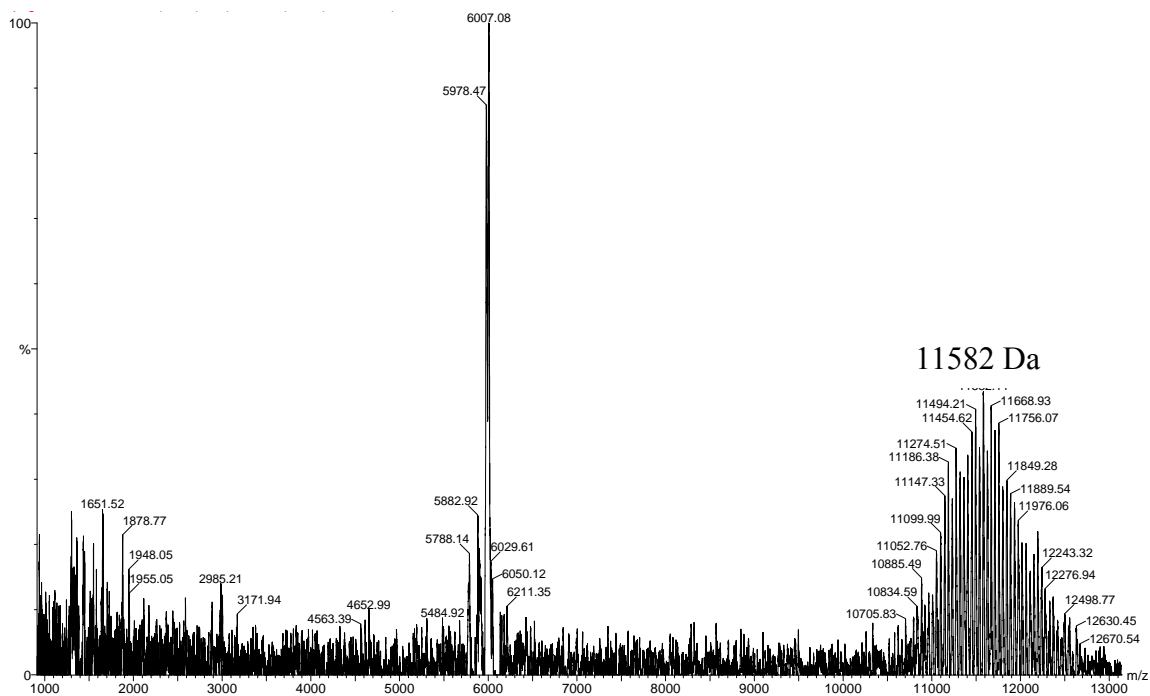


Figure 6.12. MALDI-TOF MS of PEGylated di-BOC insulin prior to eliminating unreacted components with a 2500:1 molar ratio of sinapic acid to analyte

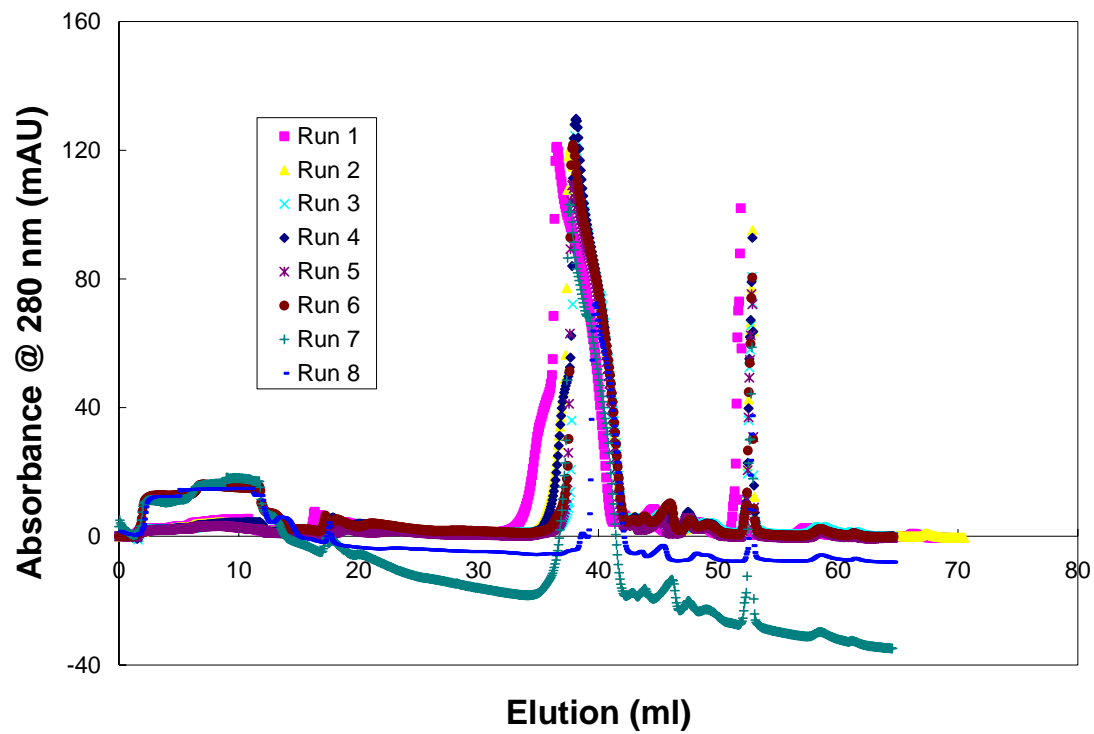


Figure 6.13. Cation exchange elution profile of PEGylated insulin following removal of the BOC groups

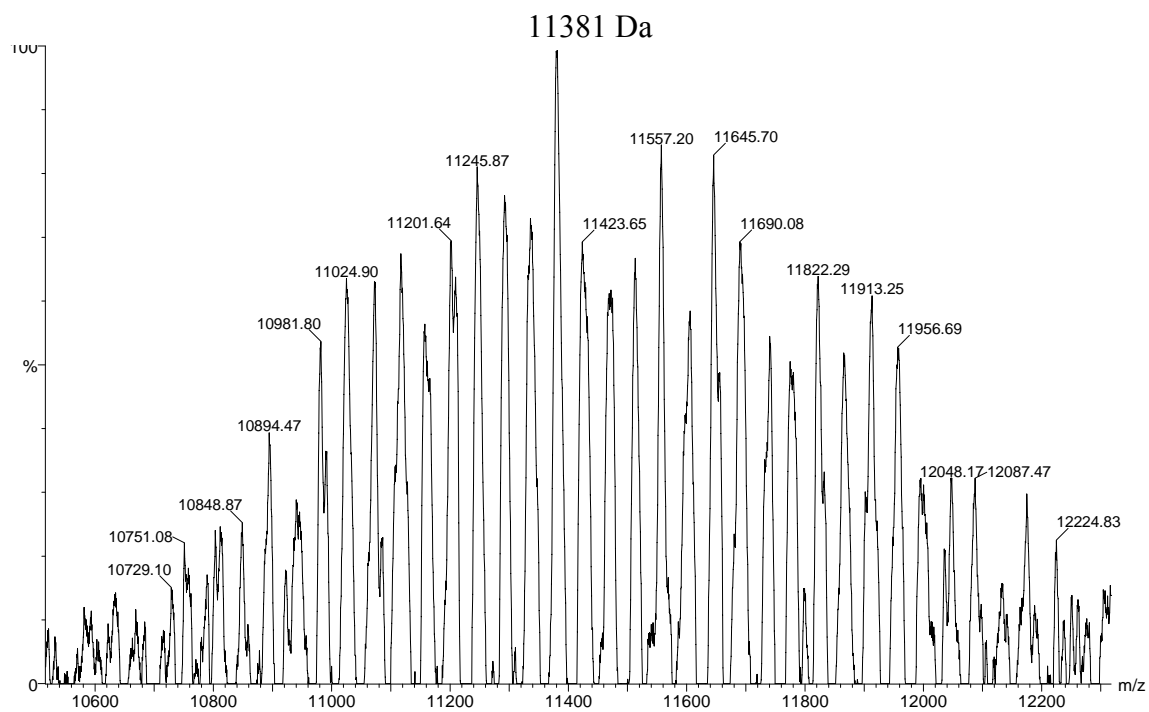


Figure 6.14. Close up view of MALDI-TOF MS of purified PEGylated insulin following removal of BOC protecting groups

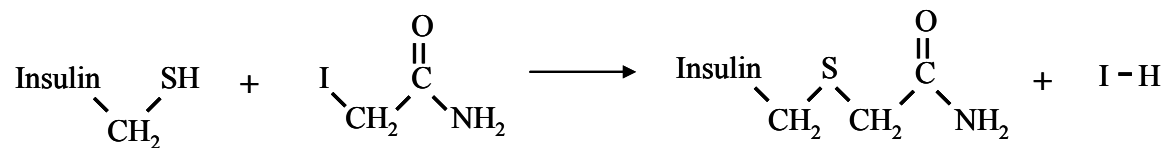


Figure 6.15. Reaction of iodoacetamide with a cysteine residue on insulin

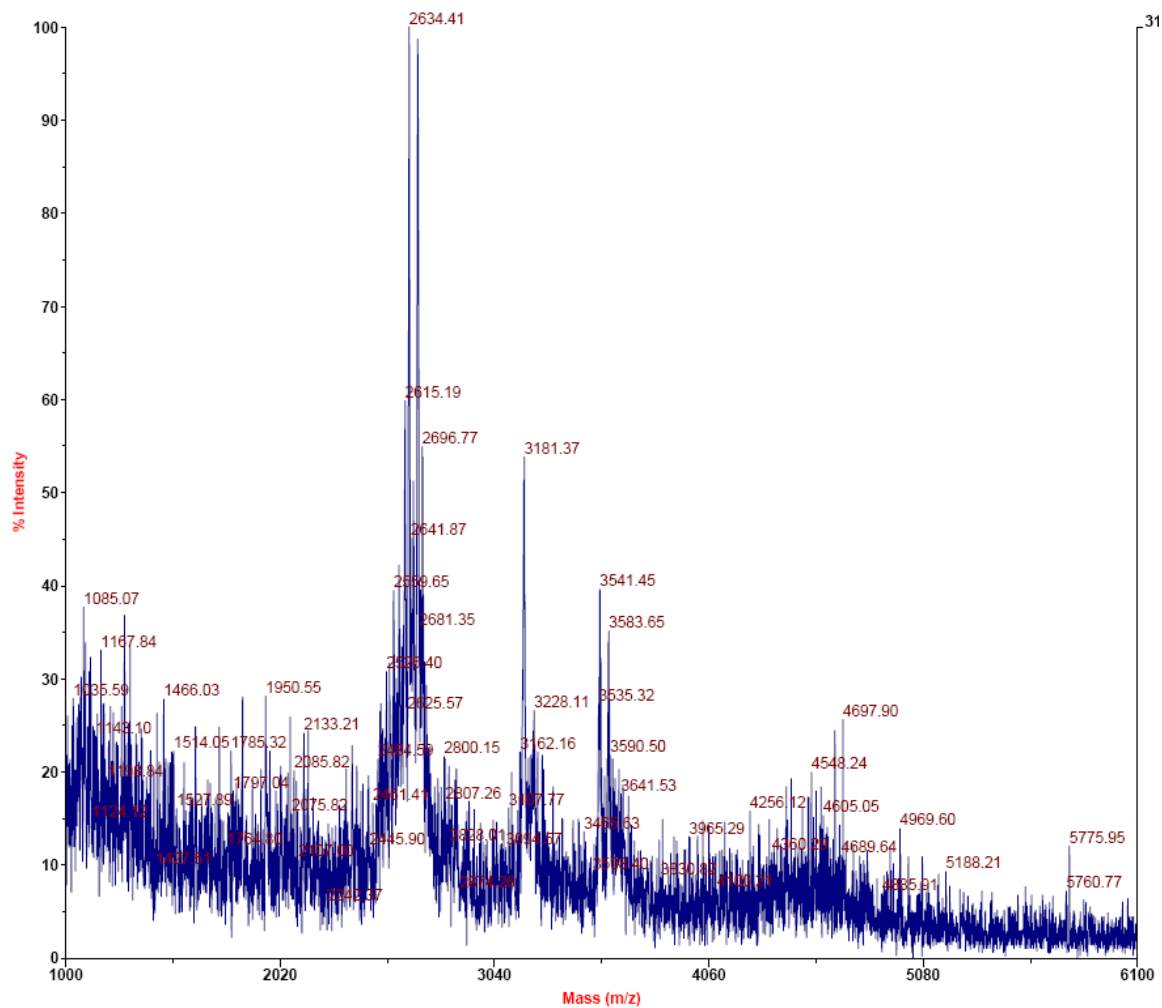


Figure 6.16. MALDI-TOF MS spectra of the A-chain of PEGylated insulin following disulfide reduction and alkylation with DTT and iodoacetamide

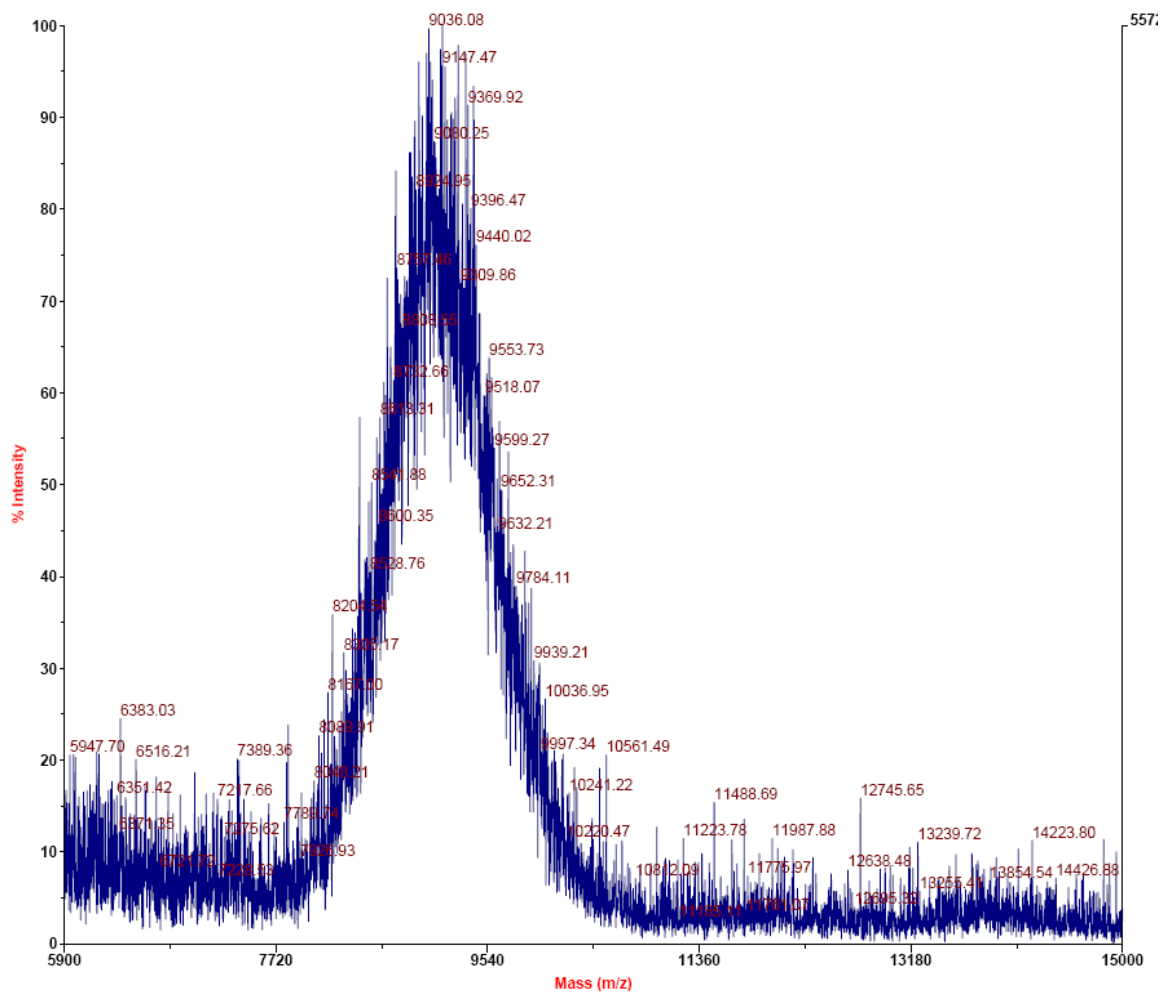


Figure 6.17. MALDI-TOF MS spectra of the B-chain of PEGylated insulin following disulfide reduction and alkylation with DTT and iodoacetamide

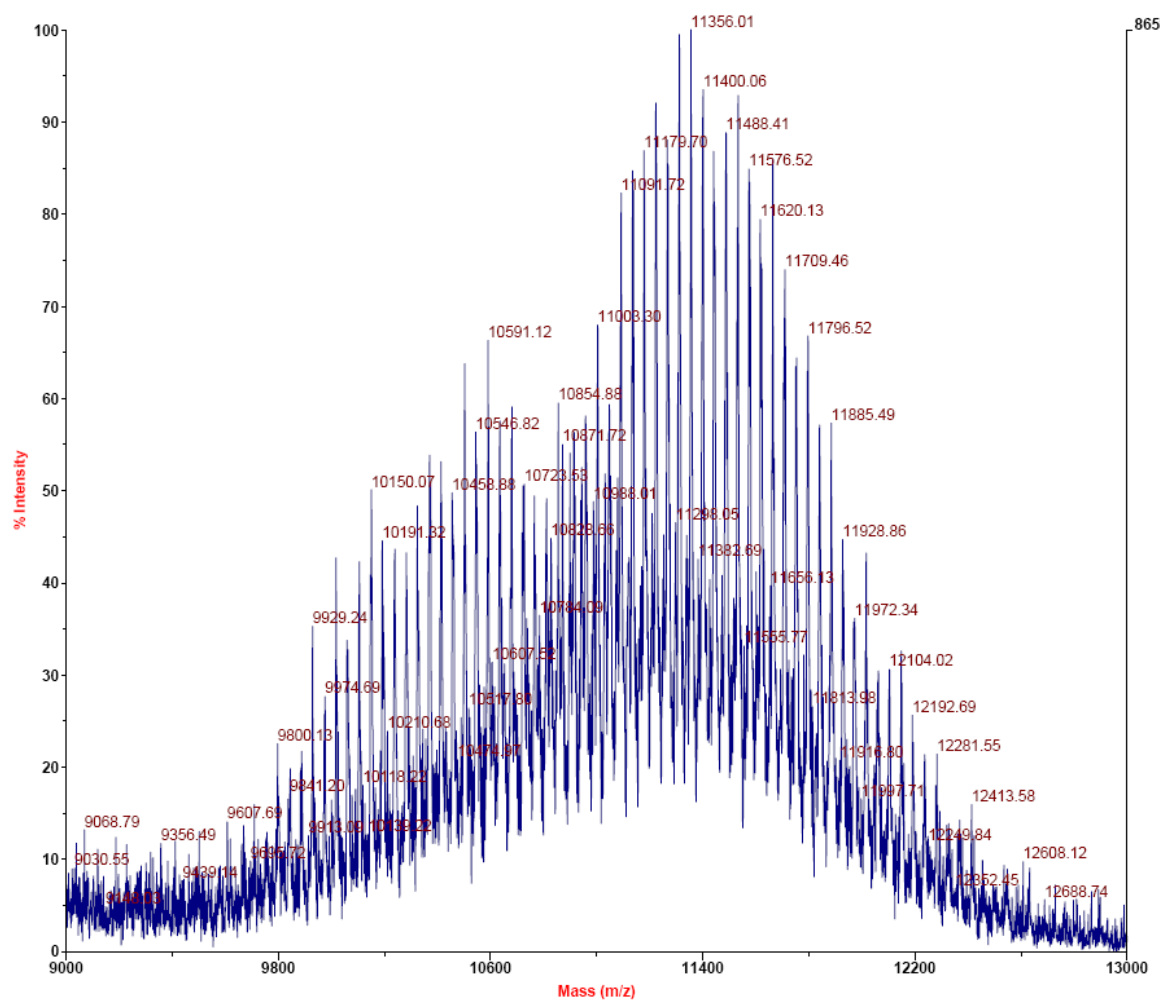


Figure 6.18. MALDI-TOF MS spectrum for the trypsin digested PEGylated insulin sample

6.5. References

1. Perakslis, E., A. Tuesca, and A. Lowman, *Complexation hydrogels for oral protein delivery: an in vitro assessment of the insulin transport-enhancing effects following dissolution in simulated digestive fluids*. J Biomater Sci Polym Ed, 2007. **18**(12): p. 1475-90.
2. Nakamura, K., et al., *Oral insulin delivery using P(MAA-g-EG) hydrogels: effects of network morphology on insulin delivery characteristics*. J Control Release, 2004. **95**(3): p. 589-99.
3. Yamagata, T., et al., *Characterization of insulin protection properties of complexation hydrogels in gastric and intestinal enzyme fluids*. J Control Release, 2006. **112**(3): p. 343-9.
4. Kim, B. and N.A. Peppas, *In vitro release behavior and stability of insulin in complexation hydrogels as oral drug delivery carriers*. Int J Pharm, 2003. **266**(1-2): p. 29-37.
5. Nakamura, K., et al., *Uptake and release of budesonide from mucoadhesive, pH-sensitive copolymers and their application to nasal delivery*. J Control Release, 1999. **61**(3): p. 329-35.
6. Goto, T., et al., *Gastrointestinal transit and mucoadhesive characteristics of complexation hydrogels in rats*. Journal of Pharmaceutical Sciences, 2006. **95**(2): p. 462-469.
7. Sahlin, J.J. and N.A. Peppas, *Enhanced hydrogel adhesion by polymer interdiffusion: use of linear poly(ethylene glycol) as an adhesion promoter*. J Biomater Sci Polym Ed, 1997. **8**(6): p. 421-36.
8. Stephenson, S.L. and A.J. Kenny, *Metabolism of neuropeptides. Hydrolysis of the angiotensins, bradykinin, substance P and oxytocin by pig kidney microvillar membranes*. Biochem J, 1987. **241**(1): p. 237-47.
9. Blanchette, J. and N.A. Peppas, *Cellular evaluation of oral chemotherapy carriers*. J Biomed Mater Res A, 2005. **72A**(4): p. 381-8.
10. Ichikawa, H. and N.A. Peppas, *Novel complexation hydrogels for oral peptide delivery: in vitro evaluation of their cytocompatibility and insulin-transport enhancing effects using Caco-2 cell monolayers*. J Biomed Mater Res A, 2003. **67**(2): p. 609-17.

11. Peppas, N.A. and N.J. Kavimandan, *Nanoscale analysis of protein and peptide absorption: insulin absorption using complexation and pH-sensitive hydrogels as delivery vehicles*. Eur J Pharm Sci, 2006. **29**(3-4): p. 183-97.
12. Torres-Lugo, M., et al., *pH-Sensitive hydrogels as gastrointestinal tract absorption enhancers: transport mechanisms of salmon calcitonin and other model molecules using the Caco-2 cell model*. Biotechnol Prog, 2002. **18**(3): p. 612-6.
13. Bernkop-Schnurch, A. and A. Scerbe-Saiko, *Synthesis and in vitro evaluation of chitosan-EDTA-protease-inhibitor conjugates which might be useful in oral delivery of peptides and proteins*. Pharm Res, 1998. **15**(2): p. 263-9.
14. Bernkop-Schnurch, A., *The use of inhibitory agents to overcome the enzymatic barrier to perorally administered therapeutic peptides and proteins*. J Control Release, 1998. **52**(1-2): p. 1-16.
15. Larionova, N.V., et al., *Biodegradable cross-linked starch/protein microcapsules containing proteinase inhibitor for oral protein administration*. Int J Pharm, 1999. **189**(2): p. 171-8.
16. Sood, A. and R. Panchagnula, *Peroral route: an opportunity for protein and peptide drug delivery*. Chem Rev, 2001. **101**(11): p. 3275-303.
17. Ge, Y.C. and R.G. Morgan, *The effect of trypsin inhibitor on the pancreas and small intestine of mice*. Br J Nutr, 1993. **70**(1): p. 333-45.
18. Zalipsky, S., *Chemistry of polyethylene glycol conjugates with biologically active molecules*. Adv Drug Deliv Rev, 1995. **16**: p. 157-182.
19. Veronese, F.M. and G. Pasut, *PEGylation, successful approach to drug delivery*. Drug Discov Today, 2005. **10**(21): p. 1451-8.
20. Roberts, M.J., M.D. Bentley, and J.M. Harris, *Chemistry for peptide and protein PEGylation*. Adv Drug Deliv Rev, 2002. **54**(4): p. 459-76.
21. Greenwald, R.B., et al., *Effective drug delivery by PEGylated drug conjugates*. Adv Drug Deliv Rev, 2003. **55**(2): p. 217-50.
22. Lindsay, D.G. and S. Shall, *The acetylation of insulin*. Biochem J, 1971. **121**(5): p. 737-45.

23. Baudyš, M., Uchio, T., Hovgaard, L., Zhu, E. F., Avramoglou, T., Jozefowicz, M., Rihová, B., Park, J. Y. Lee, H. K., Kim, S. W., *Glycosylated insulins*. J Control Release, 1995. **36**: p. 151-157.
24. Baudyš, M., et al., *Physical stabilization of insulin by glycosylation*. J Pharm Sci, 1995. **84**(1): p. 28-33.
25. Calceti, P., et al., *Development and in vivo evaluation of an oral insulin-PEG delivery system*. European Journal of Pharmaceutical Sciences, 2004. **22**(4): p. 315-323.
26. Uchio, T., et al., *Site-specific insulin conjugates with enhanced stability and extended action profile*. Adv Drug Deliv Rev, 1999. **35**(2-3): p. 289-306.
27. Hinds, K., et al., *Synthesis and characterization of poly(ethylene glycol)-insulin conjugates*. Bioconj Chem, 2000. **11**(2): p. 195-201.
28. Markussen, J., et al., *Immobilized insulin for high capacity affinity chromatography of insulin receptors*. J Biol Chem, 1991. **266**(28): p. 18814-8.
29. Konigsberg, W., *Reduction of disulfide bonds in proteins with dithiolthreitol*. Methods Enzymol, 1972. **25**: p. 185-188.

CHAPTER 7: *IN VITRO* AND *IN VIVO* TESTING OF PEGYLATED INSULIN WITH P(MAA-g-EG) HYDROGELS

7.1. Introduction

The evaluation of a design for oral insulin delivery requires a thorough knowledge of several important parameters influencing the system such as the physiology, pharmacokinetic and pharmacodynamic (PK/PD) profile, and designed delivery mechanism. Poly(methacrylic acid-g-ethylene glycol), P(MAA-g-EG), hydrogels have already exhibited the ability to adequately inhibit the degradation of insulin in the gastric environment [1, 2], bind to the mucus layer of the small intestine [3, 4], reduce enzymatic activity in the lumen of the small intestine [5, 6], locally and reversibly permeate the tight junctions the epithelial layer [7], and deliver insulin to the bloodstream in a number of *in vitro* and *in vivo* tests [8-10]. The current results of previous work has been somewhat promising with bioavailabilities as high as 9.5 % [8]. One limitation of the current design is that while P(MAA-g-EG) reduces enzymatic activity of the pancreatic enzymes present in the lumen and brush-border of the small intestine, most insulin that is released from the hydrogel does not remain localized to the hydrogel. Only insulin which is still in very close proximity to the hydrogel will be able to utilize its enzyme reducing effects and exhibit a sustained presence in the GI tract. Increasing the residence time as an undigested protein in the small intestine should greatly increase the likelihood that it will be absorbed as an intact protein by paracellular transport. As discussed in Chapter 6, insulin PEGylation can greatly increase the enzymatic resistance of the protein. This behavior was apparent in the very low amount of degradation of the protein when exposed to a concentrated amount of a pancreatic and

brush-border enzymes [11-14]. By combining the increased enzymatic resistance of PEGylated insulin with P(MAA-g-EG) hydrogels the bioavailability of the protein may be increased following oral delivery. The *in vitro* interaction between a PEGylated insulin molecule and P(MAA-g-EG) hydrogels should also change. In Chapter 5, the uptake and release of insulin from the hydrogel was characterized and appeared to be at least partially dependent on the weak bonds formed between the protein and the hydrogel. A PEG modified insulin molecule should retain these bonds, but additional bonds may be possible between the hydrogel and the PEG chain of the conjugate. Modifying the characteristics of insulin through PEGylation will also have an impact on its biological effect, as is seen for other PEG modified proteins.

In this work, the *in vitro* application of the P(MAA-g-EG) hydrogels with PEGylated insulin is performed. The uptake and release of PEGylated insulin is measured for three different hydrogel formulations in a similar fashion as was tested for regular human insulin. In doing so, changes in the loading or release behavior with PEGylated insulin can be attributed to the presence of the covalently attached PEG moiety. Characterization of the interaction between PEGylated insulin and P(MAA-g-EG) hydrogels may further bolster the conclusions reached based on the testing with native human insulin and insulin glargine.

Application of this drug delivery design is also investigated using an *in vivo* model in rats. Because the protein is inherently different, its activity must be compared to the native insulin molecule. From this testing, the PK/PD profiles can be determined based on different dosing techniques used to determine bioactivity of PEGylated insulin. The use of human insulin in rats is critical because the human an insulin glargine can be

distinguished from one another using enzyme linked immunosorbent assay (ELISA) to determine concentration. The biological effect of human insulin in rats, however, is nearly identical to that of murine insulin. The combined system is also challenged with the most rigorous *in vivo* work performed with P(MAA-g-EG) on rats using *in situ* dosing techniques. In doing so, significant insight can be gained for future designs and approaches for oral insulin delivery with P(MAA-g-EG) hydrogels.

7.2. Materials and Methods

7.2.1. Materials

The materials used to make PEGylated insulin and P(MAA-g-EG) hydrogels were the same as used in previous chapters. Bicinchoninic acid (BCA) assays were purchased from Pierce Chemical Company (Rockford, IL). Enzyme linked immunosorbent assays were purchased from ALPCO diagnostics (#80-INSHU-E10, Salem, NH). Male Sprague Dawley rats between 280-320 g were purchased from Harlan (Indianapolis, IN). Isoflurane, pentobarbital, and euthanasia solution were provided by the veterinary staff at Thomas Jefferson University. An insulin pump was used for subcutaneous dosing of insulin (Disetronic Roche Diagnostics, Palo Alto, CA). Blood glucose meters and glucose strips were purchased from Hemocue (Lake Forest, CA). Liquid diet mix was purchased from Bio-Serv (Frenchtown, NJ).

7.2.2. Synthesis of P(MAA-g-EG) Hydrogels

Only three formulations of P(MAA-g-EG) hydrogels were used for this testing due to the limited amount of PEGylated insulin available. The three formulations used were chosen to contain low, medium, and high levels of covalent crosslinks based on their formulations which were 0.75/33, 1.25/50, and 2.0/66, respectively, where the ratios represent mol% of PEGDMA/wt% of monomer present during polymerization. Two different types of each formulation were tested. The first set of hydrogels had a 1:1 monomer ratio of MAA:EG groups. This is the monomer ratio which has been used throughout this entire work. A second set of hydrogels had a 3:2 monomer ratio of MAA:EG. These samples were only tested in this chapter and were examined to emphasize the interaction between P(MAA-g-EG) hydrogels and PEGylated insulin as will be discussed in the results of this chapter.

7.2.3. PEGylated Insulin Loading and Release

The loading of regular human insulin and PEGylated insulin was performed according to the same techniques as seen in Chapter 5 for regular human insulin. Release studies were performed in PBS at pH levels of 4.7, 5.6, 6.2, 6.8, and 7.4 to adequately encompass the range in which P(MAA-g-EG) exhibits the largest change in swelling and ionic state. The protein concentrations were determined for the *in vitro* testing using a bicinchoninic acid (BCA) protein assay. This assay does not distinguish between different types of proteins, so standard curves were established for both human insulin and PEGylated insulin against the supplied bovine serum albumin standards. Briefly, aliquots of 25 μ l of solution were added to a clear, polystyrene, flat-bottomed, 96-well

plate. Each well was filled with 200 μ l of working reagent which was supplied by the manufacturer. The well was then covered and allowed to incubate at 37 °C for 30 minutes. The plate was allowed to cool to room temperature before measuring the total absorbance of each well at 550 nm using a plate reader (BioTek Elx800, Winooski, VT).

7.2.4. *In Vivo* Determination of PEGylated Insulin Bioactivity

All *in vivo* studies performed in this work were approved by the Institutional Animal Control and Use Committee (IACUC) at Thomas Jefferson University under protocol number 355 version V. The bioactivity of PEGylated insulin was measured against native human insulin following intravenous (IV) and subcutaneous (SC) injection into healthy rats. Male Sprague Dawley rats between 280-320 grams were allowed to acclimatize to their environment for a minimum of 3 days before use. The rats were fasted overnight to reduce their endogenous stores of glycogen which would counteract an induced hypoglycemic effect caused by insulin. During fasting, the rats were placed in cages with wire mesh bottoms which allowed feces to drop through the wiring so that they would not ingest them during the night. They were provided with unlimited amounts of water during their fast. The following morning, the rats were put under general anesthesia by a SC injection of 40-50 mg/kg of pentobarbital. Once anesthetized, each rat was weighed to determine accurate dosing levels and restrained in the supine position under a neonatal heating lamp by surgical tape. The rats were placed on a small piece of cardboard covered with aluminum foil to reflect the radiant heat back into the animal and help maintain their body temperature. Each rat was connected by a nose cone to a source of 100 % oxygen flowing through an isoflurane vaporizer. General anesthesia was

maintained throughout the test with 1-2 % isoflurane. The body temperature of each rat was monitored using an anal thermometer and maintained between 98-100 °F. Up to six rats could be connected in series under the neonatal lamp and connected to the vaporizer.

Blood samples were collected directly from the jugular veins which were accessed bilaterally by incisions of about 2 cm along the trachea anterior from the clavicle. Cotton balls were placed over the incision sites and intermittently saturated with normal saline to maintain the pliability and hydration of the tissues. Blood samples of 0.2 ml were collected with a 1.0 ml syringe equipped with a 27-gauge needle. For intravenous (IV) testing, the doses were injected directly into the circulation using the jugular vein. Blood samples were taken at 1, 5, 10, 15, 30, 45, 60, 120, 180, 240, 300, and 360 minutes following dosing. Three baseline samples were also taken following surgery, but prior to dosing to establish the initial blood glucose levels in each rat. Subcutaneous (SC) testing doses were injected under the skin of the rat in the abdomen using an insulin pump. Blood samples were taken following SC injection at 1, 5, 10, 15, 30, 45, 60, 120, 180, 240, 300, 360, 420, and 480 minutes. Three baseline samples were also taken as was done for IV testing. Following the testing the rats were euthanized using a 0.5 ml IV injection of the euthanasia solution according to the Panel on Euthanasia of the American Veterinary Medical Association.

The sample groups for IV and SC studies were dosed with either phosphate buffered saline (PBS), regular human insulin, or PEGylated insulin. Solution concentrations were adjusted such that a 200 µl dose would be administered for a 300 gram rat at the desired dosing levels of IU/kg. The rats tested with insulin or PEGylated insulin were given doses of 1.0 IU/kg for IV and SC studies or 4.0 IU/kg in one test for

SC administration. The dose at 4.0 IU/kg was too high for the rats and induced acute hypoglycemia which was counteracted by IV administration of glucose. Once glucose was administered, the blood glucose levels of the rats were no longer valid, but the rate of onset for the drugs still provided useful information for the pharmacokinetics of the drugs. Levels for IU of PEGylated insulin were based on the same as that for human insulin of 6 nmol/IU [15]. The conversion of nmol to μg for PEGylated insulin was then adjusted according to the increased molecular weight of the protein conjugate.

7.2.5. *In Situ* Testing of P(MAA-g-EG) Hydrogels

In an attempt to simulate an orally delivered dose, samples were placed *in situ* into the small intestines of rats. The method used in this study were somewhat different from previously reported methods in an attempt to more accurately mimic oral administration of P(MAA-g-EG) hydrogels. *In situ* testing on anesthetized rats was used rather than trying to examine the behavior in conscious rats for several reasons. First, orally dosing conscious rats is quite difficult because they will resist the dose and not normally eat a pill. Second, the number and frequency of blood samples used in this study would have been very difficult in conscious rats and impossible to take from the jugular vein. Third, by working with anesthetized animals, as many as six rats could be run in a single day. That would not have been possible with conscious rats due to the additional handling and restraint involved.

In an attempt to maintain normal GI enzymatic activity the rats were switched to an all liquid diet 48 hours prior to testing. By delivering an all liquid diet to the rats their GI tract was free from solid materials and feces but still working on digesting the food through enzymatic degradation. The diet consisted of 1 kcal/ml of mix with 35 % of

calories from fat, 18 % from protein, and the remaining 47 % from carbohydrates. The liquid diet was mixed with water and supplied as the only source of food and water for the rats during their fast. The rats were given 100 ml of the liquid diet 48 hours before testing. An additional 80 ml was provided 24 hours prior to testing. The liquid diet was removed the evening prior to testing approximately 14-16 hours prior to testing and the rats were given unlimited water overnight. By removing the liquid diet the night before testing again the glycogen and glucose stores of the rats were reduced and the chyme in the small intestine was greatly reduced but not eliminated.

Anesthesia, restraint, and blood sampling was performed in the same fashion as was done for the bioactivity determination. In this study the controls and samples were dosed directly to the small intestines of the rats. The peritoneal cavity was accessed through a midline incision. Doses of normal saline, unloaded P(MAA-g-EG) particles, insulin in PBS (20 IU/kg), insulin loaded P(MAA-g-EG) particles (20 IU/kg), PEGylated insulin in PBS (20 IU/kg), or PEGylated insulin loaded P(MAA-g-EG) particles (20 IU/kg) were preloaded into a 18-gauge silicon intraspinal catheter. Minimal solution volumes were used for each type of dose. For saline, 400 μ l of solution was dosed. Insulin solutions were made in PBS at 500 μ g/ml and PEGylated insulin solutions were made at 2 mg/ml. Doses were administered accordingly to deliver 20 IU/kg rat based on the conversion of 6 nmol/IU. For insulin and PEGylated insulin loaded polymer samples an adequate amount of polymer was first weighed into a 0.6 ml centrifuge tube. The polymer was suspended by 50 μ l of PBS at pH = 2.7. The low pH solution was used for the suspension to ensure that the polymer would not swell and release its contents until after it was dosed to the small intestine. The catheter was pre-filled with normal saline at

pH = 7.4 and connected to a 1 ml syringe with 200 μ l of saline in it. This volume served as the liquid to rinse out all of the solution or polymer suspension present in the catheter. The suspended polymer particles were drawn into the silicone catheter from the tip. By drawing the suspension into the tip of the catheter rather than trying to fill from the back the polymer remained within the length of the catheter and could be easily rinsed out. This process was repeated two or three times to ensure complete transfer of the polymer from the centrifuge tube to the catheter. The volume of the catheter was measured and determined to be between 220-250 μ l. By using less than that volume for polymer doses, mixing of the low pH and neutral pH buffers could be minimized. In experimental samples where the suspending buffer was at pH = 7.4 the polymer rapidly swelled and either could not be drawn into the catheter or clogged the catheter and could not be removed for dosing.

The pylorus of the rat was used as the anatomical marker for the start of the small intestine. The doses were administered to the duodenum just below the duodenal curve. The intestines were accessed using a 14-gauge Touhy needle. The 18-gauge catheter could then be fed into the small intestine through the needle. The catheters were marked for length every 2 cm. A length of 8-10 cm of the catheter was gently fed into the small intestines of each rat at which point the access point of the intestine was clamped to prevent backflow of the dosed liquid. The full amount of liquid or polymer suspension was then dosed directly and the catheter was slowly withdrawn from the intestine. The access point was clamped closed such that only the side of the intestines was occluded and movement of gastric juices could still proceed down the GI tract. The peritoneal cavity was then clamped closed for the duration of the test. Blood samples were

withdrawn from the jugular vein at 1, 5, 10, 15, 30, 45, 60, 120, 180, 240, 300, 360, 420, and 480 minutes following dosing. Three baseline samples were also taken to establish normal glycemic levels for each rat. Following each test, the rats were euthanized with a 0.5 ml IV injection of euthanasia solution according to the Panel on Euthanasia of the American Veterinary Medical Association.

7.2.6. Glucose and Insulin Determination

The blood samples from the *in vivo* testing were first tested for levels of glucose by two different blood glucose analyzers in mg/dl, the standard measurement for blood glucose concentrations. This required roughly 20 μ l of whole blood per sample. Both machines were verified using a control cuvette daily to ensure proper operation. The remaining blood was transferred to a serum separator tube and stored on ice for the duration of the test. When time permitted throughout the test the whole blood samples were centrifuged at 7500 rpm and the plasma was removed using a 200 μ l pipette. The plasma samples were centrifuged a second time to eliminate any bubbles and then stored on ice until the end of the test. Following testing the plasma samples were stored at -80 °C until they could be assayed for insulin concentration.

The concentration of human insulin or PEGylated insulin in the rat plasma was determined using enzyme linked immunosorbent assay (ELISA). The kits purchased from ALPCO diagnostics had a cross reactivity with rat insulin of only 0.7 %, so any detected changes in insulin concentrations were attributed exclusively to the human insulin which was dosed to the rats. A standard curve of PEGylated insulin was also generated on the ELISA plates and used to adjust the concentrations determined directly from plasma. The

ELISA plates were pre-coated with an insulin antibody to which insulin or PEGylated insulin would bind. The procedure required 25 μ l of a standard or sample in each well to be tested. The range of the kit was 3-200 μ IU/ml. Any samples which tested high out of range were diluted to 1/100 or 1/1000 concentration using the zero standard provided with the ELISA kit.

7.2.7. Statistics

A one-way analysis of variance (ANOVA) of individual data groups was used to distinguish statistically relevant differences between the groups. The confidence value of $p = 0.05$ or 0.01 was used and is indicated with the data represented in the figures at the end of the chapter.

7.3. Results and Discussion

7.3.1. PEGylated Insulin Loading

The loading for PEGylated insulin was first attempted using P(MAA-g-EG) hydrogels of formulations 0.75/33, 1.25/50, and 2.0/66 in which a 1:1 ratio of MAA:EG monomers was present. No loading of PEGylated insulin was observed with these samples. The same hydrogel formulations were able to load insulin at least to some degree as described in Chapter 5. The change in the ratio of the MAA:EG monomers caused by the addition of the PEGylated insulin may have caused the PEGylated insulin to be excluded from the hydrogel network. To investigate this hypothesis, a series of P(MAA-g-EG) hydrogels with the same formulations in terms of PEGDMA content and

monomer weight fraction were made with a 3:2 ratio of MAA:EG. If the complexation of the hydrogel is improved by moving toward a 1:1 ratio then the addition of PEGylated insulin should improve the complexation in these formulations.

The loading efficiencies for insulin and PEGylated insulin are shown in Figure 7.1. The loading of PEGylated insulin achieved the highest loading efficiencies of the three different formulations considered. It also had a higher loading efficiency than regular insulin in the P(MAA-g-EG) formulations made with a 3:2 ratio of MAA:EG. Interestingly, the loading efficiency for regular insulin increased when the monomer ratio was changed from 1:1 to 3:2 for formulations 1.25/50 and 2.0/66, but not for formulation 0.75/33. However, PEGylated insulin in the formulation 0.75/33 had significantly higher loading efficiency than insulin for either monomer ratio with 90.4 % of available PEGylated insulin loaded into the hydrogel. This result indicates that the PEGylated insulin does interact with the P(MAA-g-EG) hydrogel in a favorable manner with regard to its loading. Even when insulin cannot be efficiently loaded into the hydrogels due to very low crosslink density, as is the case with formulation 0.75/33, PEGylated insulin can be incorporated within the hydrogel and maintain its presence in excess of 90 % efficiency. Therefore the conjugation of PEG to insulin increases the attractive forces between the protein conjugate and the hydrogel. This is most likely due to the hydrogen bonds which can be formed between MAA and the PEG group now conjugated to insulin. This results further supports the findings in Chapter 5 which suggests that the interaction between P(MAA-g-EG) and insulin controls uptake and release more so than the diffusive restrictions of the network mesh size.

The release of insulin and PEGylated insulin from P(MAA-g-EG) hydrogels polymerized with a 3:2 ratio of MAA:EG is shown in Figure 7.2. In a similar fashion as was seen for regular insulin in Chapter 5, the release of insulin and PEGylated insulin did not exceed 20 % until the pH of the release buffer was 6.2 or greater. There was one exception to the rule with regular human insulin in the same formulation (0.75/33) as was seen before and presented in Chapter 5. For insulin, the fractional release for samples at $\text{pH} \geq 6.2$ exceeded 80 % with insulin for all three formulations except for one sample which still exceeded 70 %. However, for PEGylated insulin an increasing release trend was seen as the pH of the release buffer increased from 6.2 to 7.4. Additionally, the relative release amounts of PEGylated insulin were always lower than those seen for native human insulin between $\text{pH} = 6.2\text{-}7.4$. These results indicate that PEGylated insulin maintained a greater affinity for the P(MAA-g-EG) hydrogels than native human insulin. Because of that, the fractional release of PEGylated insulin did not exceed 67 % until the pH of the release buffer was at $\text{pH} = 7.4$. This behavior could be advantageous for oral insulin delivery because the protein will maintain a higher concentration within the hydrogel as it passes through the GI tract. Previous work has already shown that insulin can be protected only when it is in close proximity to P(MAA-g-EG). If the release is sustained for a significant period of time through the intestine based on local pH, then the possibility for protein transport can be sustained as the polymer moves down the GI tract.

7.3.2. Bioactivity and PK/PD for IV Administration

The applicability of PEGylated insulin for the treatment of diabetes relies on its ability to maintain its biological activity following modification. If the bioactivity of the

modified insulin is lost, then it has little clinical potential for oral delivery. The determination of the bioactivity is generally found by comparing its effect to IV administration of a control drug. In this experiment the comparison was made with regular human insulin in rats. A control group of PBS was also used to eliminate the effects of the surgeries on the biological effects seen in the rats.

The biological effect can be measured according to pharmacokinetic (PK) or pharmacodynamic (PD) behavior. As defined by Gibaldi and Perrier, pharmacokinetics is the study of the time course of drug and metabolite levels in different fluids, tissues, and excreta of the body, and of the mathematical relationships required to develop models to interpret such data [16]. Pharmacodynamics, on the other hand, is the science of evaluation of the drug action on the body as well as the relationship between drug concentration and effect [17]. A simpler description often used as a heuristic is that the pharmacokinetics is what a drug does to the body and pharmacodynamics is what the body does to the drug. The pharmacodynamic behavior of insulin is primarily related to the blood glucose (BG) levels in the circulation due to its effect on insulin receptors and subsequent transfer of glucose to the liver, muscular, and adipose tissues. Other effects of insulin are also related to its pharmacodynamic behavior, however, in this study only blood glucose was considered.

A chart of the pharmacokinetic behavior of insulin and PEGylated insulin following IV and SC delivery of 1 IU/kg in healthy male Sprague Dawley rats is shown in Figure 7.3. This figure displays the full scale of the concentrations determined using ELISA from blood serum levels. The concentrations are very high following IV administration because both PEGylated and regular insulin are delivered directly to the

bloodstream. For healthy adults, insulin concentrations reach concentrations of 60-90 $\mu\text{U}/\text{ml}$ (360-540 pmol/l) for postprandial levels [18]. The IV concentrations are greater than 150 times that of normal postprandial circulating levels immediately following dosing, but the levels rapidly drop due to clearance and binding to insulin receptors. A closer look at the lower concentrations gives more information of the pharmacokinetics of IV and SC administration and the differences between regular and PEGylated insulin. Figure 7.4 displays the insulin and PEGylated insulin concentrations following IV administration of 1.0 IU/kg in rats. Initial points are excluded because their concentrations exceed 500 $\mu\text{IU}/\text{ml}$. Normal human insulin drops below 500 $\mu\text{IU}/\text{ml}$ 10 minutes after IV administration, but PEGylated insulin required 30 minutes to drop to the same level. Normal levels for postprandial concentrations of insulin ($< 100 \mu\text{IU}/\text{ml}$) are reached for normal human insulin after 30 minutes. After 60 minutes the concentration of normal human insulin is 14.6 $\mu\text{IU}/\text{ml}$ and it is almost completely cleared from the circulation after 120 minutes. PEGylated insulin, on the other hand, sustained significant plasma concentrations for the duration of the 6 hour test. It does not drop below 100 $\mu\text{IU}/\text{ml}$ until 120 minutes after administration and maintains a concentration of 43.1 $\mu\text{IU}/\text{ml}$ after 6 hours. These results indicate that PEGylated insulin is slower to be cleared by the body and may also have a slower binding to the insulin receptor. Because it has a higher residence time in the bloodstream, the biological effect of PEGylated insulin in the body may also be sustained when compared to that of normal human insulin.

The natural pharmacodynamic action of insulin is to transport glucose into the tissues of the body. When insulin levels exceed basal levels in the absence of a meal they induce a hypoglycemic effect. In order to determine the biological activity of PEGylated

insulin must induce the same effect. The pharmacodynamic effect of the IV administered insulin and PEGylated insulin can be seen in Figure 7.5. A control group of PBS is also displayed in the figure. The BG levels are represented as the fraction of the initial values measured by baseline blood samples. Both regular human insulin and PEGylated insulin induce hypoglycemia in healthy male Sprague Dawley rats following IV administration. A drop in the fractional BG levels was also exhibited after administering only PBS, indicating that a drop was induced by the surgical technique alone. Therefore, the BG levels for insulin and PEGylated insulin were normalized by this surgery-induced drop as is seen in Figure 7.5b. The pharmacodynamic effect of both regular human insulin and PEGylated insulin were very similar to one another. The area above the normalized curve (AAC) was calculated as the sum of the area of consecutive trapezoids between the curve and 1. The AAC values were then used to determine the biological activity of PEGylated insulin were determined. The AAC values for normal human insulin were 61.63 after 4 hours and 61.69 after 6 hours versus 68.42 and 75.43 for PEGylated insulin after 4 and 6 hours, respectively. The units for these values are:

$$AAC [=] \left(\frac{C(t)}{C_o} \right) * \min \quad (\text{Eqn 7.1})$$

where $C(t)$ is the concentration of glucose at time t and C_o is the initial concentration of glucose. According to these values the bioactivity of PEGylated insulin is 111.0 % and 122.3 % that of normal human insulin following IV administration after 4 and 6 hours, respectively. While these bioactivity values may seem misleading they are explained not by the potency of PEGylated insulin, but in its increased residence time in the bloodstream. The reduced rate of clearance causes it to have an extended action and therefore a prolonged hypoglycemic effect. The potency of PEGylated insulin versus

regular insulin requires more information for the binding coefficient and residence time of each species with the insulin receptor which cannot be determined using these methods. A summary of the PK/PD data for IV insulin and PEGylated insulin administration is given in Table 7.1. Significant changes in the PK/PD profile were not expected following IV administration of PEGylated insulin versus that of regular human insulin. Administration of the proteins by IV injection does not allow a pharmacokinetic determination because they are placed directly into the circulation. Each induces a rapid hypoglycemic effect because of the high initial concentrations. While elevated, the endogenous production of insulin in healthy rats is effectively stopped and the transport of glucose from the bloodstream is carried out by the exogenous insulin or PEGylated insulin. The PK/PD profile for PEGylated insulin following SC dosing is much more likely to exhibit a more profound difference from regular human insulin because of the altered PK behavior.

7.3.3. Bioactivity and PK/PD for SC Administration

Subcutaneous administration is the typical route of delivery for insulin. Therefore a comparison between PEGylated insulin and regular human insulin following SC injection is meaningful in addition to the standard IV comparison. The PK profile of SC administered insulin and PEGylated insulin at doses of 1.0 IU/kg is given in Figure 7.6. A dose of PBS was also administered as a control group. The concentrations of both insulin and PEGylated insulin initially increase following dosing as they are absorbed into the bloodstream. Regular human insulin levels reach a maximum concentration (C_{\max}) after 30 minutes at 132.5 μ IU/ml. PEGylated insulin levels do not reach C_{\max} until

120 minutes after dosing at 195.0 $\mu\text{IU/ml}$. The time for maximum concentration is referred to as t_{max} . Similar to IV dosing, the PEGylated insulin exhibits a sustained elevation in concentration versus that of regular human insulin. The concentration of regular human insulin decreases to near zero after 300 minutes while PEGylated insulin still has a concentration of 13.5 $\mu\text{IU/ml}$ at the completion of the test at 480 minutes.

The pharmacokinetic profile of PEGylated insulin when delivered subcutaneously indicates a slower rate of absorption from the interstitial fluids to the bloodstream. This is most likely due to the increased size of the protein conjugate and is exhibited by the later peak concentration. As insulin and PEGylated are absorbed into the bloodstream they are concomitantly removed by metabolism in the liver and the reticuloendothelial system (RES). This is the reason that the concentrations never reach the incredibly high levels seen following IV administration. The maximum concentration for the insulin or PEGylated insulin occurs when the rate of clearance is greater than the rate of absorption. Because SC administration deposits only a finite amount of insulin or PEGylated insulin, the rate of absorption decreases as the local amount is reduced. Regular human insulin is rapidly absorbed from the SC depot, thus the rate of absorption also decreases rapidly. The rate of clearance from the bloodstream quickly supersedes the rate of absorption and C_{max} occurs with a t_{max} of 30 minutes. The reduced rate of absorption of PEGylated insulin means that the rate of absorption also decreases more slowly than for regular insulin. In conjunction with the lower rate of clearance from the bloodstream, as was indicated by the IV data described above, t_{max} does not occur until 120 minutes. Additionally, the value of C_{max} in comparison to regular human insulin is significantly higher. The relative rates of absorption and clearance also account for the

higher value for C_{\max} exhibited for PEGylated insulin versus that of regular human insulin. A summary of this data is given in Table 7.1.

The pharmacodynamic effect of subcutaneously administered insulin and PEGylated insulin is seen in Figure 7.7. Again the effects of the surgery induced a drop in BG levels indicated by the control group dosed with only PBS. A normalized version of this chart is seen in Figure 7.7b in which the effects of the surgery on glucose levels are removed. A similar trend is exhibited in the BG levels as was seen for insulin levels in the plasma: a delayed onset of action followed by a sustained effect for PEGylated insulin when compared to regular human insulin. The hypoglycemic effect of regular human insulin is almost instantaneous and can be seen after only 5 minutes. PEGylated insulin, however does not exhibit a hypoglycemic effect until after 30 minutes have passed. After 60 minutes, the BG concentration drops to 90% of initial values. The maximum hypoglycemic effect for normal insulin is seen after 60 minutes when BG levels are at 52.9 % of initial levels. For PEGylated insulin, the maximum hypoglycemic effect occurs 360 minutes after SC administration at when BG levels are 58.6 % that of the initial levels. This sustained effect is due to the extended residence time of PEGylated insulin in the bloodstream as was seen in the pharmacokinetic data. This lengthened duration of action is a very interesting result for PEGylated insulin because it indicates that it can have a sustained effect in comparison to regular insulin. If the same behavior can be observed when PEGylated insulin is absorbed across other tissues, such as the intestinal epithelium, then it may be able to induce a greater effect than regular insulin.

The bioavailability of subcutaneously delivered PEGylated insulin was determined by comparison to regular human insulin delivered in the same fashion. The

values for the AAC of the normalized curves determined as the sum of consecutive trapezoids integrated to 1 were 97.3 and 111.8 for normal insulin after 6 and 8 hours, respectively. The AAC values for PEGylated insulin were 98.2 and 142.9 for 6 and 8 hours, respectively. The units of these values are the same as found for IV dosing. Using these AAC values, the biological activity of PEGylated insulin was 100.9 % and 127.8 % that of regular human insulin. Similar to the IV dosed insulin samples, the higher bioactivity is due to the sustained hypoglycemic effect induced by PEGylated insulin, not an increase in potency of the PEG-modified insulin species.

7.3.4. *In Vivo* Effect of a High Dose of Insulin and PEGylated Insulin

An early test was performed in which a dose of 4.0 IU/kg was given to rats through SC injection. This dose ended up being too high for the rats and induced acute hypoglycemia which had to be countered through the intravenous administration of glucose to keep the animals from expiring. The tests were not repeated and subsequent doses were lowered for later tests. Nonetheless, the information gathered on the BG levels prior to the administration of additional glucose gives further information for the pharmacodynamic effect of PEGylated and regular human insulin in rats. The data is truncated at the point when exogenous glucose administration occurred and is shown in Figure 7.8. For normal human insulin, this occurred 60 minutes after dosing. PEGylated insulin, however, did not require exogenous glucose administration over the duration of this shortened 4 hour study. These results further indicate the reduced rate of absorption of PEGylated insulin. Even when the dose was 4.0 IU/kg, PEGylated insulin did not induce acute hypoglycemia which would have manifested itself as seizures in the rats.

The BG levels did continue to drop even after 4 hours, though, and a severe hypoglycemic state may have eventually occurred in these rats.

7.3.5. *In Situ* Testing

The design of the *in situ* testing method was adapted from previous methods used by our group and others working on oral insulin delivery with P(MAA-g-EG) hydrogels [10, 19]. The methods used in this study were in an attempt to more accurately mimic an orally delivered dose on fully anesthetized animals and there were several key changes. First, previous designs used a closed-loop *in situ* design in which the insulin loaded polymer was placed into the ileum of rats. By placing the samples in the ileum, the duodenum and jejunum are directly bypassed, which would not happen following oral administration. The current method dosed into the duodenum in a location that is close to where the pH shift would occur in the GI tract. Second, the closed-loop method isolates a segment of the small intestine by tying off the section to be dosed using sutures. By closing a segment, normal peristalsis in the intestine cannot occur. The current method was an open loop technique in which the intestine were not occluded above or below the site selected for dosing. Third, previous closed-loop methods thoroughly washed the intestine in the targeted tissues prior to dosing. In doing so, the mucus layer and luminal and brush-border enzymes are reduced by physical removal. This would greatly alter the environment normally found in the GI tract and should falsely increase the amount of insulin which can be transported across the epithelial layer. In the current method, the intestines were not pretreated in any way in an attempt to maintain normal levels of mucus and enzymatic activity. Fourth, the fasting period in previous methods was 24

hours or more. The current techniques only used a 12 hour fast, close to a normal overnight fast. Extended periods of fasting reduce the enzymatic activity in the GI tract. Finally, by using a dosing method which used a catheter and guide needle an attempt was made in the current method to minimize physical manipulation of the intestines. This was not attempted in previous closed-loop techniques.

The serum insulin and PEGylated insulin levels following *in situ* dosing can be seen in Figure 7.9. The maximum concentration seen by any sample was 11.5 $\mu\text{IU/ml}$ for PEGylated insulin loaded hydrogels. This is equivalent to the normal basal levels of insulin which are between 5 and 15 $\mu\text{IU/ml}$. However, in order to induce a hypoglycemic effect in healthy rats, plasma concentrations of PEGylated or regular human insulin must exceed basal levels in the absence of a meal. Circulating concentrations of PEGylated insulin remained above 5 $\mu\text{IU/ml}$ for 180 minutes following dosing of PEGylated insulin loaded polymer samples. Interestingly, the levels of PEGylated insulin following dosing as a solution into the duodenum also increased above basal levels and reached a maximum concentration of 10.4 $\mu\text{IU/ml}$ one minute after dosing. The plasma concentration quickly dropped and only remained above 5 $\mu\text{IU/ml}$ for 15 minutes. For regular human insulin delivered as a solution or from insulin loaded polymer particles, the maximum plasma concentration never reached 5 $\mu\text{IU/ml}$ at any point throughout the test.

The normalized relative blood glucose levels for the rats dosed by *in situ* administration can be seen in Figure 7.10. None of the rats tested exhibited a hypoglycemic effect. This is expected based on the levels of insulin seen in the PK data. Because the plasma concentrations for PEGylated and regular human insulin never

exceed basal levels, a hypoglycemic effect should not occur. A sustained increase of BG is seen for all samples due to the sympathetic effects caused by the surgery. Because the circulating insulin levels never exceeded basal concentrations, the endogenous glucose production by the healthy rats was able to compensate for the increased concentrations. Nonetheless, the transfer of some insulin and PEGylated insulin was apparent from the ELISA data represented in Figure 7.9. The lack of the expected pharmacodynamic effect is due to the fact that healthy rats were used in a test where the increase in insulin concentration did not approach or exceed postprandial levels. Using a higher dose, or a diabetic rat model, would likely exhibit a more significant PD effect.

Several important results are inferred from this *in situ* dosing study. First, PEGylated insulin was able to be absorbed from the small intestine to a greater extent than that seen for native human insulin. This was true when the protein was administered as a solution as well as following its incorporation into P(MAA-g-EG) hydrogels. This is most likely due to the additional enzymatic resistance of the PEGylated species. In fact plasma concentrations for PEGylated insulin delivered as a solution exceeded those of insulin following its incorporation into P(MAA-g-EG) hydrogels. Therefore, by PEGylating insulin, its absorption was increased in relation to normal human insulin. Secondly, the presence of P(MAA-g-EG) only slightly increased the absorption of insulin and PEGylated insulin from the small intestine. The hydrogel is highly effective at maintaining the integrity of insulin in a gastric environment; however upon exposure to the intestinal environment the release apparently occurs too rapidly for the hydrogel to greatly enhance the protein absorption. This rapid release was seen with *in vitro* testing presented in Chapter 5. Insulin and PEGylated insulin are most likely released to a large

extent into the lumen of the small intestine and do not localize with the hydrogel on the apical surface of the epithelium. Third, because the pharmacokinetic and pharmacodynamic effect of P(MAA-g-EG) hydrogels loaded with regular human insulin was significantly lower than what has been seen in previous studies, it is clear that the closed-loop *in situ* technique induces insulin transport across the intestinal epithelium. While this gives good results and a higher apparent bioavailability, it falsely increases the insulin absorption in a non-physiological way. The techniques used in this work more adequately mimic the natural pathway for orally administered drugs and drug formulations.

There are still significant limitations to the open-loop method used in this study. The most important one is the large reduction in intestinal motility induced by the surgical technique. A study performed by De Winter et. al. showed that abdominal surgery on rats caused a very large drop in the movement of a dye through the intestines [20]. If peristalsis is lost, the drug loaded polymer systems may not adequately bind to the mucus layers of the small intestine. Further, the release of PEGylated insulin did not approach 100 % until the pH of the release buffer was 7.4. This pH level is achieved in the GI tract, but not until the most proximal areas of the small intestine such as the ileum or in the colon. If the movement of the PEGylated insulin loaded polymer was restricted, then the release of the protein may not have completely occurred.

7.4. Conclusions

Regular human insulin and PEGylated insulin was successfully loaded into P(MAA-g-EG) hydrogels with low, moderate, and high levels of crosslinking formulated

with a MAA:EG ratio of 3:2. Loading efficiencies were higher than those seen for P(MAA-g-EG) with a 1:1 ratio of monomers for insulin for all three formulations. PEGylated insulin loading was not observed in the hydrogel formulations with a 1:1 monomer ratio. However, in hydrogels formulated with a MAA:EG ratio of 3:2 PEGylated insulin had the highest loading efficiencies for all three levels of crosslinking, most prominently in formulation 0.75/33 with greater than 90 % of available protein loaded into the hydrogel. The same hydrogel formulation with monomer ratios of 1:1 and 3:2 had loading efficiencies lower than 55 % for regular human insulin. The addition of PEGylated insulin to the hydrogels formulated with a 3:2 monomer ratio increased the amount of PEG available for complexation with MAA groups, thus shifting the monomer ratio closer to 1:1. Hydrogels formulated with a 1:1 ratio had shown the highest levels of complexation in previous work [21]. Therefore the increased availability of hydrogen bonding with MAA is likely the reason for the increased loading efficiencies of PEGylated insulin.

The release of PEGylated insulin and regular insulin from hydrogels with a 3:2 monomer ratio showed similar release tendencies with minimal protein loss until the pH of the release buffer was at 6.2 or greater. The fractional release of PEGylated insulin increased as the pH increased from 6.2 to 7.4 and was lower than regular human insulin for these pH levels. These results indicate that PEGylated insulin maintained a greater affinity for P(MAA-g-EG) hydrogels than regular human insulin. This could be advantageous in future designs for oral insulin delivery because of the potential for sustained localization of the drug within the hydrogel.

The retention of the bioactivity of PEGylated insulin was confirmed using intravenous (IV) and subcutaneous (SC) dosing. A hypoglycemic effect was seen for both methods of administration for PEGylated and regular human insulin at a dosing level of 1.0 IU/kg in healthy male Sprague Dawley rats. In IV dosing, the PK/PD profile exhibited a sustained elevation in PEGylated insulin concentrations for the entire duration of the 6 hours test versus that of regular human insulin, although the induced hypoglycemia was almost identical. The bioactivity of PEGylated insulin following IV administration was 111.0 % and 122.3 % that of regular human insulin based on the ratio of AAC values of relative blood glucose levels after 4 and 6 hours, respectively. Subcutaneous administration yielded significantly altered PK/PD profiles for PEGylated insulin. PEGylated insulin had a slower absorption and sustained hypoglycemic along with a higher C_{max} than seen for regular human insulin. Initially regular human insulin had higher plasma concentration levels and a greater drop in blood glucose levels. After 60 minutes the plasma concentration of PEGylated insulin exceeded that of regular human insulin and maintained a higher concentration until 8 hours following administration. After 120 minutes the hypoglycemic effect of PEGylated insulin was greater than that of regular human insulin and lower blood glucose concentrations were maintained through the remaining duration of the 8 hour test. The bioavailability of PEGylated insulin for SC administration was 100.9 % and 127.8 % that of regular human insulin after 6 and 8 hours, respectively.

Previous work on PEGylated insulin suggested that the molecular weight of PEG greater than 750 Da would cause a decrease in the biological activity of insulin [14]. However, the results of the work presented in the current study indicate that PEGylated

insulin in which a 5000 Da PEG chain conjugated to the PheB1 site of insulin fully maintained its biological activity *in vivo*. This is an important result because higher MW PEG species are able to impart more of the beneficial effects of PEGylation on proteins than lower MW PEG chains. Most important to oral insulin delivery is the increased resistance to proteolytic degradation caused by PEG conjugation. The additional benefit of the improved interaction with P(MAA-g-EG) hydrogels enhances the potential for the oral delivery of PEGylated insulin.

The administration of P(MAA-g-EG) loaded with regular human insulin or PEGylated insulin using *in situ* dosing exhibited limited transport of insulin to the bloodstream and a negligible hypoglycemic effect with 20 IU/kg doses. The highest amount of transport into the bloodstream was seen from PEGylated insulin loaded polymer samples which achieved plasma concentrations in the range of basal insulin levels for 180 minutes following dosing. PEGylated insulin delivered *in situ* as a solution also achieved plasma concentrations in the basal range, though only for 15 minutes following administration. Regular human insulin never achieved plasma concentrations greater than the minimum level for basal levels in the bloodstream administered as a solution or from insulin loaded polymer samples. Because the concentrations never exceeded basal levels for either PEGylated or regular human insulin, a hypoglycemic effect was not seen for the healthy rats tested in this study. The same study performed on diabetic rats would likely have exhibited a drop in blood glucose because the levels of PEGylated insulin in the bloodstream did increase to what would be expected in healthy animals for 3 hours. One important consideration for these results lies in the fact that the intestinal motility was significantly reduced by the *in situ* testing. Because the polymer

never proceeded down the GI tract, it may not have reached areas of the small or large intestine with the highest pH. As seen in the *in vitro* studies of PEGylated insulin with P(MAA-g-EG) hydrogels, the release did not approach 100 % until the release buffer was at pH = 7.4. Therefore, a significant portion of dosed PEGylated insulin may have remained within the hydrogel and not been available for absorption. If true, the potential bioavailability of PEGylated insulin may have been higher than seen in this study.

Another conclusion of this work is that the open-loop technique used for the *in situ* testing of this work is superior to the closed-loop technique used in previous studies. By dosing to the duodenum rather than the ileum the drug loaded polymer is exposed to the first area of the small intestine which would exhibit a near neutral pH. The open-loop design allows the natural movement of the lumen down the small intestine. The closed-loop method physically prevents this movement. The open-loop method requires less manipulation of the intestinal tract than the closed-loop method. Finally, the open-loop technique does not wash or clean the small intestines prior to dosing, thus maintaining near normal enzymatic activity and mucus layer integrity. The closed-loop technique washes the section of the intestines to be dosed which physically removes a large portion of the mucus layer and luminal and brush-border peptidases thereby skewing the absorption and degradation of insulin. Overall, the open-loop *in situ* method maintains a more normal state of the GI tract than the closed-loop method and more accurately simulates an oral dose in anesthetized rats. However, the technique can still be improved such that it does not cause such a reduction in the natural intestinal motility which would be seen in rats.

Table 7.1. PK/PD summary of IV and SC administration of insulin and PEGylated insulin at 1.0 IU/kg to healthy male Sprague Dawley rats

	IV administration		SC administration			
	AAC $\left(\frac{C(t)}{C_o}\right) * \text{min}$	Bioavailability	AAC $\left(\frac{C(t)}{C_o}\right) * \text{min}$	Bioavailability	C_{max} ($\mu\text{IU/ml}$)	t_{max} (min)
Human insulin	61.69	N/A	111.8	N/A	132.5	30
PEGylated insulin	75.43	122.3 %	142.9	127.8 %	195.0	120

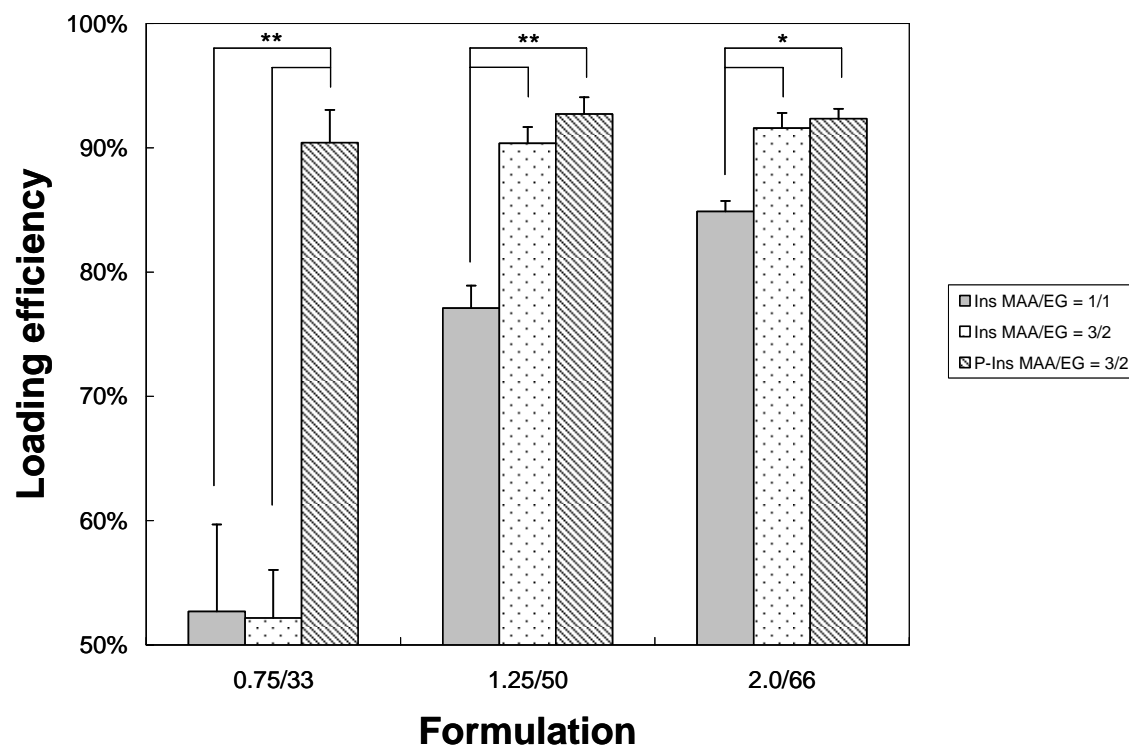


Figure 7.1. Loading efficiencies for regular human insulin and PEGylated insulin in P(MAA-g-EG) hydrogels with MAA/EG monomer ratios of 1/1 or 3/2 (+ S.D., ** $p < 0.01$, * $p < 0.05$)

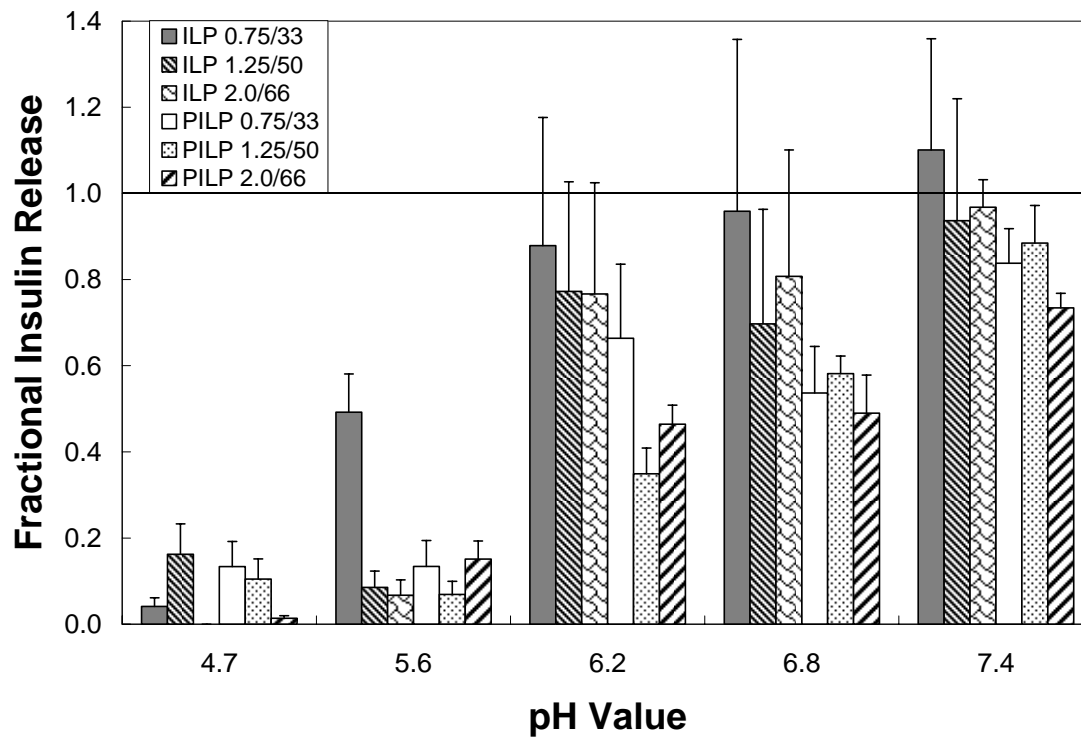


Figure 7.2. Insulin loaded polymer (ILP) and PEGylated insulin loaded polymer (PILP) release from P(MAA-g-EG) hydrogels with a MAA:EG monomer ratio of 3:2 following 3 hours of dissolution in PBS at 37 °C (+ S. D., n = 3)

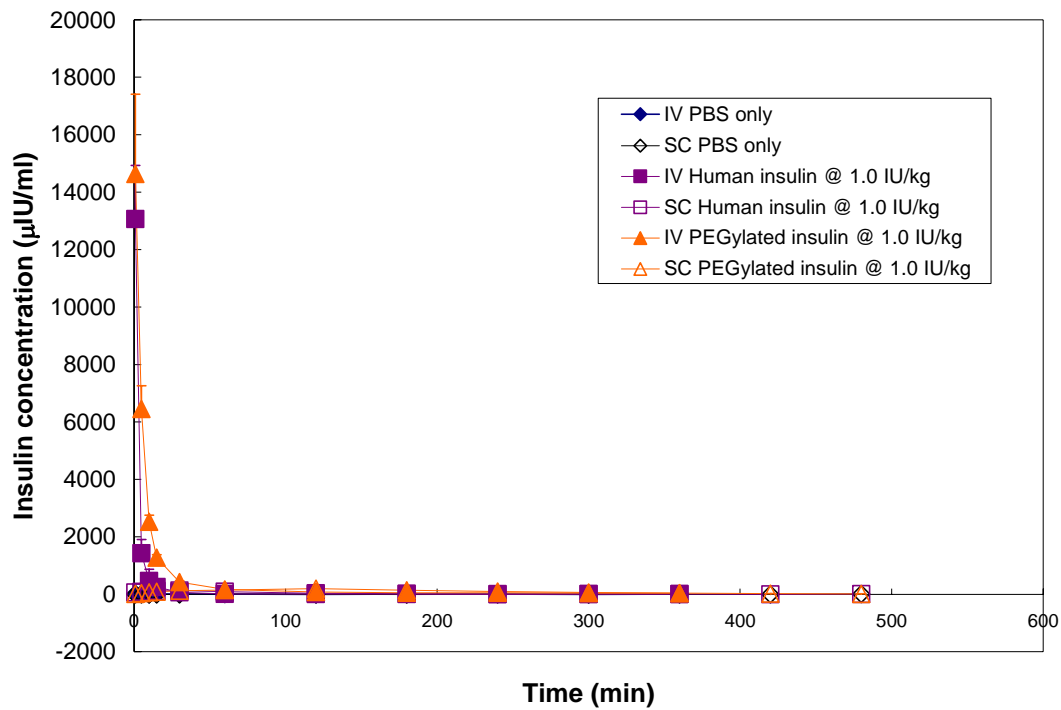


Figure 7.3. Insulin and PEGylated insulin plasma concentrations following IV and SC injection of 1.0 IU/kg in rats (+ S. D., n = 6)

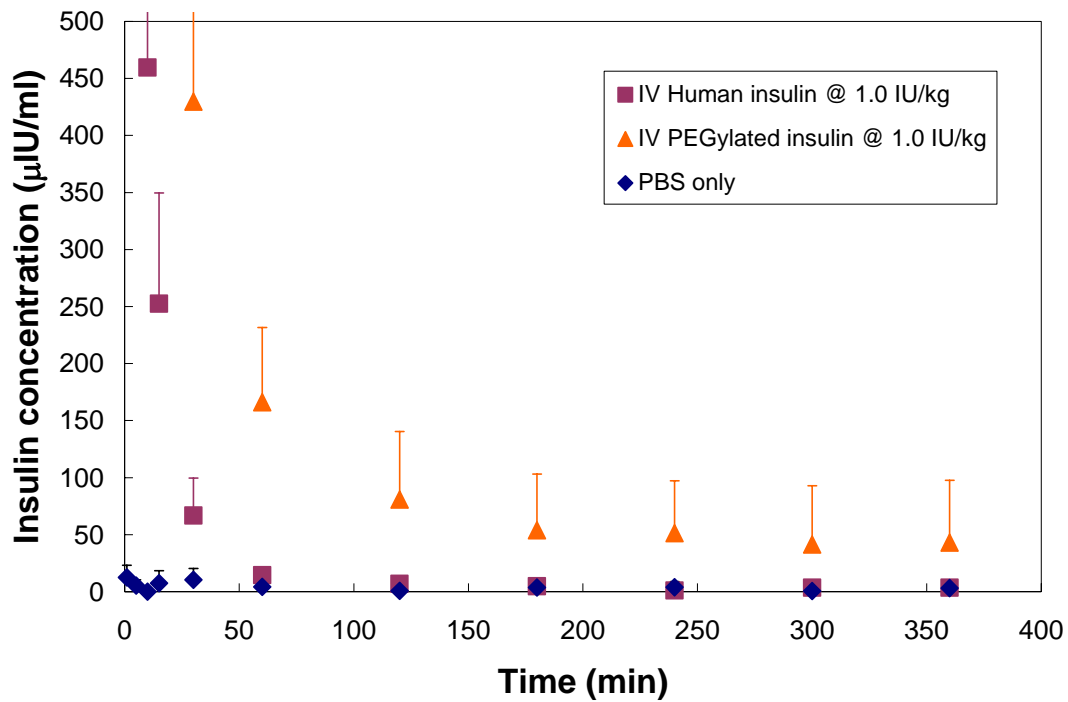


Figure 7.4. Zoom in of insulin and PEGylated insulin plasma concentrations in healthy male Sprague Dawley rats following IV injection of 1.0 IU/kg (+ S.D., n = 6)

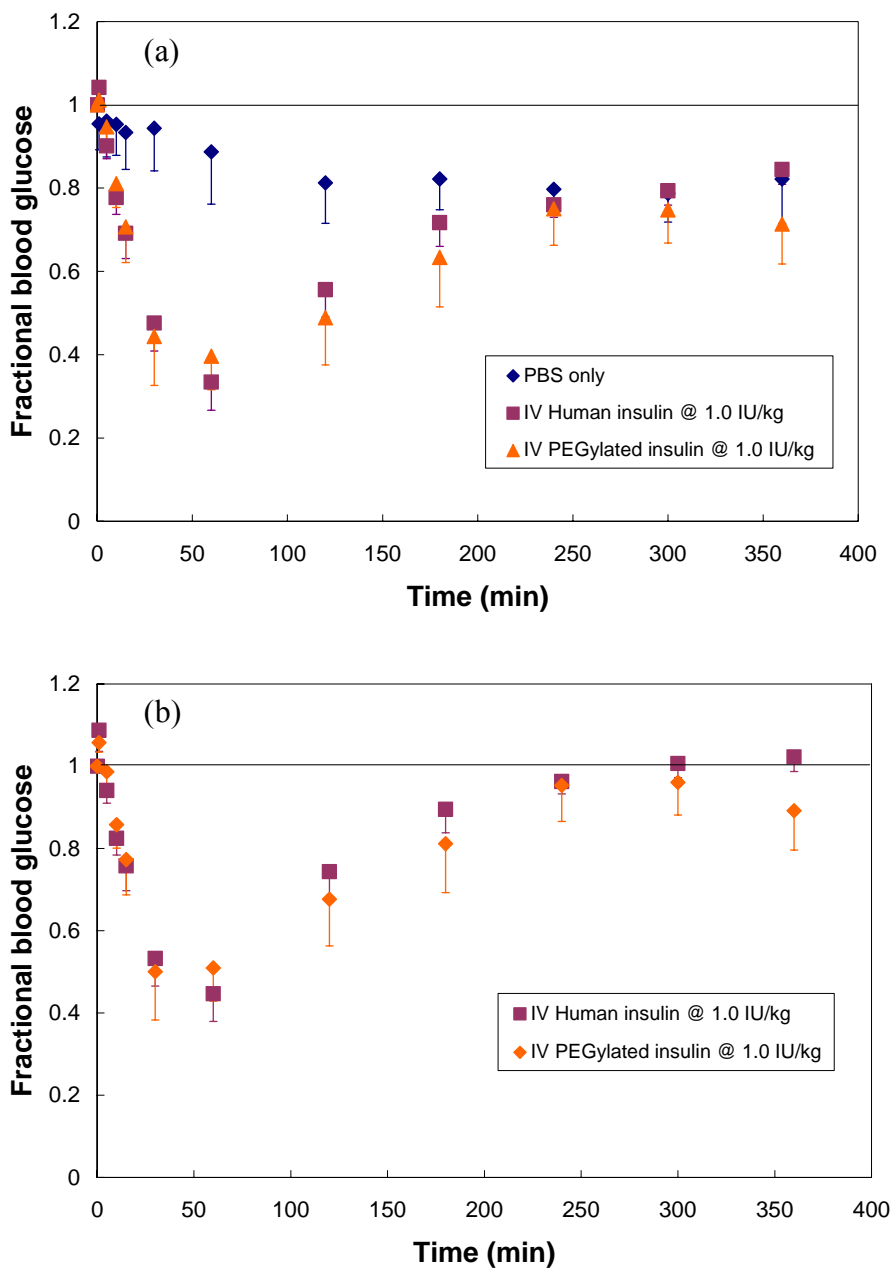


Figure 7.5. (a) Blood glucose levels and (b) normalized blood glucose levels of healthy male Sprague Dawley rats following IV administration of 1.0 IU/kg of insulin and PEGylated insulin (- S.D., n = 6)

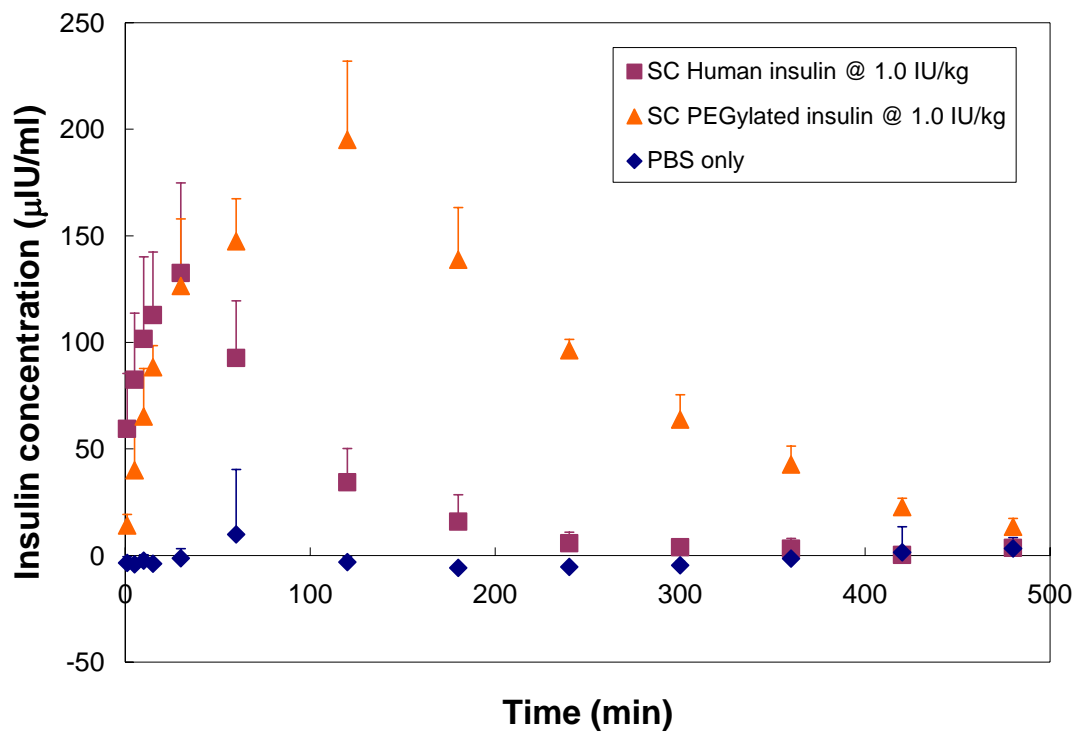


Figure 7.6. Insulin and PEGylated insulin plasma concentrations following SC injection of 1.0 IU/kg in healthy male Sprague Dawley rats (+ S. D., n = 6)

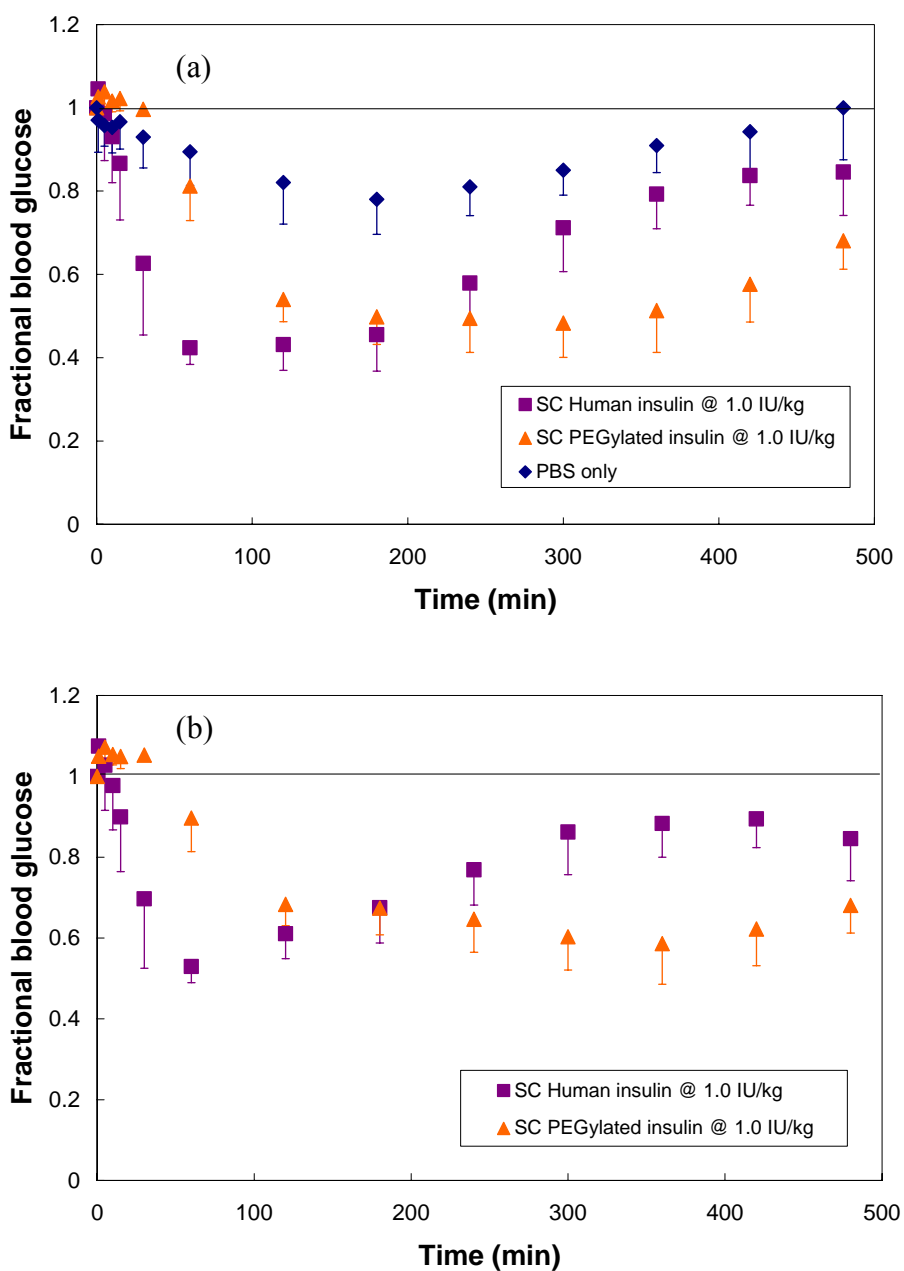


Figure 7.7. (a) Blood glucose levels and (b) normalized blood glucose levels of healthy male Sprague Dawley rats following SC administration of 1.0 IU/kg of insulin and PEGylated insulin (- S.D., n = 6)

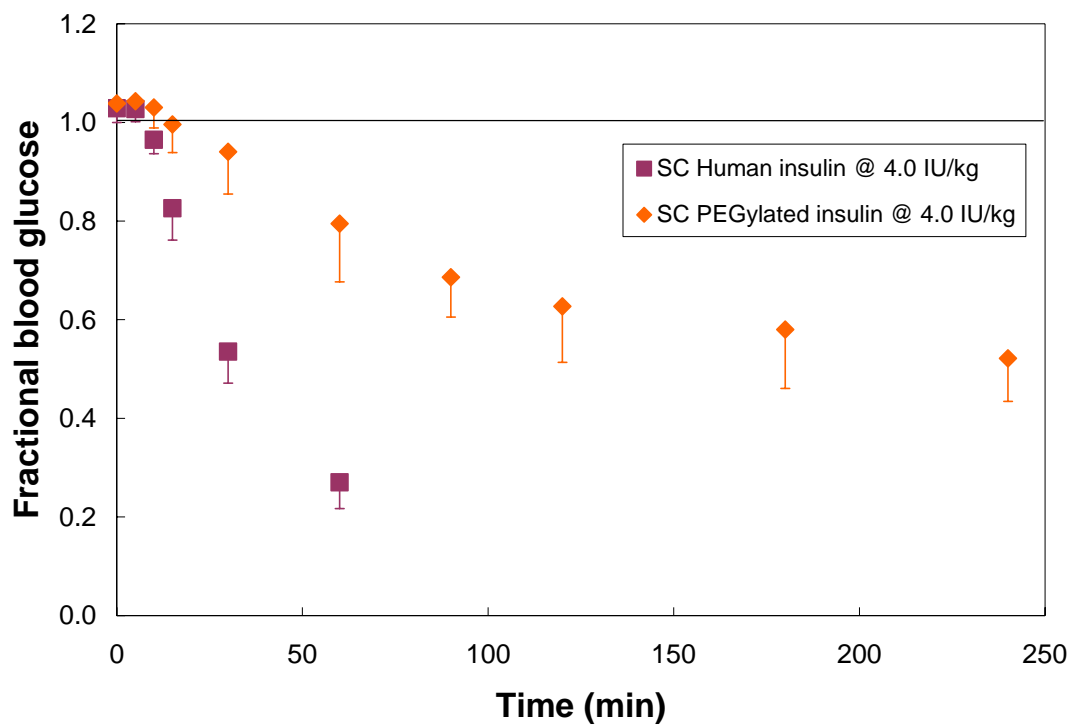


Figure 7.8. Blood glucose levels of healthy male Sprague Dawley rats following SC administration of 4.0 IU/kg of insulin and PEGylated insulin (- S.D., n = 4)

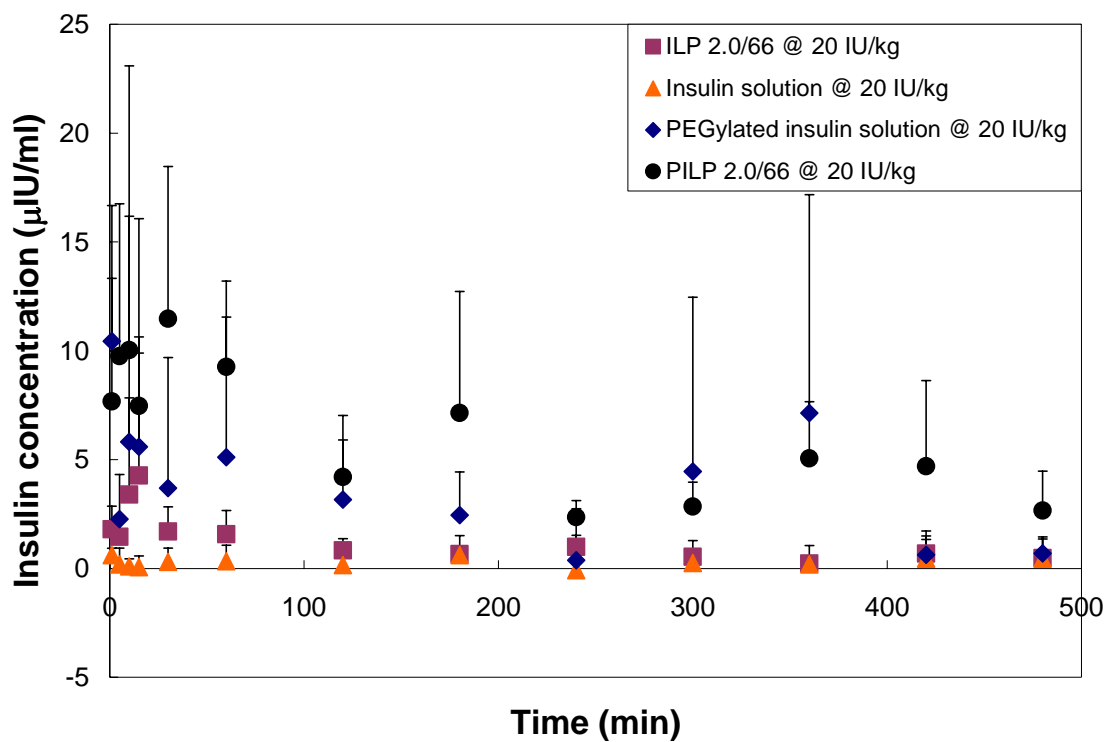


Figure 7.9. Insulin and PEGylated insulin plasma concentrations following *in situ* administration of solutions or protein loaded polymers to the duodenum of healthy male Sprague Dawley rats at 20.0 IU/kg (+ S.D., n = 6)

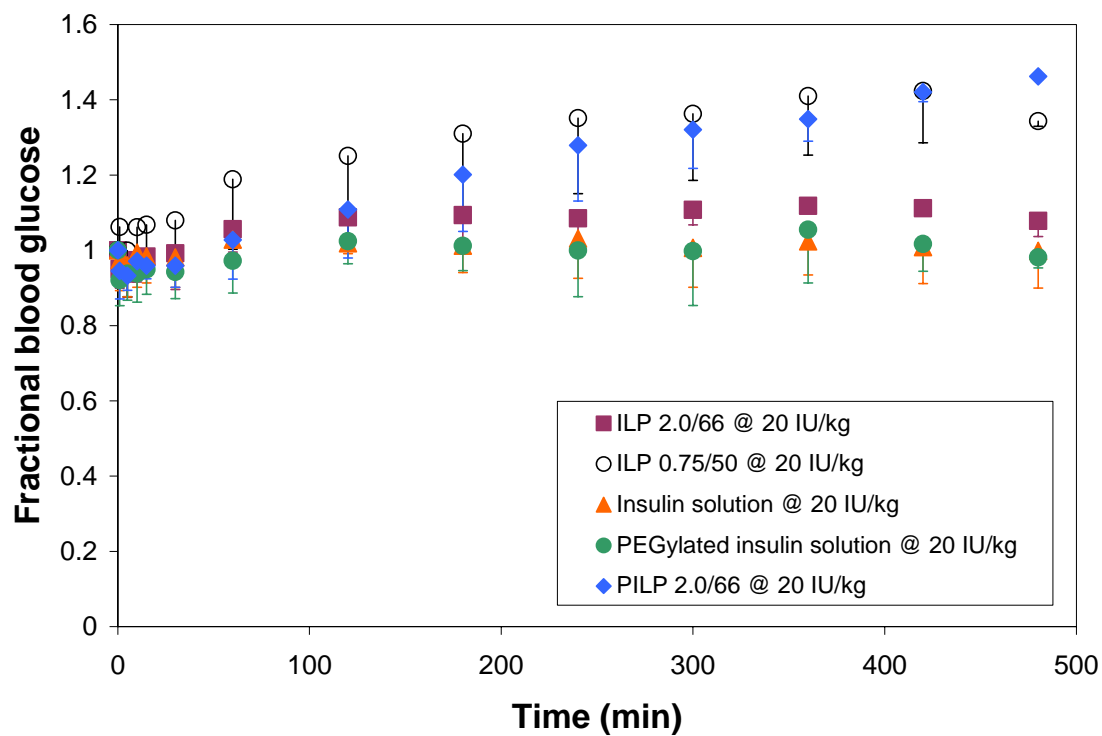


Figure 7.10. Normalized blood glucose levels of healthy male Sprague Dawley rats following *in situ* administration of 20.0 IU/kg of insulin and PEGylated insulin solutions and insulin and PEGylated insulin loaded polymers (- S.D., n = 4-6)

7.5. References

1. Perakslis, E., A. Tuesca, and A. Lowman, *Complexation hydrogels for oral protein delivery: an in vitro assessment of the insulin transport-enhancing effects following dissolution in simulated digestive fluids*. J Biomater Sci Polym Ed, 2007. **18**(12): p. 1475-90.
2. Kim, B. and N.A. Peppas, *In vitro release behavior and stability of insulin in complexation hydrogels as oral drug delivery carriers*. Int J Pharm, 2003. **266**(1-2): p. 29-37.
3. Goto, T., et al., *Gastrointestinal transit and mucoadhesive characteristics of complexation hydrogels in rats*. Journal of Pharmaceutical Sciences, 2006. **95**(2): p. 462-469.
4. Torres-Lugo, M., et al., *pH-Sensitive hydrogels as gastrointestinal tract absorption enhancers: transport mechanisms of salmon calcitonin and other model molecules using the Caco-2 cell model*. Biotechnol Prog, 2002. **18**(3): p. 612-6.
5. Yamagata, T., et al., *Characterization of insulin protection properties of complexation hydrogels in gastric and intestinal enzyme fluids*. J Control Release, 2006. **112**(3): p. 343-9.
6. Madsen, F. and N.A. Peppas, *Complexation graft copolymer networks: swelling properties, calcium binding and proteolytic enzyme inhibition*. Biomaterials, 1999. **20**(18): p. 1701-8.
7. Ichikawa, H. and N.A. Peppas, *Novel complexation hydrogels for oral peptide delivery: in vitro evaluation of their cytocompatibility and insulin-transport enhancing effects using Caco-2 cell monolayers*. J Biomed Mater Res A, 2003. **67**(2): p. 609-17.
8. Morishita, M., et al., *Novel oral insulin delivery systems based on complexation polymer hydrogels: single and multiple administration studies in type 1 and 2 diabetic rats*. J Control Release, 2006. **110**(3): p. 587-94.
9. Lowman, A.M., et al., *Oral delivery of insulin using pH-responsive complexation gels*. J Pharm Sci, 1999. **88**(9): p. 933-7.

10. Nakamura, K., et al., *Oral insulin delivery using P(MAA-g-EG) hydrogels: effects of network morphology on insulin delivery characteristics*. J Control Release, 2004. **95**(3): p. 589-99.
11. Patton, J.S., et al., *Compositions of chemically modified insulin*, in Patent # 6890518 B2 United States Patent Office. 2005, Nektar Therapeutics: USA.
12. Still, J.G., *Development of oral insulin: progress and current status*. Diabetes Metab Res Rev, 2002. **18**(Suppl 1): p. S29-S37.
13. Calceti, P., et al., *Development and in vivo evaluation of an oral insulin-PEG delivery system*. European Journal of Pharmaceutical Sciences, 2004. **22**(4): p. 315-323.
14. Hinds, K.D. and S.W. Kim, *Effects of PEG conjugation on insulin properties*. Adv Drug Deliv Rev, 2002. **54**(4): p. 505-30.
15. Volund, A., *Conversion of insulin units to SI units*. Am J Clin Nutr, 1993. **58**(5): p. 714-5.
16. Gibaldi, M., Perrier, D., *Pharmacokinetics*. 1975, New York: Marcel Dekker.
17. Lees, P., F.M. Cunningham, and J. Elliott, *Principles of pharmacodynamics and their applications in veterinary pharmacology*. J Vet Pharmacol Ther, 2004. **27**(6): p. 397-414.
18. Nolte, M.S., Karam, John H., *Pancreatic Hormones & Anitdiabetic Drugs*, in *Basic and Clinical Pharmacology, 10th Edition*, B.G. Katzung, Editor. 2007, McGraw-Hill: New York.
19. Morishita, M., et al., *Mucosal insulin delivery systems based on complexation polymer hydrogels: effect of particle size on insulin enteral absorption*. J Control Release, 2004. **97**(1): p. 115-24.
20. De Winter, B.Y., et al., *Effect of different prokinetic agents and a novel enterokinetic agent on postoperative ileus in rats*. Gut, 1999. **45**(5): p. 713-8.
21. Lowman, A.M. and N.A. Peppas, *Analysis of the complexation/decomplexation phenomena in graft copolymer networks*. Macromolecules, 1997. **30**(17): p. 4959-4965.

CHAPTER 8: CONCLUSIONS AND RECOMMENDATIONS FOR FUTURE WORK

8.1. Conclusions

The oral delivery of insulin for the treatment of Type 1 and Type 2 diabetes remains an elusive goal. The challenges of the enzymatic and physical barrier in the gastrointestinal tract can be addressed to a large extent by hydrogels composed of polymethacrylic acid grafted with polyethylene glycol chains (P(MAA-g-EG)). The overall goal of this work was to further investigate the interaction between P(MAA-g-EG) hydrogels and insulin and to improve the overall design of the delivery system by using PEG modified insulin.

A significant body of work characterizing the hydrogel structure was presented in Chapter 4. Throughout this work the ratio of the monomers remained 1:1 in terms of the monomeric repeat groups, MAA:EG. The crosslink density of these hydrogel formulations was altered by using monomer concentrations of 33, 50, or 66 wt% in solution and PEGDMA 200 concentrations of 0.375, 0.75, 1.25, and 2.0 mol%. All formulations were characterized according to their swelling and mechanical characteristics. They all exhibited an increase in swelling and decrease in tensile modulus as the pH of the buffer increased. The apparent pKa of the hydrogel based on these studies was between 5.8 and 6.0. The swelling and tensile data was then used to model the network characteristics of each formulation at each pH tested. The average molecular weight between crosslinks, \overline{M}_e , and the network mesh size, ξ , both increased with increasing pH in the same fashion as the swelling and mechanical data. Irrespective of environmental pH, increasing crosslink density was seen with increasing concentrations

of monomers and PEGDMA. Higher crosslink density caused decreases in \overline{M}_e and ξ at all pH levels. The variance for ξ between different P(MAA-g-EG) formulations was not very large and ranged between 7 nm and 12 nm at pH = 2.2 and 15 nm and 28 nm at pH = 6.8.

In vitro testing with insulin and insulin glargine was used to elucidate the mechanism of the protein loading and release from P(MAA-g-EG) hydrogels. Insulin was successfully loaded into all 11 formulations tested and the loading efficiency increased with increasing crosslink density. Insulin glargine was also loaded into 4 hydrogel formulations with the same result. The release of these proteins from P(MAA-g-EG) generally did not exceed 20 % until the pH of the release buffer exceeded both the pKa of the hydrogel and the pI of the incorporated protein. The exception to this rule was seen in the most loosely crosslinked hydrogel formulation investigated which indicated that a critical mass of polymer is required in the hydrogel to maintain a high retention of insulin near the ionic transition points of the hydrogel and the protein. In conjunction with the results from Chapter 4, these results suggested that insulin and insulin glargine were maintained within the hydrogel at low pH levels due in large part to weak bonds formed between P(MAA-g-EG) and the protein. At low pH, the network mesh size of the hydrogel was more than 5 times the hydrodynamic radius of an insulin monomer for all formulations investigated. At this ratio, the proteins would have slowly diffused from the hydrogel unless local interactions, such as hydrogen bonding, were able to further restrict their release. The release results indicated that the release of the insulin and insulin glargine at pH levels above the ionic transition points occurred because of the loss of these bonds and ionic repulsion between the hydrogel and the protein. By understanding

this interaction, more thoughtful approaches to oral protein delivery using P(MAA-g-EG) hydrogels can be attempted in the future.

In Chapter 6, the conjugation of PEG to insulin is described and characterized. The modification known as PEGylation was achieved specifically at the PheB1 residue of insulin in order to maintain its biological activity. In order to do so, the alternative free amine groups of insulin had to be modified by a protecting group prior to PEGylation. This was achieved through with di-t-butyl dicarbonate to create diboc treated insulin. Crude diboc treated insulin created through this reaction was purified using ion exchange chromatography (IEC) and characterized using RP-HPLC and MALDI-TOF MS. The purified di-BOC_{LysB29/GlyA1} insulin was subsequently reacted with amine reactive mPEG-SPA. Following reaction, the protecting BOC groups were removed and PheB1-mPEG-insulin was purified using IEC. The site of PEG modification was confirmed using MALDI-TOF MS following degradation of the conjugate using DTT or trypsin digestion. This work indicated that a site specific, mono-substituted PEGylated insulin can be made. The final yield was rather low for this process with 6.7 % of initial insulin being recovered as the desired product. However, the majority of loss occurred in the diboc treatment step. As a proof of concept this process was shown to be reversible such that impure side products of the protection reaction could be recovered and used again as a reactant. In doing so, the efficiency of this process could be easily improved and scaled up with a higher efficiency for the synthesis of PEGylated insulin product.

In vivo testing with PEGylated insulin and regular human insulin exhibited retention of the biological activity of PEGylated insulin. Dosing healthy male Sprague Dawley rats with 1.0 IU/kg of PEGylated insulin and regular human insulin caused

increases in plasma protein concentrations and drops in blood glucose levels. Based on IV administration the bioactivity of PEGylated insulin was 111.0 % and 122.3 % that of regular human after 4 and 6 hours, respectively. Subcutaneous administration yielded bioavailability of PEGylated insulin of 100.9 % and 127.8 % that of regular human insulin after 6 and 8 hours, respectively. This testing proved that PEGylated insulin in which a 5000 Da PEG chain conjugated to the PheB1 site of insulin fully maintained its biological activity *in vivo*. When delivered *in situ* to the duodenum of rats using an open-loop technique very little protein transport occurred from 20 IU/kg doses. The highest plasma concentrations were achieved with PEGylated insulin loaded polymer samples, achieving basal levels for 180 minutes following dosing. However, no hypoglycemic effect occurred in correlation with the increase in plasma levels of PEGylated insulin. The open-loop technique more accurately mimicked an actual oral dose than previously used closed-loop techniques and showed that previous results were skewed by the closed-loop method. However, the effect of the open-loop method on normal intestinal motility is a concern that should be addressed in future studies using this technique.

8.2. Recommendations for Future Work

There are several critical improvements in the design of this drug delivery system that are clearly indicated by this work. The network structure of P(MAA-g-EG) is less important than its ionization and the formation of weak bonds between the hydrogel and insulin. Previous investigations with protein delivery using P(MAA-g-EG) has either overlooked this potential interaction when investigating the mechanisms involved in drug loading and release [1] or mentioned it in passing without further investigation [2]. This

interaction can be utilized in other ways that have yet to be investigated and could significantly enhance future designs. Therefore, future work with P(MAA-g-EG) should take into account the pI and charge density of the protein to be investigated in an attempt to further enhance its loading and release. If unfavorable, the protein can be altered with PEG or another molecule or polymer that improves its interaction with P(MAA-g-EG). Alternatively, because the hydrogel becomes negatively charged, the drug could be designed to have a positive charge at neutral pH levels. In doing so, the drug should stay localized within the hydrogel in the lumen of the GI tract and have a greater likelihood of being transferred across the intestinal epithelium once the hydrogel binds to the mucus because glycoproteins in the mucus are also negatively charged [3].

In designing a method by which insulin or another drug is delivered more effectively delivered directly to the mucosal layer covering epithelial cells, the mucoadhesive behavior of P(MAA-g-EG) should be improved. The mucoadhesive behavior of these hydrogels has been characterized and is due to either the adsorption or diffusion theory of mucoadhesion, both of which are based on non-specific interactions [4-6]. Improving the mucoadhesion has already been investigated with P(MAA-g-EG) using wheat germ agglutinin (WGA) which is conjugated onto one end of a PEG chain with the other end containing a methacrylate group [7]. Initial results indicated that the loading of insulin was not greatly affected and that the mucoadhesion was increased in these hydrogels.

Improving the mucoadhesion can only address one of the problems in the current designs of P(MAA-g-EG). Another major concern is the likelihood for a majority of insulin release occurring into the lumen of the small intestine rather than into the brush

border of the epithelium. One approach which would be generic in design would be to have a unidirectional release of the protein toward the side of the hydrogel which is bound to the mucosal layer. If the release could be controlled in this way, then release of the protein to the lumen of the GI tract would first require that the protein diffuse through the mucus layer thus coming in close contact with the apical side of epithelial cells and greatly increasing the opportunity for paracellular transport in the presence of P(MAA-g-EG) hydrogels.

Alternatively, the conjugated PEG group could be used as a linker. By using PEG as a linker the benefits exhibited in this work could be retained and another material could be attached which would improve the drug delivery design. One obvious choice would be a material such as transferrin or vitamin B₁₂ which is transcytosed across epithelial cells, though these choices may be limited by total amount of transport and size of the conjugated group. Another choice would be some material which improves its interaction with P(MAA-g-EG) such as a cationic moiety of some sort. This would require quite a bit of work and would likely be difficult to create without significant loss during synthesis. Nonetheless, it could represent a promising alternative if carefully performed.

Finally, the *in vivo* testing design should be improved in future studies with P(MAA-g-EG). An optimal test would be performed on conscious animals in which the material is actually dosed orally. This can be done and is currently done for quite a few studies with rats [8], however, in a study in which blood samples have to be frequently drawn it represents a significant challenge. Also, when antagonized, rats and other animals exhibit increases in blood glucose levels which would skew results found using

these techniques. A similar approach to what was performed on the *in situ* testing in this work is a good alternative to oral administration, though further improvement is possible. The most notable problem with the methods used here is the severe drop in intestinal motility of the rats. Transit in the GI tract of rats was inhibited in a study by De Winter et. al. in which the rate of transport in the intestine was tracked using Evans blue dye. The transit of the dye was affected by surgical techniques with decreasing rates of transit where skin incision > laparotomy > laparotomy plus mechanical stimulation of the intestines [9]. Each surgical technique caused a significant drop from control rats. However, a significant increase in the intestinal motility was apparent after dosing with a prokinetic agent, cisapride. If this were administered during the *in situ* methods used in this study, it would more accurately mimic the natural movement in the GI tract.

8.3. References

1. Morishita, M., et al., *Elucidation of the mechanism of incorporation of insulin in controlled release systems based on complexation polymers*. J Control Release, 2002. **81**(1-2): p. 25-32.
2. Torres-Lugo, M. and N.A. Peppas, *Transmucosal delivery systems for calcitonin: a review*. Biomaterials, 2000. **21**(12): p. 1191-6.
3. Frey, A., et al., *Role of the glycocalyx in regulating access of microparticles to apical plasma membranes of intestinal epithelial cells: implications for microbial attachment and oral vaccine targeting*. J Exp Med, 1996. **184**(3): p. 1045-59.
4. Goto, T., et al., *Gastrointestinal transit and mucoadhesive characteristics of complexation hydrogels in rats*. Journal of Pharmaceutical Sciences, 2006. **95**(2): p. 462-469.
5. Smart, J.D., *The basics and underlying mechanisms of mucoadhesion*. Adv Drug Deliv Rev, 2005. **57**(11): p. 1556-68.
6. Torres-Lugo, M., et al., *pH-Sensitive hydrogels as gastrointestinal tract absorption enhancers: transport mechanisms of salmon calcitonin and other model molecules using the Caco-2 cell model*. Biotechnol Prog, 2002. **18**(3): p. 612-6.
7. Wood, K.M., G. Stone, and N.A. Peppas, *Lectin functionalized complexation hydrogels for oral protein delivery*. J Control Release, 2006. **116**(2): p. e66-8.
8. Damgé, C., P. Maincent, and N. Ubrich, *Oral delivery of insulin associated to polymeric nanoparticles in diabetic rats*. J Control Release, 2007. **117**(2): p. 163-170.
9. De Winter, B.Y., et al., *Effect of different prokinetic agents and a novel enterokinetic agent on postoperative ileus in rats*. Gut, 1999. **45**(5): p. 713-8.

CHAPTER 9: VITA

Anthony was born in Fort Wayne, Indiana on September 10, 1978. He graduated from Northrop High School in Fort Wayne in 1997. He then enrolled at Northwestern University in Evanston, Illinois in September of the same year. While at Northwestern, Anthony held a summer internship at Essex Group Corporation in Fort Wayne, Indiana. His work there investigated the wear effects on magnetic wiring and failure analysis following long-term and short-term high impulse current. Anthony graduated from Northwestern University in June 2001 with a B.S. in Chemical Engineering and took a position at Eastman Chemical Company in Carpentersville, Illinois as a chemist. At Eastman, he worked in a group specializing in the design and production of unsaturated polyester resins in the composite polymer group. Anthony developed 11 new commercial products during his tenure at Eastman for several different applications. He also earned his professional certification as a composite technician and assisted with the implementation of ISO 9001-2000 for the technology group. He collaborated with U.S. EPA on protocol for styrene suppressant testing which resulted in reduced hazardous air pollutant content in many current products. His findings were presented at the National Composites Fabricators Association Conference in the fall of 2003. Anthony matriculated to Drexel University in Philadelphia, Pennsylvania in September of 2003 in the Department of Chemical and Biological Engineering to pursue his M.S. degree. After joining the research group of Dr. Anthony Lowman he decided to pursue his Ph.D. Anthony has coauthored several peer reviewed publications and presented his work at several national and international conferences. He defended his Ph.D. degree on February 22, 2008.